H24/3499

MONASH UNIVERSITY
THESIS ACCEPTED IN SATISFACTION OF THE
REQUIREMENTS FOR THE DEGREE OF
DOCTOR OF PHILOSOPHY
ON..... 7 February 2003 .....
.....[redacted]....
Sec. Research Graduate School Committee

Characterisation of a *Mycobacterium smegmatis* Transposon Mutant with Defects in Cell Envelope Mannolipid Synthesis

Svetozar Kovačević
B.Sc. (Hons)

A thesis submitted
as a requirement for the degree of
Doctor of Philosophy
under the supervision of

Prof. R. L. Coppel
and
Dr. H. Billman-Jacobe

Department of Microbiology
Monash University
Melbourne, Australia
October 2002

MONASH
UNIVERSITY

Post-Examination Amendments
January 2003

Page 3	**Section 1.1.2.**	"*tuberculosis*" should read "*M. tuberculosis*".
Page 4	**Line 6**	A comma following "*M. tuberculosis*" should be inserted.
Page 4	**Line 7**	The comma following "antibiotics" should be omitted.
Page 10	**Line 25**	The word "would" should be omitted.
Page 11	**Line 22**	The word "glycosylated" should be replaced with "glycolylated".
Page 11	**Line 26**	The statement "The second main difference…" is not accurate; the DAP-DAP linkage is not unique in that it is also found in *Escherichia coli*.
Page 12	**Line 6**	The sentence "A truncated galactan backbone…" should be replaced with "The galactan backbone is typically 32 residues in length".
Page 16	**Line 27**	In reference to the indicated paragraph on DIMs: phthiocerols are fatty alcohols, not fatty acids.
Page 16	**Line 32**	The words "the on" should be replaced with "on the".
Page 17	**Line 5**	The words "β-diol fatty acids" should read "β-diols".
Page 21	**Line 13**	This statement is supported by the identification of PIM_6 in *M. smegmatis* and *M. bovis* (Reference 182).
Page 63	**Line 1**	The word "in" should be omitted.
Page 75	**Line 12**	"J. H. Pattesron" should read "J. H. Patterson".
Page 78	**Section 2.4.4.**	While MYCO481 extracts show a great deficiency in rhamnose, a marked deficiency is also apparent in MYCO479 extracts. The significance of this observation is unknown. However, it is evident that the reduction in rhamnose in both mutants corresponds with a reduction in LAM-derived sugars.
Page 80	**Line 30**	"feint" should read "faint".
Page 115	**Line 30**	"that" should read "than".
Page 173	**Line 3**	"…that that…" should read "…than that…".
Page 173	**Line 9**	Following the sentence "…change in the mutant.": Similarly, the defined Middlebrook media can be supplemented with additional NaCl to examine the effect of salt concentration on the stability of the mutant PIM/LAM phenotype.
Page 185	**Line 21**	The word "in" should be omitted.
Page 223	**Line 4**	"interfer" should read "interfere".

Table of Contents

Chapter 4

MYCO481 and MYCO479 are lpqW *Mutants with Identical Tn*611 *Insertion Sites* 119

List of Figures and Tables

Chapter 1

Mannosylated Glycolipids of the Mycobacterial Cell Envelope

Chapter 2

Transposon Mutants That Have PIM and LAM Abnormalities

Chapter 3

MYCO481 and MYCO479 Demonstrate Defects in PIM/LAM Biosynthesis

Chapter 4

MYCO481 and MYCO479 are lpqW *Mutants with Identical Tn*611 *Insertion Sites*

Chapter 5

MYCO481 Undergoes Change to Resemble MYCO479

Chapter 6

lpqW and the PIM/LAM Phenotype

Chapter 7

An Unusual Pair of Mutants with Great Potential

Statement of Authorship

I declare that the work presented for examination in this thesis has been conducted by myself, except where acknowledgment has been given in the relevant sections of text and the figure legends. The work described in this study has not been presented for examination for any other degree or at any other tertiary institution.

Svetozar Kovačević, B.Sc. (Hons)
Monash University
October 2002

Summary

Members of the genus *Mycobacterium* include the causative agents of the important human diseases tuberculosis and leprosy. Mycobacteria are also a major source of infection in HIV infected individuals. In recent times, the number of tuberculosis cases has increased in the population. The emergence of multi-drug resistant strains has compounded the growing number of infections and highlighted a need for effective new drugs.

The genus is characterised by a complex, lipid rich cell envelope that provides the bacterium with a robust peripheral layer. The mycobacterial cell envelope contains several classes of unique components that have been implicated in the disease process. One of these classes, the mycobacterial mannolipids, include the phosphatidylinositol mannosides (PIMs) and lipoarabinomannan (LAM). Apart from a structural importance in the cell envelope, PIMs and LAM have shown several immunomodulatory activities that are thought to be important in the pathogenesis of the organism. The unique nature of PIMs and LAM make their biosynthetic pathway a target for the development of novel antimycobacterial agents. The details of the pathway are incompletely understood, and many of the corresponding genes remain unidentified. The main aim of this study is to improve our understanding of the PIM/LAM biosynthetic pathway and to identify novel genetic determinants associated with the pathway. This was achieved using a transposon mutant of the non-pathogenic *Mycobacterium smegmatis*.

The *M. smegmatis* transposon mutant described in this study was found to have a complex phenotype characterised by several unusual abnormalities in PIM and LAM biosynthesis. The biosynthetic defect manifested itself as a novel metabolic blockage that resulted in reduced LAM or the loss of some PIMs together with the accumulation of a PIM metabolic intermediate. The transposon insertion was found to be located within an open reading frame of unknown function, designated *lpqW*. Interestingly, the mutant was found to be unstable on certain media, with distinct differences in PIM and LAM content between the unstable and stable forms. The transposon disrupted gene *lpqW* was then tested for its role in the observed PIM and LAM abnormalities by complementing the mutant

with an intact *lpqW* derived from the wild-type *M. smegmatis* chromosome. A novel, uncharacterised gene was implicated in both PIM and LAM biosynthesis by relating the biochemical observations with the genetic data.

The mutant phenotype defined by this study is completely novel and as such will form an important contribution to the body of knowledge. The multi-faceted nature of the mutant phenotype provides the foundation for further studies into the complexities of PIM and LAM biosynthesis.

Acknowledgements

I would like to extend sincere gratitude to my supervisors Ross Coppel and Helen Billman-Jacobe, who guided me through what was a challenging but immensely rewarding experience. I appreciate the opportunities they provided me with and thank them for their supervision. Special thanks to Helen for always being there to offer her knowledge and support whenever I needed it. Helen, I always appreciated our conversations and your commitment to my work. Thank you Helen, I feel privileged to be your first doctoral student.

Thank you, Ross, for your continued guidance and unique perspective on the project. Your insights were always appreciated, as was your ability to distil an often convoluted set of results into something that made undeniable sense. Your seemingly endless reserves of scientific knowledge always managed to put an interesting spin on much of my work.

I would also like to acknowledge the input of Malcolm McConville, whose expertise and advice shaped the project into a very interesting story. Mal, your tremendous enthusiasm for my work was always appreciated, and I thank you for giving me the opportunity to spend a lot of time in your lab. Your ideas and suggestions were crucial to the study. You were the best PhD supervisor I never had!

Sincere thanks to John Patterson, who trained me in Mal's lab and was always available for advice and assistance. Thank you for everything, Patto, I couldn't have done it without you. It was a privilege to do my PhD with you, thanks for being such a great guy. And thank you for being so patient.

Special thanks to Yasu Morita, who also showed a lot of enthusiasm for my work. Thank you for all of our great discussions, Yasu. Your insights added a lot to the study and made me appreciate the work from a much deeper perspective. You were an excellent teacher and I thoroughly enjoyed working with you, it was a pleasure.

I would also like to thank the members of the Billman-Jacobe, Coppel and McConville labs for all the support and encouragement. Thanks to Tony Korman for all the great discussions on music, film and sport (and occasionally science) and

to Dharshini Jeevarajah for being a great buddy and keeping me in check when things went awry. Dharsh, you were great to work with and fun to be around, thank you for putting up with me. I really appreciate it. Thanks also to Carolyn Trower and Ben Popp for all the fun moments; Agnieszka Topolska for your fascinating perspectives on life, the universe and everything; and to Ruth Haites for all of your help in the lab. Thanks also to Ingrid Olsen, Stephen Doughty, Arena Yao, Jia Jing Lee, Simon Sheridan, Ellen Taig, René Velasquez, Paul Crellin, David Lea-Smith and Kerith Shuckey for being a part of what was a very interesting ride.

Special thanks to Lyndal Borrell and Lukasz Kedzierski for being great friends throughout the last few years. Thanks for listening guys, I appreciate all of the laughs we shared. Thanks to Brian Cooke, John Menting and Simon Weisman for the wonderful evening transportation service and great after hours conversations. A truly enlightening experience, gentlemen, thank you.

Finally, I would like to thank my family, in particular my brother Sam. Thank you for understanding when I was rarely at home and seemed like I cared more for my experiments than for all of you. I love you all and I thank you for your encouragement and support.

Acronyms and Abbreviations

%	Percent
°C	Degrees celcius
µCi	Microcurie
µg/ml	Micrograms per millilitre
µl	Microlitre
µm	Micrometre
µM	Micromolar
[^{3}H]	Tritium
Ac_3PIM_2	Triacylated phosphatidylinositol dimannoside
Ac_3PIM_4	Triacylated phosphatidylinositol tetramannoside
Ac_3PIM_6	Triacylated phosphatidylinositol hexamannoside
Ac_4PIM_2	Tetraacylated phosphatidylinositol dimannoside
Ac_4PIM_6	Tetraacylated phosphatidylinositol hexamannoside
AG	Arabinogalactan
AIDS	Acquired Immune Deficiency Syndrome
AM	Arabinomannan
APC	Antigen Presenting Cell
Approx.	Approximately
Ara	D-arabinofuranose
ATP	Adenosine triphosphate
BCA	Bicinchoninic acid
BCG	Bacille Calmette-Guérin
BLAST	Basic Local Alignment Search Tool
bp	Base pairs
BSA	Bovine serum albumin
BY	Beef-Yeast media
CDP-DAG	Cytidine-diphosphate diacylglycerol
CHO	Chinese Hamster Ovary
Ci/mmole	Curie per millimole
CL	Cardiolipin

cm	Centimetre
cpm	Counts per minute
CR	Complement Receptor
DAT	Diacyl trehalose
DIG	Digoxygenin
DIM	Dimycocerosate
DMSO	Dimethyl suphoxide
DMT	Dimycoloyl trehalose
DNA	Deoxyribonucleic acid
DPM	Decaprenol phospho-mannose
EDTA	Ethylene diamine tetraacetic acid
EGTA	Ethylene glycol tetraacetic acid
ESI-MS	Electrospray Ionisation – Mass Spectroscopy
FPP	Farnesyl diphosphate
g	Grams
g/cm^3	Grams per cubic centimetre
Gal	D-galactofuranose
GC-MS	Gas Chromatography – Mass Spectroscopy
GDP	Guanosine diphosphate
Glc	D-glucopyranose
GM-CSF	Granulocyte Macrophage - Colony Stimulating Factor
GPL	Glycopeptidolipid
GPP	Geranyl diphosphate
HIV	Human Immunodeficiency Virus
HMDS	Hexamethyldisilazane
HPM	Heptaprenol phospho-mannose
HPTLC	High Performance Thin Layer Chromatoraphy
IFN$_\gamma$	Interferon gamma
IL	Interleukin
Ino	D-*myo*-inositol
IPP	Isopentenyl diphosphate
kb	Kilobase pairs
LAM	Lipoarabinomannan

LB	Luria-Bertani media
LM	Lipomannan
LOS	Lipooligosaccharide
M	Molar
MAC	*Mycobacterium avium* Complex
mAGP	Mycolylarabinogalactan-peptidoglycan
MALDI-TOF-MS	Matrix Assisted Laser Desorption Ionisation – Time of Flight – Mass Spectroscopy
MAME	Mycolic acid methyl ester
Man	D-mannopyranose
MBP	Mannose Binding Protein
MDR	Multi-Drug Resistant
mg/ml	Milligrams per millilitre
min(s)	Minute(s)
ml	Millilitre
mM	Millimolar
mm	Millimetre
MMA	Momomethyl amine
MR	Mannose Receptor
MSH	Mycothiol
nm	Nanometre
nmole	Nanomole
NMR	Nuclear Magnetic Resonance
nsGPL	Non-specific glycopeptidolipid
ORF	Open Reading Frame
PAGE	Polyacrylamide Gel Electrophoresis
PBS	Phosphate-buffered saline
PCR	Polymerase Chain Reaction
PE	Phosphatidylethanolamine
PG	Phosphatidylglycerol
PGL	Phenolic glycolipid
PI	Phosphatidylinositol
PI-GAM	Phosphoinositol – glyceroarabinomannan

PIM	Phosphatidylinositol mannoside
PI-PLC	Phosphatidylinositol phospholipase C
PPLO	Pleuropneumonia-like organism media
PPM	Polyprenol phospho-mannose
PPT	Polyphthienoyl trehalose
Rha	L-rhamnopyranose
rpm	Revolutions per minute
SDS	Sodium dodecyl sulphate
SL	Sulpholipid
ssGPL	Serovar-specific glycopeptidolipid
TAE	Tris-acetate ethylene diamine tetraacetic acid
TAG	Triacylglycerol
TMCS	Trimethylchlorosilane
TFA	Tri-fluoroacetic acid
TGF_β	Transforming Growth Factor beta
TLCK	*N*-α-p-tosyl-L-lysine chloromethyl ketone hydrochloride
TMS	Tri-methyl silyl
TNF-α	Tumor Necrosis Factor alpha
v/v	Volume per volume
w/v	Weight per volume

Chapter 1
Mannosylated Glycolipids of the Mycobacterial Cell Envelope

The genus *Mycobacterium* is distinguished by its complex and lipid-rich cell envelope, the organisation of which is unique to the genus and consists of a diverse array of unusual lipids and carbohydrates. This chapter will provide a broad overview on the composition, architecture and biological importance of the mycobacterial cell envelope, with particular attention to the mannose-containing glycolipids phosphatidylinositol mannoside (PIM) and lipoarabinomannan (LAM).

1.1 Mycobacteria and Human Disease

1.1.1 Mycobacterial Pathogens

While most mycobacteria are non-pathogenic saprophytes, several species are the causative agents of potentially fatal human diseases. Members of the *Mycobacterium tuberculosis* complex, which includes *M. tuberculosis*, *Mycobacterium bovis* and *Mycobacterium africanum*, are responsible for one of the most medically significant diseases in human history, tuberculosis. *M. tuberculosis* infects 1.7 billion people world-wide (almost one third of the world's population) and causes in excess of two million deaths per year (208), the most for any single infectious agent (28). The incidence of new infections is also alarming. Globally, approximately 8.4 million new infections were estimated in 1999 (207). Of all people infected, approximately 5% to 15% will go on to develop *tuberculosis* disease. Although the incidence of *tuberculosis* in the developed world had declined in previous decades, the number of new cases has shown a marked increase within the last 10 to 15 years. This is largely due to two factors: the emergence of multiply-drug resistant strains, and the advent of the world-wide AIDS pandemic. In 1990, approximately 10% of the world's AIDS sufferers had *tuberculosis*, while 50% of AIDS patients in Africa were infected (87). A more recent report estimates that *tuberculosis* accounts for approximately 15% of AIDS

deaths worldwide (208).

Mycobacterium leprae is the causative agent of another significant human disease, leprosy. *M. leprae* is an obligate intracellular pathogen. Leprosy affects approximately six million people worldwide, and is endemic in parts of Asia, Africa, Latin America and the Pacific. The disease is often associated with rural areas and poverty and the majority of individuals infected with *M. leprae* do not become diseased. This is thought to be due to a natural immunity that exists within the population (73).

As with *M. leprae*, *Mycobacterium ulcerans* appears to be a human specific pathogen and is probably found in water reservoirs (191). The disease is most prevalent in parts of Africa and Australia and manifests itself as an ulcerating tissue necrosis that is generally localised to the limbs and extremities. Unlike other mycobacteria, *M. ulcerans* appears to produce a polyketide-based toxin (74, 89). The transmission and epidemiology of the disease are not well understood (83).

Several species of mycobacteria act as opportunistic pathogens. The *Mycobacterium avium* complex, or MAC, includes the species *M. avium* and *Mycobacterium intracellulare* (81). MAC species are the most common cause of non-tuberculous mycobacterial infections. As with *M. tuberculosis*, MAC species are a common source of infection in HIV-infected individuals (93). The incidence of MAC infections in HIV patients peaked in the early to mid 1990s, but improved prophylaxis strategies and survival rates have led to a reduction in the number of infections (94, 151). Despite the decline, MAC infection of HIV infected individuals remains high in certain regions. A recent study of South African patients found that 10% were infected with MAC, while 54% carried *M. tuberculosis* (161).

Other species of mycobacteria act as opportunistic pathogens in individuals with a suppressed immune system. Most of these species are found in soil, water, and in animals and most infections appear to be acquired from the natural reservoirs by the inhalation of droplet nuclei or by direct inoculation through injury. No evidence of person-to-person spread has been reported (92).

Mycobacterium kansasii can cause a *tuberculosis*-like pulmonary disease and is able to infect other tissues as a result of direct inoculation. Pulmonary, nervous system and disseminated *M. kansasii* disease has also been observed in

AIDS patients. *Mycobacterium marinum* normally inhabits marine organisms, with human infections usually resulting from injuries associated with marine environments. *Mycobacterium paratuberculosis* has been associated with Crohn's disease, while *Mycobacterium scrofulaceum* is a rare cause of lymph node infection (81, 92).

All of the above mentioned species exhibit a slow growth rate which is characteristic of the genus. However, several species show a more rapid growth rate. Most of the rapid growing mycobacteria are non-pathogenic, but some species can cause human disease. *Mycobacterium fortuitum* and *Mycobacterium chelonae* are common soil and water inhabitants, which when inoculated during surgery or trauma can cause infections. *Mycobacterium smegmatis* is considered a non-pathogen, but in rare cases can cause soft tissue and bone infections (92).

1.1.2 The Success of Mycobacteria as Human Pathogens

Several intrinsic and acquired traits of the mycobacteria make them highly successful human pathogens. In most cases *tuberculosis* infections can be effectively treated with a combination of drugs, incorporating two or more of isoniazid, rifampicin, ethambutol, pyrazinamide, cycloserine and streptomycin.

However, the emergence of multi-drug resistant (MDR) strains of *M. tuberculosis* has become a cause for concern (208). MDR *M. tuberculosis* is resistant to at least isoniazid and rifampicin, which are the two main anti-mycobacterial drugs used to treat the infection. Recent surveys report that the global incidence of MDR strains is 3.2%, but this figure is much higher in certain regions (65). Countries of the former Soviet Union such as Estonia (14.1% MDR), Kyrgyzstan (11.2%), Latvia (9.0%), Ukraine (8.9%) and Russia (6.0%) have relatively high rates of MDR *M. tuberculosis*, while regions of China (Henan Province, 11%) and Russia (Ivanovo, 9%) also have high MDR rates (65). Provinces of India have also reported high numbers of MDR strains (65, 217). It is thought that a lack of compliance to the lengthy period required to treat *tuberculosis* together with inadequate supervision of the treatment program by healthcare workers has contributed to the rise in the prevalence of MDR strains (208). The emergence of MDR *M. tuberculosis* can contribute to the economic burden of public health in developing countries, as the cost of managing a case of

MDR *tuberculosis* in London is in excess of £60,000. This is many times more than the cost required to treat a drug-susceptible case of *tuberculosis*. The economic burden becomes more significant when dealing with large populations such as those of India and China, where a low percentage of MDR can still translate into hundreds of thousands of cases (217).

In addition to the emergence of MDR *M. tuberculosis* the intrinsic resistance of *M. avium* to many antibiotics, including isoniazid, compounds the problem of MAC infections in AIDS patients. Apart from an innate resistance to many antibiotics (101) and chemotherapeutic agents, mycobacteria are also resistant to various chemical disinfectants, drying, and alkali. It is believed that this robust nature of mycobacteria, as well as at least some of its associated pathogenic features, can be attributed to the highly complex and unusual structure of the mycobacterial cell envelope. The individual components of the cell envelope and their distribution within the structure influence mycobacterial cell morphology, permeability to solutes, response to drugs, host-cell interactions and intracellular survival. By influencing these factors, the envelope plays an important role in determining the success of a mycobacterial infection (102). Interestingly, several key drugs specifically target mycobacterial cell envelope biosynthetic processes. Isoniazid affects fatty acid metabolism and in particular mycolic acid biosynthesis (34), cycloserine targets peptidoglycan biosynthesis (56), while ethambutol has been shown to target cell envelope arabinan synthesis (129).

1.2 The Mycobacterial Cell Envelope

1.2.1 The Cell Envelope as a Virulence Factor

Pathogenic mycobacteria such as *M. tuberculosis* and *M. avium* are spread by the inhalation of aerosolised bacteria within droplet nuclei. Coughing, sneezing or talking by infected individuals with pulmonary disease can generate these. To establish infection, the bacteria reach the terminal air spaces of the lung where they multiply and are ingested by alveolar macrophages. In the case of some infections, the mycobacteria can exist in a dormant state and remain in host cells for long periods. The organism eventually destroys the macrophage and is re-phagocytosed by mononuclear phagocytes, which travel to other parts of the body via the blood

stream and lymphatic system (87).

Since mycobacteria are intracellular pathogens, the cell envelope plays an important role in the initial entry into the host phagocyte. This step is dependant on interactions between components of the host cell surface, and those of the mycobacterial surface (67). Hence, the mycobacterial cell envelope and its components will dictate the nature of host-cell entry, particularly those components which are surface exposed. The envelope components located in the deeper layers of the structure may also play a role in pathogenesis, perhaps once the mycobacterium has established itself inside the host cell where it needs to resist the hosts antimicrobial defence mechanisms.

M. tuberculosis is known to bind to a restricted set of macrophage receptors (67). These receptors bind to a variety of glycoconjugates, many of which constitute mycobacterial cell envelope components. These include the phosphatidylinositol mannosides (PIMs) and the structurally related lipoarabinomannans (LAMs).

1.2.2 The Cell Envelope: A Structural Model

The mycobacterial envelope is a multi-layered, complex structure consisting of phospholipids, glycolipids, polysaccharides and proteins. Many of these components have unusual structures that are unique to the mycobacteria. While many of the structures which make up the cell envelope are well characterised, the way in which the individual molecules are organised to form the envelope is less clear. Models which attempt to explain the ultrastructure of the mycobacterial envelope have been based on electron microscopy of thin sections of bacterial cells (35) and when coupled with the accumulated biochemical and structural data, allow a theoretical picture of how the main envelope components are arranged (156, 157).

Conventional electron microscopy staining has revealed a layered structure for the periphery of mycobacterial cells (Figure 1.1). The innermost layers resemble a classic plasma membrane bilayer structure, appearing as two electron dense layers separated by a lipid-rich, poorly staining electron transparent layer. The dense layers represent the polar headgroups of the membrane phospholipids, while the

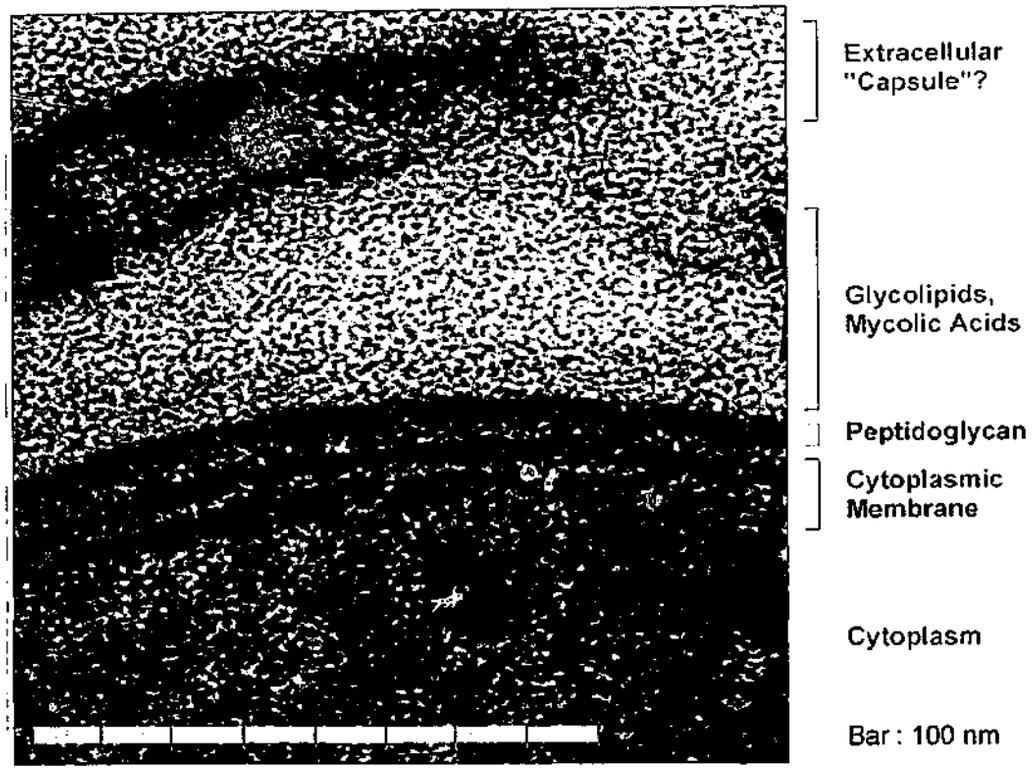

Figure 1.1
Electron micrograph of the *Mycobacterium kansasii* cell envelope.
The labels to the right of the micrograph indicate the possible nature of each layer of the envelope structure.
(Adapted from references 156, 157).

transparent layer is attributed to the acyl chains of the phospholipids. The outer leaflet of the membrane is usually slightly thicker than the inner leaflet. This is thought to be due to additional carbohydrate head-group components of glycosylated phospholipids being located preferentially in the outer leaflet of the membrane. These are likely to include the aforementioned PIMs, lipomannan (LM) or LAM (36).

The next electron dense layer beyond the plasma membrane is thought to be the peptidoglycan, due to its expected location and staining properties (156, 157). External to this layer is a thick, electron transparent zone which is likely to be rich in hydrophobic substances, given the poor staining properties of such molecules (51). Because the peptidoglycan is known to be covalently attached to the carbohydrate macromolecule arabinomannan (125), which is in turn esterified with mycolic acids (6), this electron transparent zone is thought to correspond to a vast, lipid-rich mycolic acid layer.

In 1982, Minnikin (131) proposed a model to define the structure of the mycolic acid layer. In the model, the mycolic acids of the cell envelope formed an array of hydrophobic chains, packed side-by-side perpendicular to the plane of the cell surface and plasma membrane. Furthermore, the model suggested that the mycolic acids formed an inner leaflet of an assymetric bilayer, where the outer leaflet consisted of various "extractable lipids" of the envelope. The outer layer lipids included the various glycolipids which are abundant in the cell envelope, with their structures varying from species to species. It was proposed that the acyl chains of these lipids are intercalated with the mycolic acid chains, forming an external hydrophobic barrier which was highly impermeable to polar solutes. Studies by Nikaido *et al.* (146) examining the arrangement of *M. chelonae* envelope mycolic acids support this model.

What lies beyond the proposed mycolic acid monolayer is less well understood. Expanding on the Minnikin model, Liu *et al.* (117) proposed a model for the *M. chelonae* cell envelope in which C_{14}-C_{18} triglycerides intercalated with the mero-mycolate branches. Daffé and Draper (51) discussed the possibility of triacylglycerols with longer acyl chains fulfilling this role. Variations on this concept have been suggested. Brennan and Nikaido (36) raise the possibility of glycolipids with medium-length acyl chains (i.e. those containing mycocerosic,

mycolipenic or mycolipanolic acids) intercalating with the mycolic acids. In addition, lipoconjugates with shorter acyl chains such as PIMs and phosphatidyl ethanolamines (PEs) would be arranged with the medium-length acyl compounds to form a monolayer. This in turn formed an asymmetric bilayer with the mycolic acids. The outer leaflet of this bilayer would show an increased fluidity when compared to the mycolic acid layer, and would vary between the mycobacteria depending on the lipid profile of that species. In support of this concept, Liu *et al.* (117) suggested that the amount of glycopeptidolipids (GPLs, a glycolipid) found in *M. chelonae* was sufficient to cover the surface of the bacterial cell.

McNeil and Brennan (126) also added cell wall-associated proteins to the model and proposed that the highly glycosylated phospholipid, LAM, spanned the entire envelope by being anchored to the plasma membrane and reaching through to the exterior. Porin proteins have also been identified and are thought to traverse the glycolipid/mycolic acid bilayer (36, 200, 201). The limited understanding of the proposed mycolic acid/glycolipid bilayer highlights a need to resolve the arrangement of this part of the cell wall.

Electron micrographs of cells grown in static culture also show that the most external layer of the cell is electron dense, and highly variable in thickness and density (35). This layer may correspond to the carbohydrate-protein rich "capsule" of mycobacteria, a structure suggested by Rastogi *et al.* (168). The finding that lipids were present in this material and that the amounts of lipids increased in the deeper parts of the capsule, as well as increasing in variety, led Daffé and Draper to propose a model for the outermost part of the envelope (51). The lipids associated with the capsule, particularly those within the deeper portion, formed the outer lipid monolayer of the glycolipid-mycolic acid bilayer. The lipids within this outer leaflet are thought to exist within the deeper part of the capsular polysaccharide-protein matrix, while other lipids are found throughout the whole capsular layer. Much of the theory behind the architecture of the mycobacterial cell envelope stems from an advanced knowledge of the composition and structure of its individual components. A diagram of the mycobacterial cell envelope which attempts to combine the main features of the various models discussed within this section is depicted in Figure 1.2.

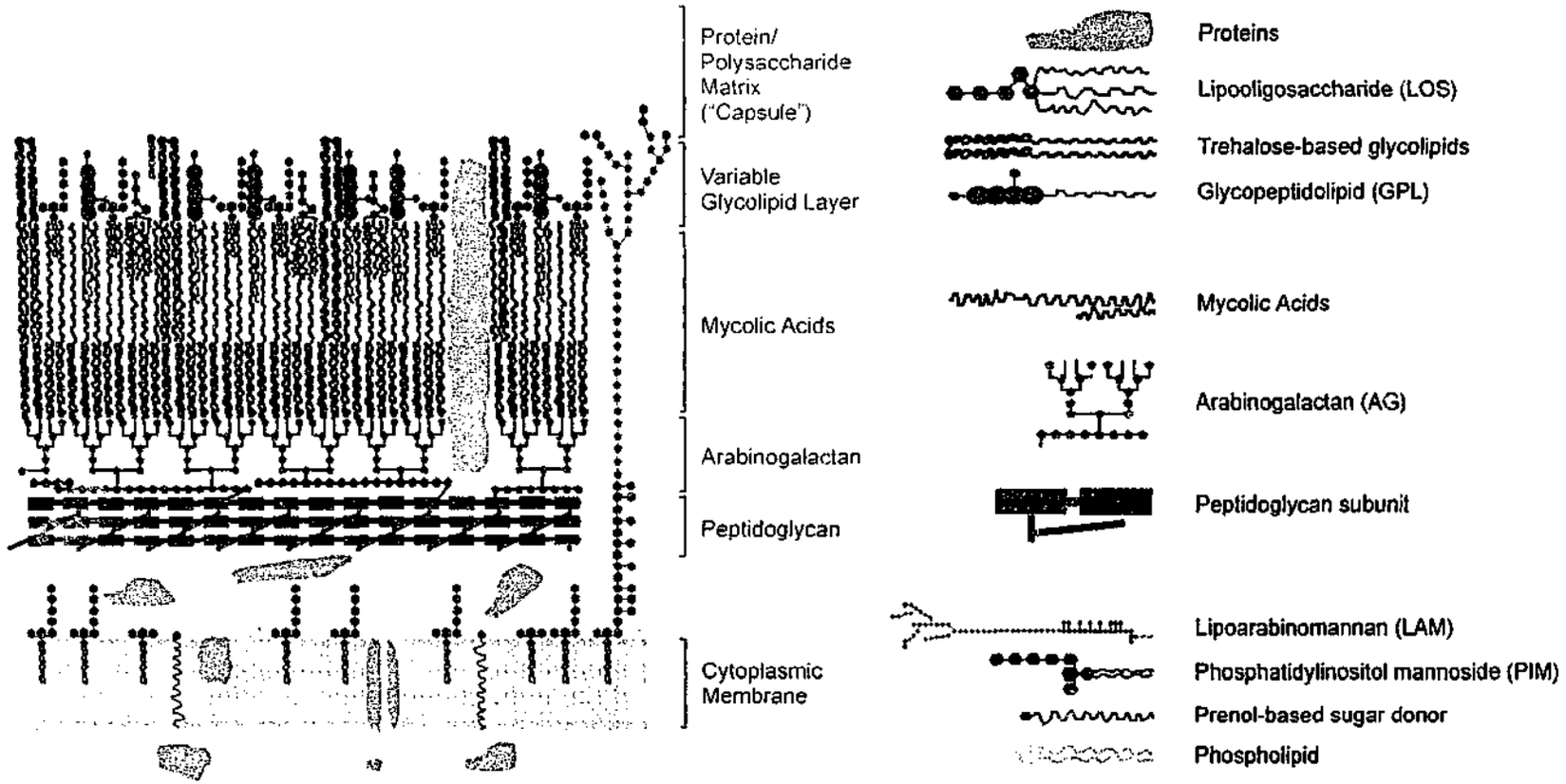

Figure 1.2
A generalised structure for the mycobacterial cell envelope.
This proposed organisation of the mycobacterial cell envelope is based on several models. Electron microscopy images, the demonstration of structural linkages within the mycolyl-arabinogalactan-peptidoglycan (mAGP) complex, and subcellular localisation studies are combined with hypothetical lipid arrangements to result in what appears to be a highly compiex, unique structure. (Adapted from references 131, 36 and 51).

1.2.3 Components of the Envelope

The Cytoplasmic Membrane

As with other biological membranes, the mycobacterial plasma membrane consists of a bilayer of phospholipids. The lipids of the mycobacterial plasma membrane are mostly phosphodiacylglycerols derived from phosphatidic acid. The acyl components of the phospholipids consist of a heterologous mixture of saturated, unsaturated and methyl-branched fatty acid residues. These most commonly include palmitic (C_{16}), stearic (C_{18}) and 10-methyl octadecanoic (tuberculostearic, C_{19}) acids (51).

The predominant types of phospholipids found in the membrane are phosphatidylinositol (PI) and the PIMs, which are restricted to the actinomycetes (36, 82). Phosphatidylglycerol (PG), cardiolipin (CL), phosphatidylethanolamine (PE) are also found (36). Interestingly, PEs and PIMs are also present in appreciable amounts within the outermost layers of the mycobacterial cell envelope (150). LMs and LAMs are hyper-glycosylated PIMs which are thought to be integrated in the mycobacterial plasma membrane (95) due to the presence of a structural component resembling PIM which may act to anchor the lipoglycans within the plasma membrane (41). Both PIMs and LAM have been found in all of the mycobacterial species tested (51).

Proteins are also incorporated into the plasma membrane. They are largely involved in the respiratory and electron transport pathways of the bacterium, including cytochromes, succinate dehydrogenase and NADH oxidase (51). Various transporters, biosynthetic enzymes and carriers also make up the protein composition. Many other proteins are thought to be present within the membrane, where a mixture of species-specific and conserved polypeptides would reside. Porin-like proteins have been isolated from *M. chelonae* and *M. smegmatis*, and are thought to have a functionally similar role to the porins of Gram-negative bacteria. These proteins act to transport hydrophilic solutes through the hydrophobic layers of the cell envelope. While they are unlikely to be membrane bound, porins are thought to form channels through the vast cell wall skeleton (see below) to facilitate nutrient transport (200, 201).

The plasma membranes of mycobacteria and related families also contain glycosyl-isophosphoprenols ("polyprenols") which are involved in the biosynthesis

of cell wall polysaccharides such as peptidoglycan. Polyprenols act as carriers of biosynthetic intermediates (21). Mycobacteria contain decaprenols (C_{50}) and heptaprenols (C_{35}), while other bacteria possess undecaprenols (C_{55}) (36). Examples of mycobacterial polyprenols include β-D-arabinofuranosyl phosphodecaprenol, which has been implicated in arabinogalactan and LAM biosynthesis (206) and 6-*O*-mycoloyl-β-mannopyranosyl-phosphooctohydro-heptaprenol (24), which is involved in mycolic acid biosynthesis.

The Cell Wall Skeleton

The mycobacterial cell wall skeleton consists of peptidoglycan, arabinogalactan and mycolic acids. These components are covalently linked together to form a complex macromolecule, often referred to as the mycolylarabinogalactan-peptidoglycan (mAGP) complex. This structure defines the basic shape of the mycobacterial cell (51). A schematic model of the mAGP complex, encompassing peptidoglycan, arabinogalactan and mycolic acids, is shown in Figure 1.3.

Peptidoglycan is a complex polymer consisting of glycan chains formed from alternating sugar units of *N*-acetyl-D-glucosamine and muramic acids. These sugar units are attached via a β(1→4) linkage. Tetrapeptide chains are linked to the muramic acid residues, acting to cross-link the glycan chains together to form a single laminated molecule. Mycobacterial peptidoglycan has two distinct structural features. Firstly, the muramic acid residues of the glycan polymers are *N*-glycosylated in mycobacteria and related genera (81), whereas *N*-acetylated muramic acid residues are found in the common bacterial peptidoglycan. The tetrapeptide linker in all mycobacterial peptidoglycans consists of L-alanyl-D-isoglutaminyl-*meso*-diaminopimelyl-D-alanine, except for that found in *M. leprae*, where the L-alanine residue is replaced by a glycine (62). The second main difference seen in mycobacterial peptidoglycan is within the peptide linker, where unique bonds between two residues of diaminopimelic acid occur in addition to the usual links between diaminopimelic acid and D-alanine.

The cell wall peptidoglycan is covalently linked to another polysaccharide, arabinogalactan (AG) (124). The linkage is mediated by a molecule consisting of agalactofuranosyl unit of the AG attached to position 4 of an L-rhamnopyranosyl residue. The rhamnose substitutes position 3 of an *N*-acetyl-D-glucosamine unit,

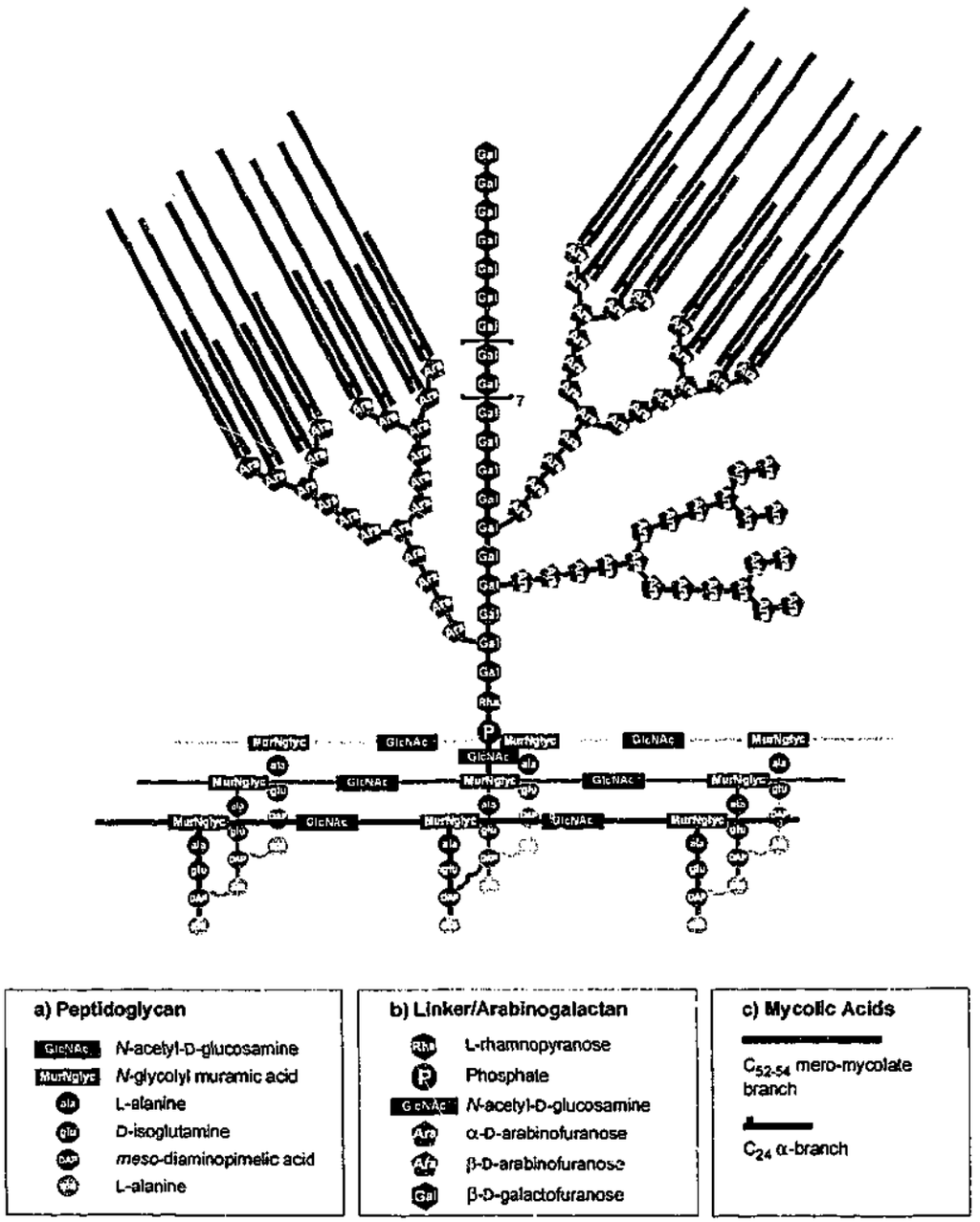

Figure 1.3
Schematic representation of the mycolylarabinogalactan-peptidoglycan complex.
a) Peptidoglycan. The structure is conserved amongst the mycobacteria, except in *M. leprae*, where the L-alanine residue is replaced by glycine.
b) Arabinogalactan. A truncated galacan backbone is shown; an additional 12 galactose residues are present. The degree of mycolic acid substitution varies between species.
c) Mycolic acids. The α-branch is conserved between species; the mero-mycolate branch can include *cis*- and *trans*-double bonds, methyl branches, cyclopropane rings and oxygen groups. Mycolic acid types are defined by these additions, which vary between species.

which in turn is connected to position 6 of a muramic acid residue in the peptidoglycan via a phosphodiester linkage (125). Approximately 10-12% of the peptidoglycan muramic acid residues are linked to AG (36).

AG is composed of a linear galactan backbone with arabinan chains branching off the galactan chain. Structurally, the galactan core of AG is composed of linear, alternating 5- and 6-linked β-D-galactofuranose units (36), typically being 32 residues long (51). Three arabinan chains are attached to the 5-position of 6-linked galactofuranose units near the proximal portion of the galactan core. The arabinan chains consist of 5-linked α-D-arabinofuranose units (approximately 27 units per chain), with branching structures occurring at the terminal residues by 3-, 5-linked α-D- and β-D-arabinofuranose units. This branching structure of the arabinan is referred to as the hexaarabinofuranosyl unit (50). The structure of AG does not appear to vary amongst the mycobacteria (51).

Mycolic acids are attached to the hexaarabinofuranosyl units via ester linkages (6). Mycolic acids are bound in clusters of four to the 5-positions of arabinofurans within the unit (34). In *M. tuberculosis* AG, two of the three arabinan branches are usually substituted with mycolic acids with the third branch remaining unmycolated. *M. bovis* BCG, *M. leprae*, and *M. smegmatis* AG tends to be less mycolated than *M. tuberculosis* AG (125).

Mycolic acids are high molecular weight, long chain α-alkyl, β-hydroxy fatty acids that are found in all mycobacteria and related genera (51). Mycobacteria possess the longest-chain mycolic acids. Most of the mycolic acids found in mycobacteria are esterified to AG, but are also present in some cell envelope glycolipids. Mycolic acids consist of two main lipid components. The shorter lipid component, the α-branch, consists of a C_{24} saturated fatty acid. Except for minor variations in chain length, the α-branch is conserved amongst the different types of mycolic acids found (21). The larger fatty acid component, the mero-mycolate branch, contains a very long carbon chain of almost C_{60}. The mero-mycolate is structurally endowed with *cis* and *trans* double bonds, cyclopropane structures, methyl branches and oxygen groups in addition to a characteristic β-hydroxy group. The types of functional groups present in the mero-mycolate chain vary, and it is on this basis that several classes of mycolic acids have been defined.

The different classes of mycolates include α-, α'-, epoxy-, keto-, methoxy-

and wax ester-mycolic acids. The α- and α'-mycolic acids are devoid of additional oxygen groups, while the other classes contain characteristic substitutions. Furthermore, each class of mycolic acid includes structural variants in chain length, methyl branching, and in the degree of saturation (36), leading to considerable structural diversity between species. Mycobacteria generally contain a mixture of the different classes of mycolic acids (51), and most species elaborate different types of mycolates. This characteristic has been useful as a tool in mycobacterial taxonomy (190). The mycolic acid content of selected fast and slow growing species is listed in Table 1.1a. Slow growers such as *M. tuberculosis* and *M. leprae* elaborate the more cyclopropanated mycolic acids (keto- and methoxy-mycolates), while MAC organisms possess the wax-ester mycolic acids. The rapid grower *M. aurum* also produces keto- and methoxy-mycolic acids (51, 54, 118), while *M. smegmatis* produces epoxy-mycolic acids (64). The α-mycolic acids have been found in all mycobacterial species examined (36).

Extractable Lipid Components of the Cell Envelope

The mycobacterial cell envelope contains a large collection of waxes, lipids and glycolipids that are not covalently bound to the mAGP complex. Many of the molecules exhibit antigenic properties and immunomodulatory functions, and have been structurally characterised. As described in the various cell envelope models, it is thought that the lipids predominantly reside outside of the mAGP complex. The precise locations of many of the lipids and their architectural roles in the cell envelope have not been defined. The types of glycolipids found in the cell envelope differ between the species, suggesting that the glycolipid layer shows variation amongst the genus. Table 1.1 lists the predominant extractable lipids found in selected mycobacteria.

As well as being found in the plasma membrane, PIMs have been located in the outer layers of the envelope (150). It is thought that LAM may also be present in this layer (36). Glycopeptidolipids (GPLs) are major glycolipids found in a range of mycobacteria, including *M. smegmatis*, *M. chelonae*, *M. fortuitum*, MAC, *M. abscessus*, *M. peregrinum*, *M. senegalense*, *M. porcinum* and *M. simiae* and are unique to the genus (36, 51). GPLs are not found in mycobacteria which contain another cell envelope component, the phenolic glycolipids (PGLs). *M. smegmatis*

Species	a) Mycolic Acid Composition	b) Main Glycolipid Species
Slow Growers		
M. tuberculosis	α-, methoxy-, keto-	PIM, SL, PDM, DAT,
M. avium complex	α-, keto-, wax ester-	PIM, GPL
M. leprae	α-, keto-	PIM, PGL, PDM
Rapid Growers		
M. fortuitum	α-, α'-, epoxy-	PIM, GPL, LOS
M. chelonae	α-, α'-	PIM, GPL
M. smegmatis	α-, α'-, epoxy-	PIM, GPL, LOS

Table 1.1
Variation in the mycobacterial cell envelope of selected species.
While the structures of the peptidoglycan and arabinogalactan are highly conserved, mycobacterial species show variation in the types of mycolic acids present and the composition of the peripheral glycolipid layer. Shown here are some of the more commonly encountered species.
a) The mycolic acid structures have been useful in mycobacterial taxonomy, where divisions were found to correspond to the broad taxonomic groupings of "slow growers" and "rapid growers".
b) Details on the glycolipid composition of mycobacterial species are incomplete. Presented are the more abundant glycolipids: phosphatidylinositol mannosides (PIMs), glycopeptidolipids (GPLs), lipooligosaccharides (LOSs), phenolic glycolipids (PGLs), phthiocerol dimycocerosates (PDMs), diacyltrehaloses (DATs) and sulpholipids (SLs). Other glycolipids which are commonly found amongst the genus include triacylglycerols (TAGs) (149), and monomycoloyl- and dimycoloyl trahaloses (MMTs and DMTs, with *M. leprae* only showing MMTs) (61).

This table was adapted from Brennan and Nikaido (36).

produces a simple form of the glycolipid, referred to as non-specific GPL ("nsGPL"). In *M. avium*, GPLs are more elaborately glycosylated to form serotype-specific GPLs ("ssGPL"), the structures of which vary between serotypes. The ssGPLs are frequently used as serological typing antigens, based on specific sero-reactivity to the variable oligosaccharide moieties (4, 43). Following phagocytosis, species of the *Mycobacterium avium* complex are usually surrounded by a coating of GPL-rich material and have various immunomodulatory functions (43, 91, 197).

The cell envelope contains a variety of trehalose-containing glycolipids, where the types and structures of these components vary between the species. Lipooligosaccharides (LOSs) are glycolipids found within the cell envelopes of *M. smegmatis*, *M. kansasii*, *M. malmoense*, *M. szulgai*, *M. gordonae* and *M. fortuitum*. The *M. tuberculosis* Canetti strain also contains LOS. Like GPLs, the structures of LOSs are variable, where the composition of the oligosaccharide side-chain is strain-specific (4). Diacyl trehaloses (DATs) are polar glycolipids isolated from *M. tuberculosis*. DATs have been found in virulent strains of *M. tuberculosis* (19), such as $H_{37}R_v$ (150). Dimycoloyl trehalose (DMT, or "cord factor") is an ubiquitous trehalose-based lipid found in the cell envelopes of all mycobacterial species tested so far, with the exception of *M. leprae* (36, 61). Structurally, the trehalose core of DMTs are elaborated with mycolic acids (21), where different combinations of mycolic acid residues are found in different species. Polyphthienoyl trehaloses (PPTs) are a non-polar class of acylated glycolipid found in virulent strains of *M. tuberculosis*, such as $H_{37}R_v$, but being absent from the avirulent $H_{37}R_a$ and Canetti strains. PPTs are highly acylated trehaloses, with the acyl substituents being found on several positions of the core trehalose moiety (52). Sulpholipids (SLs) are another type of trehalose-containing lipid found in *M. tuberculosis* (21).

Dimycocerosates (DIMs) are wax-like compounds found within the cell envelopes of the *M. tuberculosis* complex, as well as *M. marinum*, *M. kansasii*, *M. gastri* and *M. ulcerans*. DIMs are structurally based on the straight-chain fatty acids phthiocerol (DIM class I) or phthiodiolene (DIM class II) (150) and also contain mycocerosic acids (C_{27}-C_{34}). Structural differences exist between the species, based the on types of DIMs present and the length of the fatty acid portions (53).

Phenolic glycolipids, or PGLs, are cell-surface located molecules (150)

found in *M. kansasii*, *M. marinum*, *M. ulcerans*, *M. bovis*, *M. leprae*, and the *M. tuberculosis* Canetti strain (4, 36, 51). Structurally, PGLs consist of a conserved lipid core component which is attached to an oligosaccharide component. The oligosaccharide component is variable between different species and strains (4). The lipid components consist of mycocerosic acids and C_{36} β-diol fatty acids. DIMs have been found in all species which possess PGLs (4, 51). In tissue sections of *M. leprae* infected cells the organism is usually surrounded by a dense layer peripheral to the cell wall, primarily consisting of the cell envelope glycolipid PGL-1. This specific glycolipid has been shown to mediate the phagocytosis of *M. leprae* (177).

Triacylglycerols (TAGs) are ubiquitous compounds found in mycobacteria and are surface exposed in at least *M. avium*, *M. smegmatis* and *M. aurum* (150). Little is known about the function of TAGs. Liu *et al.* (117) have proposed that TAGs play a structural role in the cell wall of *M. chelonae*.

Evidence for a Mycobacterial "Capsule"

Several studies have reported that an electron-transparent zone is observed surrounding some virulent mycobacteria under electron microscopy, when grown intracellularly (reviewed in (51)). This led to the idea that pathogenic mycobacteria may produce an extracellular "capsule". Rastogi *et al.* (168) found that various slow-growers, rapid-growers, pathogens and non-pathogens all demonstrated a polysaccharide-containing outer layer which varied in thickness and continuity among the species tested. Further studies have shown that this outermost layer mainly consists of polysaccharides and proteins, with small amounts of lipids (114, 115, 150).

The main carbohydrate found in the mycobacterial capsule is a D-glucan, comprising approximately 70% of the capsular carbohydrates (115). D-arabino-D-mannan (AM) and D-mannan are found in the capsule in lesser amounts, totalling approximately 30% of the capsular carbohydrates (149). Capsular material has also been shown to contain several proteins. It is possible that these proteins are secreted to the extracellular environment, and are present in the capsule *en route* through the external layers of the envelope (51). The protein composition is likely to vary according to the species, where a mixture of conserved and species-specific proteins are expected to be found.

A minor component of capsular material (1-6%) consists of glycolipids.

These are assumed to reside within a polysaccharide-protein matrix to make up the composition of the capsule. Furthermore, the majority of the capsular glycolipids tend to be located within the deeper portions of the capsule, as demonstrated by sequential glass bead and detergent extractions from *M. tuberculosis* (149). In *M. tuberculosis* Canetti, the glycolipids located on the surface of the capsule were found to be PGLs, PIMs, PEs, LOSs, DIMs and DATs. The glycolipids found within the deeper layers of the capsule were PPTs, DMTs and TAGs. PIMs and PEs were also found to be surface-exposed in several other species, while in *M. avium* and *M. smegmatis* GPLs were surface exposed. TAGs were found to be surface exposed in *M. smegmatis*, *M. avium* and *M. aurum*, while *M. aurum* also appeared to have DMTs exposed. LAMs do not appear to be located in the mycobacterial capsular material (150). This diversity in capsular lipid composition reflects the diversity in the range of glycolipids found between species, and further compicates the proposed structure of the outermost layer of the envelope.

1.3 Mannosylated Phospholipids in Mycobacteria

The mycobacterial cell envelope contains several biologically important mannosylated phospholipids, the PIMs, LMs and LAMs. These lipids exist as a variety of structures and are abundant within the envelope. They have been identified in every mycobacterial species from which they have been sought, and relatively minor structural differences are seen between the species (36).

1.3.1 Structural Definition

Phosphatidylinositol Mannosides (PIMs)

PIMs exist as a class of structurally related glycolipids whose basic structures were determined in the 1960s (113) (Figure 1.4). PIMs contain a diacyl-glycerol moiety, where the C1-position of the glycerol is typically esterified with 10-methyl-octadecanoic acid (C_{19}, or tuberculostearic acid), while the 2-position usually contains a hexadecanoic acid (C_{16}, palmitic acid) residue. Variations on the acylation state of the glycerol exist. The palmitic and tuberculostearic acid residues sometimes occupy different positions, while rare examples of C_{14} acylation have been found. Mono-acylated ("*lyso*") forms of the glycerol have also been characterised and have either a single palmitic or tuberculostearic acid chain (104).

a) Phosphatidylinositol dimannoside (PIM_2)

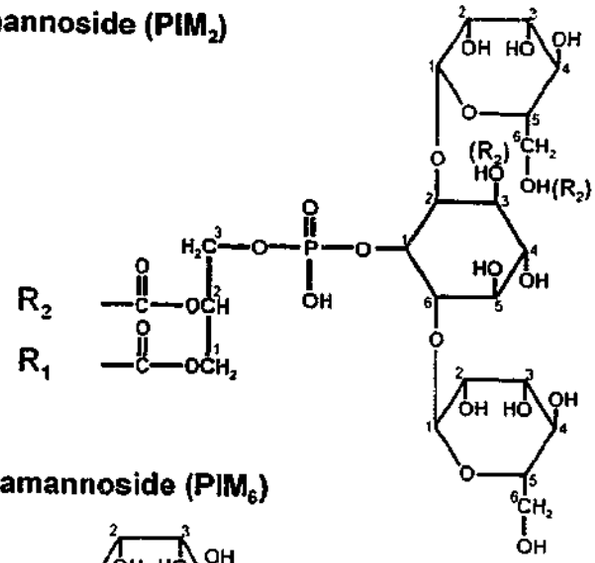

b) Phosphatidylinositol hexamannoside (PIM_6)

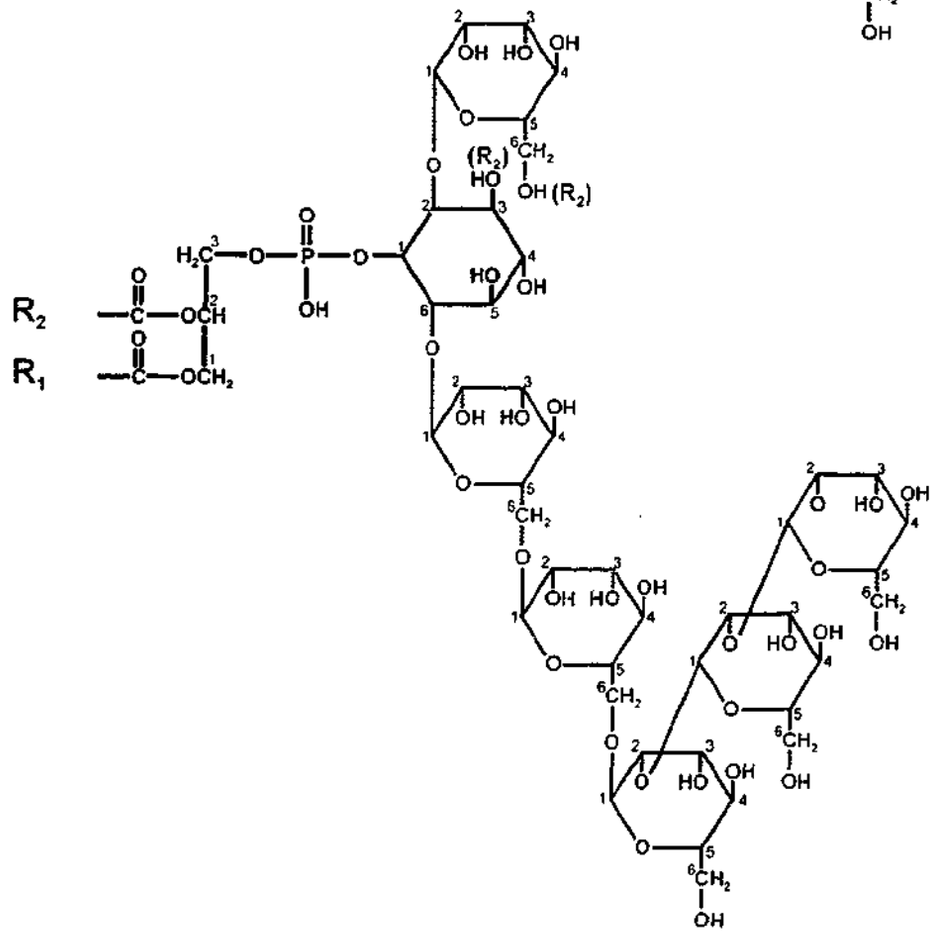

Figure 1.4
Structure for mycobacterial phosphatidylinositol mannosides (PIMs).
a) Phosphatidylinositol dimannoside (PIM_2);
b) Phosphatidylinositol hexamannoside (PIM_6).
In each case, the glycerol moiety may have one, two or no acyl chains. R_1 is usually a tuberculostearic acyl group (C_{19}) while R_2 is usually palmitic acid (C_{16}). Further acylation with palmitic acid can be found on the inositol and mannose residues, indicated by (R_2).

The 3-position of the glycerol is substituted with a phosphate. The phosphate is in turn attached to the 1-position of a D-*myo*-inositol (113). Linked to the 2- and 6-positions of the *myo*-inositol unit are α-D-mannopyranose units, which are attached via their 1-position. These mannose residues vary in number according to a specific PIM, and it is on this basis that PIM nomenclature is based. The most simply mannosylated PIM is PIM_2, which contains two mannose units (Figure 1.4a). The more elaborate PIMs contain additional mannose substitutions. PIM_3, PIM_4, PIM_5 (113) and PIM_6 (41) contain a total of three, four, five and six mannose residues, respectively (Figure 1.4b). The linkages between the mannose units exist as $\alpha(1\rightarrow6)$ for PIM_2 to PIM_4, or as both $\alpha(1\rightarrow6)$ and $\alpha(1\rightarrow2)$ for PIM_5 and PIM_6 (182).

PIMs have varying degrees of acylation of the sugar units (33, 152), resulting in heterogeneity amongst PIMs with the same number of mannose units. A palmitic acid residue is commonly found on the 6-position of the mannose attached to the 2-position of the inositol (104), while fatty acid substitution on the 3-position of the *myo*-inositol has also been reported (78). The possibility of acylation on the 6-position of the mannose linked to the 6-position of the *myo*-inositol has also been proposed (104). PIMs therefore vary in their degree of acylation as well as their mannosylation state, where a total of one to four acyl chains and one to six mannose residues are found. Recent studies adopt the general Ac_XPIM_Y nomenclature, where X refers to the total number of acyl groups while Y represents the total number of mannose residues (108).

The acylation states of PIM_2 and PIM_6 from the *M. tuberculosis* Erdman strain have been the most extensively characterised (104). The PIMs were found to exist as Ac_2-, Ac_3-, and Ac_4- forms, their relative abundances varying between preparations. Ac_2PIM_2 was mostly found in the *lyso*-form, where the glycerol moiety contained a single palmitic or tuberculostearic acid substitution while either one of the mannose residues or the inositol residue can also be acylated. The Ac_3-form of PIM_2 was more common. The PIM_2 had two acyls on the glycerol moiety (palmitic and/or tuberculostearic) with an additional palmitic acid residue attached to the 6-position of the mannose on the 2-position of the inositol. Ac_4PIM_2 was defined as being acylated as with the Ac_3- form with the addition of a further palmitic acid substitution, possibly on the 3-position of the inositol or the 6-

position of the mannose attached to the 6-position of the inositol. Ac_2-, Ac_3-, and Ac_4- forms of PIM_6 were also identified. The acylation states of PIMs from *M. bovis* have also been investigated (79). The significance of this variety in acylation states is not clear. It has been proposed that the variations in acyl groups have a role in regulating the biosynthesis of PIMs and their related molecules (104, 136).

Early studies on *M. tuberculosis* and *M. phlei* showed that PIM_2 and PIM_5 were the main accumulating forms of PIM in the cell envelope (33, 113, 152). However, more recent studies indicate that acylation variants of PIM_2 and PIM_6 are the only PIM species to accumulate in the cell envelope structure in *M. tuberculosis*, *M. bovis* and *M. smegmatis* (41, 104, 182). One report found that PIMs made up 40% of the phospholipids extracted from *M. smegmatis*, with PIM_2 accounting for 73% of the total PIMs and PIM_5 making up 23% (186), although given more recent structural studies the PIM_5 is likely to represent PIM_6.

Lipomannan (LM) and Lipoarabinomannan (LAM)

Structurally, both LM and LAM are hyper-glycosylated extensions of PIMs (41). LM is a multi-mannosylated extension of PIM_2, PIM_3 or PIM_4, while further arabinosylation of LM results in LAM. The PIM-like component of LAM is commonly referred to as the anchor portion because it may embed the base of the molecule in the lipid bilayer of the plasma membrane. The anchor is structurally identical to the phosphatidylinositol moiety of PIMs (95), with α-D-mannopyranose residues attached to the 2- and 6-positions of the inositol (Figure 1.5a).

Structural variation has been demonstrated in anchor structures from different species and strains. These variations occur with the acylation state of the anchor. Palmitic and tuberculostearic acid are found attached to the glycerol moiety of the PIM-like anchor (95), while traces of other fatty acids have also been found (116, 144). Most commonly, the anchor is acylated with palmitic and/or tuberculostearic acid at the 1- and 2-positions of the glycerol, with palmitic acid acylating the 6-position of the mannose residue connected to the 2-position of *myo*-inositol. This finding led to the hypothesis that Ac_3PIM_2 may act as the specific precursor for LM/LAM biosynthesis (23, 104). However, it remains possible that Ac_3PIM_3 or Ac_3PIM_4 fulfil this role.

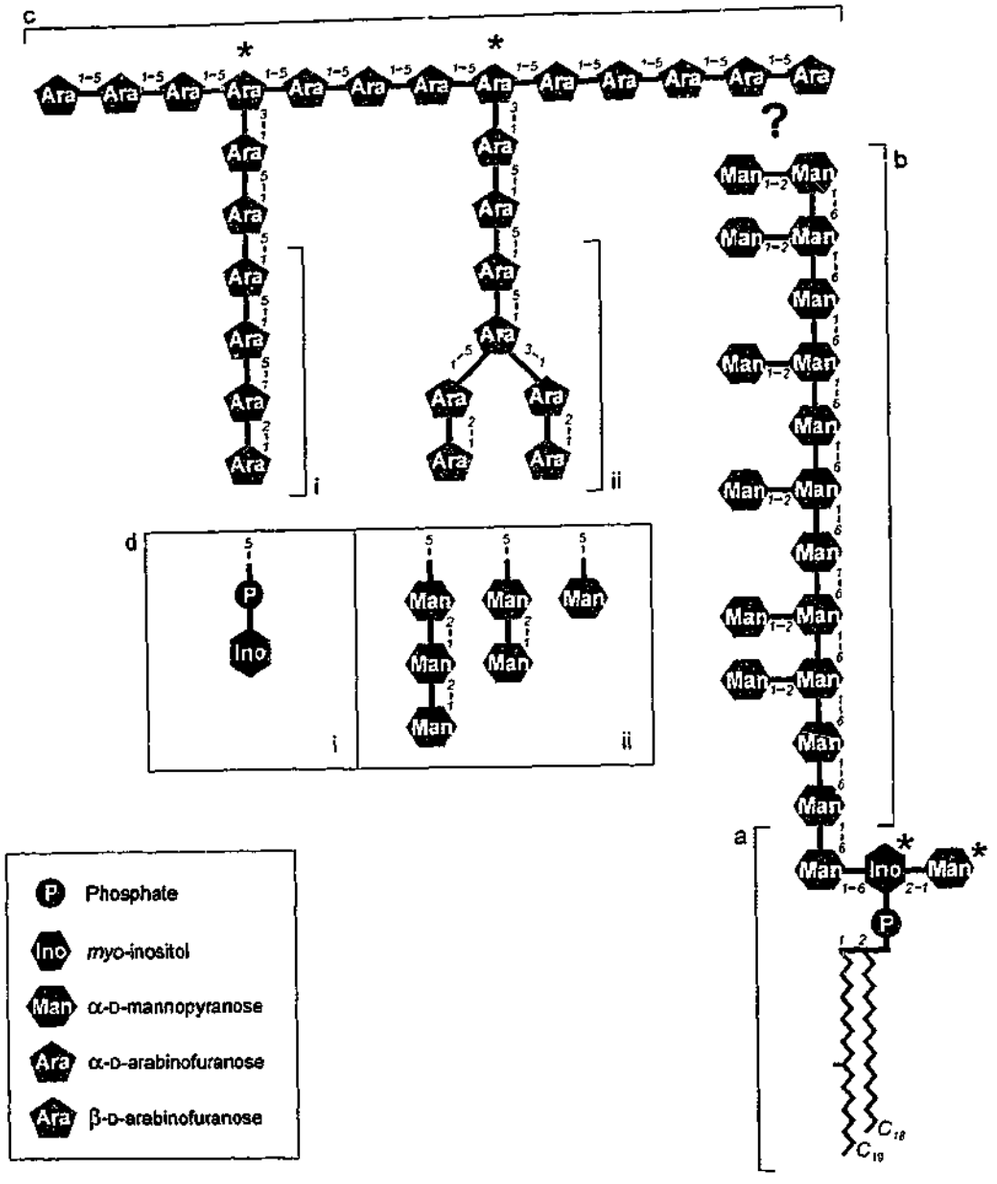

Figure 1.5
Proposed structure for mycobacterial lipoarabinomannan (LAM).
a) Phosphatidylinositol anchor. The glycerol moiety may have one, two or no acyl chains, while the mannose and inositol residues marked with * may or may not be acylated. Variation in the acylation of the anchor structure is not only present between species, but within the LAM population of any given strain.
b) Mannan core. The length of mannan chain and degree of branching varies.
c) Arabinan branch. The site of attachment to the mannan core is unknown. The arabinan branch contains (i) tetra-arabinosyl as well as (ii) hexa-arabinosyl side chains. The length of chain and number and type of branching is thought to vary. Succinic or lactic acid may also be attached at positions marked with *.
d) Arabinan capping structures. (i) Inositol phosphate caps, commonly found in rapid-growing species such as *M. smegmatis*. (ii) Oligomannoside caps, typical of slow-growing species such as *M. tuberculosis*.

Recent improvements in the techniques used to extract LAM have resulted in the selective extraction of two separate pools of the molecule, the "parietal" and the "cellular" LAM (76, 144). The parietal LAMs were easily extractable from intact cells with aqueous ethanol and are thought to reside in the more peripheral layers of the cell envelope. By comparison, the cellular LAMs were extracted from cells that had been mechanically disrupted and may be more strongly associated with the cell. Cellular LAMs may be located within the more internal layers of the envelope, perhaps attached to the cytoplasmic membrane.

There are some differences between the structures of parietal and cellular LAMs. The parietal LAM anchor of *M. smegmatis* is non-acylated, and was named phosphoinositol-glyceroarabinomannan (PI-GAM) (77), while the cellular LAM anchor was acylated with palmitic and tuberculostearic acids (42). *M. bovis* BCG parietal LAM had a single novel fatty acid residue on the 1-position of the glycerol (144). The cellular LAMs had di-, tri- and tetra-acylation with palmitic and tuberculostearic acid, containing a mixture of *lyso*- and di-acylated glycerols, acylated mannoses and acylated *myo*-inositol (145). *M. tuberculosis* $H_{37}R_v$ parietal LAMs were acylated at one position of the glycerol and singly acylated on either a mannose or *myo*-inositol, while the cellular LAM existed in a variety of acylation states (76). These findings suggest that the acylation state of cellular LAM anchors is more diverse and elaborate than those seen in the parietal LAMs, which may explain the differences in extractability and possible difference in cell envelope location (76).

As with PIMs, a mannan core extends from the 6-position of the *myo*-inositol (41, 95, 202). The core consists of a linear (1→6) α-D-mannopyranose chain which varies in the chain length (44) (Figure 1.5b). Some of the mannose residues within the chain are substituted at the 2-position by single α-D-mannopyranose units to form several short branches along the core (41). An exception to this structure has recently been reported for *M. chelonae* LAM, where mannose residues are substituted at the 3-position with α-D-mannopyranose units (84).

The degree of branching within the mannan core also varies. *M. bovis* BCG was shown to contain 18 mannose units within the core, with 67% of the residues

being branch points (202). The *M. smegmatis* mannan core contained 26 mannose units, with a branching degree of 50% (103). However, the exact composition of the mannan core varies between preparations (42).

The structure of LM is identical to the anchor and mannan core of LAM (95). The mannan core of LAM is further extended with (1→5)-linked α-D-arabinofuranose chains (Figure 1.5c) (40). The precise mode of attachment of the arabinan branches to the mannan core has not been defined. Branching exists within the arabinan chain where some of the arabinose residues are substituted at the 3-position with an α-D-arabinofuranose side-chain. In *M. tuberculosis*, two types of side chains have been characterised. One contains a linear tetra-arabinosylfuranoside chain, while the other type consists of a branched hexa-arabinosylfuranoside structure (Figure 1.5c) (40). Both types of branches are terminated with β-D-arabinofuranose. The number of side chains and the degree of branching are likely to vary between species and individual cultures (42). Variation in the arabinan component of LAM has not been extensively examined. One study reports that both types of arabinan branches were found in *M. smegmatis* in approximately equal amounts (103).

The arabinan chain can also be substituted by succinic acid. One to four residues of succinate were found esterified to the 2-position of 3,5-linked arabinose residues in *M. bovis* BCG LAM (Figure 1.5c), their presence varying between cultures (59). Evidence of succinate as well as lactate substitution has also been reported for *M. smegmatis* (204) and *M. tuberculosis* (148).

The structure of LAM is completed by the addition of oligo-mannose or inositol-phosphate caps on the termini of the arabinosyl side branches (Figure 1.5d). This gave rise to a nomenclature which differentiates LAM based on the type of capping found on the molecule. LAM capped with oligomannosides are often referred to as "ManLAM", while LAM exhibiting the inositol-phosphate caps are referred to as "AraLAM", due to the absence of mannose caps (164). LAM from the rapid growing species *M. chelonae* is unusual in that it lacks both mannosyl and inositol-phosphate caps, and therefore could not be classified as either ManLAM or AraLAM. The authors referred to the novel structure as "CheLAM" (84). Further variations on the cap structures are also apparent. Another recent report described

the presence of a novel methylthiopentose substituent of the mannose cap structures in *M. tuberculosis* LAM (199).

The degree of mannose-capping varies according to the species and strain. Mannose capping of LAM was initially thought to be a feature of pathogenic strains, but structural analyses of ManLAM from various strains of the *M. tuberculosis* complex do not support this view. LAM from the virulent *M. tuberculosis* Erdman strain is capped with one, two or three mannose residues, the majority of caps containing two mannoses (45). Only the di- and tri-mannoside caps were present on the tetra-arabinosyl branches, while each type of mannoside cap was present on the hexa-arabinosyl branches (44). Nigou *et al.* (144) showed that in *M. bovis* BCG, the oligomannoside caps were present on both types of arabinan branches. The virulent *M. tuberculosis* $H_{37}R_v$ shows a slightly higher amount of capping than the avirulent *M. tuberculosis* $H_{37}R_a$, while LAM from the highly virulent *M. tuberculosis* Erdman strain is more extensively capped than the LAM of either of the above strains (45, 103). LAM from the non-virulent, attenuated *M. bovis* BCG is capped to a similar extent to that of *M. tuberculosis* Erdman (164), with a significantly higher degree of capping seen in the parietal LAM extracts than that in the cellular LAMs (144). In contrast, *M. leprae* exhibits a low degree of mannose capping (103). Hence, rather than being associated with pathogenicity, mannose capping appears to be characteristic of slow growing mycobacteria.

Inositol-phosphate capping of the so-called AraLAM is more typically seen in the fast-growing mycobacteria. The caps of AraLAM consist of an inositol phosphate moiety which is attached to the 5-position of the terminal arabinose within tetra-arabinosyl branches (Figure 1.5d) (77). Khoo *et al.* (103) found that 20% of the arabinan branches in an unidentified fast-growing mycobacterium were inositol capped, while Gilleron *et al.* (77) found that approximately 40-50% of arabinan side-chains in *M. smegmatis* PI-GAM were capped with the inositol phosphate.

While the basic structure of LAM is understood, the finer details of its structure and composition are still being determined. Evidently, LAM shows subtle structural variation and many of the apparent species-specific differences have not been studied in detail. Furthermore, the structure of LAM within any one cell is

thought to be heterogeneous, complicating the detailed study of LAM composition and structure.

1.3.2 Cell Envelope Location

PIMs are a major component of the cell envelope, and are easily extractable from mycobacterial cells. Some PIMs are loosely associated with the cell and can be removed using mechanical abrasion. This led to the notion that PIMs are surface exposed. In studies aimed at elucidating the proposed capsule structure, PIMs were recovered from material removed from mycobactera by agitating the cultures with glass beads (150). Hoppe *et al.* were also able to demonstrate that PIMs were surface exposed (90). It was shown that *M. tuberculosis* and *M. smegmatis* were able to bind to non-phagocytic cells. This binding was blocked by a monoclonal antibody which was specific for polar PIMs, and did not show any cross-reactivity to mannose-capped LAM from *M. tuberculosis* (90).

While these reports strongly suggest that at least some PIMs are present on the surface of the mycobacterial cell, their structural nature implies that like other phospholipids, PIMs should be resident in the cytoplasmic membrane. The observation that in electron micrographs the outer leaflet of the plasma membrane is usually thicker than the inner leaflet gave rise to the theory that the more glycosylated phospholipids, such as PIMs, would reside in the outer leaflet (36). If this were the case, the oligomannosyl chains of the PIMs would face out from the membrane, towards the peptidoglycan. It has been reported that PIMs constitute 37% of the phospholipids in the cytoplasmic membrane and 56% of the total phospholipids in the cell wall structure of *M. bovis* BCG (82). An attempt at localising PIMs to subcellular fractions of *M. leprae* showed that they were present in fractions corresponding to membranes and cell wall material (123). Clearly, further studies aimed at localising PIMs within the cell envelope are warranted.

The envelope location of LAM is somewhat controversial. One model proposes that the PIM-like anchor is integrated in the plasma membrane (41) while the arabinomannan portion may traverse the entire envelope structure. It was previously thought that this highly immunogenic molecule was surface exposed, since anti-LAM antibodies have been shown to bind to the surface of intact *M. tuberculosis* (95). However, the antibodies used cross-reacted with arabinomannans

(AMs), which are abundant in the capsule (90). LAM is not extracted from capsular material, casting uncertainty on the surface location of LAM within the cell envelope (150). It has been suggested that LAMs may well be anchored in the plasma membrane, but may not traverse the entire envelope. Rather, LAMs may act to link the plasma membrane with the cell wall skeleton (51). The structural differences between the so called parietal and cellular LAMs extracted from the same culture lend favour to the notion that LAMs may be anchored in the cytoplasmic membrane in addition to being found in the more peripheral layers of the envelope (76, 144). It seems likely that the location of individual molecules is determined by structural differences. For example, the degree of acylation of the anchor component of LAM perhaps influences whether or not the molecule is anchored to a lipid-rich structure such as the plasma membrane. Similarly, the differences in extractability between the proposed parietal and cellular LAM pools may be due to the differences in acylation, relative to the strength of the LAMs association with the plasma membrane.

1.3.3 Biological Functions of Mannosylated Phospholipids

Pathogenic mycobacteria are usually phagocytosed by cells of the host's immune system, where an intracellular infection can be established. To initiate phagocytosis, the host cell typically recognises the surface molecules of the foreign bacterium. Upon phagocytosis, the processes of microbial internalisation, destruction, antigen presentation and signalling to other components of the innate immune system via cytokine release follow. The mannosylated glycolipids of mycobacteria appear to be important in several of these steps. Furthermore, the fine structural features of PIMs and LAM are able to influence specific immune responses in the infected host cell.

Interaction with the Host Cell

M. tuberculosis binds to a restricted set of macrophage receptors, including complement receptors (CR1, CR3 and CR4) and the mannose receptor (MR) (67). The host cell receptor CR3 demonstrates a broad ligand specificity, including complement protein C3bi and a range of carbohydrates which include β-glucan, *N*-acetyl-D-glucosamine and mannose containing polysaccharides. Recognition is mediated via a lectin site within the receptor (198). *M. tuberculosis* is pre-

opsonised with complement proteins before being phagocytosed via CR3 (111). Entry through this receptor is thought to promote phagocytosis without activating the host cells bactericidal respiratory burst mechanism (18).

Ligands for the MR include glycoconjugates terminating in mannose, fucose and *N*-acetyl-D-glucosamine, with attachment to the receptor promoting non-opsonic phagocytosis (196). MR is usually expressed by non-activated, differentiated tissue-dwelling macrophages (63). Mannose residues bind to the MR via a Ca^{2+} dependant carbohydrate recognition domain within the receptor (196). Hence, mycobacteria may use this receptor to directly enter resident alveolar macrophages in the lung (67). Another component of the host defence is the mannose binding protein (MBP), a serum constituent with similar binding properties to the MR. MBP acts to opsonise bacterial surfaces by binding to mannose conjugates and subsequently activates the classical complement pathway (193).

The finding that PIMs are surface exposed (150) suggests that they may play an important role as ligands for host cell receptors. Hoppe *et al.* (90) found that PIMs act as mycobacterial adhesins for non-phagocytic cells, by both direct and opsonisation-dependant means. Upon finding that *M. tuberculosis* $H_{37}R_v$ and *M. smegmatis* bound to non-phagocytic Chinese Hamster Ovary (CHO) cells more efficiently after opsonisation, a surface-exposed ligand for MBP was isolated. The ligand was found to be polar PIM (PIM_5 or PIM_6). Hence, the PIM mannose moieties were thought to directly bind to a host cell mannose binding lectin molecule on the surface, such as the MR, while also facilitating opsonisation with MBP to bind to a host cell MBP receptor.

Interestingly, different strains of *M. tuberculosis* have differing degrees of PIM surface exposure (49). Strains which have less PIM exposed contain more abundant capsular surface polysaccharides, while strains which show a greater degree of PIM exposure contain less surface polysaccharides. Strains with abundant capsular polysaccharides bound to CR3 in a direct, non-opsonic manner, wheras strains with more exposed PIMs require opsonisation to mediate binding to CR3 (49).

The binding of LAM to host cell surfaces has also been investigated in some detail. Strains of *M. tuberculosis* bind to the complement receptors CR1, CR3 and

CR4 of monocyte-derived macrophages, with the virulent $H_{37}R_v$ and Erdman strains also binding to the MR (176). The ManLAM of *M. tuberculosis* Erdman is a ligand for the MR, specifically via the terminal oligomannoside cap structures. In contrast, LM and the AraLAM from an avirulent fast-growing *Mycobacterium* species adhere less efficiently (178). The less virulent *M. tuberculosis* $H_{37}R_v$ and the avirulent $H_{37}R_a$ bind to the MR less efficiently than the highly virulent Erdman strain. Comparable amounts of mannose-capping occurs in each strain, implying that other structural features of the LAMs may also influence the degree of binding (179).

MBP can also bind to LAM and can enhance the phagocytosis of *M. avium* by neutrophils (162). The same study also demonstrated that purified ManLAM, AraLAM and LM, and PIMs (from *M. tuberculosis* $H_{37}R_v$, a rapid growing *Mycobacterium* species and *M. tuberculosis* Erdman, respectively) bound to MBP, with ManLAM showing the strongest binding. This suggests that MBP acts to opsonise either whole cells or components shed from the internalised bacterium, thereby aiding in the recognition of the organism by the hosts immune system.

Interference with Host-Cell Components

Internalised mycobacteria shed lipids, including PIMs and LAMs, into the host phagocyte (11). Shortly after the infection of macrophages with *M. bovis* BCG, PIMs and LAMs were seen to migrate from the phagosome to endosomal and lysosomal compartments, as well as vesicles in close proximity to the host cells Golgi apparatus and endoplasmic reticulum. Vesicles containing the PIMs/LAMs may also be internalised by neighbouring macrophages. PIM_6 and LAM are able to integrate into monocytic plasma membranes (97). LAM was found to integrate into host cell membranes rich in endogenous phosphatidylinositol-containing molecules via the acyl groups of the LAM anchor structure. This was observed with both ManLAM and AraLAM, with integration being inhibited by the removal of those acyl groups.

The role of these glycolipids in intracellular trafficking is unclear. Perhaps by distributing PIMs and LAMs throughout the infected cell, the mycobacterium can modulate the functions of the entire host cell by means of "remote control". Trafficking and localisation of PIM and LAM within the host cell may also act to modulate the hosts signalling pathways. In eukarotic cells, PI-containing molecules

commonly act as cell signalling messengers. The insertion of PIMs and LAMs in close proximity to these molecules may disrupt these signals and hence alter the functions of the host cell. A recent study supports the notion that LAM can interfere with host cell signalling. Maiti *et al.* (120) reported that ManLAM from *M. tuberculosis* Erdman is able to activate a host cell enzyme, phosphatidylinositol-3-kinase (PI-3K) which acts to phosphorylate the host cell Bad protein, which in its phosphorylated state promotes cell survival. When Bad is not phosphorylated, it acts as an apoptotic protein. The structural feature of LAM that triggers this activity was not defined. This may be one of the mechanisms that mycobacteria use to improve the survival of the host cell and thereby prolong the infection period, favouring the survival of the pathogen (120).

LAM has also been shown to activate Src homology 2 containing tyrosine phosphatase (SHP-1), a protein which is important for cell signal termination in pathways involved in macrophage activation and intracellular killing mechanisms (107). In this case the polysaccharide moiety of the LAM was thought to be responsible for the observed effect. LAM has also been shown to inhibit protein kinase-C activity (39). Protein kinases are involved in activating the production of reactive oxygen intermediates in the infected macrophage (71).

Modulating Cytokine Expression in Infected Cells

PIMs and LAMs are able to modulate other branches of the immune system by affecting the levels of cytokine expression in the host cell. Tumor necrosis factor alpha (TNF-α) acts to stimulate the bactericidal activity of phagocytes, eliciting a protective immune response. During *M. tuberculosis* infection, TNF-α is involved in granuloma formation which acts to prevent the spread of infection (106). LAM induces TNF-α secretion (133, 134) and the extent of its effect is dependant on LAM structure. AraLAM is a far more potent inducer of TNF-α secretion than ManLAM (46), implying that the type of cap structures on the LAM are important. However, since LAM, LM and PIM are all able to increase TNF-α secretion, the anchor structure may also be important. Differences in the ability to induce TNF-α may be determined by the acylation state of the anchor. When LAM is de-acylated, its ability to induce TNF-α secretion is reduced markedly (10).

Parietal and cellular LAMs show differences in their ability to induce TNF-α. The *M. smegmatis* parietal LAM, or PI-GAM, was still able to induce TNF-α

quite strongly despite the absence of acylation. *M. smegmatis* cellular LAM, which is acylated at the anchor, is far less active as an inducer of TNF-α. This implies that the acylation state alone is not sufficient for modulating this activity, and that other LAM structural motifs are an important determinant in the ability of LAM to modulate TNF-α secretion (77, 144). LAM has been shown to induce the secretion of several other cytokines, including pro-inflammatory (IL-1, IL-6, IL-8 and GM-CSF) and anti-inflammatory (IL-10, IL-12 and TGF-β) cytokines (203). It seems that AraLAM is a more potent inducer of cytokines than ManLAM. A recent study testing the ability of LAM to induce TNF-α and IL-8 secretion in macrophages found that the AraLAM of *M. smegmatis* was a far more potent inducer of the cytokines than *M. tuberculosis* ManLAM or the cap-deficient *M. chelonae* CheLAM (84). This supports the notion that inositol-phosphate capping influences the ability of LAM to induce at least some cytokines.

AraLAM from an unidentified fast-growing mycobacterial species induced IL-1, IL-6, IL-8 and IL-10 production to a significantly greater extent than ManLAM (10, 55, 214, 215). AraLAM was able to induce the macrophage KC and JE genes, which encode for neutrophil and monocyte chemoattractants, respectively, wheras ManLAM was unable to induce these genes (169, 170). ManLAM, however, was found to block IFNγ-activated bactericidal functions and downregulate IFNγ-inducible genes in the macrophage (39, 183, 184). PIMs have also demonstrated the ability to increase cytokine levels, including IL-6, IL-8 and GM-CSF (10, 213).

Inhibition of Other Immune Mechanisms

PIMs and LAMs affect other functions of the infected host cell and immune system. For example, the carbohydrate moiety of LAM is able to scavenge oxygen radicals (39). ManLAM and PIMs from *M. tuberculosis* suppress T-cell proliferation by inhibiting antigen processing in antigen presenting cells (APCs) (10, 133). Gilleron *et al.* (79) recently showed that when PIMs isolated from *M. bovis* BCG were injected into mice, they were able to induce granuloma formation. The predominant PIM species present in the granuloma material were triacyl- and tetracyl-PIM_2 and PIM_6 species. Interestingly, deacylated PIMs did not induce granulomas. Only the acylated forms of PIM_2 and PIM_6 were able to recruit natural killer T cells at the granuloma site. PI, which has no mannan, was also effective in

causing the formation of a granuloma. Therefore, the mannan portion of the PIM is unlikely to play a role in the process. Clearly, the structure and variation in PIMs and LAMs influence host cell responses and therefore these molecules have a special significance in the mycobacterial infection process.

1.3.4 Biosynthesis of Mannosylated Phospholipids

The importance of PIMs and LAM in mycobacterial infection has made its biosynthetic pathway an attractive target for the development of novel anti-mycobacterial drugs. Despite recent advances, several crucial steps of the pathway are still poorly understood. The structural relationship between PIMs, LMs and LAMs suggests that PIMs act as biosynthetic precursors for LAMs. Recent studies shed light on several of the key steps in the process.

The availability of the *M. tuberculosis* $H_{37}R_v$ genome sequence (47) has permitted a comprehensive analysis of cell envelope biosynthesis through predictive genetics. Out of a total of 3924 potential open reading frames (ORFs), *M. tuberculosis* appears to devote a striking amount of its genome to genes potentially involved in cell envelope biosynthesis (Table 1.2). Many genes would be required to produce the enzymes and components necessary for PIM and LAM biosynthesis, a large number of which have not been identified. A model for the biosynthetic pathway is presented in Figure 1.6, highlighting the large number of gene products that are potentially involved in regulating, catalysing or supplying for each step of the pathway.

Phosphatidylinositol (PI) Biosynthesis

The presence of PI in prokaryotes is not common and is far more abundant in mycobacteria than in any other bacterial genera (173). PI synthesis has been thoroughly investigated in eukaryotes, and this system has served as a model for the mycobacterial PI synthesis pathway.

In eukaryotes, hexokinase converts glucose to glucose-6-phosphate, which is then converted to inositol-1-phosphate by the enzyme inositol-1-phosphate synthase (INO1p) (121). The *M. tuberculosis* INOp (encoded by the gene Rv0046c) is the functional homologue of the yeast INOp and is able to complement a yeast INO1p mutant (7).

Inositol-1-phosphate is subsequently converted to free inositol by the enzyme inositol monophosphate phosphatase (IMP). Parish *et al.* (153) had isolated

Fatty acid degradation	119
Synthesis of fatty acids/mycolic acids	27
Modification of fatty acids/mycolic acids	14
Acyltransferases, mycoloyl transferases and phospholipid synthesis	25
Mycocerosic acid, polyketide and phenolphthiocerol synthesis	30
Degradation of polysaccharides, lipopolysaccharides and phospholipids	8
Esterases and lipases	27
Surface polysaccharides, lipopolysaccharides, proteins and antigens	39
Cell wall/peptidoglycan	28
Miscellaneous transferases	61
Putative lipoproteins	65
Conserved membrane proteins	17
Other membrane proteins	211
[1]Conserved hypothetical proteins	915
[2]ORFs with no similarity to database entries	606

Table 1.2

Potential cell envelope biosynthetic genes of the *Mycobacterium tuberculosis* $H_{37}R_v$ genome.

The complete genome of *M. tuberculosis* $H_{37}R_v$ contains 3924 potential genes, many of which seem to be involved in cell envelope biosynthesis. Several of the genes show strong matches to known counterparts in other species, but many show poor or no similarity to any database entries.

(1) These putative genes show matches to database entries that have no known function.

(2) A large number of ORFs encode for proteins that have no similarity to any database entries (47).

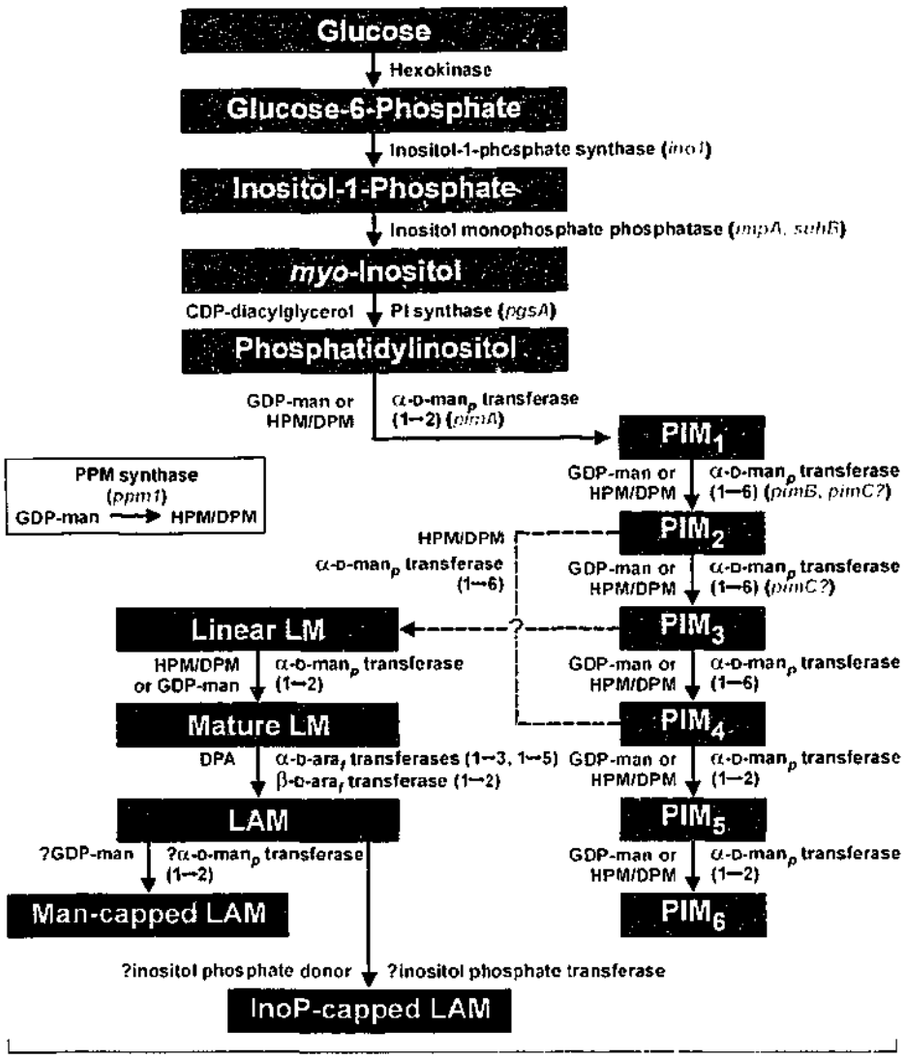

Figure 1.6
Proposed biosynthetic pathway for PIMs and LAM in mycobacteria.
The biosynthesis of phosphatidylinositol mannosides (PIMs) and lipoarabinomannan (LAM) is thought to occur via the sequential addition of glycosyl residues to a phosphatidylinositol (PI) precursor. PIM_1 to PIM_6 represent PI substituted with 1 to 6 mannose units. At some point, PIM_2, PIM_3 or PIM_4 is further mannosylated to form lipomannan (LM), which is arabinosylated to form LAM. Capping of the arabinose branches with oligomannosyl units or inositol phosphate caps complete the molecule. In most cases, the enzymes and glycosyl carriers involved in each step have not been confirmed. Guanosine di-phospho-mannose (GDP-man), the polyprenol phosphomannoses (PPMs; heptaprenol phospho-mannose (HPM), decaprenol phospho-mannose (DPM), and decaprenol phospho-arabinose (DPA)) donate sugar units to the growing molecule via specific α-D-mannopyranosyl or α- and β-D-arabinofuranosyl transferases. Predicted enzymes are listed in green, while their corresponding glycosyl donors are listed in red. Identified mycobacterial open reading frames corresponding to these enzymes are listed in grey. PIM and LAM intermediates can be mono-, di-, tri- or tetra-acylated.

a *M. smegmatis* transposon mutant that was disrupted in an ORF resembling mammalian IMP genes, and designated the *M. smegmatis* gene *impA*. The gene showed strong similarity to the *M. tuberculosis* ORF Rv1604. The *M. smegmatis impA* transposon mutant produced less PIM_2 than the wild-type, but the disruption of *impA* did not cause a complete loss of the PIM. Other, functionally redundant enzymes may compensate for the loss of *impA*. A recent study supports this notion. Nigou *et al.* (143) found that *M. tuberculosis* had four ORFs which possessed a key inositol monophosphatase signature (137): Rv2701c (*suhB*), Rv3137, Rv1604 (*impA*) and Rv2131 (*cysQ*). Recombinant, purified SuhB was able to hydrolyse inositol-6-phosphate, while also being able to hydrolyse other polyol phosphates to a lesser extent.

Free inositol is converted to PI by the transfer of phospho-diacylglycerol to the inositol, probably using cytidine-diphosphate diacylglycerol (CDP-DAG) as a donor (158). The enzyme involved in this conversion is CDP-DAG:*myo*-inositol transferase, or PI synthase. This reaction has been demonstrated in *M. smegmatis* (173) using purified cell envelope fractions in a cell-free assay for PI synthesis. Purified cytosolic and cytoplasmic membrane fractions did not catalyse PI biosynthesis in the cell-free system, suggesting that PI synthase occurs in the cell wall. Significant PIM_2 synthesis occurred in combined cell wall/cytoplasmic membrane fractions, with little synthesis seen in the cell wall fraction alone. This suggests that while PI synthase activity is localised to the cell wall, the newly synthesised PI must be transferred to the cytoplasmic membrane to be further mannosylated into PIMs.

The *M. tuberculosis* PI synthase has a conserved PI synthase motif, identified by Jackson *et al.* as being encoded by Rv2612c (*pgsA*) (98). When *M. tuberculosis pgsA* was overexpressed in *M. smegmatis*, there was a 2 to 2.5-fold increase in PI synthase activity (98). Jackson *et al.* noted that *pgsA* is located within a five-ORF cluster which is likely to be involved in PIM biosynthesis (Figure 1.7). The proposed cluster is also found in *M. smegmatis*. The ORF immediately upstream of *pgsA*, Rv2613c, encodes for a protein with no assigned function. The three ORFs downstream from *pgsA*, however, have putative roles in PIM biosynthesis. Rv2611c shows some similarity to bacterial acyltransferases, while Rv2610c contains a motif found in bacterial α-mannosyltransferases,

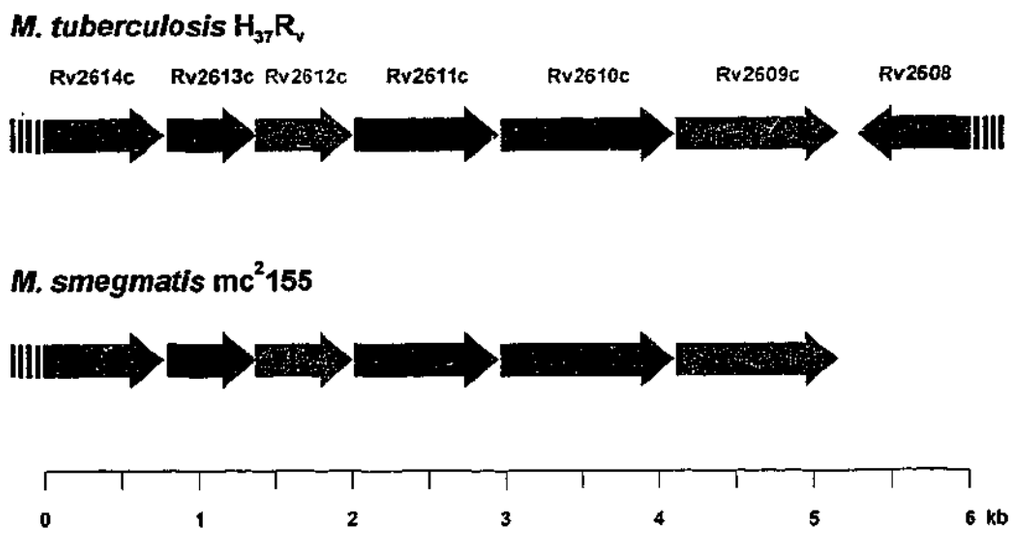

M. tuberculosis ORF	*M. smegmatis* Homologue % Amino Acid Identity/Similarity	Proposed Function
Rv2608	NM	*M. tuberculosis* PPE family
Rv2609c	67, 79	Putative GDP-mannose hydrolase
Rv2610c	82, 88	*pimA:* α-mannosyltransferase
Rv2611c	74, 84	Similarity to bacterial acyltransferases
Rv2612c	66, 81	*pgsA:* phosphatidylinositol synthase
Rv2613c	79, 88	Unknown function
Rv2614c	82, 89	*thrS:* probable threonyl-tRNA synthetase

Figure 1.7
Conservation of the *M. tuberculosis* PIM biosynthetic cluster in *M. smegmatis*.
The sequencing projects for *M. tuberculosis* $H_{37}R_v$ (47) and *M. smegmatis* mc^2155 (TIGR) were accessed to compile genomic maps of the proposed PIM biosynthetic region described by Kordulakova *et al.* (108).
The *M. tuberculosis* $H_{37}R_v$ numbering system (47) was applied for each ORF. The proposed function of each ORF is listed, together with their amino acid sequence similarities to the likely *M. smegmatis* homologues. NM: no matches found.

EXF(G/C)XXXE (75), which is thought involved in binding to guanosine-diphosphate mannose (GDP-man). Rv2609c contains the *mutT* domain signature characteristic of GDP-man hydrolases (72), and is perhaps involved in the regulation of GDP-man within the cell. The observation that these five ORFs appear to be transcribed in the same direction suggests that this cluster may represent a PIM biosynthetic operon. Homologues of *pgsA* have been was identified in *M. smegmatis* and *M. leprae*. Disruption of *pgsA* in *M. smegmatis* was lethal, suggesting that PI or its derivatives are essential for cell viability. Two other *M. tuberculosis* ORFs, *pgsA2* (Rv1822) and *pgsA3* (Rv2746c), have also been identified as potential PI synthases (47). The biosythetic function of these genes have not been confirmed.

Phosphatidylinositol Mannoside (PIM) Biosynthesis

PI is mannosylated to form the PIMs. The mannose donor in these reactions has been identified as GDP-man (32, 33). The mannose from the GDP-man donor is presumably transferred to PI via an α-D-mannosyltransferase. Since the addition of mannose to PI to form PIM_1 involves an α(1→2) linkage, and the mannosylation of PIM_1 to form PIM_2 involves an α(1→6) linkage, different mannosyltransferases are likely to be involved in each step (194). Kordulakova *et al.* recently confirmed the product of Rv2610c as the enzyme that converts PI to PIM_1 in *M. tuberculosis* $H_{37}R_v$, and was designated *pimA* (108). Overexpression of *the M. smegmatis* homologue in its native host resulted in an approximately 6-fold increase in incorporation of [^{3}H]inositol into PIMs. Moreover, membrane fractions from *M. smegmatis* overexpressing PimA increased the incorporation of GDP-[^{14}C]man into PIM_1 species, demonstrating that PimA has α-mannosyltransferase activity. This was further confirmed when PimA was overexpressed in *E. coli*. Crude extracts were able to synthesise PIM_1 from GDP-[^{14}C]man and bovine PI, conclusively demonstrating that *pimA* encodes for an α-D-mannose-α(1→2)-phosphatidyl-*myo*-inositol transferase. The presence of a potential transmembrane domain within the PimA sequence is consistent with the localisation of its activity in membrane fractions as well as the likely subcellular location for PIM biosynthesis.

Interestingly, *pimA* was also found to be essential in *M. smegmatis*. Kordulakova *et al.* demonstrated that a targetted disruption mutant of *pimA* was only viable in the presence of a temperature-sensitive complementation plasmid

containing a functional *pimA* (108). When the complementing plasmid was lost, the mutant was not viable. This work provides the first evidence that PIM_1 is essential for mycobacterial survival. Together with the finding that *pgsA* is also essential for survival, this implies that the other genes of the proposed PIM biosynthetic cluster may also be important to cell viability.

Schaeffer *et al.* (175) identified the mannosyltransferase responsible for mannosylating PIM_1 to form PIM_2. A *M. tuberculosis* genomic library was transformed into *M. smegmatis* and grown in the presence of D-mannosamine (ManN), a mannose analogue which terminates mannan chain elongation. The rationale was to select for clones of *M. smegmatis* that were resistant to ManN by virtue of overexpression of a *M. tuberculosis* gene, thereby overcoming the effects of ManN. A ManN-resistant *M. smegmatis* clone containing the *M. tuberculosis* Rv0557 gene was isolated. The enzyme encoded by Rv0557 had the mannosyltransferase GDP-mannose binding motif (75) and was named *pimB*. Overexpression of *pimB* resulted in a 1.7-fold increase in PIM_2 biosynthesis. Furthermore, recombinant PimB protein catalysed the formation of tri-acylated PIM_2 from tri-acyled PIM_1 in a cell-free system. The conversion was inhibited by the addition of ManN, demonstrating that *pimB* encoded the α-D-mannosyltransferase responsible for mannosylating Ac_3PIM_1 to form Ac_3PIM_2. The PimB amino acid sequence contains a potential transmembrane domain, which would be consistent with the observation that mannosylation activity may occur within the cytoplasmic membrane (173).

PIM_2 is sequentially converted to PIM_3 and PIM_4, presumably via the action of (1→6) α-D-mannosyltransferases that are yet to be completely identified. Kremer *et al.* (110) searched the *M. tuberculosis* CDC1551 genome sequence to identify further potential mannosyltransferases. An ORF which showed 33% identity to PimB, RvD2-ORF1, contained the mannosyltransferase motif and was designated *pimC*. To examine its activity, *pimC* was overexpressed in *M. smegmatis* and membrane fractions were analysed. The fractions were able to incorporate label from GDP-[^{14}C]man into PIM_2 and PIM_3, suggesting that PimC catalyses the formation of PIM_3. Interestingly, *pimC* is absent in *M. tuberculosis* $H_{37}R_v$, but present in the $H_{37}R_a$ and Erdman strains as well as 17 out of 80 clinical isolates tested. The gene is also present in *M. bovis* BCG and *M. avium*, but absent

in *M. smegmatis* and *M. leprae*. The absence of the gene in *M. leprae*, which has been described as possessing a minimal gene set for mycobacteria (48), suggests that *pimC* is not essential. This notion was supported by the finding that a *pimC* targetted disruption mutant of *M. bovis* BCG showed no growth impairment and contained a PIM and LAM complement which was similar to that of the wild-type. This result also implies that the enzyme/s involved in PIM_3 synthesis have functional redundancy in the form of alternate enzymes encoded by other genes. This also raises the possibility that *pimB* is also non-essential. GDP-mannose probably acts as the mannose donor in each mannosylation step (32, 33), although more recent work supports the role of polyprenol phosphomannoses as the sugar donors (23).

One of these mannosylation steps is thought to be the point at which PIMs are converted into LMs and LAMs. Either PIM_2, PIM_3 or PIM_4 can be further mannosylated to form linear LM but it is not known which of these PIMs is the true precursor of LM since the mannan backbone of LM and the mannose side-chains of PIM_2, PIM_3 and PIM_4 consist of (1→6) linked α-D-mannose units. The acylation state of the precursor may play an important role in determining whether a PIM is further metabolised to LM/LAM, or whether the PIMs are converted to the higher order PIM_5 and PIM_6 (23, 104, 136).

PIM_5 and PIM_6 are not likely to act as precursors for LM/LAM, since their mannose chains contain (1→2) linkages which are not found within the linear mannan backbone of LM (41). Whether it is metabolised into LM or not, PIM_4 is further mannosylated to form PIM_5, which in turn is mannosylated to form PIM_6. Both steps appear to use GDP-man as a mannose donor (33). The mannosyltransferases involved in these final steps of PIM synthesis have not been identified.

Lipomannan (LM) and Lipoarabinomannan (LAM) Biosynthesis

The discovery that the anchor structure of LAM resembled that of PIMs (95) led to the notion that LAMs were synthesised as hyperglycosylated extensions of the simpler PIMs. Further evidence for this was provided by Gilleron *et al.* (79), who observed that the acylation variants of PIMs closely resembled those of the LAM anchor, where the sites for acyl substitutions and the types of fatty acids found in each case were the same. It is therefore likely that an appropriately

acylated PIM_2, PIM_3 or PIM_4 is further mannosylated to form linear LM. The mannose donor in this case has been identified as either a heptaprenol phospho-mannose (C_{35}, HPM) (Figure 1.8a) or a decaprenol phospho-mannose (C_{50}, DPM) (Figure 1.8b) (23), with the corresponding (1→6) α-D-mannosyltransferase yet to be identified. The subsequent addition of (1→2) α-D-mannosyl units to form mature LM is thought to be mediated by either a DPM/HPM or GDP-man donor via the action of an unidentified (1→2) α-D-mannosyltransferase (20). The mechanism for the addition of arabinose units to the LM to form LAM is not clear. Individual arabinoses are transferred to the growing arabinan via a decaprenol phospho-arabinose (C_{50}, DPA) donor (Figure 1.8c) (112, 206, 209).

Recent work has shed light on polyprenol biosynthesis. Polyprenols are thought to be synthesised with the condensation of two C_5 lipids, isopentenyl diphosphate (IPP) and dimethylallyl diphosphate, to form the C_{10} lipid geranyl diphosphate (GPP). An individual C_5 IPP unit is subsequently added to GPP, producing a C_{15} farnesyl diphosphate (FPP). FPP is then further extended with the addition of seven C_5 IPP units to form the C_{50} decaprenol diphosphate. This precursor is then presumably de-phosphorylated and substituted with either a mannose or arabinose unit to form DPM or DPA, respectively (180). Two *M. tuberculosis* ORFs which may encode enzymes that catalyse the incorporation of IPP into decaprenol diphosphate have been identified through cloning and subsequent overexpression in *M. smegmatis*. The first ORF, Rv1086, encodes for the enzyme that converts GPP to FPP and was designated farnesyl diphosphate synthase. The product of the second ORF, Rv2361c, extended FPP into decaprenol diphosphate and was named decaprenol diphosphate synthase. Farnesyl diphosphate synthase activity in the recombinant *M. smegmatis* was located in both cytosolic and cytoplasmic membrane fractions, while decaprenol diphosphate synthase was active in membrane fractions. This corresponded with the presence of a potential transmembrane domain in the Rv2361c amino acid sequence, while such a domain was not apparent in the farnesyl diphosphate synthase sequence (180). The membrane-bound location of the polyprenol synthetic enzyme is compatible with the notion that LAMs are at least initially bound to the cytoplasmic membrane. The polyprenol chain is then substituted with a mannose unit from a GDP-man donor via the action of a polyprenol monophosphomannose

a) Heptaprenol phospho-mannose (HPM)

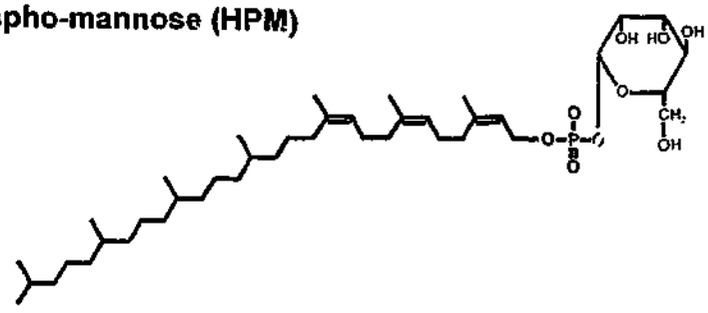

b) Decaprenol phospho-mannose (DPM)

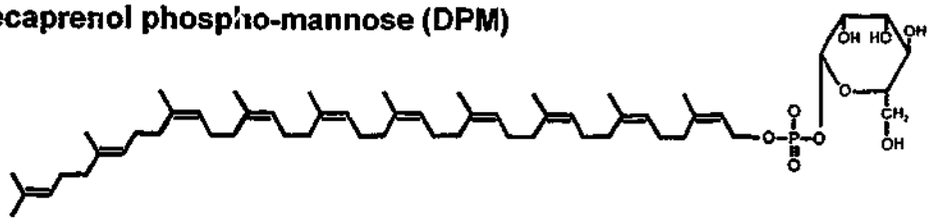

c) Decaprenol phospho-arabinose (DPA)

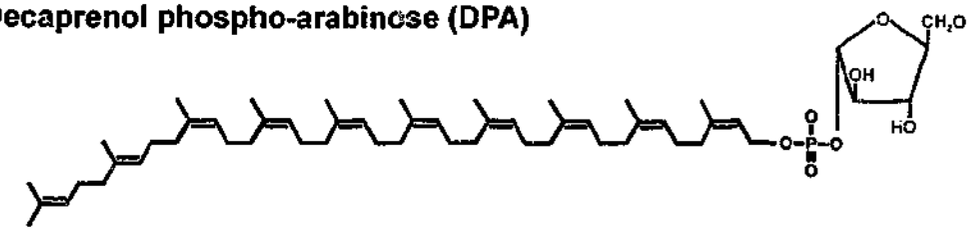

Figure 1.8
Structures for mycobacterial polyprenol carriers.
Each of these polyprenols act as sugar donors in the biosynthesis of lipomannan and lipoarabinomannan.
a, b) Heptaprenol phospho-mannose (HPM) and decaprenol phospho-mannose (DPM) donate mannose units.
c) Decaprenol phospho-arabinose (DPA) is an arabinose donor, and is also involved in arabinogalactan biosynthesis.

(PPM) synthase. The product of *M. tuberculosis* Rv2051c, designated Ppm1, was found to catalyse this step and was identified via similarities to eukaryotic dolichol monophosphomannose (PPM) synthases (86). *M. smegmatis* lysates overexpressing Ppm1 were able to catalyse the transfer of mannose from GDP-[^{14}C]man to HPM and DPM, as well as a novel C_{40} prenol species. Interestingly, the gene was found to contain two functionally distinct domains. The N-terminal portion contained several potential transmembrane domains and showed some similarity to bacterial acyltransferases, while the C-terminal region showed the PPM synthase activity. Homologues for *ppm1* were found in *M. smegmatis*, *M. leprae* and *M. avium*, where the two regions are apparently encoded by separate, adjacent ORFs which may form an operon (86). The compatibility of the *M. tuberculosis* genes in *M. smegmatis* implies that the polyprenol biosynthetic mechanism is similar in both species. The targetted disruption of these genes with a view to abolishing polyprenol biosynthesis may well be lethal for many mycobacterial species. It is, however, possible that a functional redundancy exists given the fundamental role of these enzymes in cell envelope component synthesis.

Unidentified arabinosyltransferases are probably responsible for adding the arabinose units from DPA donors to the growing arabinan branches of LAM. Much of the work in this area has stemmed from the observation that ethambutol, an antimycobacterial drug, inhibits the extension of arabinan chains in cell envelope arabinogalactan and LAM. Wolucka *et al.* (206) showed that ethambutol treatment of the drug-susceptible *M. smegmatis* led to an accumulation of DPA and HPA, suggesting that the targets for ethambutol were arabinosyltransferases. It was subsequently shown that ethambutol inhibited the extension the arabinan chains in AG and LAM to differing extents (206).

To identify genes which conferred resistance to ethambutol, Belanger *et al.* (12) transformed a genomic DNA cosmid library of the ethambutol-resistant *M. avium* into the susceptible *M. smegmatis* and screened for ethambutol resistant clones. This led to the identification of three ORFs; one ORF showed homology to transcriptional activators and was named *embR* (or *embC*), while the other two ORFs showed no similarity to database sequences but showed high similarity to each other. These were designated *embA* and *embB*, their products being possible

targets for ethambutol. Hybridisation studies showed that homologues to these genes were present in other mycobacteria.

A spontaneous ethambutol resistant mutant of *M. smegmatis* was isolated. The mutant demonstrated a normal AG biosynthetic profile while producing truncated forms of LAM (105, 129). The extent of LAM truncation was proportional to the concentration of ethambutol in the medium, and high concentrations of the drug resulted in the truncation of both AG and LAM (105). This suggested that the spontaneous *M. smegmatis* mutant had altered *embAB* homologues, producing enzymes that were no longer being affected by ethambutol. If this were the case, *embAB* specifically encode for AG arabinosyltransferases. Since the truncated arabinans of LAM appeared at higher concentrations of the drug, it is possible that the arabinosyltransferases responsible for LAM biosynthesis show a weaker affinity for ethambutol and are only affected at the higher concentrations. This also implied that the arabinans of AG and LAM, while structurally similar, were synthesised via separate pathways and that different arabinosyl transferases showed different sensitivities to ethambutol (60, 129). It was subsequently shown that targetted disruption of *M. smegmatis embA* and *embB* resulted in a reduction in the arabinose content of AG. More specifically, the hexaarabinosyl motif characteristic of AG was altered. This suggests that EmbA and EmbB are involved in the later stages of arabinan assembly in AG biosynthesis (68).

It appears that *embAB* do not encode for arabinosyltransferases involved in LAM biosynthesis. Further biosynthetic details about the arabinan branches of LAM are lacking. Whether the arabinosyls are transferred after the mannan core is complete or while it is being synthesised is also unknown, since the site of arabinan attachment to the mannan has not been defined.

LAM biosynthesis is thought to be completed by the addition of the mannose or inositol-phosphate caps. The presence of mono-, di- and tri-mannosyl caps suggest that mannose residues may be added onto the arabinan branch one by one, but this is yet to be shown. The biosynthetic processes involved in the production and attachment of the inositol-phosphate caps are also not known. The capping of some branches and not others suggests that some kind of regulatory mechanism exists to mediate the degree of capping, perhaps in response to

environmental stimuli. It is not known whether any acylation of the LAM molecule occurs after the addition of the arabinan chains and the caps, or during an earlier stage of the biosynthetic process. The various acyltransferases needed to complete these modifications are yet to be identified.

While a great deal of biosynthetic details have been determined, many steps of the PIM/LAM biosynthetic pathway and the role of acylation in the biosynthesis of these molecules remain poorly understood.

1.4 Project Rationale and Objectives

1.4.1 Cell Envelope Components as Novel Drug Targets

Therapeutic agents such as isoniazid, ethambutol and cycloserine have been useful in treating mycobacterial infections. Each of these drugs target a component of the mycobacterial cell envelope. However, the emergence of MDR *M. tuberculosis*, compounded by the ongoing problem of opportunistic mycobacterial infections in AIDS patients, has re-focussed efforts to identify targets for new anti-mycobacterial agents. In the search for novel drug targets, the mycobacterial cell envelope has received much of the recent attention. Its structure is complex, diverse and crucial to the integrity of the mycobacterium. Further, many of the envelopes constituents are restricted to the genus, making the development of new, specifically anti-mycobacterial agents possible.

A thorough understanding of the envelope's structure and biosynthetic processes is required for the design of new drugs. While the structures of the envelope's components are well known, and a fairly detailed level of understanding regarding its synthesis has been achieved, the corresponding genetic background is by comparison poorly understood. Identifying mycobacterial genes which encode for parts of the envelope's biosynthetic machinery will foster a better understanding of the structure's synthesis and will aid in the rational design of new antimycobacterial agents.

1.4.2 Mycobacterium smegmatis: A Laboratory Model

In the past, a lack of established tools for the genetic manipulation of mycobacterial pathogens has hampered progress of their study. Additionally, the

pathogenicity and specialised growth conditions of some mycobacteria present practical problems. Consequently, many researchers use *M. smegmatis* as a laboratory model, as it overcomes some of the problems faced when working with a pathogen.

Conveniently, *M. smegmatis* is a rapid grower which is able to form visible colonies within three days. Pathogens such as *M. tuberculosis* require up to 6 weeks for visible colony growth. Secondly, *M. smegmatis* is non-pathogenic, only causing rare infections in immunocompromised hosts. Perhaps most importantly, *M. smegmatis* produces a cell envelope which is highly similar to other mycobacteria, including the pathogens. This similarity is also reflected at the genetic level, where *M. smegmatis* has been shown to contain homologues to many genes identified in pathogenic species. Various genetic manipulation techniques, such as random transposon mutagenesis (85), gene disruption by homologous recombination and mycobacterial gene overexpression (100, 192) are relatively well developed in *M. smegmatis.*

Table 1.3 presents a list of recent studies in which *M. smegmatis* has been used to aid in the identification of cell envelope biosynthetic genes in pathogens such as *M. tuberculosis*. The genes have been either been directly studied in *M. smegmatis*, first identified in *M. smegmatis* and subsequently identified in the pathogen, or the pathogen gene has been cloned into a *M. smegmatis* host. Recombinant *M. smegmatis* has also been a common source for cell-free assays to test the activity of pathogen-derived enzymes. Genetic determinants for several important components of the cell envelope have been identified using *M. smegmatis*. The model has also proven useful in determining the genetic basis of resistance to existing anti-mycobacterial drugs; the *M. tuberculosis* targets for isoniazid, ethambutol and cycloserine have all been defined (see Table 1.3) using *M. smegmatis.*

The recent release of the *M. tuberculosis* $H_{37}R_v$ (47) and *M. leprae* (48) genome sequences, as well as the current sequencing projects for *M. bovis* BCG and *M. avium*, have facilitated the direct study of these pathogens. Indeed, various techniques for the genetic manipulation of *M. tuberculosis* have recently been developed. These include allelic exchange, transposon mutagenesis (31, 160) and signature-tagged mutagenesis, an approach which identifies genes that are

Envelope Component	Gene	Function	Species of Origin	Reference
Glycolipids				
PIM	*impA*	Inositol monophosphate phosphatase	*M. smegmatis* mc^{2}155	(153)
	pimB (Rv0557)	Mannosyl transferase	*M. tuberculosis* $H_{37}R_v$	(175)
	pgsA (Rv2612c)	Phosphatidylinositol synthase	*M. tuberculosis* $H_{37}R_v$	(98)
	pimC	Mannosyl transferase	*M. tuberculosis* CDC1551	(110)
	pimA (Rv2610c)	Mannosyl transferase	*M. tuberculosis* $H_{37}R_v$	(108)
GPL	*Ser2* locus	Various	*M. avium* serotype 2	(16)
	rtfA	Rhamnosyl transferase	*M. avium* serotype 2	(66)
	mps	Peptide synthetase	*M. smegmatis* mc^{2}155	(26)
	mtf1	Methyl transferase	*M. smegmatis* mc^{2}155	(155)
LOS, DAT, DMT, PPT, SL	*otsA* (Rv3490)	Trehalose-6-phosphate synthase	*M. tuberculosis* $H_{37}R_v$	(58)
	otsB (Rv2006)	Trehalose-6-phosphate phosphatase	*M. tuberculosis* $H_{37}R_v$	(58)
	treY (Rv1563c)	Maltooligosyl trehalose synthase	*M. tuberculosis* $H_{37}R_v$	(58)
	treZ (Rv1562c)	Maltooligosyl trehalose trehalohydrolase	*M. tuberculosis* $H_{37}R_v$	(58)
	treS (Rv0216)	Trehalose synthase	*M. tuberculosis* $H_{37}R_v$	(58)
DIM, PGL	ORF3	Mycocerosic acid acyl co-enzyme A synthase	*M. bovis* BCG	(69)
Fatty Acids	*pncA*	Pyrazinamidase	*M. tuberculosis* (various)	(181, 30)
	fas1	Fatty acid synthase I (pyrazinamide target)	*M. tuberculosis* $H_{37}R_v$	(216)
Cytoplasmic Membrane				
Polyprenols	Rv1086	Farnesyl diphosphate synthase	*M. tuberculosis* $H_{37}R_v$	(180)
	Rv2361c	Decaprenol diphosphate synthase	*M. tuberculosis* $H_{37}R_v$	(180)
	Rv2051c	Polyprenol monophosphomannose synthase	*M. tuberculosis* $H_{37}R_v$	(86)

Table 1.3
The use of *M. smegmatis* in studying the genetics of cell envelope biosynthesis.
The identification of cell envelope biosynthetic genes, predominantly those in *M. tuberculosis*, has been facilitated by the use of *M. smegmatis* as a laboratory host. All of the above studies employed *M. smegmatis* in a variety of ways to help identify and assign functions to genes from other mycobacteria. In many cases, the *M. smegmatis* gene itself has been cloned and shows sequence and/or functional similarity to the gene from the pathogenic species. The figure is continued on the following page

Envelope Component	Gene	Function	Species of Origin	Reference
mAGP Complex				
Mycolic Acids	*cmaA1* (Rv3392c)	Cyclopropane-mycolic acid synthase 1	*M. tuberculosis* $H_{37}R_a$	(212, 172)
	cmaA2 (Rv0503c)	Cyclopropane-mycolic acid synthase 2	*M. tuberculosis* Erdman	(80, 172)
	mmaA1-4 (Rv0645c-0642c)	Methoxy-mycolic acid synthases	*M. tuberculosis* $H_{37}R_a$	(211, 172)
	inhA (Rv1484)	Enoyl-acyl carrier protein reductase (fatty acid synthase II)	*M. tuberculosis* $H_{37}R_v$	(8)
	mabA (aka *fabG1*) (Rv1483)	3-ketoacyl reductase	*M. tuberculosis* $H_{37}R_v$	(9)
	kasA, *kasB* (Rv2245, Rv2246)	Acyl carrier protein synthases (fatty acid synthase II)	*M. tuberculosis* $H_{37}R_v$	(109)
	fbpC (Antigen 85C) (Rv0129c)	Mycolic acid transfer to arabinogalactan?	*M. tuberculosis* 103	(99, 17)
Arabinogalactan	Rv3808c	Galactosyl transferase	*M. tuberculosis* $H_{37}R_v$	(130)
	glf (Rv3809c)	UDP-galactopyranose mutase	*M. tuberculosis* $H_{37}R_v$	(205)
	embA	Arabinan synthesis	*M. smegmatis* mc^2155	(68)
	embB	Arabinan synthesis	*M. smegmatis* mc^2155	(68)
	embC	Arabinan synthesis	*M. smegmatis* mc^2155	(68)
	rfbA (aka *rmlA*) (Rv0334)	Glucose-1-phosphate thymidyl transferase	*M. tuberculosis* $H_{37}R_v$	(119)
Peptidoglycan	*ponA*	Penicilin binding protein 1 (transglycosylase/transpeptidase)	*M. smegmatis* mc^2155	(25)
	ddlA	D-alanine-D-alanine ligase (D-cycloserine target)	*M. smegmatis* mc^2155	(13)
	alrA	D-alanine racemase	*M. smegmatis* mc^2155	(37)
Cell Envelope Transport				
Porin	*mspA*	Porin channel monomer	*M. smegmatis* mc^2155	(142)

Table 1.3
The use of *M. smegmatis* in studying the genetics of cell envelope biosynthesis.
The figure is continued from the previous page.

expressed *in vivo* inside the infected macrophage (38). Allelic exchange methods for *M. bovis* BCG (147, 159) and *M. intracellulare* (122) have also been developed. Genetic manipulation of *M. avium* remains underdeveloped. The genes of interest can be identified based on sequence similarity to functional counterparts in other genera and isolated directly from the genome. At this point, the gene can be expressed to produce protein, or a disrupted copy of the gene can be introduced into the pathogen to produce a knock-out strain. Conversely, mutant libraries can be constructed and used to screen for altered phenotypes and the corresponding gene then identified. It can therefore be argued that the *M. smegmatis* model has become somewhat redundant.

Still, the emergence of genetic manipulation techniques for organisms such as *M. tuberculosis* along with the availability of genome sequence does not signify the end of *M. smegmatis* as a model. The structures of *M. smegmatis* and *M. tuberculosis* PIMs and LAMs have been described in detail earlier in this chapter, and show minor structural differences. This is also the case for many other components of the cell envelope. Accordingly, the biosynthetic processes and corresponding genetics are expected to be very similar between the two species. The sequencing of the *M. smegmatis* genome is currently in progress.

The apparent conservation of cell envelope composition and architecture between *M. smegmatis* and the mycobacterial pathogens means that *M. smegmatis* is useful as a laboratory model. Indeed, many recent cell envelope composition and biosynthetic studies still use *M. smegmatis* as a means of determining a pathogen genes function using a variety of techniques (see Table 1.3). This is especially so for studies focussing on PIM and LAM biosynthesis. However, the use of *M. smegmatis* as a model for cell envelope biosynthesis needs to be questioned in cases where the study target has been shown to be different to the pathogens. This would be particularly important in virulence studies, as *M. smegmatis* is not a pathogen.

1.4.3 Aims of this Study

The main aim of this investigation is to improve the understanding of the PIM/LAM biosynthetic pathway by analysing a mutant which shows defects in the synthesis of these molecules. This will be achieved by characterising a *M.*

smegmatis transposon mutant that has PIM and LAM abnormalities. The characterisation of the aberrant PIM/LAM content and biosynthesis in the mutant provides clues to the order of the PIM and LAM biosynthetic pathway and how the synthesis of the two molecules is related.

As discussed earlier in this chapter, the underlying genetics of PIM/LAM biosynthesis are incompletely understood, especially for the sections of the pathway beyond PIM_2 synthesis. Once PIM and LAM defects are characterised, the site of transposon insertion in the mutant will be identified. By correlating observed PIM/LAM defects with the genetic mutation, a gene which is associated with the synthesis of these important molecules may be identified.

Characterisation of the mutant phenotype provides the basis for further detailed studies of how PIM and LAM biosynthesis are affected in the mutant, ultimately improving our understanding of the mechanics of this important pathway. The mutant can also be of use in determining the influence of PIMs and LAMs in mycobacterial infections. In the longer term, a thorough understanding of the PIM/LAM biosynthetic pathway will facilitate the identification of targets for novel antimycobacterial agents.

Chapter 2
Transposon Mutants That Have PIM and LAM Abnormalities

2.1 Rationale and Objectives

2.1.1 Transposon Mutants with Potential Cell Envelope Defects

In order to identify genes that are involved in cell envelope biosynthesis, transposon mutants with an altered colony morphology were examined. Variations in colony morphology have sometimes been shown to be due to a difference in cell envelope composition, affecting the physical and chemical properties of the cell surface and thereby influencing the colony morphology of the strain. Colony morphology defects that have been linked to altered or depleted cell envelope components commonly involve glycopeptidolipids (15, 26, 155) or lipoligosaccharides (14).

This study examines a Tn*611* transposon mutant of *M. smegmatis* which showed an aberrant colony morphology when compared to the wild-type strain. The mutant MYCO481 was initially isolated from a library of transposon mutants based on an unusual colony morphology. As the results presented in this chapter will show, the aberrant MYCO481 colony phenotype was found to be unstable on certain media, giving rise to a distinct form of the strain (named MYCO479) which resembled the wild-type colony morphology more closely.

The focus of this chapter is to define phenotypic differences between the two mutants and the wild-type strain by examining their cell envelope components. Defining the mutant phenotype in detail may offer clues as to the function or identity of the disrupted gene/s in the transposon mutants, which will be examined in detail in Chapter 4.

2.1.2 Aims of this Section

The first objective of this section was to assess if the differences in the colony morphologies of the mutants featured in this study were consistent in different media. The possibility that biochemical distinctions exist between the two mutants was then examined in detail. The second aim was to determine if any differences were observed in the major *M. smegmatis* cell envelope components, including GPLs, PIMs, LAMs, mycolic acids, arabinogalactan and other extractable sugars. The strains were grown in Middlebrook 7H9 medium. If major differences were found, the composition of the two mutants would again be examined under PPLO medium culturing conditions to observe if the difference in colony morphology coincided with the same biochemical differences observed when the strains were grown in Middlebrook 7H9 medium.

2.2 Materials and Methods

2.2.1 Chemicals and Reagents

All chemicals and reagents used in this study were supplied by BDH Laboratory Supplies, Bio-Rad Laboratories, Difco Laboratories, ICN Biomedicals Inc., Sigma-Aldrich Co. and Univar Corporation. Media ingredients were supplied by Difco Laboratories and Oxoid Ltd. DNA restriction and modification enzymes were supplied by New England Biolabs Inc., Pharmacia Biotech, Promega Corporation and Roche Molecular Biochemicals.

2.2.2 Isolating Transposon Mutants on Different Media

The *M. smegmatis* Tn*611* transposon mutant library used in this study was grown in Middlebrook 7H9 media, constructed as per Guilhot *et al.* (85). The library was then plated onto BY media and colonies with morphologies distinct from the wild-type were isolated. The transposon mutant examined in this study was then plated onto LB, PPLO and Middlebrook 7H10 agar to assess the influence of media on colony morphology.

Mycobacterial Culture: Strains and Media

The *M. smegmatis* strains used in this study are listed in Appendix 1. Luria Bertani (LB) media was prepared as described in Sambrook *et al.* (174). A modified recipe for Pleuropneumonia-like organism (PPLO) media was prepared

for the growth of mycobacteria. Middlebrook 7H9 broth and 7H10 agar were prepared according to the suppliers instructions (Difco Laboratories). Where required, filter-sterilised 20% (v/v) Tween-80 was also added to a final concentration of 0.05% (v/v). Media formulations are listed in detail in Appendix 2. Transposon mutants MYCO481 and MYCO479 were always cultured in the presence of kanamycin.

Incubation Conditions

All mycobacterial cultures were incubated aerobically at 37°C or 39°C. In most cases, *M. smegmatis* colonies appeared after 3-5 days of incubation on agar media. For liquid cultures, single colonies of *M. smegmatis* were picked, inoculated into 10 ml of broth and grown for 3-5 days. This was referred to as the "starter culture". The starter culture was then used to inoculate a larger broth by applying 1 ml of starter culture per 100 ml of medium in each case. The cultures were then allowed to grow for a further 1-2 days. For all broths, shaking at 160 to 200 rpm was applied in order to aerate the cultures.

2.2.3 Cell Envelope Component Extraction

Covalently and non-covalently linked components of the mycobacterial cell envelope were sequentially extracted using organic solvent, mild base and acid extraction. A summary of the procedure is presented in Figure 2.1, which outlines the sequential extraction technique detailed below.

Culture Preparation

M. smegmatis cultures were grown at 39°C. After incubation, cells were collected into pre-weighed 50 ml polypropylene tubes by centrifugation at 3000 rpm for 10 mins using a Jouan CR 1000 centrifuge. The cell pellet was then resuspended in 50 ml of 1 × PBS, harvested by centrifugation as before, and the resulting pellet weighed. Pellets from different source cultures were equalised for their weight by resuspending the pellet in a proportional volume of 1 × PBS and removing a portion of that volume to leave identical volumes in each sample. The equalised cell material was then recovered by centrifugation. The cell pellets were either stored away at -20°C, or immediately subjected to the extraction process.

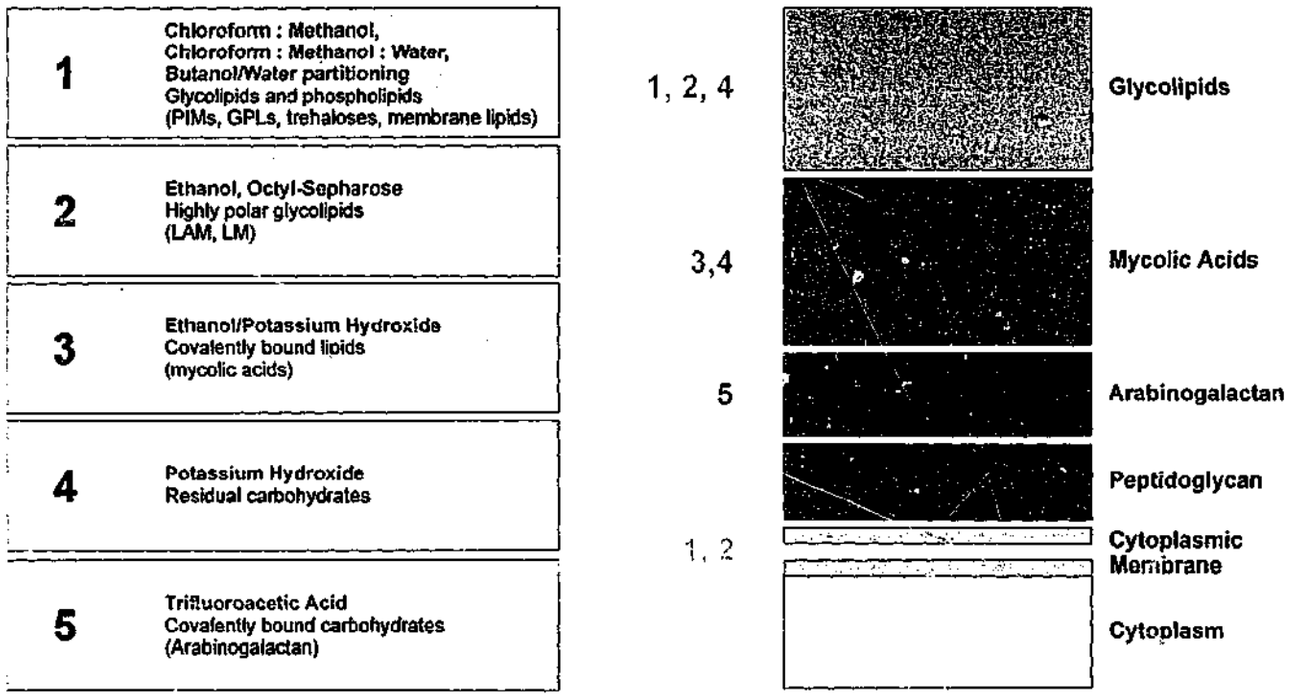

Figure 2.1
Overview of the sequential extraction process of *M. smegmatis* cell envelope components.
To obtain fractions of the *M. smegmatis* cell envelope, a series of extractions were performed in the order shown at left of the figure. Each part of the procedure was expected to isolate cell envelope components such as those listed with each extraction step. (PIM: phosphatidylinositol mannoside; GPL: glycopeptidolipid; LAM: lipoarabinomannan; LM: lipomannan). The likely source of the material extracted with each step is outlined in relation to the general structure of the cell enevelope, shown to the right of the figure.

relation to the general structure of the cell enevelope, shown to the right of the figure.

Extraction of Non-Covalently Bound Lipids and Glycolipids

The lipid extraction process used for this study was derived from the method described by Folch *et al.* (70). Cell pellets were resuspended in a volume of chloroform : methanol (2 : 1, v/v) which was equivalent to 20 times the pellet weight. Approx. 10 acid-washed glass beads (0.4-0.6 mm, Sigma) were added to the cell suspension. The cells were then shaken for two hours at room temperature using a Dynamax Flask Shaker set at a moderate speed. Following incubation, the cells were recovered by centrifugation (3000 rpm, 10 mins), and the solvent supernatant decanted to a new tube. The pellets were then resuspended in a fresh volume of chloroform : methanol (2 : 1, v/v), and shaken for a further two hours as before. The cells were again harvested by centrifugation, and the resulting solvent supernatant pooled with the previous solvent extract. The remaining pellet was then resuspended in chloroform : methanol : water (1 : 2 : 0.8, v/v/v), using the same volume as that used for the previous two chloroform : methanol (2 : 1, v/v) extractions. The cells were incubated and recovered as above. The resulting chloroform : methanol : water (1 : 2 : 0.8, v/v/v) extract was decanted and stored in a new tube. Both chloroform : methanol (2 : 1, v/v) and chloroform : methanol : water (1 : 2 : 0.8, v/v/v) extracts were stored at -20°C until required.

Butanol Partitioning

Butanol-water partitioning was employed in order to remove salts from the solvent extracts. The resulting butanol phase was expected to contain lipidic molecules including PIMs, GPLs, and LOSs. The aqueous phase was likely to contain more polar, glycosylated compounds such as LMs and various glycans. Two ml of pooled chloroform : methanol (2 : 1, v/v) and 1 ml of chloroform : methanol : water (1 : 2 : 0.8, v/v/v) extracts were concentrated into a 1.5 ml polypropylene tube by evaporation under a stream of nitrogen (N_2) gas. One hundred µl of water and 200 µl of water-saturated 1-butanol were then added to the dried extracts to create a bi-phasic system. The tubes were vortexed for 30 seconds to emulsify the lipids, and centrifuged for 1 minute at 13000 rpm to separate the phases. The upper 1-butanol phase was removed to a new tube. One hundred µl of 1-butanol was added to the remaining lower aqueous phase, and the tubes vortexed and centrifuged as before. The upper 1-butanol phase was then pooled with the 1-

butanol phase from the previous partitioning. One hundred µl of water was then added to the pooled 1-butanol phases, and the tube re-vortexed and centrifuged as before. The resulting 1-butanol phase was removed to a new tube, while the remaining aqueous phase was pooled with the aqueous phase left over from the previous partitioning step.

Both the 1-butanol and aqueous phases were then concentrated by evaporation using a Savant Speed Vac Plus SC110A concentrator. The 1-butanol phase was resuspended in 20 µl of pure solvents lower phase (chloroform : methanol : water, 86 : 14 : 1, v/v/v) (70), while the aqueous phase was resuspended in 20 µl of water. In each case, resuspension of the lipids was achieved by vigourous vortexing or short bursts in a sonic bath (Decon F5300b). The lipids were stored at -20°C until required, and analysed by HPTLC (section 2.2.4) or GC-MS (section 2.2.5).

Alkaline Methanolysis of Extractable Glycopeptidolipids (GPLs)

Twenty µl of 1-butanol phase derived from the chloroform : methanol (2 : 1, v/v) extract was dried under N_2 and resuspended in 200 µl of 0.2 M NaOH in methanol. The reaction was incubated at 37°C for 1 hour, and neutralised by adding 1 M acetic acid to a pH of approx. 6.0. The amount of acetic acid needed to reach this pH was determined emperically each time. Once neutralised, the reaction was concentrated by evaporation under N_2, and butanol extracted as described above. The resulting 1-butanol phase was then analysed by HPTLC (section 2.2.4).

Ethanol Refluxing and Octyl-Sepharose Purification

The de-lipidated cell pellet was then refluxed in aqueous ethanol to extract non-covalently bound, highly glycosylated molecules. This extract was then passed through an octyl-sepharose column, which binds lipidic molecules. Highly glycosylated lipids such as LMs, LAMs and residual polar PIM species were expected to bind to the column, while components such as mannans and arabinomannans would be collected in the eluate. The bound and unbound material was then analysed for monosaccharide composition by methanolysis and subsequent GC-MS.

The extraction method used in this study is adapted from one described by Nigou *et al.* (144). The de-lipidated pellets were resuspended in 5 ml of freshly prepared 50% (v/v) ethanol, and approx. 5-10 anti-bumping granules (BDH

Laboratory Supplies) were added. The mixture was then refluxed by incubating the cells at 100°C for 2 hours. After refluxing, the cells were harvested by centrifugation (3000 rpm, 10 mins), and the refluxate supernatant removed to a new tube. The cell pellet was then resuspended in a fresh aliqout of 5 ml 50% (v/v) ethanol, refluxed again and re-centrifuged as before. The resulting supernatant was pooled with the refluxate from the previous step and stored at -20°C until required.

Purification of glycolipids from ethanol extracts was performed as follows. One ml of pooled refluxate was concentrated in a 1.5 ml polypropylene tube by evaporation under N_2. The dried material was then resuspended in 500 µl of 5% (v/v) 1-propanol / 0.1 M ammonium acetate, and applied to a 1 ml octyl-sepharose column (Amersham Pharmacia Biotech). Before the sample was applied, the column was equilibrated by flowing through 1 ml volumes of the following solutions: 4 × 5% (v/v) 1-propanol / 0.1 M ammonium acetate, 2 × 40% (v/v) 1-propanol, 2 × 50% (v/v) 1-propanol, 2 × 60% (v/v) 1-propanol, 4 × 5% (v/v) 1-propanol / 0.1 M ammonium acetate. The sample was then bound to the column for 10 minutes. Bound sample was then eluted from the column by passing through 1 ml volumes of the following solutions: 4 × 5% (v/v) 1-propanol / 0.1 M ammonium acetate, 2 × 30% (v/v) 1-propanol, 2 × 40% (v/v) 1-propanol, 2 × 50% (v/v) 1-propanol, 2 × 5% (v/v) 1-propanol / 0.1 M ammonium acetate. Each elution was collected into separate 1.5 ml tubes.

Twenty µl of each elution was then applied to a HPTLC plate as ten 2 µl aliquots. The plated was then stained with orcinol (section 2.2.4) to detect which fractions contained glycolipids. Typically, the first two 5% (v/v) 1-propanol / 0.1 M ammonium acetate elutions contained some material, which corresponds to glycolipids which were not bound to the octyl-sepharose. The second 30% (v/v) 1-propanol and first 40% (v/v) 1-propanol elutions also contained glycolipid, corresponding to material which was bound to the column and was eluted with the propanol. The elutions of interest were stored at -20°C until required.

Base Ethanolysis and Hydrolysis

With the cell pellet now largely devoid of glycolipids, a base hydrolysis was performed to cleave the covalent linkages between the mycolic acids and arabinogalactan. This was achieved by alkaline ethanolysis. The de-lipidated, refluxed pellets were resuspended in 2 ml of 0.1 M potassium hydroxide (KOH) in

ethanol and incubated at 37°C for 48 hours. The resulting extract was collected by removing the cells via centrifugation (3000 rpm, 10 mins), with the supernatant being removed to a new tube. The cells were then resuspended in 2 ml of chloroform : methanol (1 : 1, v/v), and incubated at room temperature for 1 hour with shaking. The solvent was recovered by centrifugation and pooled with the 0.1M KOH in ethanol extract. Two point eight ml of water was then added to the pooled extract to create a biphasic system. The upper phase was neutralised by the addition of 1M hydrochloric acid, the amount required being determined empirically. Once neutralised, the lower phase was removed and added to a fresh tube.

Mycolic acid methyl esters (MAMEs) were generated by subjecting the KOH/ethanol extract to acidic methanolysis according to a method derived from one described by Minnikin *et al.* (132). Fifty µl of the lower phase was concentrated by evaporation and resuspended in 500 µl of toluene. Five hundred µl of methanol and 20 µl of sulfuric acid were then added, and the mixture incubated at 50°C overnight. After incubation, 200 µl of hexane was added to create a bi-phasic system. The tube was then vortexed, centrifuged briefly and the upper, hexane phase removed to a new tube. MAMEs partition to the hexane phase. MAMEs were then resolved by HPTLC (section 2.2.4).

The cell pellet was then subjected to a KOH hydrolysis, which is expected to extract any remaining non-covalently bound molecules left over after alkaline ethanolysis. The pellets were resuspended in 2 ml of 0.1M KOH and incubated at 37°C for 48 hours. The resulting extract was recovered by centrifugation (3000 rpm, 10 mins) and the supernatant transferred to a new tube. Twenty µl of the extract was then spotted onto a HPTLC plate as ten 2 µl aliquots. The plated was then stained with orcinol (section 2.9.1) to gauge an idea of the amount of sugar present in the extract. The resulting extracts were then examined for monosaccharide composition via methanolysis and GC-MS (section 2.2.5).

Mild Acid Hydrolysis

Mild acid hydrolysis was employed to remove the final layer of the envelope beyond the peptidoglycan. The treatment is expected to hydrolyse the acid-labile *N*-acetyl glucosamine-1-phosphate linkages attaching the arabinogalactan molecules to the cells peptidoglycan layer. The de-lipidated pellet

was resuspended in 1 ml of 40 mM tri-fluoroacetic acid (TFA) and incubated at 100°C for 12 mins. The resulting cell/hydrolysate mixture was dried down under N_2 and resuspended in 2 ml water. The cells were then harvested by centrifugation (3000 rpm, 10 mins) and the water removed to a new tube. The remaining cell pellet was hydrolysed again for a further 20 mins, dried, resuspended in 2 ml of water, and the cells harvested by centrifugation. The second water supernatant was then pooled with the first extraction. Twenty µl of the pooled extract was then applied onto a HPTLC plate and stained with orcinol (section 2.2.4) to detect the amount of sugar present in the extract. Qualitative and quantitative differences in arabinogalactan were then assessed by GC-MS compositional analysis (section 2.2.5).

2.2.4 *High Performance Thin Layer Chromatography (HPTLC)*

Resolving Glycolipids

GPLs and PIMs were examined by HPTLC and carbohydrate staining with orcinol/sulfuric acid to visualise the resolved glycolipids. In order to visualise PIMs, 4 µl of the 1-butanol phases from both the chloroform : methanol (2 : 1, v/v) and chloroform : methanol : water (1 : 2 : 0.8, v/v/v) extracts were applied onto a 10 cm silica gel 60 aluminium-backed HPTLC plate (Merck). The 1-butanol phases from both the chloroform : methanol (2 : 1, v/v) and chloroform : methanol : water (1 : 2 : 0.8, v/v/v) extracts were loaded as a combined sample.

The plates were then developed in a HPTLC tank (Alltech) using the solvent chloroform : methanol : 1 M ammonium acetate : 13 M ammonia : water (180 : 140 : 9 : 9 : 23, v/v/v/v/v). This was referred to as "Solvent System A". The HPTLC was developed until the solvent front was within 0.5 to 1 cm of the end of the plate. The plates were then allowed to dry and sprayed with orcinol stain (180 mg orcinol in 5 ml water, 75 ml ethanol, 10 ml sulfuric acid). The plates were baked at 100°C for 3 to 5 minutes to visualise the result.

When required, individual PIM species were purified as follows. PIMs were resolved by HPTLC using Solvent System A. Individual species were purified by scraping off strips of silica containing the PIM of interest and collecting the silica in a 1.5 ml tube. PIMs were eluted by incubating the silica in 200 µl of chloroform : methanol : water (10 : 10 : 3, v/v/v) for two hours, with

gentle agitation. The silica was then concentrated by centrifugation (13,000 rpm, 5 mins) and the solvent supernatant removed. A fresh 200 µl aliquot of chloroform : methanol : water (10 : 10 : 3, v/v/v) was then added to the silica, and re-incubated for a further two hours. The silica was again concentrated and the supernatant pooled with the first elution. The pooled eluates were dried down using the Savant Speed Vac Plus SC110A concentrator and resuspended in 50 µl of chloroform : methanol : water (10 : 10 : 3, v/v/v). Yield was assessed by running a sample of the purified PIM by HPTLC using Solvent System A. After development, the plates were stained with orcinol to visualise PIMs.

GPLs were resolved by loading 4 µl of the 1-butanol phase from the NaOH-treated glycolipids (section 2.2.3) onto a silica-backed HPTLC plate. The plates were developed in chloroform, dried, and re-developed in chloroform : methanol (9 : 1). This was referred to as "Solvent System B". The HPTLC was developed until the solvent front had migrated to within 0.5 to 1 cm of the end of the plate. The plates were then air dried and stained with orcinol.

Resolving Mycolic Acid Methyl Esters (MAMEs)

MAMEs were resolved by loading 40 µl of the hexane phase (section 2.2.3) onto a HPTLC plate. The plate was developed twice with petroleum spirits : diethyl ether (85 : 15, v/v), referred to as "Solvent System C". The plate was then air dried and sprayed with chromic acid stain (10 × stock: 5 g potassium chromate in 5 ml water, 95 ml sufuric acid; Diluted to 1 × with water for use). The plate was air dried and baked at 150°C for 15 mins to visualise the result.

2.2.5 Compositional Analysis

The monosaccharide composition of the sub-fractions described above were determined after cleaving sample components into constituent monosaccharides by acidic methanolysis. This reaction results in the formation of methyl glycoside products. The reaction products were then converted to tri-methylsilyl esters and analysed for monosaccharide composition by gas chromatography - mass spectroscopy (GC-MS).

Sample Preparation

Solvent-extracted glycolipids were prepared for compositional analysis as follows. The 1-butanol phases from both the chloroform : methanol (2 : 1, v/v) and

chloroform : methanol : water (1 : 2 : 0.8, v/v/v) extracts (section 2.2.3) were sampled directly for compositional analysis. The corresponding aqueous phases were dried and resuspended in 500 µl of water. The samples were then de-salted by passage through an AG_{50}/AG_3 column (Bio-Rad) (200 µl of each resin), freeze-dried, resuspended in 200 µl of water and the entire amount used for compositional analysis.

Glycolipids purified by octyl-sepharose were prepared for analysis as follows. The first two 5% (v/v) 1-propanol / 0.1 M ammonium acetate elutions, corresponding to glycolipids which were not bound to the octyl sepharose and the second 30% (v/v) 1-propanol and first 40% (v/v) 1-propanol elutions, corresponding to material which was bound to the column, were freeze dried. The "unbound" and "bound" samples were then pooled by resuspending one of each pair of tubes in 1 ml of water and adding the contents of the tube to its matching pair. The pooled fractions were then freeze-dried again. The resulting pooled "unbound" sample was resuspended in 1 ml of 5% (v/v) 1-propanol / 0.1 M ammonium acetate, while the pooled "bound" sample was resuspended in 1 ml of 30% (v/v) 1-propanol. The glycolipids were then sampled for compositional analysis. For most experiments, only the "bound" sample was analysed, as this represented the crude LM/LAM fraction. In these cases, equal amounts of the second 30% (v/v) 1-propanol and first 40% (v/v) 1-propanol elutions were sampled directly for compositional analysis.

To prepare the KOH and TFA extracts for compositional analysis, the extracts were freeze-dried and resuspended in water to their original volumes (i.e. 2 ml for the KOH extract, 4 ml for the TFA extract). An aliquot of the extract was then adjusted to a volume of 500 µl with water and de-salted through an AG_{50}/AG_3 column (200 µl of each resin). The resulting flow-through was collected, freeze dried and resuspended in 200 µl. One hundred µl was then sampled for compositional analysis.

Methanolysis

Each sample was combined with 10 µl of 0.1 mM *scyllo*-inositol (1 nmole) as an internal standard, and concentrated in a glass capillary tube by evaporation using a Savant Speed Vac Plus SC110A concentrator. For each experiment, a "standards" tube containing 10 µl each of *myo*-inositol, D-arabinose, D-mannose, D-

glucose, D-galactose and L-rhamnose (all 0.1 mM) was also included for each analyses. After drying, each sample was washed by resuspending in 15 µl of methanol and re-dried. Fifty µl of 0.5 M methanolic-HCl (Supelco) was then added to each tube. The methanolysis reactions were incubated under vacuum for 16 hours at 80°C. After incubation, the reactions were neutralised with 10 µl of fresh pyridine, then dried with the Savant Speed Vac Plus SC110A concentrator. Methanolysis products were stored at room temperature until required.

TMS Derivatisation

For compositional analysis, the methanolysis products were converted to their tri-methyl silyl derivatives by TMS derivatisation, which adds volatile tri-methyl sialyl groups to the methyl glycosides. The methanolysis products were resuspended in 15 µl of fresh derivatisation reagent (pyridine : hexamethyldisilazane (HMDS) : trimethylchlorosilane (TMCS), 9 : 3 : 1, v/v/v), and incubated for 30 mins at room temperature. Derivatisation reagent was evaporated under N_2, resuspended in 50 µl n-hexane, and sampled for GC-MS analysis.

Gas Chromatography-Mass Spectroscopy Analysis (GC-MS)

Samples were analysed using a Hewlett Packard HP6890 Series GC System and a 5973 Mass Selective Detector. The following running conditions were followed. The instrument commenced the analysis with an oven starting temperature of 140°C, held for 1 min. The oven temperature then increased at 5°C per min to 250°C, with a 10 min hold at 250°C. Temperature then increased at 15°C per min to 265°C and held for 5 mins at this temperature. The inlet temperature was held at 180°C and the transfer line into the MS unit held at 270°C.

The data generated provided information on the monosaccharide composition of each sample in relation to the included standards. Standard response factors were calculated by dividing the peak area of each sugar standard with the area of the *scyllo*-inositol standard. The amount of sugar in each sample was then calculated by dividing the peak area of each sugar in the sample with the standard response factor for that sugar. This figure was then divided by the area of the *scyllo*-inositol standard in that sample, giving the amount of sugar in the sample in nmole. These figures were then adjusted to represent compositional data in nmole/g

of wet weight cells. The calculated data from the GC-MS results in are included in Appendix 3.

2.2.6 The Effect of Culturing Conditions on Cell Envelope Composition

The affect of media on the biochemical composition of the transposon mutants MYCO481 and MYCO479 was tested by culturing the mutant through PPLO media. Single colonies were grown and isolated from either PPLO or Middlebrook 7H10 agar plates and further cultured in PPLO broth. The PIM profiles and LAM content of the mutants were then determined as described above in sections 2.2.3 to 2.2.5.

2.3 A Transposon Mutant with an Unstable Colony Morphology

2.3.1 MYCO479 and MYCO481: Two Mutants or One?

Initial Observations

The Tn*611* transposon mutant examined in this study was designated MYCO481. The mutant was initially selected on BY agar, which is similar in composition to LB agar. MYCO481 formed colonies that were approx. 0.5 mm in diameter compared to a typical 2 mm in diameter for wild-type *M. smegmatis* on these agar plates. The morphology of wild-type colonies did not change through subculture, retaining their size and surface properties. When MYCO481 was plated onto LB agar, a mixture of colonies were evident. A number of colonies similar in size to the wild-type were observed as a minority; however, small colonies of 0.5 to 1 mm in diameter formed the vast majority of colonies on the agar plate. These colonies were referred to as the "small" variants of the transposon mutant, while the mutant colonies which resembled the wild-type were referred to as the "large" variants. To discount the possibility that this observation was merely a result of contamination in the strain, isolated small colonies were subcultured onto fresh LB plates, and generated the same large/small colony mixture. When transposon mutant colonies of the large diameter were subcultured onto fresh plates, all of the resulting colonies retained the large morphology. Hence, it appeared that the small

colony form of the transposon mutant was unstable and gave rise to a mixture of small and large variants through subculture on LB agar.

To test if this phenomenon was evident in a different media, MYCO481 was plated onto modified PPLO agar. If the small colony form of the mutant is a result of a severely impaired cell envelope structure, it may not be able to propagate well on LB agar. PPLO is a media designed for culturing the more fragile, peptidoglycan-deficient *Mycoplasma* species, and hence may have been useful for culturing enfeebled mutants. The *M. smegmatis* wild-type was plated onto PPLO, and the resulting colonies were 3 to 4 mm in diameter. The morphology was maintained through subculture of the colonies. When the transposon mutant was plated onto PPLO agar, a homogeneous population of small, 0.5 to 1 mm diameter colonies were observed. Subculturing the small colony onto fresh media still resulted in a pure population of small colonies, but further subculturing of the small colony resulted in the emergence of the large colony variant. When the large colonies were isolated and subcultured, they remained large in size. These mutant colonies showed a similar diameter to those of the wild-type, but showed a more flattened colony. This result suggested that it was possible to isolate the small form of the transposon mutant on PPLO agar as a homogenous population.

MYCO481 and MYCO479

For the purposes of this study, the wild-type and the original MYCO481 transposon mutant were inoculated onto LB agar (Figure 2.2). A single colony of the wild-type was isolated and plated onto PPLO agar. This plate was then used to create a stock of the wild-type strain. The MYCO481 LB agar plate showed the typical mixture of large and small colonies. A single small mutant colony was isolated from the LB agar plate and subcultured twice on PPLO. The resulting colonies were collected and stored as "MYCO481", consisting of a homogenous population of the small colony variant of the transposon mutant. Similarly, a large mutant colony variant was chosen and inoculated onto a PPLO agar plate, and subcultured again to ensure purity. These colonies were then stored as "MYCO479" to distinguish from the original form of the MYCO481 mutant.

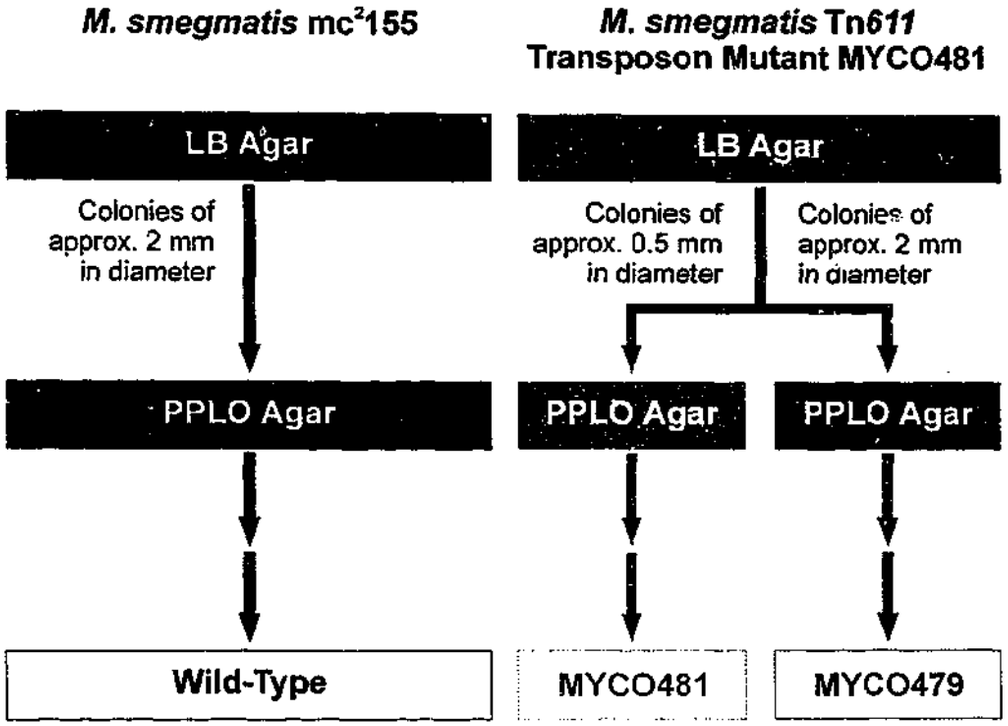

Figure 2.2
Derivation of strains used in this study.
M. smegmatis mc²155 (188) and the Tn*611* transposon mutant MYCO481 were plated onto LB agar. In the case of mc²155, a single colony was isolated and plated onto PPLO agar. This plate was used to create the "wild-type" stock used in this study. Plating the original MYCO481 stock onto LB agar resulted in a mixed population of "large" (approx. 2 mm in diameter) and "small" (approx. 0.5 mm in diameter) colonies. Each colony type was picked and streaked to purity on PPLO agar. The distinctive "small" colony form was designated "MYCO481", while the "large" colony form was called "MYCO479". Subculturing steps are represented by the arrows.

2.3.2 *Colony Morphology Varies in Different Media*

To confirm that the PPLO-derived stocks of the wild-type and the transposon mutants (MYCO479/MYCO481) produced the expected colony morphology after being stored, samples of the stock were serially diluted in PPLO broth and plated onto LB and PPLO agar. The strains were also plated onto Middlebrook 7H10 agar, which is a defined medium commonly used in the propagation of mycobacteria. When each strain was plated onto LB agar (Figure 2.3a), the expected colony morphologies were observed. The wild-type produced colonies of 2 mm in diameter. Plating MYCO481 resulted in the previously observed mixture of large and small colony variants, the small colonies being approx. 1 mm in diameter. The large colony form of the mutant, MYCO479, generated colonies which resembled those of the wild-type. On PPLO agar, the wild-type and MYCO479 produced colonies of approximately 3 to 4 mm in diameter (Figure 2.3b). Mutant MYCO479 formed colonies with a slightly less undulated surface morphology than those seen in the wild-type. Plating out MYCO481 resulted in a homogeneous population of small colonies, being 0.5 to 1 mm in diameter. Similar growth characteristics to this phenotype were also observed in liquid culture. When small, PPLO-derived colonies of MYCO481 were grown in PPLO broth, the culture grew more slowly and achieved a noticeably lower turbidity than that of the wild-type and MYCO479.

The strains were then plated onto Middlebrook 7H10 agar (Figure 2.3c). Surprisingly, each strain generated large colonies of 4 to 5 mm in diameter. As seen with PPLO agar, MYCO479 colonies showed a more flat surface morphology than the wild-type, while MYCO481 colonies looked identical to those of the wild-type. It was subsequently observed that subculturing each strain on Middlebrook 7H10 agar resulted in no variation in colony morphology. MYCO481 always yielded large colonies, as did the wild-type and MYCO479. No obvious growth differences were observed when the wild-type and mutant strains were grown in Middlebrook 7H9 broth.

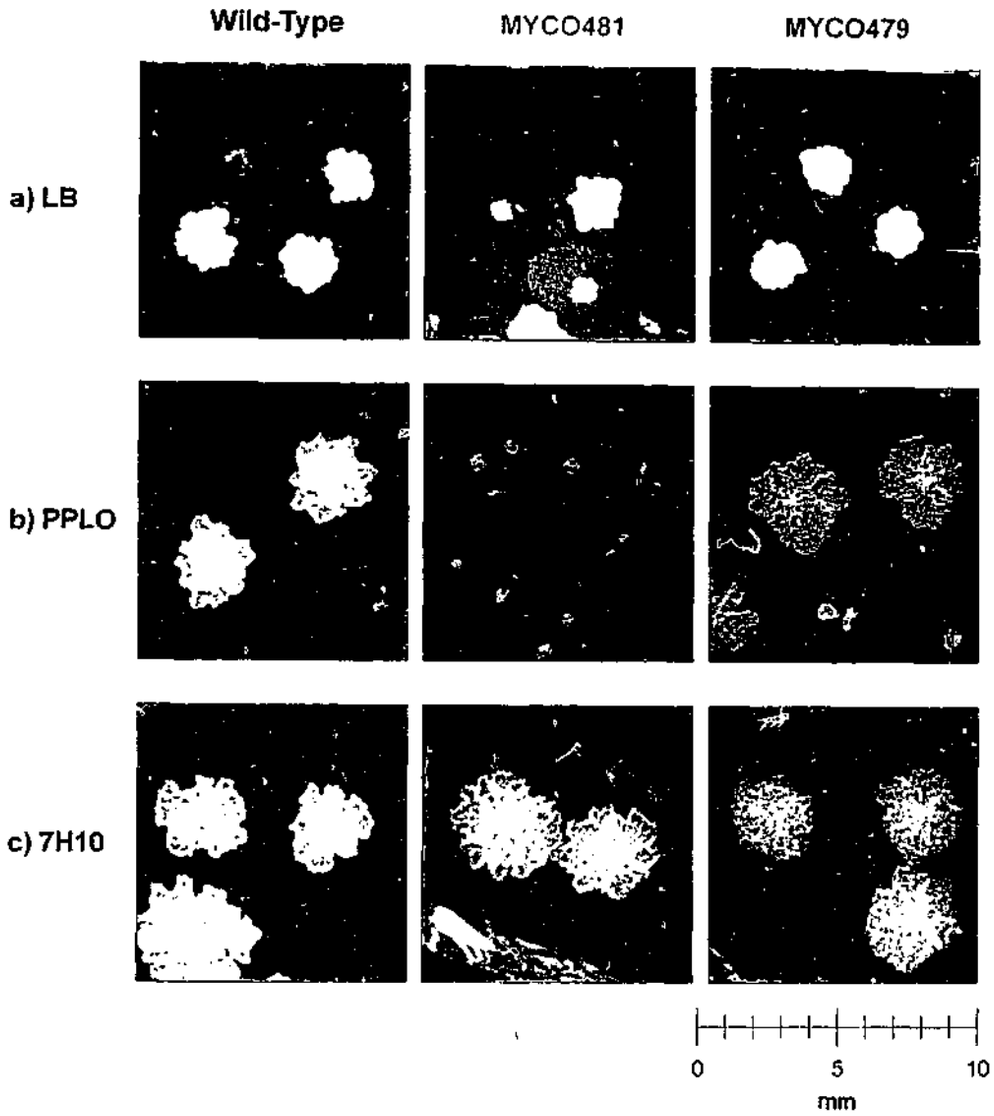

Figure 2.3
A transposon mutant with varying colony morphology.
The wild-type, mutant MYCO481 and mutant MYCO479 were serially diluted and plated out on three different media to assess colony morphology.

a) When plated onto LB agar, the wild-type and mutant MYCO479 generate large colonies of approx. 2 mm in diameter. Mutant MYCO481 typically generates a mixture of small (approx. 1 mm) and large (approx. 2 mm) colonies.

b) Plating each strain onto PPLO agar resulted in the wild-type and mutant MYCO479 generating large colonies of approx. 3 to 4 mm in diameter. When mutant MYCO481 was plated a homogeneous population of small colonies was observed, being 0.5 to 1 mm in diameter.

c) When plated onto Middlebrook 7H10 agar, all three strains generated colonies of approximately equal diameter (approx. 4 mm).

The scale is provided in millimetres (mm).

2.3.3 Colony Morphology in Different Culture Media Conditions

Each strain was grown under four different media conditions. Colonies that were grown on PPLO agar then subcultured into PPLO broth were designated as the "PPLO/PPLO" series, while those that were subsequently subcultured in Middlebrook 7H9 broth were designated "PPLO/7H9". Conversely, colonies which were initially grown on Middlebrook 7H10 agar then subcultured into Middlebrook 7H9 broth were designated the "7H10/7H9" series, whereas those that were subcultured in PPLO broth were called the "7H9/PPLO" series. Broth cultures derived from each of the culturing regimens were then serially diluted and plated onto PPLO and Middlebrook 7H10 agar. The number and size of the colonies that grew on the agar plates were then recorded (Table 2.1).

The wild-type and MYCO479 always formed large colonies irrespective of the medium used or the culturing regimen. MYCO481 formed exclusively large colonies on Middlebrook 7H10 plates, regardless of whether the source colony used to inoculate the broth was grown on PPLO (small colony) or Middlebrook 7H10 (large colony) agar. In contrast, MYCO481 cultures that were plated on PPLO agar resulted in a mixed population of small and large colonies, with small colonies predominating. These results indicated that cultivation in PPLO broth or Middlebrook 7H9 broth did not seem to influence the final colony morphology of MYCO481. Rather, MYCO481 formed small colonies on PPLO agar and normal, large sized colonies on Middlebrook 7H10 agar.

2.4 Transposon Mutants Show Novel PIM and LAM Composition

Since the colony morphology of MYCO481 is unaffected through subculture using Middlebrook 7H10 agar, and the morphology matches that of the wild-type and MYCO479, the media was used to grow the strains for biochemical analysis. The raw compositional data presented in this chapter is provided in Appendix 3.

Culturing Conditions	Colonies Counted on PPLO Agar	
	Large	Small
a) PPLO/PPLO		
Wild-Type	456	0
MYCO479	32	0
MYCO481	18	155
b) PPLO/7H9		
Wild-Type	81	0
MYCO479	121	0
MYCO481	0	83
c) 7H10/7H9		
Wild-Type	298	0
MYCO479	362	0
MYCO481	0	5
d) 7H10/PPLO		
Wild-Type	268	0
MYCO479	96	0
MYCO481	5	165

Table 2.1
Colony morphology observed on PPLO agar is maintained after changing culturing conditions.
The wild-type and the two transposon mutants MYCO479 and MYCO481 were grown under the following four culture conditions:

a) Colonies which were grown on PPLO agar then subcultured into PPLO broth were designated the "PPLO/PPLO" series;

b) Colonies which were grown on PPLO agar and were subcultured in Middlebrook 7H9 broth were designated the "PPLO/7H9" series;

c) Colonies which were grown on Middlebrook 7H10 agar then subcultured into Middlebrook 7H9 broth were designated the "7H10/7H9" series;

d) Colonies which were grown on Middlebrook 7H10 agar and were then subcultured in PPLO broth were called the "7H10/PPLO" series.

At the end of each round, the culture was serially diluted and aliquots were spread onto PPLO agar. Plates which yielded countable colony numbers were then scored for the number of small colonies and normal ("large") colonies.

2.4.1 Compositional Analysis of Glycolipid Extracts

Plasma membrane and cell wall lipids were initially extracted from the wild-type and mutant strains with chloroform : methanol (2 : 1, v/v), then recovered by bi-phasic partitioning in 1-butanol and water. Lipids of greater polarity were then extracted with the more polar solvent mixture of chloroform : methanol : water (1 : 2 : 0.8, v/v/v), and partitioned between butanol and water. The butanol and aqueous phases from each solvent extraction were then analysed for monosaccharide composition by GC-MS.

The data from the butanol partitioned material of the two solvent extractions were then combined for analysis (Figure 2.4a). The combined butanol phase was dominated by mannose, inositol and rhamnose. The inositol and mannose were likely to be derived from the ubiquitous PI and PIMs, which are expected to partition into the less polar butanol phase as they are phospholipids endowed with short oligosaccharides. The mutants MYCO481 and MYCO479 show mildly elevated inositol and mannose levels when compared to the wild-type. The rhamnose detected in the extract is likely to be derived from the other main envelope glycolipid species of *M. smegmatis*, the GPLs.

The compositional data from the aqueous phases of each solvent extraction was then combined for analysis (Figure 2.4b). This extract contained predominantly glucose, most likely derived from non-lipidic cytoplasmic or capsular glucans. To more clearly represent the relative abundance of other sugars, the glucose data is not presented in the figure (see Appendix 3). Small amounts of inositol and mannose were detected, possibly from the more polar PIM species such as PIM_6 which were not partitioned into the butanol phase (Figure 2.4a), as well as longer-chain LMs. MYCO481 extract contained almost twice as much mannose as the wild-type or MYCO479, but given the small amount of sugar extracted, the difference may not be significant. A small amount of galactose was also detected.

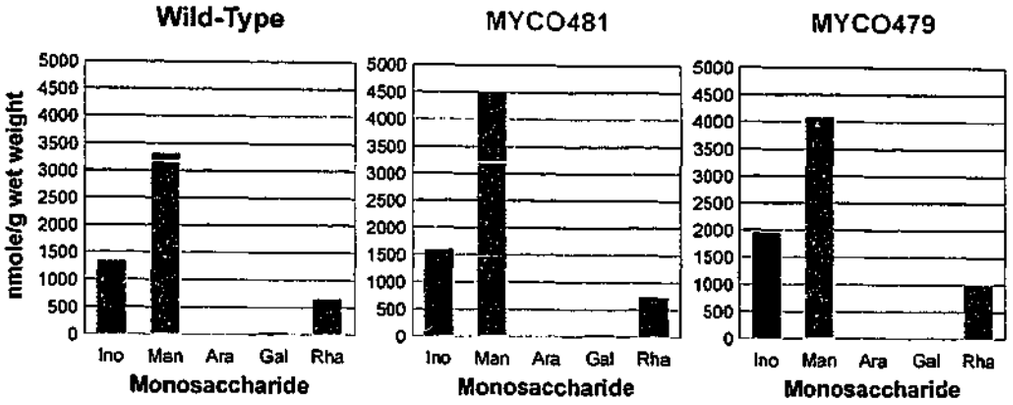

a) Combined Butanol Phases

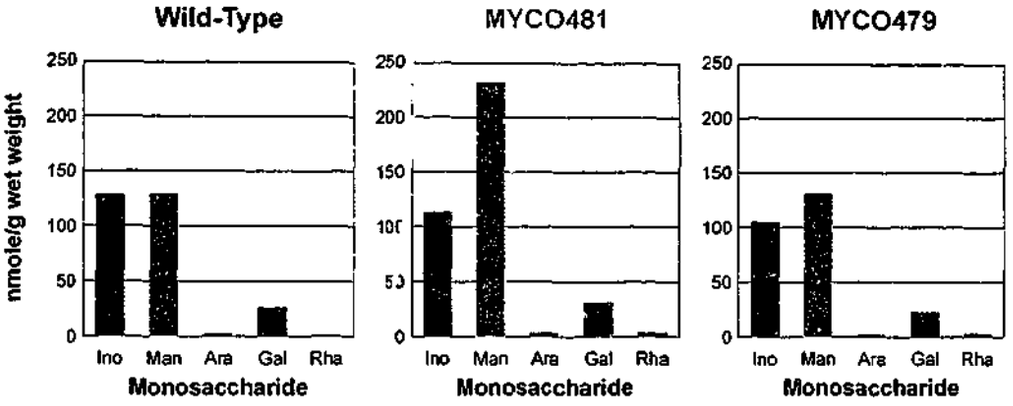

b) Combined Aqueous Phases

Figure 2.4
Compositional analysis of solvent-extractable lipids in *M. smegmatis*.
Cell pellets of the wild-type and mutant strains MYCO481 and MYCO479 were subjected to a solvent extraction with chloroform : methanol (2 : 1, v/v), then chloroform : methanol : water (1 : 2 : 0.8, v/v/v) to remove non-covalently bound lipids. The resulting extracts were dried and butanol/water partitioned. The butanol and water phases were subjected to methanolysis and analysed for monosaccaride composition by TMS-derivatisation and GC-MS. The monosaccharides presented are: *myo*-inositol (Ino), D-mannose (Man), D-arabinose (Ara), D-galactose (Gal) and L-rhamnose (Rha).

a) Combined values for the butanol phases of chloroform : methanol (2 : 1, v/v) and chloroform : methanol : water (1 : 2 : 0.8, v/v/v) extracts.

b) Combined values for the aqueous phases of chloroform : methanol (2 : 1, v/v) and chloroform : methanol : water (1 : 2 : 0.8, v/v/v) extracts.

The values given are nmole of sugar per gram of cell pellet wet weight (nmole/g wet weight).

2.4.2 HPTLC Analysis of Glycolipid Extracts

GPL Profile

In order to specifically examine GPLs, a sample of the butanol phase from the chloroform : methanol (2 : 1, v/v) extract was resolved by HPTLC. This fraction contained the most rhamnose, a key constituent sugar of GPLs (see Figure 2.4a). GPLs show heterogeneity due to acetyl groups which are variably attached to the glycolipid. To simplify the GPL profile, the lipids extracted with chloroform : methanol (2 : 1, v/v) were subjected to an alkaline methanolysis. The process cleaves ester-linked fatty acids and acetyl groups from glycolipids. In the case of GPLs, the acetyl groups are removed while the amide-linked fatty acid of the glycolipid is resistant to the process. De-acetylation acted to reduce the heterogeneity of the GPL pool and resulted in four GPL species designated GPL-1, GPL-2, GPL-3 and GPL-4. GPL-1 and GPL-2 correspond to de-acetylated species with a tri-methylated rhamnose, while GPL-3 and GPL-4 contain a di-methylated rhamnose. Further, GPLs –1 and –3 contain an additional *O*-methyl substituent on a hydroxyl group of the GPL fatty acid, accounting for their increased mobility compared to GPLs –2 and –4, respectively (155). Following alkaline methanolysis, each of the four GPL structures expected for *M. smegmatis* were observed (Figure 2.5), indicating that the mutants contained a GPL profile which resembles that of the wild-type.

PIM Profile

The butanol phases from the chloroform : methanol (2 : 1, v/v) and chloroform : methanol : water (1 : 2 : 0.8, v/v/v) solvent extracts were rich in inositol and mannose, and therefore likely to contain PIMs. Samples of these fractions were pooled and resolved by HPTLC (Figure 2.6). In the wild-type, four distinct glycolipid species dominated the sample, and were putatively identified as acylation variants of PIM_2 (PIM_2-A, -B) and PIM_6 (PIM_6-A, -B) in order of increasing polarity. PIM_2 and PIM_6 are the main forms of PIMs that accumulate in *M. smegmatis* (182). The PIM profile of MYCO481 resembled that of the wild-type. In contrast, extract from MYCO479 contained a distinctly different PIM profile. While the PIM_2 species were present, the PIM_6 variants were absent. Furthermore, MYCO479 accumulated two novel glycolipid species which were not

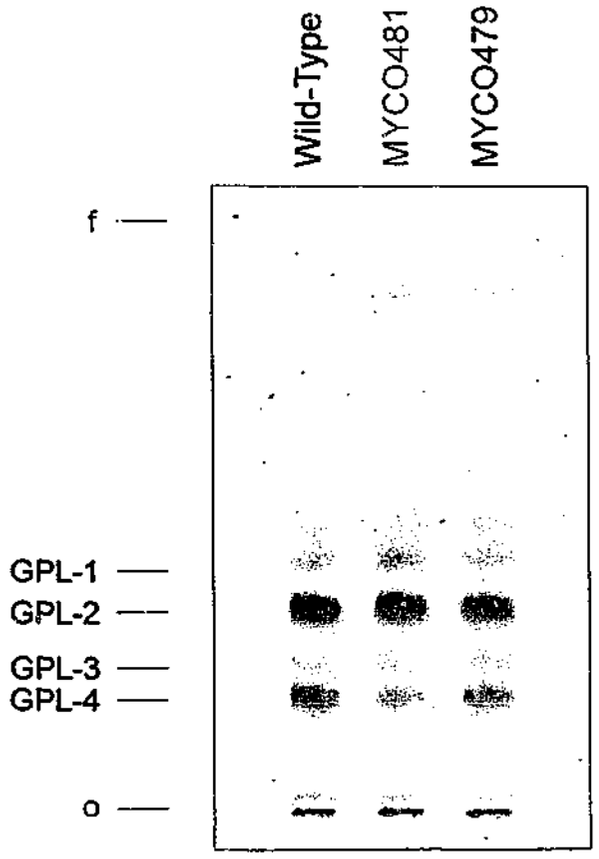

Figure 2.5
Analysis of *M. smegmatis* glycopeptidolipids.
Lipids of the wild-type and the mutants (MYCO481 and MYCO479) were extracted with chloroform : methanol (2 : 1, v/v), dried down and partitioned in butanol and water. Solvent extracts were subjected to deacetylation by alkaline methanolysis.

The plate was developed using Solvent System B and stained with orcinol to visualise glycolipids. Solvent System B resolves glycopeptidolipids (GPLs) (155).

Indicated are GPL-1 and GPL-2 (containing 2,3,4-methylated rhamnose), GPL-3 and GPL-4 (containing 3,4-methylated rhamnose). GPL-1 and GPL-3 contain an additional *O*-methyl substituent on the fatty acid hydroxyl group.

The sample origin is designated by an "o", while the solvent front is indicated by an "f".

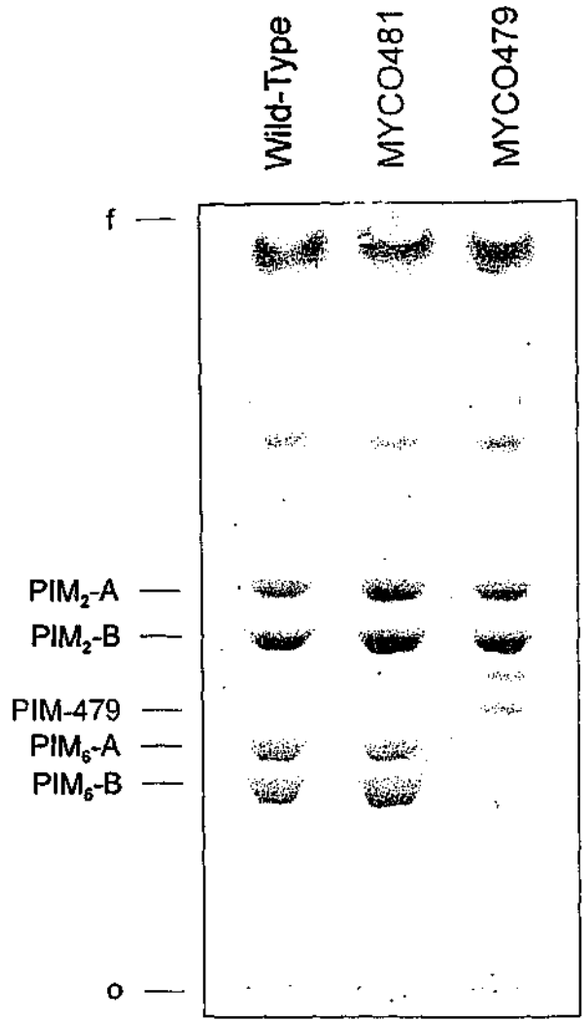

Figure 2.6
***M. smegmatis* MYCO479 lacks polar PIMs and accumulates a novel species.**
Lipids of the wild-type were extracted with chloroform : methanol (2 : 1, v/v) and chloroform : methanol : water (1 : 2 : 0.8, v/v/v). The extracts were partitioned in butanol and water. The butanol phase from each extraction was pooled, sampled and resolved by HPTLC. The plate was developed using Solvent System A and stained with orcinol to visualise glycolipids.

PIM-479 was only seen in MYCO479, which also lacked polar PIM_6 species.

The sample origin is designated by an "o", while the solvent front is indicated by an "f".

apparent in either the wild-type or MYCO481 extracts. The more polar of the novel species was putatively identified as a PIM, and named PIM-479.

2.4.3 MYCO479 Lacks PIM_6 and Accumulates PIM_4

In order to confirm the identity of the putative PIMs, a sample of butanol-partitioned chloroform : methanol (2 : 1, v/v) extract from the wild-type was resolved, and the individual bands corresponding to the four main PIM species were purified from the HPTLC plate. PIM-479 from the equivalent MYCO479 extract was also purified for analysis. The purified PIMs were subjected to GC-MS compositional analysis. The results showed that each species contained inositol, mannose, palmitic acid and tuberculostearic acid. This implied that each species was indeed a PIM. A sample set of data is shown in Figure 2.7a, showing the GC trace for PIM_2-B. The GC-MS analysis was performed by J. H. Pattesron (unpublished results).

A combination of electrospray ionisation - mass spectroscopy (ESI-MS) and matrix-assisted laser desorption ionisation - time of flight - mass spectroscopy (MALDI-TOF-MS) was used to determine the atomic mass of each PIM. By taking into account the observed atomic mass values and the relative polarity of each PIM by HPTLC, a predicted PIM structure was assigned and its corresponding predicted atomic mass calculated to determine the identity of each purified PIM. A sample set of data for purified PIM_2-B is presented in Figure 2.7b, while the data for each PIM is summarised in Table 2.2. The atomic mass of PIM_2-A matched that of a PIM_2 species with two palmitate chains in addition to the palmitic and tuberculostearic acid groups on the glycerol moiety of the structure, and was assigned the trivial name "Tetraacyl-PIM_2" (Ac_4PIM_2). PIM_2-B showed an atomic mass consistent with a single additional palmitate group distinct from those of the glycerol, and was named "Triacyl-PIM_2" (Ac_3PIM_2). Similarly, the atomic masses generated for PIM_6-A and PIM_6-B were consistent with two and one additional palmitic acid group, respectively. These PIMs were assigned the names "Tetraacyl-PIM_6" (Ac_4PIM_6) and "Triacyl-PIM_6" (Ac_3PIM_6). These results confirmed that the wild-type accumulates PIM_2 and PIM_6, each existing as two acylation variants. Since glycolipids of identical mobility were seen in MYCO481 extracts, it was assumed that this mutant contains a normal complement of PIMs.

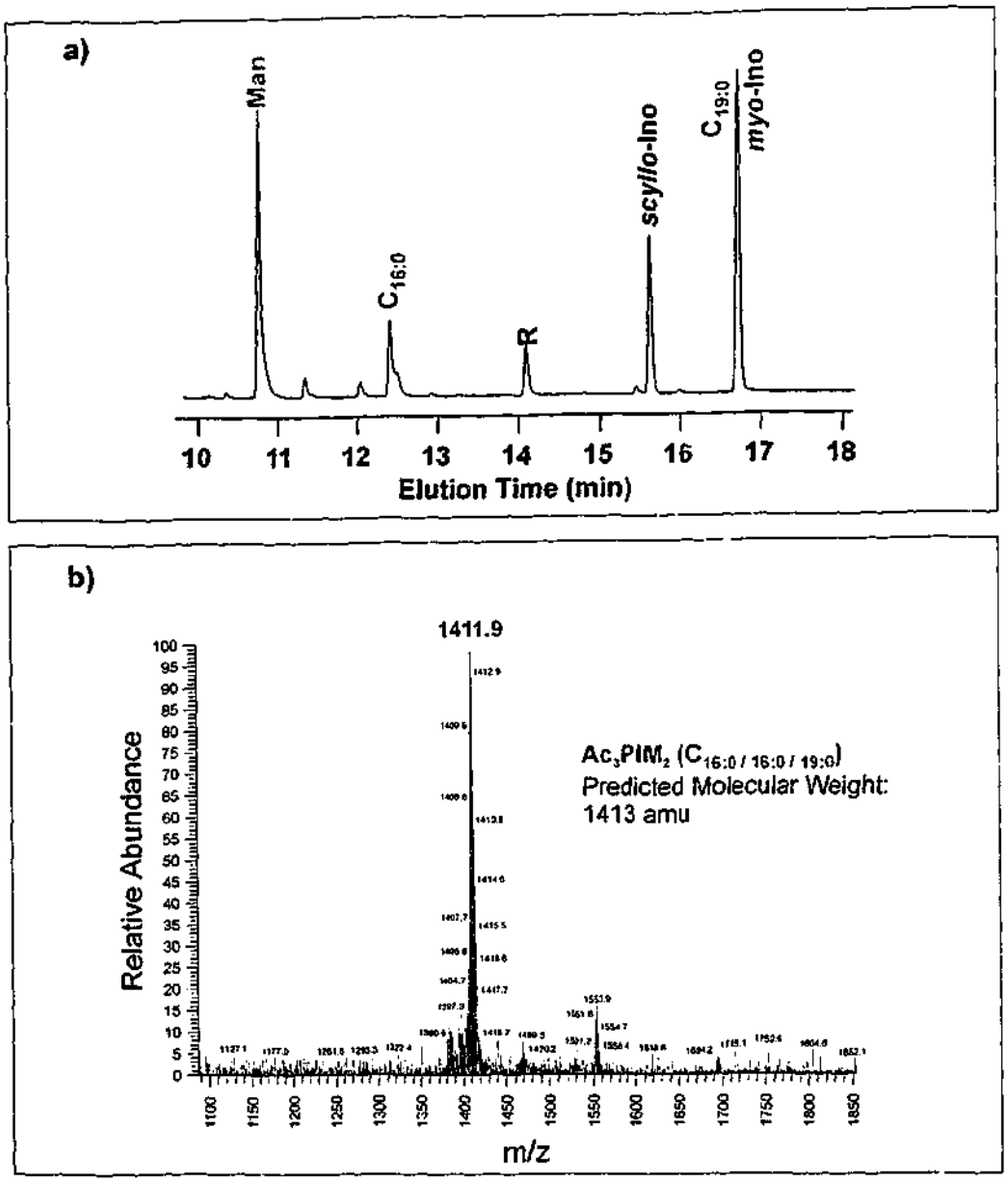

Figure 2.7
Identification of PIM_2-B as Ac_3PIM_2.
Glycolipids which were identified as putative phosphatidylinositol mannosides (PIMs) were purified by HPTLC and subjected to spectroscopy.
a) Gas Chromatography - Mass Spectroscopy (GC-MS) was used to provide compositional data for each putative PIM. The result presented shows that the species contained the key components of PIMs: α-D-mannose (Man), *myo*-inositol (*myo*-Ino), palmitic acid ($C_{16:0}$) and tuberculostearic acid (10-methyl octadecanoic acid, $C_{19:0}$). Peaks corresponding to a reagent component (R) and the internal standard *scyllo*-inositol (*scyllo*-Ino) are also indicated.
b) Electrospray Ionisation - Mass Spectroscopy (ESI-MS) was one of the techniques used to determine the mass of each PIM in atomic mass units (amu) represented by the mass/charge ratio (m/z). In this case, the atomic mass of the predominant ion closely corresponded to the predicted mass for Ac_3PIM_2. The data presented in this figure was generated by J. H. Patterson (unpublished results).

Glycolipid	Mass Spectroscopy				
	Predicted Structure	Predicted Mass (amu)	Observed Mass (amu)	Method	Trivial Name
PIM_2-A	$[C_{16}]_3C_{19}$-PIM_2	1651	1650.00	ESI-MS	Ac_4PIM_2
PIM_2-B	$[C_{16}]_2C_{19}$-PIM_2	1413	1411.90	ESI-MS	Ac_3PIM_2
PIM_6-A	$[C_{16}]_3C_{19}$-PIM_6	2298	2297.01	MALDI-TOF-MS	Ac_4PIM_6
PIM_6-B	$[C_{16}]_2C_{19}$-PIM_6	2061	2063.00	MALDI-TOF-MS	Ac_3PIM_6
PIM-479 (MYCO479)	$[C_{16}]_2C_{19}$-PIM_4	1737	1733.00	ESI-MS	Ac_3PIM_4

Table 2.2
Identification of PIM species.
PIM_2-A, PIM_2-B, PIM_6-A, PIM_6-B and PIM-479 were resolved by HPTLC using Solvent System A and purified.
The atomic mass of each PIM was determined by either Electrospray Ionisation - Mass Spectroscopy (ESI-MS) or Matrix Assisted Laser Desorption Ionisation - Time Of Flight - Mass Spectroscopy (MALDI-TOF-MS). Observed atomic masses were recorded in atomic mass units (amu). The observed atomic masses closely corresponded to predicted masses for the following PIMs: Ac_4PIM_2, Ac_3PIM_2, Ac_4PIM_6 and Ac_3PIM_6. Ac_3PIM_4 is unique to MYCO479.

The data presented in this table was generated by J. H. Patterson (unpublished results).

The mobility of PIM-479 did not match any PIM seen in the wild-type or MYCO481, and was therefore likely to a PIM of novel structure. The atomic mass of PIM-479 was consistent with a PIM species with four mannose residues and a palmitic acid residue in addition to the invariant palmitate and tuberculostearate on the glycerol. On this basis, PIM-479 was assigned the trivial name "Triacyl-PIM_4" (Ac_3PIM_4). Hence, MYCO479 accumulated Ac_3PIM_4, a novel species not seen in the wild-type or MYCO481.

The ESI-MS and MALDI-TOF-MS data was generated by J. H. Patterson (unpublished results).

2.4.4 MYCO481 Extracts Contain Reduced Amounts of LAM

Octyl-sepharose-bound material from ethanol extracts of each of the strains was expected to contain the hypermannosylated PIM, LM and LAM species. In order to compare LM/LAM content in each of the strains, octyl-sepharose-bound glycolipids as well as sample which did not bind to the octyl-sepharose ("unbound" fraction) were analysed for sugar composition by GC-MS.

The bound material was designated the crude "LM/LAM fraction". The major constituents in this fraction were mannose and arabinose (Figure 2.8a). When compared to the wild-type, MYCO481 showed a clear reduction in inositol, mannose and arabinose, which are the constituent sugars of LAM. Inositol was present at 26% of the wild-type, mannose at 24% and arabinose at 31%. The reduction in inositol, arabinose and mannose was observed over several analyses of MYCO481 crude LM/LAM material, with the mutant sugar levels typically ranging from 10-30% of those detected in the wild-type. This result suggests that MYCO481 has a LAM deficiency, with the trend being evident in subsequent LAM content data presented in later sections of this study. MYCO481 also showed a marked decrease in rhamnose, being present at 18% of that seen in the wild-type. The presence of rhamnose in this fraction was unexpected. GPLs are expected to be the main source of rhamnose, the majority of which were extracted with chloroform : methanol (2 : 1, v/v) (Figure 2.4). It is possible that the rhamnose was derived from a novel unidentified glycolipid, and it is unknown as to why the molecule would co-purify with LM and LAM.

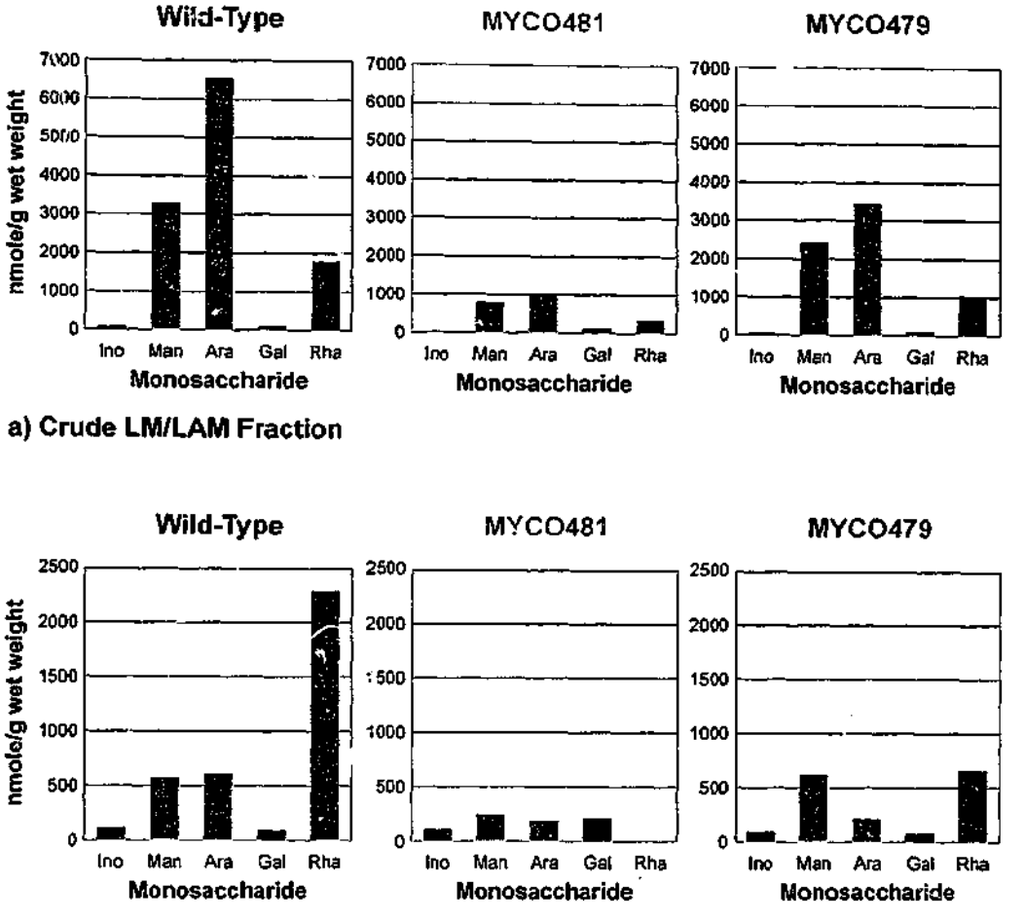

Figure 2.8
MYCO481 shows a deficiency in LAM-derived sugars.
The wild-type and mutant strains MYCO481 and MYCO479 were refluxed in 50% (v/v) ethanol to remove non-covalently bound glycolipids. Extracts were then sampled and passed through an octyl-sepharose column, which binds lipidic molecules.

a) Sample which bound to the column was collected and designated the crude lipomannan/lipoarabinomannan (LM/LAM) fraction;

b) Sample collected from washes of the column was designated the "Unbound" fraction.

The fractions were subjected to methanolysis and analysed for composition by TMS-derivatisation and GC-MS. The monosaccharides presented are: D-*myo*-inositol (Ino), D-mannose (Man), D-arabinose (Ara), D-galactose (Gal) and L-rhamnose (Rha). The values given are nmole of sugar per gram of cell pellet wet weight (nmole/g wet weight).

MYCO479 showed some reduction in the sugars which were likely to be derived from LAM. Inositol was present at 65% of that of the wild-type, mannose at 73% and arabinose at 52%. Based on these figures, it seems that MYCO479 contains less LAM than the wild-type, but not to the same extent as that seen for MYCO481. The mutant also showed reductions in galactose and rhamnose.

The "unbound" fraction (Figure 2.8b) contained predominantly inositol and mannose, although the amounts of sugar detected were generally less than those of the crude LM/LAM fraction. Interestingly, MYCO481 extracts showed a decrease in LM/LAM-derived sugars when compared to the wild-type. The source of these sugars is not clear, as LM and LAM are acylated and should therefore only be found as material bound to the octyl-sepharose. The sugars may correspond to deacylated LM/LAM, such as the reported *M. smegmatis* PI-GAM (77). Alternatively, hyperacylated LM/LAM may be forming micelles in solution that prevent them from binding to the octyl-sepharose and purifying with the bound, crude LM/LAM fraction described above. As with the crude LM/LAM fraction, the presence of rhamnose in the wild-type and MYCO479 and its complete absence in the MYCO481 fraction is interesting. The significance of this finding is unknown and worthy of examining in further detail.

2.4.5 Mycolic Acid Methyl Esters (MAMEs) and KOH Extraction

Mycolic acids were extracted from the wild-type strain and the mutants, and their corresponding methyl esters (MAMEs) were produced. *M. smegmatis* produces three types of mycolic acids: α-mycolic acid, which is ubiquitous amongst mycobacteria; α'-mycolic acid; and epoxy-mycolic acid (36, 64). MAMEs are methanolysis derivatives of mycolic acids which can be differentiated by HPTLC according to the different classes of mycolic acids (88).

The MAMEs derived from each strain were resolved by HPTLC and visualised (Figure 2.9). The results show that no obvious difference existed in the MAME profile for each strain, indicating that both MYCO481 and MYCO479 contain normal mycolic acids. The expected α- and epoxy-MAMEs are clearly present in each case, while the α'-MAME is not. The feint lipid migrating just below the α-MAME may represent the α'-MAME. The large amount of lipid

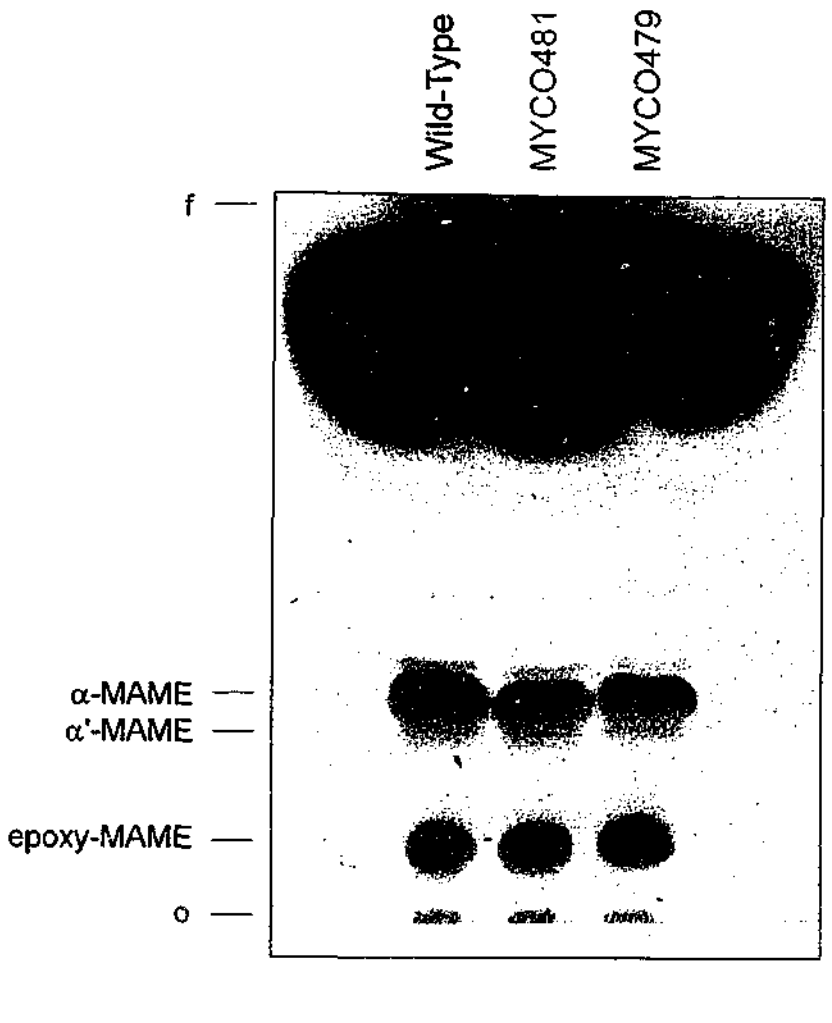

Figure 2.9
Mycolic acid methyl esters of *M. smegmatis*.
The mycolic acids of the wild-type and the mutants (MYCO481 and MYCO479) were extracted with ethanolic KOH. The extracts were then subjected to methanolysis to generate mycolic acid methyl esters (MAMEs). MAMEs were resolved by HPTLC using Solvent System C, stained with chromic acid and charred.

M. smegmatis should produce three distinct MAME derivatives of α-mycolate, α'-mycolate and epoxy-mycolate (64). The α-MAME and epoxy-MAME were apparent in all three strains; the α'-MAME may be migrating below the α-MAME.

The sample origin is designated by an "o", while the solvent front is indicated by an "f".

migrating near the solvent front may be non-hydroxylated fatty acid esters (64). With no obvious differences observed between the strains, these questions were not investigated further.

A compositional analysis was performed on the KOH extracts from each strain (Figure 2.10). The data showed that the extract contained very few carbohydrates. Although glucose, mannose and arabinose were the most predominant sugars in the extract, the relatively low amounts of sugar made it difficult to draw any significant conclusions. This data assured that the prior extractions of non-covalently bound glycolipids were complete.

2.4.6 Arabinogalactan Content

With the removal of non-covalently bound glycolipids (such as GPLs, PIMs and LAMs) and the integral, covalently bound mycolic acids, the major cell envelope component remaining beyond the peptidoglycan was expected to be arabinogalactan (AG). AG was extracted and subjected to a compositional analysis by GC-MS (Figure 2.11).

The results show that arabinose, galactose and rhamnose made up the bulk of the extract. The source of the rhamnose is unclear as the majority of the GPLs should have been removed with the chloroform : methanol (2 : 1, v/v) extraction. The rhamnose may be derived from the linker molecule which acts to covalently attach the cell envelopes AG to the peptidoglycan matrix (124). However, only one rhamnose residue per AG molecule is expected. Hence, the source of the rhamnose is unknown. The wild-type and MYCO481 showed approximately the same amount of arabinose and galactose, while the levels seen in MYCO479 were mildly reduced. Arabinose was present at 66% of the wild-type, with the galactose at 87%. These differences were not always apparent in separate AG compositional analyses, so it is unclear whether or not this difference is significant. MYCO479 also showed elevated glucose and mannose, but reduced rhamnose. Some differences in inositol levels were apparent, but the amounts extracted were small and hence the differences were probably negligible.

The published structure of AG contains 32 galactose residues and three 27-residue long arabinan chains (22, 50), resulting in a galactose : arabinose ratio of 1 : 2.53. The data from each strain indicates that approximately twice the expected

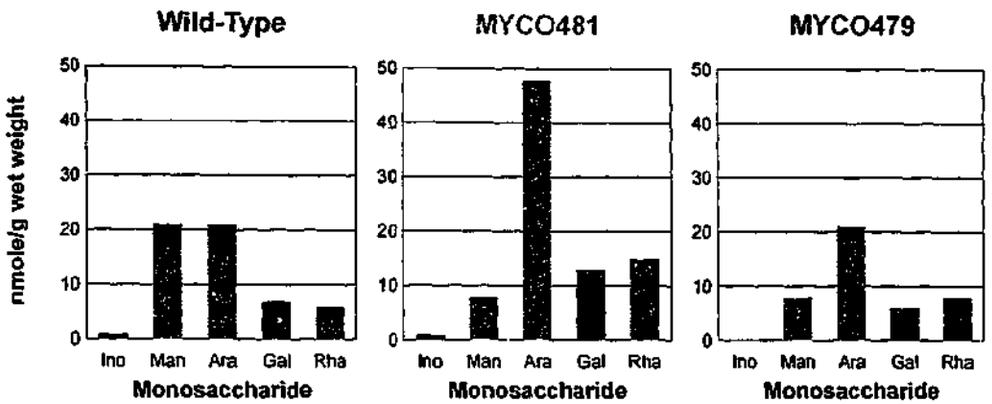

Figure 2.10
Compositional analysis of KOH-extractable carbohydrates from *M. smegmatis*. Following mycolic acid extraction, remaining non-covalently bound molecules were extracted from the wild-type and mutant strains MYCO481 and MYCO479 with 0.1 M KOH. Extracts were then sampled and subjected to methanolysis. Methanolysis products were analysed for composition by TMS-derivatisation and GC-MS.

The monosaccharides presented are: *myo*-inositol (Ino), D-mannose (Man), D-arabinose (Ara), D-galactose (Gal) and L-rhamnose (Rha).

The values given are nmole of sugar per gram of cell pellet wet weight (nmole/g wet weight).

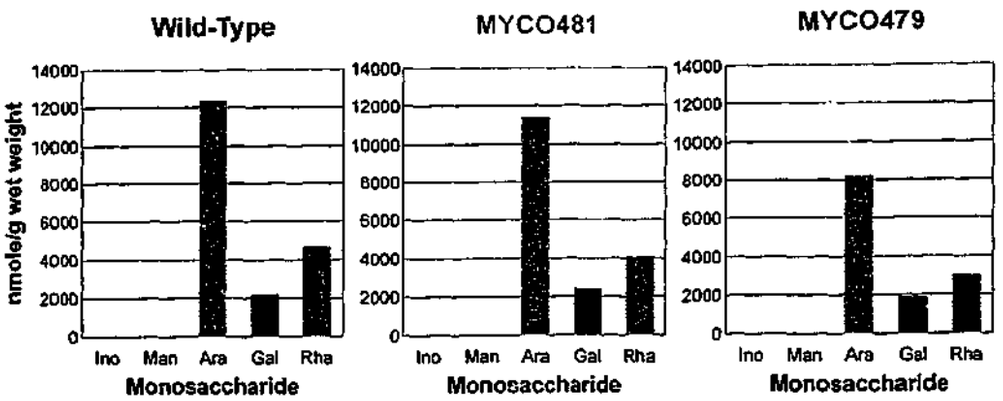

Figure 2.11
Compositional analysis of arabinogalactan-containing extracts from *M. smegmatis*.
Remaining covalently bound molecules were extracted from the wild-type and mutant strains MYCO481 and MYCO479 using tri-fluoroacetic acid (TFA) hydrolysis. Extracts were then sampled and subjected to methanolysis. Methanolysis products were analysed for composition by TMS-derivatisation and GC-MS.

The monosaccharides presented are: *myo*-inositol (Ino), D-mannose (Man), D-arabinose (Ara), D-galactose (Gal) and L-rhamnose (Rha).

The values given are nmole of sugar per gram of cell pellet wet weight (nmole/g wet weight).

amount of arabinose is present, perhaps derived from additional cell envelope arabinans in the extract.

2.5 PIM and LAM Deficiency in PPLO Media

The gross phenotypic differences seen for MYCO481 depending on the media used raised the possibility that different media conditions may result in different biochemical phenotypes. An experiment was designed to determine if the PIM-deficient phenotype of MYCO479 and the LAM-deficient composition of MYCO481 observed in cultures grown in Middlebrook media were maintained after cultivation in PPLO media. As described in section 2.3.3, media conditions were alternated from Middlebrook to PPLO media to test if this had an effect on the PIM/LAM phenotype. Wild-type, MYCO481 and MYCO479 colonies that were grown on Middlebrook 7H10 agar and subsequently inoculated into PPLO broth were designated as the "7H10/PPLO" series, while colonies grown on PPLO agar and subcultured into PPLO broth were referred to as the "PPLO/PPLO" series.

2.5.1 Growth Observations

To observe any gross qualitative differences in growth characteristics, a visual inspection of the culture was made at the conclusion of each culturing condition. In both cases, the growth of MYCO479 showed no obvious difference in final culture density to that of the wild-type, regardless of the culturing regimen. In contrast, MYCO481 cultures showed distinct growth differences to the wild-type. When a phenotypically small colony derived from PPLO agar was cultured in PPLO broth, the culture density was markedly lower than that of the PPLO-cultured wild-type. When a MYCO481 colony grown on Middlebrook 7H10 agar was cultured in PPLO broth, final culture density was greater than that of the culture inoculated with a PPLO-derived colony, but still markedly less than that of the wild-type. This may have been a result of the Middlebrook 7H10-derived colony providing a larger inoculum. Consistent with the observations of section 2.3.3, this result implied that PPLO media resulted in smaller colonies and lower yield in liquid broth than that seen for Middlebrook 7H9/7H10. The PIM and LAM content of each culture was then examined.

2.5.2 PIM Profiles

The PIMs extracted from the 7H10/PPLO series culture pellets were resolved by HPTLC (Figure 2.12a). The resulting profiles showed that when each strain was grown in PPLO broth, the same PIM profiles were observed as those derived from cultures grown in Middlebrook 7H9 broth (as shown in Figure 2.6). The wild-type and MYCO481 show a normal complement of PIMs, while MYCO479 shows the characteristic Ac_3PIM_4 species and a lack of PIM_6. The PIMs extracted from the PPLO/PPLO series showed the same results (Figure 2.12b), where MYCO479 retained its unique PIM profile when colonies were initially grown on PPLO agar and subcultured into PPLO media.

2.5.3 LAM Content

LAMs were extracted, purified and subjected to GC-MS compositional analysis (Figure 2.13). The results for the 7H10/PPLO series show that MYCO481 retained its LAM deficient phenotype. In comparison to the wild-type, MYCO481 LAM extract contained 6% as much inositol, 3% mannose and less than 1% arabinose. These deficiencies are far greater than those observed for cultures grown in Middlebrook 7H9 media (see Figure 2.8). MYCO479 also showed a greater reduction in LAM, where the constituent inositol (45%), mannose (51%) and arabinose (33%) were all reduced when compared to the wild-type. The LAM deficiencies were also evident in the PPLO/PPLO cultures. MYCO481 extracts yielded 4% as much inositol, 7% mannose and 2% arabinose as that seen in the wild-type. MYCO479 LAM extracts contained 34% inositol, 63% mannose and 35% arabinose when compared to the wild-type.

These results suggested that the PIM/LAM phenotype observed in cultures grown in Middlebrook 7H9 media was also apparent in PPLO-cultured strains, despite the fact that the two media result in very different colony morphologies for MYCO481. Cultures grown in PPLO media, however, seem to show an exaggerated LAM deficiency.

2.6 A Unique PIM/LAM Phenotype

The results presented in this chapter show that a Tn*611* transposon mutant is able to generate two different colony types on LB and PPLO agar. The "small"

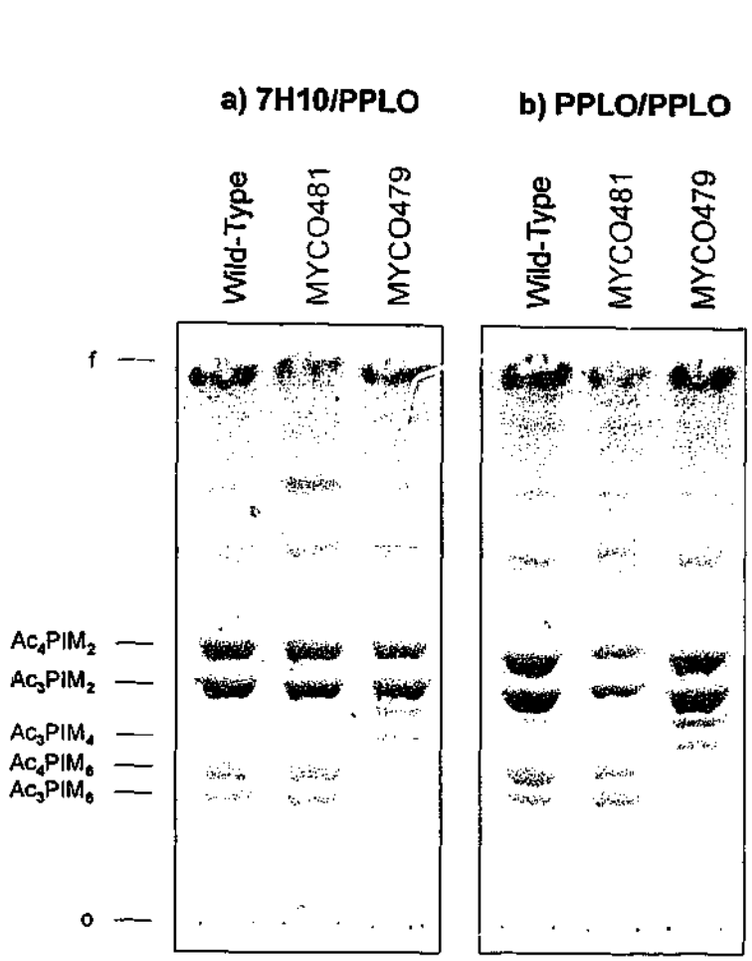

Figure 2.12
MYCO479 PIM profile is maintained in PPLO media.
The wild-type and the mutants (MYCO481 and MYCO479) were grown under the following conditions:

a) Colonies which were grown on Middlebrook 7H10 agar then subcultured into PPLO broth were referred to as the "7H10/PPLO" series;

b) Colonies which were grown on PPLO agar then subcultured into PPLO broth were designated the "PPLO/PPLO" series.

PIMs were extracted with chloroform : methanol (2 : 1, v/v) and resolved by HPTLC. The plate was developed using Solvent System A and stained with orcinol to visualise glycolipids.

The predominant PIMs are indicated. The sample origin is designated by an "o", while the solvent front is indicated by an "f".

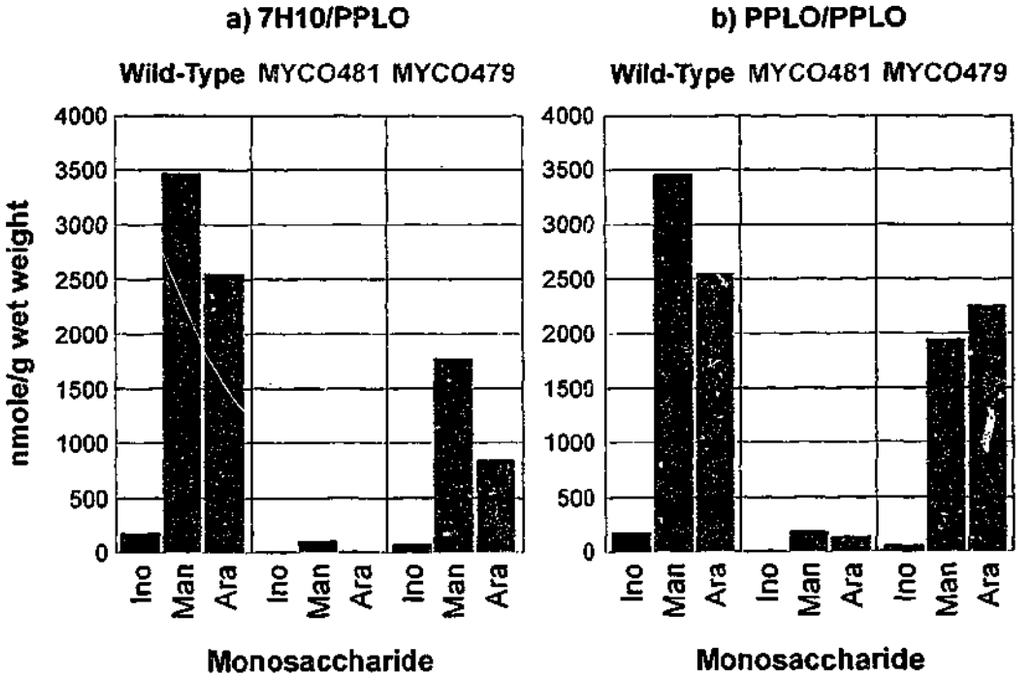

Figure 2.13
MYCO481 LAM deficiency is maintained in PPLO media.
The wild-type and the mutants (MYCO481 and MYCO479) were grown under the following conditions:

a) Colonies which were grown on Middlebrook 7H10 agar then subcultured into PPLO broth were referred to as the "7H10/PPLO" series;

b) Colonies which were grown on PPLO agar then subcultured into PPLO broth were designated the "PPLO/PPLO" series.

The resulting cell pellets were refluxed in 50% (v/v) ethanol. Extracts were then passed through an octyl-sepharose column, bound and subsequently eluted off the column.

The fractions were subjected to methanolysis and analysed for composition by TMS-derivatisation and GC-MS. The monosaccharides presented are the LAM constituents *myo*-inositol (Ino), D-mannose (Man) and D-arabinose (Ara). The values given are nmole of sugar per gram of cell pellet wet weight (nmole/g wet weight).

colony form of the mutant (MYCO481) does not appear to be stable in LB or PPLO, and eventually gave rise to a large colony type that resembles the wild-type colony morphology. The "large" variants of the mutant (MYCO479) appear stable in LB and PPLO media. The differences in colony morphology were not apparent in Middlebrook media, where both forms of the mutant yield colonies which resemble the wild-type. More interestingly, MYCO481 and MYCO479 contained cell envelope compositional abnormalities affecting the structurally related PIMs and LAM.

While MYCO481 extracts showed a normal complement of PIMs, the mutant was greatly deficient in LAM when compared to the wild-type. It is unclear as to whether the reduction in LAM content is a result of a reduction in the size of the molecules, or a reduction in the number of LAM molecules per cell. A reduction in the amounts of the key LAM constituents inositol, mannose and arabinose was always apparent in MYCO481 LAM preparations, implying a general reduction in LAM rather than the presence of truncated structural variants. This, however, is difficult to conclude in the absence of detailed structural data. The reported structure of *M. smegmatis* LAM contains a single inositol unit within the anchor portion of the molecule (95) attached to approximately 26 mannose units and 70 to 80 arabinose units (105), but the amount of mannose and arabinose is thought to vary in a LAM population which is likely to be heterogeneous in its composition (42).

In the unbound fractions, an inositol : mannose : arabinose ratio of 1 : 5.2 : 5.4 was observed for the wild-type. This suggests that more inositol and mannose are present than can be accounted for from the predicted structure of LAM. These ratios may be reflective of *M. smegmatis* PI-GAM or its non-arabinosylated precursors. PI-GAM is a form of LAM where the PIM-based anchor does not show acylation (77), and therefore may bind poorly to the lipid-binding octyl-sepharose. The additional structural variation of inositol capping on the arabinose branches may also vary the expected sugar ratio (77). It remains possible that the MYCO481 LAM contains truncated mannose and arabinose branches, with the inositol levels appearing low due to the reduction or absence of inositol capping. A detailed examination of the structure of MYCO481 LAM will further address this issue.

MYCO479 extracts also demonstrated PIM and LAM compositional defects, several of which were distinct from MYCO481. The most striking difference between MYCO479 and MYCO481 was found to be in the PIM profile. MYCO479 did not produce Ac_4PIM_6 or Ac_3PIM_6, and accumulated Ac_3PIM_4. This PIM did not accumulate in the wild-type or MYCO481. While it was demonstrated that PIM_6 was clearly absent in MYCO479, the absence of PIM_5 was not confirmed as the migratory location of PIM_5 by HPTLC was not investigated. It is possible that acylation variants of PIM_5 co-migrate with variants of PIM_4 and/or PIM_6. The ESI-MS and MALDI-TOF-MS data on the purified PIM_4 and PIM_6 species demonstrated masses which were very close to the hypothetical masses of the predicted PIM structures, implying that these species dominated the sample. The presence of PIM_5 in the mass spectra was not apparent (J. H. Patterson, unpublished results). If PIM_5 species co-migrated with PIM_4 or PIM_6 and were therefore not distinguished by the HPTLC developing system used for this study, alternative approaches can be attempted. A two-dimensional solvent system may help to resolve this limitation. Alternatively, the release and analysis of the size of the oligomannosyl head groups will determine the possible contribution and abundance of PIM_5 species in the observed PIM profiles.

The accumulation of Ac_3PIM_4 in MYCO479 also resulted in the accumulation of another, less polar glycolipid which did not accumulate in the wild-type or MYCO481. The identity of this PIM was not determined, but is likely to be a PIM_3 species or an acylation variant of PIM_2 or PIM_4. Given that the lipids migration in relation to Ac_3PIM_4 is similar to the difference in migration between Ac_4- and Ac_3PIM_6, it is possible that this lipid is Ac_4PIM_4. MYCO479 extracts also contained a reduced amount of LAM when compared to the wild-type, but not to the extent of MYCO481. It is also possible that MYCO479 produces LAM that is structurally distinct from the wild-type while being similar in composition. Detailed structural studies would address this question.

The approach used in this study was mainly compositional and needs to be expanded to examine the yield and structure of the mutant LAM more closely. The extraction technique was successful in extracting the majority of PIM, LM and LAM from the cells, as the KOH and TFA-extracted fractions are essentially devoid of mannose. A limitation of the GC-MS compositional analysis was that

while low inositol, mannose and arabinose trends were reproducible, the absolute amounts of LAM sugars tended to vary between preparations. This was especially so for arabinose. Whether this variability is reflective of the extraction or analysis technique is not clear, while the possibility of contaminating PIMs which were not removed by the previous solvent extractions can not be eliminated.

A more detailed analysis of LAM can be achieved applying the methods described by Nigou *et al.* (144). The Nigou method involves a more meticulous extraction procedure where the de-lipidated pellet is refluxed in aqueous ethanol, then the remaining pellet disrupted by sonication and French Press methods. The disrupted pellet is then refluxed again. The resulting ethanol extracts are then subjected to various purification steps, including detergent solubilisation, enzymatic digestion, phenol extraction and gel filtration. The resulting extracts differentiate between parietal and cellular LM, AM and LAM pools, as well as PIMs, peptides and other sugars which are present in the original ethanol extracts. Applying this technique should result in a purer LAM preparation, and would also be useful for examining the question as to whether or not MYCO481 shows LAM deficiencies in parietal or cellular LAM pools. This question was not examined in this study. Alternative analysis techniques such as nuclear magnetic resonance (NMR) spectroscopy can be used to provide more detailed structural data (144). Alternatively, polyacrylamide gel electrophoresis (PAGE)-based approaches (96) can help to differentiate between LM and LAM and offer an insight on the heterogeneity of the MYCO481 LAM.

The PIM and LAM abnormalities of MYCO479 and MYCO481 were maintained under different media conditions. When grown in PPLO media, extracts from both mutants demonstrated a reduced amount of LAM in comparison to cultures grown using Middlebrook media. Growth of the mutants in Middlebrook may result in a change which increases LAM levels; it is possible that the nutritional environment of the media promotes greater LAM production in the mutants. When grown in PPLO, the LAM levels of MYCO481 may present a severe disadvantage to the cell's ability to grow. The apparent increase in LAM when the mutant is grown in Middlebrook may make the deficiency more tolerable to MYCO481, which consequently produces normal colonies on Middlebrook 7H10 agar. The reduced colony size on PPLO agar may be a result of a greatly

exaggerated LAM deficiency, which is less apparent on Middlebrook 7H10 agar. The exaggerated LAM deficiency observed in PPLO-cultured MYCO481 may be explained by different growth phases between PPLO and Middlebrook 7H9-derived cultures. The apparently slow or impeded growth of the mutant in PPLO media may be representative of an earlier point in the growth cycle of the mutant in comparison to wild-type or MYCO479 cultures inoculated at the same time. Nevertheless, MYCO481 still showed a major LAM deficiency in both media. No difference in the PIM profiles of each mutant was evident when the strains were grown in either media.

No other major compositional abnormalities were observed in either mutant. GPL profiles were normal, and the MAME profiles resembled the wild-type. AG-derived sugars were also not highly different to the wild-type. Some differences in sugar composition were observed in several extracts. It is possible but unlikely that environmental contaminants contributed to the variation in some of the sugar levels, the most likely contaminant being glucose. Given the cell envelope PIM and LAM abnormalities seen in the two mutants, it is also possible that these defects result in a change in the ability of different components to be extracted, either due to a compensatory change in envelope location or composition of the molecule itself. The biosynthesis of other cell envelope components may also be increased or reduced in response to the PIM/LAM deficiency.

The findings presented in this chapter led to the definition of the "PIM/LAM phenotype". In summary, the small, unstable colony morphology of MYCO481 coincides with a major reduction in LAM. In contrast, the normal colony morphology of MYCO479 coincides with a novel PIM profile, where variants of PIM_6 are absent while PIM_4 accumulates. These findings point to a link between the colony morphologies of each strain and their biochemical composition. It appears that a reduction in LAM has a great effect on colony morphology and perhaps cell growth, while a loss of PIM_6 does not.

Chapter 3
MYCO481 and MYCO479 Demonstrate Defects in PIM/LAM Biosynthesis

3.1 Rationale and Objectives

3.1.1 A Closer Examination of PIM and LAM

With a clear PIM deficiency in MYCO479 and a markedly reduced LAM content in MYCO481, it seemed apparent that the abnormalities seen in the two mutants are connected in the sense that they are defective in what is proposed to be a shared biosynthetic pathway between PIMs and LAM. The accumulation of the novel Ac_3PIM_4 in MYCO479 raises the possibility of a metabolic blockage resulting in the loss of PIM_5 and PIM_6 synthesis. Thus, PIM_4 may exist as a precursor in the wild-type. Alternatively, the apparent PIM biosynthetic defect in MYCO479 may be due to the inability of the biosynthetic enzymes to access their required substrates or intermediates in the cell. Mutants with aberrant PIM and LAM composition such as MYCO481 and MYCO479 provide a unique opportunity to observe the biosynthesis of the various PIMs, LAM and the pathway intermediates. An examination of the mutants ability to incorporate radio-labelled mannose and inositol into nascent PIM and LAM species could provide insights on the role of Ac_3PIM_4 in the biosynthetic pathway, and how its accumulation affects other parts of the pathway.

3.1.2 Aims of this Section

The aim of this chapter was to observe PIM and LAM biosynthesis in MYCO481 and MYCO479, with a view to determine whether or not aspects of the biosynthetic processes of PIMs/LAM in the mutants were comparable to the wild-type. Exponentially growing cultures of the wild-type and the mutants were examined for their ability to incorporate tritium-radiolabelled mannose and inositol in an *in vivo* labelling experiment. By monitoring the incorporation of the label over a time course, the biosynthetic order of events can be observed and metabolic

blockages may also be revealed. In a separate experiment, cell-free lysates were radiolabelled *in vitro* with a tritiated GDP-mannose sugar donor to examine the biosynthesis of polyprenol phospho-mannose donors and other PIM metabolic intermediates.

3.2 Materials and Methods

3.2.1 Chemicals, Reagents, Strains and Culture Conditions

Suppliers for chemicals and reagents used in this study are listed in Section 2.2.1 of Chapter 2. The strains used in this study are listed in Appendix 1. *M. smegmatis* culture was performed according to Section 2.2.2 of Chapter 2, with modifications described in detail below. Media formulations are included in Appendix 2.

3.2.2 Production of Actively Growing Cultures

Exponential growth conditions were defined by determining a growth curve for the wild-type and mutant strains, as grown in Middlebrook 7H9 media. *M. smegmatis* growth curves were carried out according to the protocol described by Meyers *et al.* (128), with minor modifications. For each strain, two 200 ml Middlebrook 7H9 broths were inoculated with 2 ml of starter culture which were equalised to 200 μg/ml protein. The broths were grown for 5 days at 39°C with constant agitation, with duplicate samples being taken throughout this period at various timepoints. Upon sampling, the cells were collected by centrifugation at 13000 rpm for 5 mins (Hereaus Biofuge Pico) and washed in 1 ml of 1 × phosphate buffered saline (PBS). The PBS was prepared from a 10 × stock, comprising of 80 g NaCl, 2 g KCl, 14.4 g Na_2HPO_4 and 2.4 g KH_2PO_4 per litre (pH 7.4). The resulting cell pellets were stored at -20°C for later analysis.

Once all of the samples had been collected and washed, the pellets were resuspended in 100 μl 1 M NaOH and incubated at 100°C for 10 mins to lyse the cells. The lysates were neutralised by adding 20 μl 5 M HCl, and adjusted to 1 ml with the addition of 880 μl 1 × PBS. The samples were centrifuged at 13000 rpm for 30 mins, and 800 μl of supernatant was removed for protein concentration measurement. The absorbance of each sample at 230 nm and 260 nm was measured

using a Pharmacia LKB Ultrospec III, with the samples being diluted with 1 × PBS when required. The protein concentration in μg/ml was determined using the equation [protein concentration] = (183 × A_{230}) – (75.8 × A_{260}). Samples with a protein concentration within the range of 6 to 225 μg/ml were deemed to be within the linear range of the assay, as described by Meyers *et al.* (128). Sample protein concentrations which measured below the detection range of the assay (6 μg/ml) were excluded from the data. A curve relating protein concentration (μg/ml) to sampling time was then constructed. Logarithmic growth phase was estimated from the resulting curve and taken as the point at which the cultures were growing optimally.

3.2.3 *Radiolabelling of PIMs and LAM*

In vivo *labelling*

PIM and LAM synthesis was examined *in vivo* by labelling actively growing cells with [^{3}H]mannose and [^{3}H]inositol. The destination of the mannose and inositol labels were followed using a pulse-chase approach. *M. smegmatis* cultures were grown to mid-logarithmic phase (section 3.2.2) in 200 ml Middlelbrook 7H9 broths at 39°C. Two aliquots of 25 ml from each culture were then harvested into a pre-weighed 50 ml tube by centrifugation (3000 rpm, 10 mins, 37°C; Beckman GS-6R centrifuge). The pellet weights were recorded.

Cultures were labelled and sampled as follows. Each of the pellets were resuspended in 5 ml of Sauton's minimal medium, pre-warmed to 39°C (see Appendix 2), and the cells collected by centrifugation (3000 rpm, 10 mins, 37°C). The pellets were then resuspended in 1 ml of pre-warmed Sauton's minimal medium and incubated at 39°C for 15 mins, with shaking. This step constituted a "starvation" period. Fifty μCi of [^{3}H]mannose (17 Ci/mmole specific activity, NEN Life Sciences) or [^{3}H]inositol (1.3 Ci/mmole specific activity, Dr. Malcolm McConville) were dried down into a 1.5 ml tube and resuspended in 100 μl of Sauton's minimal medium. At the end of the 15 minute starve period, the [^{3}H]mannose or [^{3}H]inositol was added to the culture, which was then further allowed to incubate at 39°C for 10 mins with shaking. This step was referred to as the "pulse". After the 10 minute pulse period, 5 ml of Middlebrook 7H9 media pre-

warmed to 39°C was added to the cells. A 1 ml sample was immediately taken and placed on ice. The cells were incubated for a further 6 hours, with 1 ml samples being taken at 30, 60, 120, 240 and 360 mins. This was referred to as the "chase" period.

Cells from each sample were harvested by centrifugation at 13000 rpm for 5 mins at 4°C, and the supernatant removed. Glycolipids were then extracted using two 800 µl extractions of chloroform : methanol (2 : 1, v/v) and one of chloroform : methanol : water (1 : 2 : 0.8, v/v/v), as outlined in section 2.2.3. The three extracts were concentrated by evaporation under N_2 into the one 1.5 ml tube, and partitioned in 1-butanol and water (section 2.2.3). Before being dried and resuspended, 20 µl of each of the 1-butanol and water phases were sampled and measured for radioactivity counts using a Tricarb 2100TR Liquid Scintillation Analyser, according to the manufacturers instructions. One ml of Packard Emulsifier Safe liquid scintillant was used for each sample.

The 1-butanol phases were dried in the Savant Speed Vac Plus SC110A concentrator, resuspended in pure solvents lower phase (chloroform : methanol : water, 86 : 14 : 1 v/v/v) proportional to the original culture pellet weight, and 10 µl was loaded onto a HPTLC plate. The plate was developed using Solvent System A (section 2.2.4). After development, the plate was scanned for radioactivity counts using an EG&G Berthold Automatic TLC Linear Analyser. The plate was then layered with EA Scintillant Wax (EA Biotech Ltd.) and exposed to Biomax MR film (Kodak) at -70°C. The film was developed with an All-Pro 100 film developer.

The de-lipidated pellets were subjected to refluxing in 500 µl 50% (v/v) ethanol, as outlined in section 2.2.3. The entire refluxate was evaporated under N_2, and purified using a 500 µl octyl-sepharose column (see section 2.2.3). The 30% (v/v) 1-propanol and 40% (v/v) 1-propanol elutions were set aside and measured for radioactivity counts using the Liquid Scintillation Analyser, according to the manufacturers instructions. Taking pellet weight into account, the equivalent of 20% of the eluted sample was counted.

In vitro *labelling*

M. smegmatis cultures were grown to mid-logarithmic phase (section 3.2.2) in 200 ml Middlebrook 7H9 broths at 39°C. The cultures were chilled on ice and

harvested in a 250 ml GSA tube by centrifugation (10000 rpm, 15 mins, 4°C in a Sorval RC5C centrifuge, Sorval Instruments). The resulting pellet was resuspended and washed in 10 ml of 50 mM HEPES/NaOH (pH 7.4), transferred to a pre-weighed 50 ml polypropylene tube and harvested (3500 rpm, 15 mins, 4°C; Beckman GS-6R centrifuge). The supernatant was discarded, and the cells were re-washed in 50 mM HEPES/NaOH (pH 7.4). The resulting pellets were then weighed and resuspended in sonication buffer (25 mM HEPES/NaOH (pH 7.4), 25% (w/v) sucrose, 2 μM leupeptin, 0.2 M *N*-α-p-tosyl-L-lysine chloromethyl ketone hydrochloride (TLCK), 2 mM ethylene glycol-bis(β-aminoethylether)-N,N,N,N'-tetraacetic acid (EGTA)) to give an equalised final cell concentration of 1 g per 5 ml.

Weight-equalised cell suspensions were then disrupted by sonication using a Soniprep 150 Sonicator. Sonication was applied as fifteen 30 second bursts at an amplitude of approx. 26 μm, with 30 second pauses between each burst. The cell preparation was kept on ice during the entire sonication procedure. The sucrose concentration of the lysates was then adjusted to 60% by adding 90% (w/v) sucrose, and 4.2 ml of the adjusted lysate was set aside for fractionation. The remainder of the lysate was frozen in liquid N_2 and stored as unfractionated material.

The lysate was then added to the bottom of an ultracentrifuge tube, and overlaid with an 8 ml sucrose gradient. The gradient was made using an Labconco Auto Densi-Flow gradient dispenser/fraction collector, and consisted of 60 to 25% (w/v) sucrose in 25 mM Hepes/NaOH (pH 7.4), 2 μM leupeptin, 0.2 M TLCK, 2 mM EGTA. The gradient tubes were then placed in an SW41 rotor and centrifuged at 35000 rpm for 20 hours at 4°C using a Beckman L-80 ultracentrifuge. After centrifugation, 500 μl fractions were collected from the top of the gradient into 1.5 ml tubes. Twelve fractions were collected, along with an "R" ("remainder") fraction which represented the bottom of the gradient where the sample was originally loaded. One hundred μl aliquots of each fraction were set aside, with the rest of the fraction being aliquoted, frozen in liquid N_2, and stored at -70°C.

Twenty μl from each fraction was sampled and tested for reflective index using a Zeiss Refractometer to assess whether a linear sucrose gradient was sampled. Reflective index values were converted to a density value (in g/cm^3),

extrapolating from a standard curve of known sucrose densities. Five µl of each fraction was also sampled and analysed for protein content using a bicinchonic acid (BCA) assay (Bio-Rad Laboratories), as per the suppliers instructions. A bovine serum albumin stock (BSA, 2 mg/ml) was diluted and used to construct a standard curve. The results of the assay were measured at 562 nm using a Bio-Rad Model 2550 EIA reader.

Separate fractions were sampled and labelled with GDP-[^{3}H]mannose (6.3 Ci/mmole specific activity, Dr. Malcolm McConville). For each reaction, 2µl of GDP-[^{3}H]mannose (equating to approx. 150,000 cpm/µl) was evaporated under N_2 into a 1.5 ml tube. Zero point nine µl of 250 mM $MgCl_2$ and 44.1 µl of lysate were then added and the reaction incubated at 37°C for 15 mins. The reactions were then inactivated and lipids extracted by the addition of 300 µl chloroform : methanol (1 : 1, v/v), giving a final ratio of chloroform : methanol : water (10 : 10 : 3, v/v/v). The lipids were extracted overnight at -20°C.

The extractions were centrifuged for 5 mins at 13000 rpm, and the supernatant removed to a new tube. The extract was then evaporated under N_2, and the dried material subjected to butanol-water partitioning (see section 2.2.3). The resulting butanol phase was then resuspended in 10 µl of chloroform : methanol : water (10 : 10 : 3, v/v/v) with the aid of the sonic bath and vortexing. Two µl of the extract was sampled and measured for radioactivity using the Tricarb 2100TR Liquid Scintillation Analyser. The remainder of the sample was applied to a HPTLC plate, and developed using Solvent System A (section 2.2.4). After development, the plate was scanned for radioactivity counts, overlaid with scintillant wax, exposed to film and developed as described above.

3.3 The Mutants Show Various PIM/LAM Biosynthetic Defects

3.3.1 Determining Exponential Growth Phase

To define the optimal growth conditions for each strain, a growth curve was determined. Colonies of each strain were grown on Middlebrook 7H10 agar and cultured in Middlebrook 7H9 broth. During incubation, timed samples were taken

and measured for their protein concentration (Figure 3.1). No major differences were observed in the growth curves for each strain. The mutant growth rates seemed to be slightly slower than the wild-type during the exponential phase. Based on this data, optimal growth conditions were defined. Both the wild-type and the mutants reached approximately equivalent exponential growth between 21 and 24 hours and stationary phase by 45 to 50 hours.

3.3.2 In vivo *Labelling*

A pulse-chase approach was used to examine *in vivo* biosynthesis in actively growing cultures, where the incorporation of [^{3}H]mannose and [^{3}H]inositol into PIM and [^{3}H]mannose into LAM metabolic intermediates was assessed.

PIM Biosynthesis

When pulsed with [^{3}H]mannose, the wild-type strain incorporated label into PIMs (Figure 3.2a, I). From the beginning of the time course, [^{3}H]mannose was incorporated into Ac_3PIM_2, Ac_4PIM_6, Ac_3PIM_6 and several other species. These probably represent the various PIM biosynthetic precursors. Throughout the sampling period, the amount of [^{3}H]mannose incorporation into the two PIM_6 species and Ac_3PIM_2 remained high in comparison to the other glycolipids and slightly increased over time. After 120 mins, [^{3}H]mannose was also eventually incorporated into Ac_4PIM_2. The accumulation of [^{3}H]mannose into the PIM_2 and PIM_6 species implies that they are metabolic end-products. By the end of the sampling period, mannolipids that were more polar than PIM_6 were also accumulating [^{3}H]mannose; these probably represent hyperglycosylated PIMs such as LMs. Interestingly, throughout the sampling period a relatively small amount of [^{3}H]mannose was also incorporated into a mannolipid which showed the expected migration of Ac_3PIM_4. This suggests that while Ac_3PIM_4 does not accumulate in cultures (see Figure 2.6), it is synthesised in the wild-type. It was also clear that the [^{3}H]mannose did not accumulate in Ac_3PIM_4 over time, implying that Ac_3PIM_4 is a PIM biosynthetic intermediate.

When the wild-type was labelled with [^{3}H]inositol (Figure 3.2b, I), most of the label is initially incorporated into what is likely to be PI, the primary phospholipid precursor for all PIMs and LAM (173). PI migrates closely with Ac_4PIM_2, but shows a slightly different HPTLC mobility than any of the PIMs and

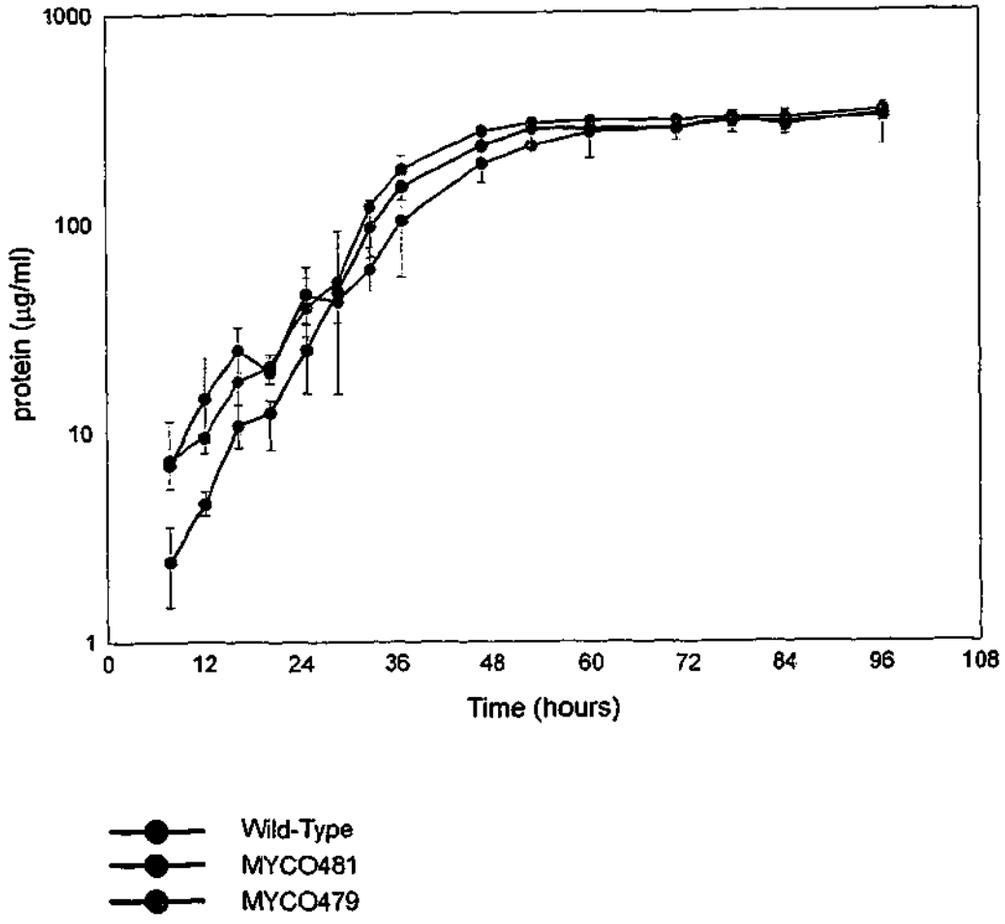

Figure 3.1
Definition of exponential growth in Middlebrook 7H9 media.
Cultures for the wild-type, MYCO481 and MYCO479 were grown to stationary phase (200 µg/ml protein concentration), inoculated into Middlebrook 7H9 broth 1 in 100, and incubated at 39°C. Samples of the growing culture were taken throughout the course of the incubation, and protein concentration in µg/mL of culture was estimated (128).

The cultures were grown in duplicate, with each culture being sampled twice (i.e. four samples per strain). The data was plotted as the mean of two duplicates, with the accompanying bars representing the maximum and minimum values for the set of four samples.

Cultures were found to be in exponential growth phase after 21-24 hours of incubation (indicated by the yellow bar), and were harvested at this point for subsequent metabolic labelling experiments.

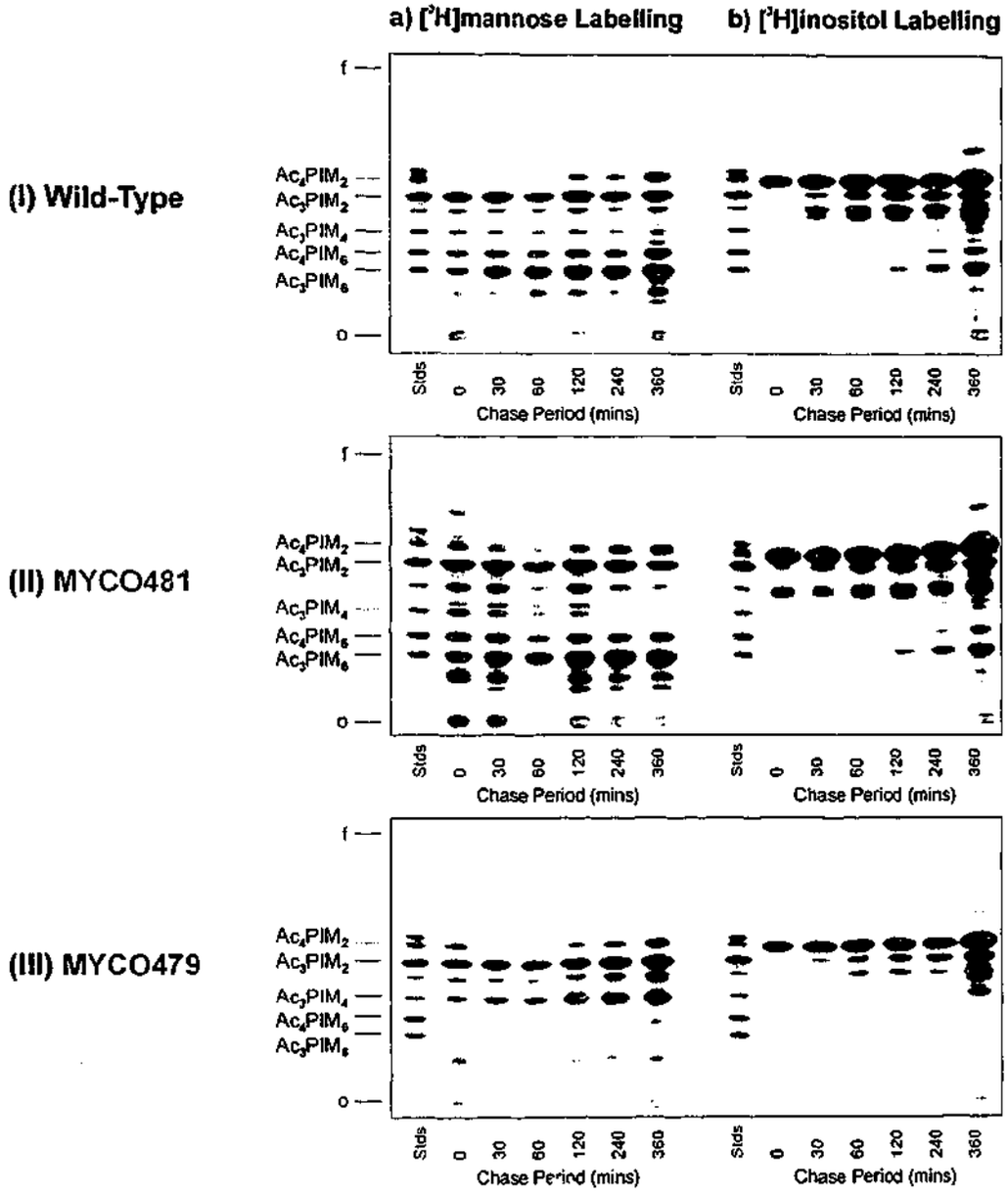

Figure 3.2
***In vivo* labelling of *M. smegmatis* PIMs.**
Actively growing cultures of (I) the wild-type, (II) MYCO481 and (III) MYCO479 were labelled with either a) [^{3}H]mannose or b) [^{3}H]inositol. After labelling, the cultures were grown in Middlebrook 7H9 media at 39°C, and the destination of the label "chased" for a period of 360 minutes. Culture samples were taken at set time points (indicated in minutes).
PIMs were extracted with chloroform : methanol (2 : 1, v/v) and chloroform : methanol : water (1 : 2 : 0.8, v/v/v), and partitioned in butanol and water. The butanol phases for each extract were sampled and resolved by HPTLC using Solvent System A to visualise lipids which had incorporated the label. A sample of [^{3}H]mannose labelled PIMs extracted from a labelled culture of the wild-type was included as standards (Stds). The plate was exposed to film to visualise label incorporation. The known PIMs are indicated. The sample origin is designated by an "o", while the solvent front is indicated by an "f".

does not appear to be labelled with mannose, consistent with the possibility that it is PI. From 30 mins, the [^{3}H]inositol becomes incorporated into Ac_3PIM_2 and lipids which migrate between Ac_3PIM_2 and Ac_3PIM_4. These may be the previously postulated PIM_3 species or acylation variants of PIM_2 and PIM_4. By 120 mins, the [^{3}H]inositol incorporated into PIM_6, which accumulates [^{3}H]inositol to the end of the sampling period. A species that appears to be Ac_3PIM_4 was synthesised after 120 mins, and did not accumulate as much [^{3}H]inositol as the PIM_2 and PIM_6 species. Hence, both the [^{3}H]mannose and [^{3}H]inositol labelling experiments show that Ac_3PIM_4 incorporates a small amount of label in comparison to PIM_2 and PIM_6, suggesting that Ac_3PIM_4 is a metabolic intermediate while PIM_2 and PIM_6 are metabolic end products. This is consistent with the abundance of PIM_2 and PIM_6 in lipid extracts from cultures when examined by HPTLC and carbohydrate staining, together with the apparent lack of Ac_3PIM_4 (see Figure 2.6).

Labelling of MYCO481 resulted in a similar overall [^{3}H]mannose incorporation profile to the wild-type (Figure 3.2a, II). However, some differences to the wild-type labelling were observed. There was greater incorporation of the [^{3}H]mannose into the highly polar potential LM species migrating below the PIM_6 species, as well as in PIM precursors migrating between Ac_3PIM_2 and Ac_3PIM_4. A similar trend was seen in the [^{3}H]inositol labelling of the mutant, where incorporation of the label into PI, Ac_3PIM_2 and the lipids migrating below PIM_2 was evident from the beginning of the time course (Figure 3.2b, II). The [^{3}H]inositol labelling characteristics of the PIM_6 species resemble those of the wild-type.

The labelling profile for MYCO479 showed a distinct difference to the wild-type and MYCO481. When pulsed with [^{3}H]mannose (Figure 3.2a, III), the label was mostly incorporated into Ac_3PIM_2 and Ac_3PIM_4. Towards the end of the sampling period, [^{3}H]mannose had gradually accumulated into Ac_4PIM_2 and Ac_3PIM_2. It was also apparent that the [^{3}H]mannose had also progressively accumulated in Ac_3PIM_4, a result not observed in MYCO481 or the wild-type. This implies that in MYCO479, Ac_3PIM_4 is present as a metabolic end product, while it acts as an intermediate in the other two strains. The [^{3}H]mannose also accumulated in mannolipids less polar than Ac_3PIM_4. This indicated that the accumulation of Ac_3PIM_4 as a metabolic end-product resulted from a blockage in the PIM

biosynthetic pathway, causing the accumulation of these other, less polar PIM precursors. If Ac_3PIM_4 represents the end of the PIM biosynthetic pathway in MYCO479, the more mannosylated PIM_5 and PIM_6 should not be synthesised. This was found to be the case. No incorporation of labelled mannose was evident in lipids which migrate at the expected positions of Ac_4- or Ac_3PIM_6.

Some incorporation of the [^{3}H]mannose was evident in bands more polar than Ac_3PIM_4. These showed a slightly different migration to the PIM_6 species and were probably short chain LMs. When MYCO479 was labelled with [^{3}H]inositol (Figure 3.2b, III), the eventual accumulation of the label in Ac_3PIM_4 was also evident, together with the lack of label incorporation into the PIM_6 species.

Incorporation of Label into LAMs

Crude LM/LAM extracts were analysed for the incorporation of [^{3}H]mannose. Incorporation of label in the form of radioactivity counts were plotted against the time of the sample during the chase period (Figure 3.3). Compared to the wild-type and MYCO479, MYCO481 showed little incorporation of the label throughout the sampling period. This is consistent with being a LAM-deficient strain and demonstrates that a reduced LAM biosynthetic activity contributed to the reduced amount of LAM end product, as observed in Chapter 2 (Figure 2.8). MYCO479 and the wild-type showed relatively similar increases in counts over time, with MYCO479 showing greater incorporation of [^{3}H]mannose at the final timepoint.

Incorporation of [^{3}H]inositol was found to be much lower than that observed for [^{3}H]mannose. This was consistent with the fact that LAM preparations should have very few inositol residues compared with mannose, which forms the long backbone of the molecule. The low counts would have contributed to a greater sampling error, and hence made it difficult to draw conclusions.

3.3.3 In vitro *Labelling*

Subcellular Fractionation

In order to examine further differences in PIM biosynthesis by the mutants, cell-free lysates and subcellular fractions were radiolabelled with GDP-[^{3}H]mannose. This experiment allowed the visualisation of PIM biosynthesis localised to fractions corresponding to the plasma membrane, where PIM

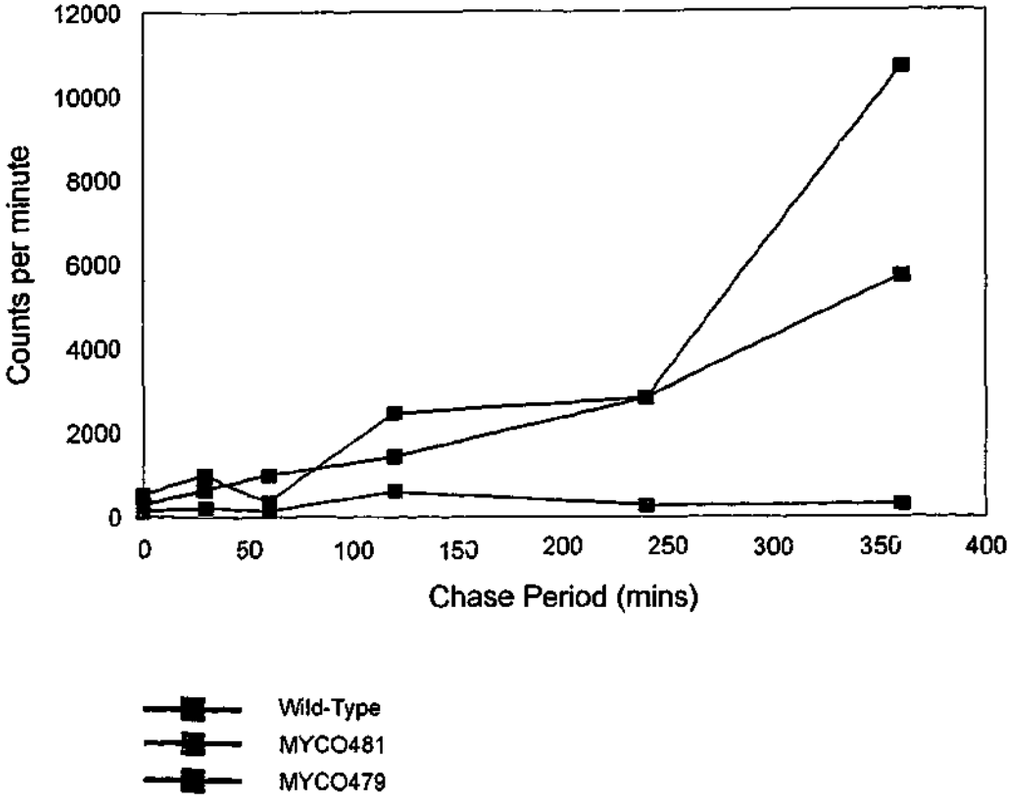

Figure 3.3
***In vivo* labelling of *M. smegmatis* LAMs.**
Actively growing cultures of the wild-type, MYCO481 and MYCO479 were labelled with [^{3}H]mannose. After labelling, the cultures were grown in Middlebrook 7H9 media at 39°C, and the destination of the label "chased" for a period of 360 minutes. Culture samples were taken at set time points (indicated in minutes).
The timed samples were extracted of PIMs and refluxed in 50% (v/v) ethanol to remove non-covalently bound glycolipids. The LAM-containing extracts were passed through an octyl-sepharose column. Sample which was bound and subsequently eluted off the column was subjected to scintillation counting to assess the amount of label incorporation. The counts were plotted against the time of the sample during the chase period, shown in minutes.

biosynthesis is likely to occur (173). Radiolabelling of polyprenol mannosides, which act as mannose donors in PIM biosynthesis, was also observed using this approach. The data for this experiment was generated with the co-operation of Dr. Y. S. Morita.

The sub-cellular fractions were analysed for their sucrose density and protein concentration (Figure 3.4). For each of the three strains, the sucrose concentration gradients were found to be near linear, with the top of the gradient being 1.08 to 1.09 g/cm^3 (corresponding to 23.6 to 25.5% (w/v) sucrose) and the bottom 1.23 to 1.24 g/cm^3 (55.2 to 57.2% (w/v) sucrose). This demonstrated that the sucrose gradients used for fractionating lysate from each strain were comparable. The protein concentration of each fraction was also assessed. In each of the three strains, protein concentration was relatively low for the first three fractions. A peak in protein concentration was observed around fractions 4 to 7 for the wild-type (corresponding to a sucrose density of 1.14 to 1.17 g/cm^3), fractions 6 to 9 for MYCO481 (1.14 to 1.19 g/cm^3) and fractions 4 to 8 for MYCO479 (1.13 to 1.17 g/cm^3). These fractions approximately corresponded to an opaque band which was visible after fractionation. This band possibly represents lipid and protein rich subcellular components, such as the plasma membrane. This peak is slightly lower for MYCO479 than in the wild-type, while the protein peak is shifted by two fractions in MYCO481. This is probably due to minor differences in the sucrose density for that particular fraction, resulting in slightly different fractionation pattern. From Fraction 10 onwards, a rise in protein concentration is seen for each strain. This is likely to represent denser membrane fragments and cytosolic material. The protein concentrations of the unfractionated material from each strain were found to be comparable, with the MYCO481 lysate being 7.52% more concentrated than the wild-type lysate, while MYCO479 was found to be 1.74% more concentrated. This demonstrated that the starting material for the subsequent fractionation and labelling experiment was equivalent.

Fractions 2, 4, 5, 6, 7, 9, 11, R and unfractionated lysate, designated "Fraction UF", were then radiolabelled by adding GDP-[^{3}H]mannose. After labelling, PIMs were extracted and resolved by HPTLC (Figure 3.5). The results show that the most efficient incorporation of the label into mannolipids coincided with the proposed membrane-enriched fractions (see Figure 3.4), which is

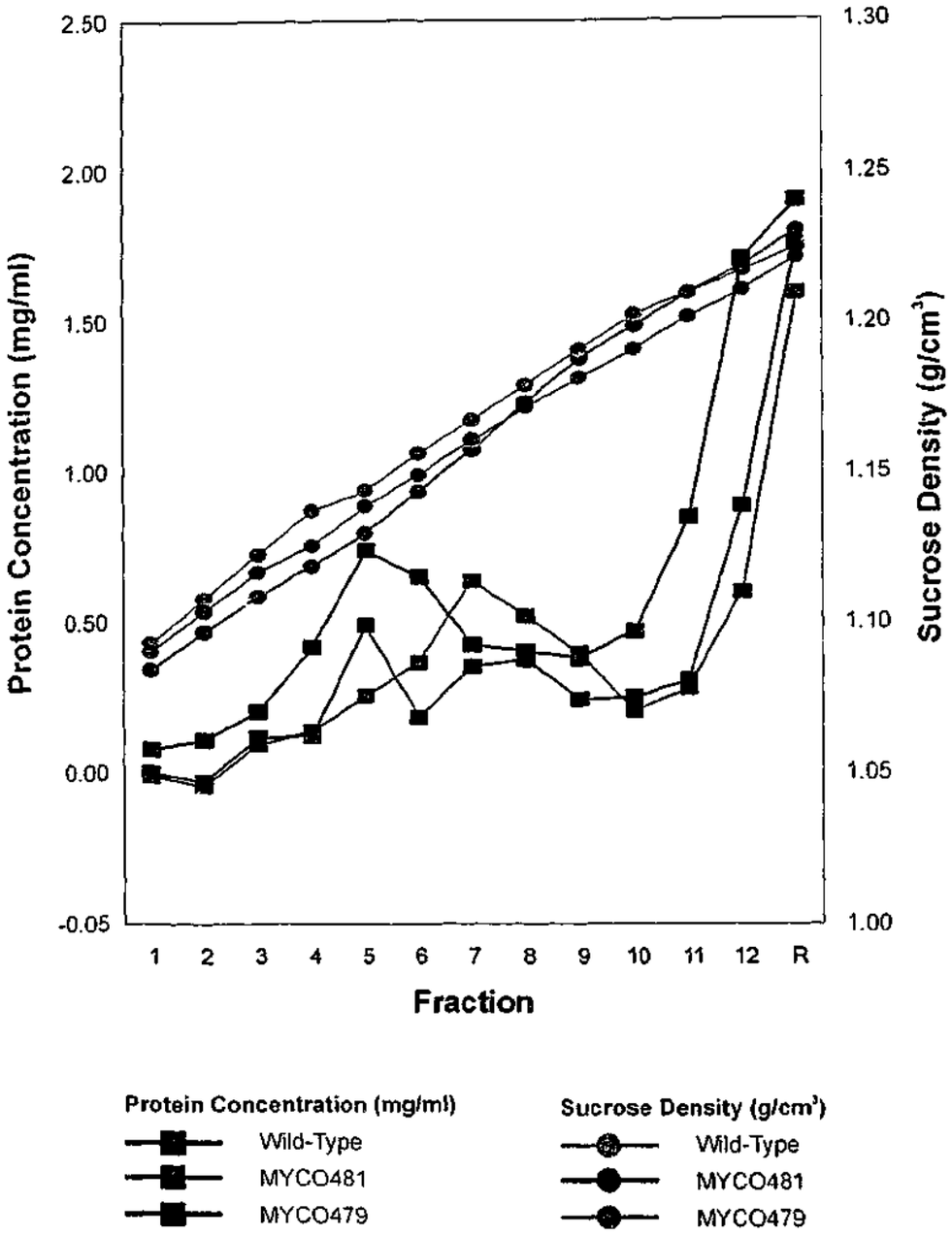

Figure 3.4
Analysis of *M. smegmatis* culture lysate fractions.
Actively growing cultures of the wild-type, MYCO481 and MYCO479 were lysed and fractionated in a 25-60% (w/v) sucrose gradient by ultracentrifugation. Fractions 1 to 12 were then collected from the top of the gradient, with Fraction R representing the remaining material at the bottom of the gradient.
Each fraction was assessed for its sucrose density by refractometry. The refractive indicies were converted to sucrose densities in g/cm^3. The protein concentration of each sample was also determined and expressed in mg/ml. Both the sucrose densities and the protein concentrations were then plotted against their corresponding fractions.

Sucrose Density (g/cm³)

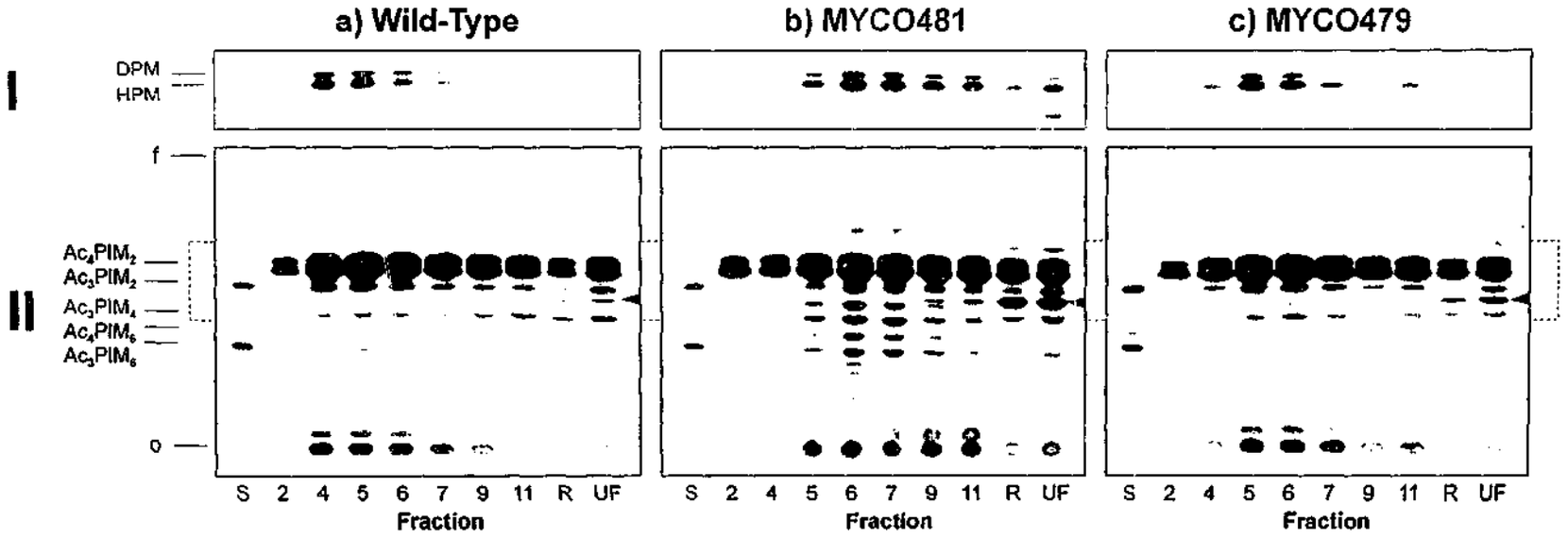

Figure 3.5

MYCO481 and MYCO479 show PIM biosynthetic defects.

Actively growing cultures of a) the wild-type, b) MYCO481 and c) MYCO479 were lysed and fractionated in a 25-60% (w/v) sucrose gradient by ultracentrifugation. Fractions 2, 4, 5, 6, 7, 9 and 11 along with remaining material from the bottom of the gradient (Fraction R) and unfractionated lysate (UF) were then labelled with GDP-[^{3}H]mannose. PIMs were extracted with chloroform : methanol : water (10 : 10 : 3, v/v/v) and the extracts resolved by HPTLC developed using Solvent System A. [^{3}H]mannose labelled PIMs extracted from a labelled culture were included as standards (S). The plates were scanned for radioactivity counts, overlaid with signal enhancer and exposed to film.

(I) Short exposure showing incorporation of [^{3}H]mannose into probable decaprenol phospho-mannose (DPM) and heptaprenol phospho-mannose (HPM);

(II) Extended exposure showing [^{3}H]mannose incorporation into the known PIM species, as indicated. An unidentified mannolipid designated "Lipid X" (indicated by red arrows) migrates between Ac_3PIM_2 and Ac_2PIM_4 and is over-synthesised in the mutants. The dotted blue line indicates the area of film presented in part (I) of the figure.

The sample origin is designated by an "o", while the solvent front is indicated by an "f".

consistent with the localisation of PIM synthesis to the plasma membrane (23, 108, 173, 175). In each strain, incorporation of the label from GDP-[^{3}H]mannose to mannolipids was most apparent in fractions corresponding to a sucrose density of 1.12 to 1.16 g/cm^3.

The HPTLC lanes containing fractions corresponding to a sucrose density of 1.14 g/cm^3 were measured for radioactivity counts, which in turn were plotted against migration distance on the HPTLC plate. The peaks corresponding to likely polyprenol phospho-mannose (PPMs, i.e. heptaprenol phospho-mannose (HPM), decaprenol phospho-mannose (DPM)) and PIMs were then integrated to give an estimate of the total number of counts for each mannolipid (Figure 3.6).

Polyprenol Biosynthetic Abnormalities

The most actively labelled lipids were observed after an overnight exposure of the HPTLC to film, and migrated as a doublet (Figure 3.5-I). The two species were probably HPM and DPM, which are involved in PIM and LAM biosynthesis (23). Polyprenol lipids act as sugar donors in glycoconjugate synthesis; HPM contains a C_{35} lipid component (C_{35}-P-mannose), while DPM contains a longer chain C_{50} lipid component (C_{50}-P-mannose). In Figure 3.5-I, the slightly more polar HPM migrated more slowly than DPM, as expected (23).

While each strain clearly synthesised the two putative prenols, it seemed that both mutants produced more HPM than DPM, while the amount of label incorporation was approximately equal between the two prenols in the wild-type. This was confirmed by quantitative measurement of the radioactivity incorporated into the two polyprenol bands (Figure 3.6). In the wild-type, DPM incorporated an approximately equal number of counts measured for each PPM. MYCO481 DPM incorporated 60% as much label as HPM, while MYCO479 DPM contained 42% of the label counted in HPM. This shows that while DPM/HPM are synthesised in approximately equal amounts in the wild-type, the two mutants produced markedly more HPM than DPM.

Interestingly, the amount of label incorporation into DPM was similar between the three strains. When compared to the wild-type, MYCO481 DPM contained 92% as much label, while MYCO479 contained 125%. In contrast, the amount of labelling seen in the HPM was found to be greater in the mutants. MYCO481 HPM contained 145% as much label as wild-type HPM, while

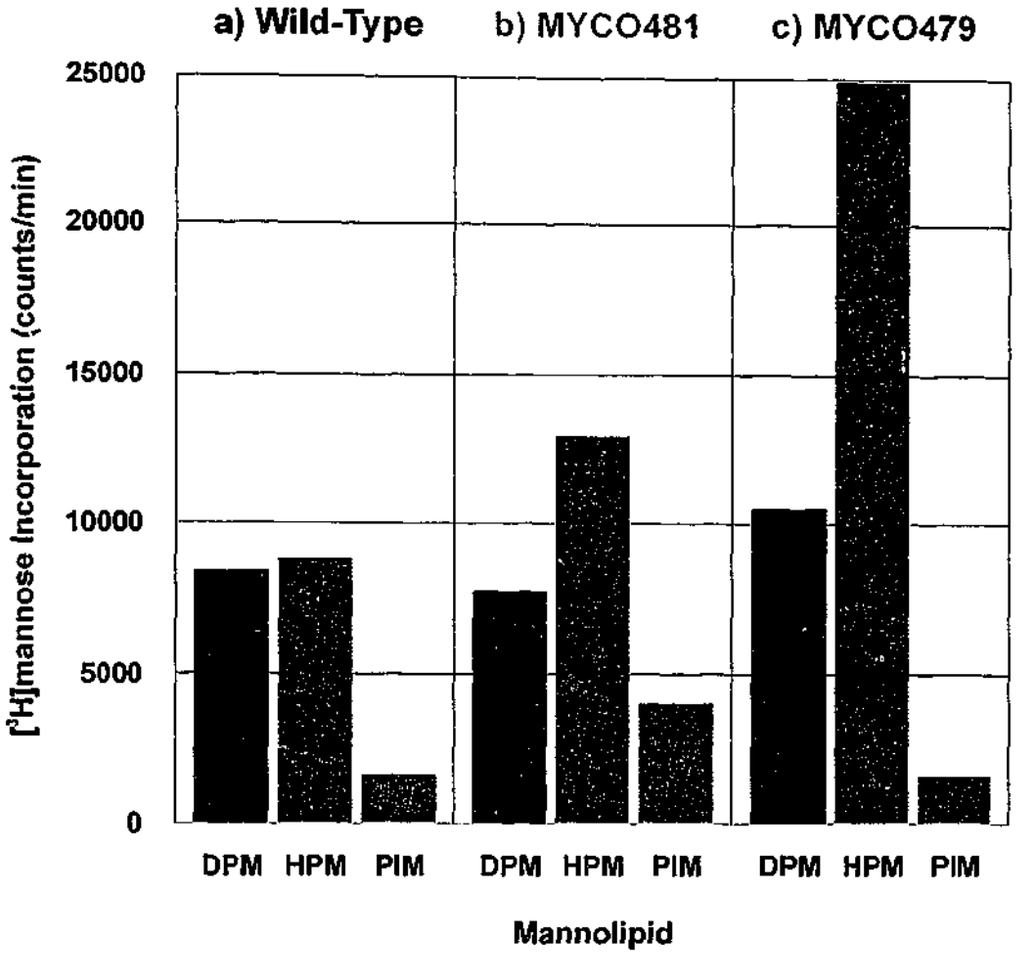

Figure 3.6
MYCO481 and MYCO479 show elevated incorporation of [^{3}H]mannose label into various mannolipids.
To quantitate the amount of label incorporation into mannose-containing lipids, fractions corresponding to a sucrose density of 1.14 g/cm^3 from the HPTLC plates shown in Figure 3.5 were scanned for radioactivity. These corresponded to: a) Fraction 5 from the wild-type; b) Fraction 6 from MYCO481; and c) Fraction 5 from MYCO479.

The peaks representing probable heptaprenol phospho-mannose (HPM), decaprenol phospho-mannose (DPM) and phosphatidylinositol mannosides (PIMs) were integrated and the radioactivity counts recorded.

MYCO479 showed 279% incorporation. Hence, both mutants over-synthesise HPM, with MYCO479 producing 2 to 3-fold more than the wild-type. Despite this, DPM synthesis levels were more comparable across the three strains.

PIM Biosynthesis

When compared to the wild-type and MYCO479, MYCO481 showed an overall higher amount of label incorporation into various PIM species, including both PIM_6 species, Ac_3PIM_4, various unidentified mannolipids which were probably PIM precursors, and Ac_3PIM_2 (Figure 3.5-II). Ac_4PIM_2 was not observed, as the bands corresponding to the heavily-labelled HPM/DPM co-migrated at their expected position on the HPTLC. Although not as well labelled, all of the lipids seen in the wild-type were apparent in MYCO481.

Being consistent with the *in vivo* labelling, MYCO479 showed no evidence of PIM_6 synthesis. Weak labelling of mannolipids more polar than Ac_3PIM_4 was apparent, but these polar mannolipids were not likely to be PIM_6 as their mobility on the HPTLC plate suggests a slightly more polar composition. These lipids are probably LAM precursors, such as LMs of various mannose chain lengths. These potential LMs were more clearly seen in the more heavily labelled MYCO481 fractions, where at least four distinct mannolipids were found to migrate below Ac_3PIM_6 (Figure 3.5b-II).

To quantitate [^{3}H]mannose incorporation into PIMs, the radioactivity peaks corresponding to mannolipids migrating below the HPM/PPM and above the sample origin were integrated. The results demonstrate that MYCO481 incorporates approximately twice as much label as the wild-type or MYCO479 (Figure 3.6). This indicates an overall increase of PIM biosynthetic activity in MYCO481. The observed elevation in biosynthetic activity is not likely to be due to a greater amount of total protein in the reaction, as the amount of protein measured in Fraction 6 (1.14 g/cm^3) of MYCO481 is less than that of Fraction 5 (1.14 g/cm^3) in either the wild-type or MYCO479 (see Figure 3.4).

MYCO481 and MYCO479 Over-Synthesise PIM_1

In addition to oversynthesising PIMs, MYCO481 incorporated radiolabelled mannose into an novel mannolipid (Figure 3.5b-II), migrating below the polyprenol phospho-mannoses in the Fraction UF lanes. The lipid was designated "Lipid X". Lipid X was also apparent in Fraction R of MYCO481, and

absent from all other fractions. Lipid X was also observed in the wild-type and MYCO479, but synthesised to a lesser extent. The lipid migrated at a position between Ac_3PIM_2 and Ac_3PIM_4. In the wild-type, the lipid incorporated less label than Ac_3PIM_2 and Ac_3PIM_4, while in the two mutants, Lipid X was labelled more than the PIMs. Label incorporation into Lipid X was quantitated by radioactivity counting (Figure 3.7). MYCO481 incorporated approximately 30 times more [^{3}H]mannose into Lipid X than the wild-type. Lipid X synthesis was also elevated in MYCO479, which incorporated approximately four times more label than the wild-type.

Unfractionated lysate from MYCO481 was subjected to a variety of chemical and enzymatic treatments to establish the identity of Lipid X (Table 3.1). It seemed likely that Lipid X was either a PIM or polyprenol derivative, given that it migrated amongst these two lipid classes and contained mannose. To address this, unfractionated lysates of MYCO481 were treated with the PPM biosynthesis inhibitor amphomycin, and labelled. The synthesis of Lipid X was found to be unaffected, implying that it was not a prenol-based molecule. Lipid X was sensitive to monomethylamine (MMA) treatment, which removes fatty acids from PIMs. Lipid X was resistant to phosphatidylinositol phospholipase C (PI-PLC) digestion. PI-PLC cleaves the phosphodiester bond of the PIM/LAM precursor PI, therefore most PIM and LAM species are expected to be resistant to this treatment. These results implied that Lipid X was a PIM species. The additional observations that the bands which were thought to correspond to DPM and HPM were amphomycin sensitive, MMA resistant and TFA labile supported the identity of these bands as polyprenol phospho-mannosides.

To determine the number of mannose units present in its sugar headgroup, Lipid X was purified and subjected to jack bean α-mannosidase (JBαM) treatment, which cleaves terminal mannoses within the PIM headgroup. The enzyme is inefficient in hydrolysing mannoses directly attached to the inositol (J. H. Patterson, unpublished results). Lipid X was resistant to this treatment, suggesting that it is a PIM_1 or PIM_2 species. To determine the number of mannose residues in Lipid X more definitively, the neutral glycan head group of the molecule was released by hydrofluoride (HF) treatment and resolved by HPTLC. HF acts to cleave phosphate ester linkages, releasing mannosylated inositol in the case of

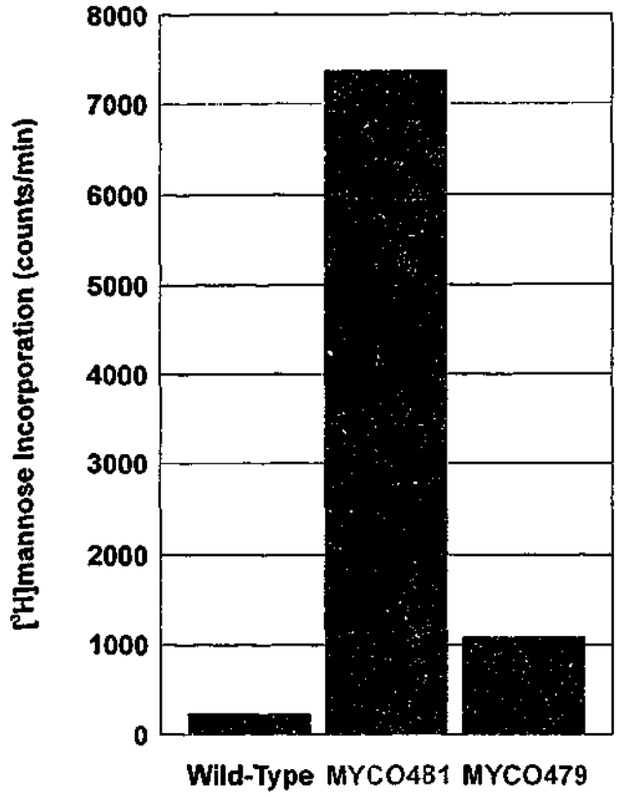

Figure 3.7
MYCO481 and MYCO479 show elevated incorporation of [^{3}H]mannose label into an unknown mannolipid (Lipid X).
To quantitate the amount of label incorporation into Lipid X, the lanes corresponding to unfractionated material from the HPTLC plates shown in Figure 3.5 were scanned for radioactivity.

The peaks representing Lipid X were integrated and the radioactivity counts for each peak recorded.

Treatment	Effect	Result	Probable Structure
PPM or PIM?			
Amphomycin	Inhibits PPM synthesis	No inhibition of synthesis	PIM
MMA	De-acylates PIMs	Sensitive	PIM
PI-PLC	Cleaves phosphodiester bond of PI	Resistant	PIM
TFA	Cleaves phospho-mannose linkage in PPMs	Resistant	PIM
PIM mannosylation			
JBαM	Cleaves bonds between mannose residues	Resistant	PIM_1 or PIM_2
MMA/HF	Releases sugar head group	TLC migration implies less than two mannose units	PIM_1
PI-PLC	Cleaves phosphodiester bond of PI	Resistant	PIM_1 (mannose on 2-position of inositol)

Table 3.1
Structural characterisation of MYCO481 Lipid X.
Lipid X was analysed either as a HPTLC-purified lipid or as unfractionated MYCO481 lysate, being subjected to the following treatments.

To differentiate between polyprenol phospho-mannose (PPM) and phosphatidylinositol mannoside (PIM): amphomycin, monomethyl amine (MMA), trifluoroacetic acid (TFA) and phosphatidylinositol phospholipase C (PI-PLC).

To determine the size of the mannan group on the PIM: jack bean alpha-manosidase (JBαM); MMA/hydrofluoride (HF); and PI-PLC.

This data was generated by Dr. Y. S. Morita (unpublished results).

PIMs. The resulting glycan from Lipid X closely migrated with monomannosylated inositol.

The mannose and inositol units of PIM headgroups can also show acylation (104). However, prior treatment of Lipid X with MMA to remove acyl chains followed by HF treatment did not alter its migration. This suggested that Lipid X is a PIM_1 species, with no additional acyl substitution on the mannose or inositol residues. The resistance of Lipid X to PI-PLC treatment also implied that the mannose unit was attached to the 2-position of the inositol. Hence, MYCO481 (and to a lesser extent, MYCO479) over synthesised a PIM_1 species in unfractionated lysates.

The data confirming the identity of the polyprenols and the purification and identification of Lipid X as PIM_1 was generated by Dr. Y. S. Morita (unpublished results).

3.4 A Complex and Unique Phenotype

The results presented in Chapter 2 of this study describe two mutants whose phenotypes were characterised by a marked reduction in LAM (MYCO481) and an abnormal PIM profile (MYCO479). These compositional differences are further complicated by various biosynthetic abnormalities in the mutants. It is now apparent that the previously described PIM/LAM phenotype represents a complex yet related set of observations which relate to the biosynthesis of PIMs and LAM.

MYCO481 over-synthesises the mannose donor HPM to approximately 1.5 times more than DPM. In the wild-type, HPM and DPM were synthesised in approximately equal amounts. More strikingly, MYCO479 synthesised almost three times as much HPM than the wild-type. Both HPM and DPM act as mannose donors in PIM and LAM biosynthesis (23). Given the prenol biosynthetic abnormalities seen in the mutants, the AG composition should be examined more closely, since decaprenol phospho-arabinose (DPA) is involved in the extension of the arabinan chain of AG (206). The observation that the synthesis of the structurally related DPM is relatively normal in the mutants implies that AG synthesis may not be affected.

MYCO481 overproduced a PIM_1 species in unfractionated lysates in the *in vitro* labelling experiment, with some synthesis also being observed in Fraction R

representing the material at the bottom of the gradient. MYCO479 also over-synthesised PIM_1, but not to the extent of MYCO481. Little synthesis of PIM_1 occurred in the other fractions, including membrane-containing fractions which were enriched for PIM biosynthesis. It is not clear why PIM_1 synthesis was not obvious in the likely membrane fractions, as the enzyme reported to convert PI to PIM_1 (PimA) is active in membrane-enriched fractions (108). However, this activity was observed for the overexpressed PimA product, such that a comparison to the observations in this study would be difficult. It is possible that other factors which were not fractionated with the membranes may be required for PIM_1 biosynthesis. This was a particularly interesting finding, as the conversion of PI to PIM_1 is thought to be the first step in PIM and LAM biosynthesis (23, 108). Since PIM_1 is overproduced to an even greater extent in MYCO481, it is unclear why the lipid does not accumulate in culture. Perhaps the excess PIM_1 in MYCO481 is fully metabolised into products further down the PIM/LAM biosynthetic pathway. It is possible that PIM_1 is the unidentified lipid which accumulates in MYCO479, migrating between Ac_3PIM_2 and Ac_3PIM_4. The lack of this lipid in MYCO481 culture suggests that it is not (see Figure 2.6).

In addition to over-synthesising PIM_1, MYCO481 was also able to synthesise a greater amount of PIMs than the wild-type. There was some evidence for this in the compositional analysis (Chapter 2), but more convincingly apparent in the *in vitro* metabolic labelling experiment. The identification of the accumulating glycolipid in MYCO479 would be informative, as would the identification of the various potential PIM precursors observed in the MYCO481 cell-free labelling experiments. Knowing the identity of each of these precursors would undoubtedly improve the basic understanding of the PIM biosynthetic pathway.

MYCO481 extracts demonstrated a great reduction in the amount of LAM-derived sugars, being found at 10-30% of the wild-type levels (Chapter 2). This LAM deficiency was supported by the *in vivo* labelling results, which show that the amount of incorporation of [^{3}H]mannose into LAM was far less that the wild-type. Since the incorporation of label in the LAM *in vivo* labelling experiment did not reach a plateau, it is possible that MYCO481 may reach a comparable level of labelling given time. Interestingly, mannolipids which may represent short-chain

LMs were present and over-synthesised in MYCO481 membrane fractions in the *in vitro* labelling experiments. LMs are thought to be LAM biosynthetic precursors (23, 41). This may be a consequence of a disruption in LAM synthesis, where LMs are not metabolised and therefore accumulate. However, this would contradict the compositional analysis which shows a reduction in all three of the LAM sugars.

While MYCO479 produces a decreased amount of LAM when compared to the wild-type (Chapter 2), labelled mannose incorporation was similar or higher to that seen in the wild-type. It is possible that LAM degradation is more active in MYCO479, such that observation of its synthesis over short periods reveals no abnormality, while examining end-products from cultures shows that the yield of LAM is reduced. The radioactivity measurements generated for the *in vivo* labelling experiment may be skewed by the presence of other labelled, mannosylated compounds such as PIMs and LMs which co-purify with LAM.

Both the overproduction of PIMs and LM in MYCO481 can be explained by a general increase in mannosyl transferase activity, but how this is related to a reduction in LAM is not clear. It would be interesting to examine the possibility of elevated mannosyl transferase activity in d. aii. One approach would be to examine the transcript levels of the PIM mannosyl transferases recently identified in *M. tuberculosis* (108, 175). Another explanation for the increased label incorporation may be that the LAM deficiency creates a disruption in the cell envelope structure which allows more label to enter the cell, but this scenario is not likely since the cell-free lysates used in the *in vitro* labelling experiments also showed increased label incorporation. The reduction of LAM synthesis in MYCO481 may increase the availability of mannose donors or mannosyltransferases for polyprenol and PIM production, explaining the elevated incorporation of label.

The metabolic labelling experiments showed that the Ac_3PIM_4 species accumulating in MYCO479 was found in the other strains, but apparently as a metabolic intermediate which incorporated but did not accumulate label. The lack of PIM_6 (and presumably PIM_5) synthesis in MYCO479 implies that the PIM biosynthetic pathway is blocked beyond the production of Ac_3PIM_4. The defect is not likely to be a result of biosynthetic enzymes being inaccessible to their substrates, as the MYCO479 *in vitro* labelling results using a cell-free reaction show no synthesis of PIM_6. It is more likely that the enzyme that metabolises PIM_4

is not functional or absent. It is not known whether one or both of the proposed biosynthetic steps leading to the production of PIM_6 from PIM_4 are defective in MYCO479. To test the functionality of the PIM_5 to PIM_6 step, labelled PIM_5 can be purified and used as a substrate in a cell-free *in vitro* labelling experiment. If MYCO479 cell-free fractions able to incorporate label into PIM_6 from PIM_5, this would imply that the defect is localised to the PIM_4 to PIM_5 step of the biosynthetic pathway.

The PIM/LAM phenotype is unique in that there have been no other reports of PIM or LAM variations of such magnitude. Parish *et al.* (153) isolated a *M. smegmatis* Tn*611* mutant which showed a reduced amount of PIM_2. The transposon disrupted the *impA* gene (inositol monophosphate phosphatase), and the mutant was initially selected because of its ability to produce very large plaques when infected with various mycobacteriophages, which the authors claimed was indicative of a cell surface abnormality. Other variations to the PIM profile have been produced by over-expressing mannosyltransferase genes in *M. smegmatis* (108, 175), but these do not represent PIM mutants.

Examples of LAM mutants with defined genetic lesions have not been published. Some studies have only managed to create structural truncations in the arabinan branch of LAM by growing *M. smegmatis* cultures in the presence of the antibiotic ethambutol. The drug appears to target arabinosyltransferase activity (60, 129). Further, the PIM profile for MYCO479 demonstrates that a cell can remain viable in the absence of PIM_5 and PIM_6, at least in the presence of an abundant PIM_4. This is in contrast to the essentiality of PI and PIM_1 (98, 108). Equally interesting, the reduction in LAM in MYCO481 shows that a strain with low levels of LAM can also remain viable.

MYCO481 and MYCO479 represent the first examples of mutants with major defects in the PIM and LAM biosynthetic pathways, as defined by the PIM/LAM phenotype. A more detailed analysis of this mutant is paramount, as further biochemical abnormalities may be identified. By further investigating the PIM/LAM phenotype and any other biochemical differences, the basic understanding of the PIM and LAM biosynthetic pathways can be improved. It is tempting to speculate that the accumulation of Ac_1PIM_4 in MYCO479 and the

LAM deficiency of MYCO481 are genetically connected. If so, the relationship between these two observations will provide insights into the as yet unidentified branching point between the PIM and LAM biosynthetic pathways.

Chapter 4

MYCO481 and MYCO479 are lpqW *Mutants with Identical Tn*611 *Insertion Sites*

4.1 Rationale and Objectives

In the preceding chapters, it was established that MYCO479 and MYCO481 have distinct compositional and biosynthetic abnormalities in the cell envelope, in particular showing PIM and LAM defects. Additionally, the strains give rise to markedly different colony morphologies on different media. The genomic locations of the mutation in each strain would therefore provide an insight into the nature of these aberrant phenotypes, and whether or not they are genetically related.

4.1.1 The *Tn*611 Mutagenesis System

The mutant isolated for this study was created by random transposon mutagenesis of the *M. smegmatis* genome with Tn*611*, according to the method detailed in Guilhot *et al.* (85). Briefly, Tn*611* consists of a kanamycin resistance marker flanked by IS6100 insertion sequences. The transposon is carried on a vector containing replication origins for mycobacteria and *E. coli*, as well as an additional resistance marker for streptomycin. The entire construct is approximately 18 kb in size and is called pCG79 (85).

Transposon mutant libraries were constructed by exploiting the inability of the mycobacterial origin of replication to function at elevated incubation temperatures. In *M. smegmatis*, replication of pCG79 proceeds at an incubation temperature of 30°C, while at temperatures of 39°C and above the plasmid is unable to replicate. Under these non-permissive conditions, the transposon is only maintained if it integrates into the chromosome. Upon insertion, one of its two IS6100 elements duplicates and along with one of the IS elements flanking the kanamycin resistance marker integrates into the genome. Consequently, the entire pCG79 plasmid is also inserted into the genome, creating an 18 kb disruption to

form a *M. smegmatis* transposon mutant. The transposon has no obvious target specificity, ensuring that the site of insertion into the genome is random (85).

Insertion events mediated by pCG79 can be detected by selecting for cells which are resistant to kanamycin and streptomycin. Putative transposon mutants of interest can then be analysed to confirm the presence of an insertion. Importantly, the location of the transposon insertion can also be determined.

4.1.2 Aims of this Section

The primary aim of this section was to identify the site of Tn*611* insertion into the *M. smegmatis* MYCO479 and MYCO481 transposon mutant genomes. The sequence data generated will be used in bioinformatic analysis to identify the region of open reading frame (ORF) that has been disrupted. The sequence surrounding the point of transposon insertion was characterised and compared to the known sequences of mycobacterial pathogens to determine if any genomic synteny, clustering of genes of related function or operon organisation was apparent. Given the distinct PIM and LAM compositional differences seen between MYCO481 and MYCO479 (Chapter 2), the location of the transposon insertion was also investigated under different culture media conditions.

4.2 Materials and Methods

4.2.1 Chemicals, Reagents and Bacterial Strains

Suppliers for chemicals and reagents used in this study are listed in Section 2.2.1 of Chapter 2. The *M. smegmatis* and *E. coli* strains used in this study are listed in Appendix 1.

4.2.2 Bacteriological Culture

The culturing conditions for *M. smegmatis* are described in section 2.2.2 of Chapter 2. *E. coli* cultures were grown in Luria Bertani (LB) medium. Media formulations for LB, PPLO and Middlebrook media are included in Appendix 2. All *E. coli* cultures were incubated aerobically at 37°C. Colonies appeared after overnight incubation on agar media. For liquid cultures, single colonies of *E. coli* were inoculated into 10 ml of broth and grown overnight. When required, the 10 ml

overnight culture was used to inoculate a larger broth, applying a 1 in 100 inoculum in each case. The cultures were then allowed to grow for a further 6-18 hours. For all broths, shaking at 160 to 200 rpm was applied in order to aerate the cultures.

4.2.3 DNA Isolation

Mycobacterial Genomic DNA

M. smegmatis genomic DNA was prepared according to a protocol adapted from Anderberg *et al.* (2). The cells from 50 ml of *M. smegmatis* culture were harvested at 3000 rpm for 10 mins in a Beckman GS-6R centrifuge. The cell pellet was then resuspended in 1 ml of TE buffer (10 mM Tris-HCl (pH 7.5), 1 mM EDTA (pH 8.0)), then 10 µl of proteinase K (20 mg/ml) and 10 mg of lysosyme were added. The cells were incubated at 37°C for 1-2 hours and harvested by centrifugation at 13000 rpm for 1 minute. The supernatant was removed, and the cells resuspended in 750 µl of 4 M guanidine thiocyanate, 25 mM sodium citrate, 0.5% (w/v) sodium lauryl sarcosinate. Approximately 100 mg of 0.10-0.11 mm glass beads (B. Braun Biotech International) were then added to the resuspended cells. The cells were disrupted using a Biospec Products Cell Disruptor for 20 seconds at the medium speed setting, then cooled on ice. The cell debris was removed by centrifugation at 13000 rpm for 1 min, and the cell lysate supernatant collected.

Seven hundred µl of TE buffer-saturated phenol : chloroform : iso-amyl alcohol (25 : 24 : 1, v/v/v, pH 7.8) was mixed with the lysate to remove proteins, and centrifuged at 13000 rpm for 10 mins to partition the organic phenol and aqueous phases. The aqueous phase was removed to a fresh tube, and the extraction with phenol repeated twice more. Residual phenol was removed by partitioning the aqueous phase with 500 µl of chloroform : iso-amyl alcohol (24 : 1). The genomic DNA in the resulting aqueous phase was precipitated (section 4.2.4) and resuspended in 200-500 µl of sterile distilled water.

E. coli *Plasmid DNA Isolation*

Plasmid DNA was extracted from 3 ml of overnight *E. coli* culture using a small scale alkaline lysis method as detailed by Ausubel *et al.* (5). The concentration of the DNA was determined by loading 1 µl onto an agarose gel and

resolving the DNA with electrophoresis and subsequent staining (section 4.2.4). All plasmids generated or used in the study are listed in Appendix 4.

4.2.4 Concentration and Quantitation of DNA

Plasmid and genomic DNA was concentrated by precipitation and subsequently quantitated according to methods described by Sambrook *et al.* (174). Spectrophotometry readings were measured using a CECIL CE 1020 Spectrophotometer. Alternatively, a known volume of DNA was resolved in an agarose gel and its resulting intensity compared with a simultaneously resolved lane of DNA markers, where the approximate concentration of each marker fragment is known.

4.2.5 Manipulation of DNA Fragments

Endonuclease Digestion and Resolution of DNA Fragments by Agarose Gel Electrophoresis

DNA digestion reactions involving restriction enzymes were used in accordance with the suppliers instructions or Sambrook *et al.* (174). DNA fragments were separated according to their size in 0.8, 1.0 or 1.5% (w/v) agarose gels prepared in Tris-acetate-EDTA (TAE) buffer (0.1% (v/v) glacial acetic acid, 2 mM $Na_2EDTA.2H_2O$ and 40 mM Tris-HCl, pH 8.5). After electrophoresis, the resolved DNA was stained with ethidium bromide (5 µg/ml, Bio-Rad) and visualised using a Spectroline TC-312A Trans-Illuminator at a wavelength of 312 nm.

Isolation of DNA Restriction Fragments

Restriction fragments and PCR products (section 4.2.7) resolved by agarose gel electrophoresis were excised and purified using the Geneclean II® Kit (Bio 101 Inc.) according to the manufacturers instructions. The DNA yield was checked by agarose gel electrophoresis (section 4.2.4).

4.2.6 Ligation of DNA Fragments

Standard Reactions

Ligations between vector and insert fragments were performed according to the methods detailed by Sambrook *et al.* (174). Ligation reactions were

transformed into *E. coli* as described in section 4.2.8. When required, termini of purified restriction fragments or PCR products were modified according to the methods detailed by Sambrook *et al.* (174).

Marker "Rescue"

Marker rescue was carried out according to the method used by Billman-Jacobe *et al.* (27). One µg of transposon mutant genomic DNA was digested with 1 µl *Eco*RI (10 units/µl), 2 µl 10 × Buffer H (Roche) and sterile distilled water to make the reaction up to 20 µl. The digest was incubated at 37°C for 4 hours, then heat inactivated at 65°C for 15 mins. The inactivated digest was then self-ligated by adding 10 µl of 10 × T4 ligase buffer, 10 µl of 10 mM ATP, 5 µl of bacteriophage T4 DNA ligase (5 units/µl) and 55 µl of sterile distilled water to a final reaction volume of 100 µl. The reaction was incubated overnight at 15°C, inactivated at 70°C for 20 mins, then transformed into *E. coli* (section 4.2.8).

4.2.7 DNA Amplification and Sequencing

Oligonucleotide primers used for DNA amplification and sequencing were synthesised on an Applied Biosystems 392 DNA/RNA Synthsiser. The sequence of each oligonucleotide is listed in Appendix 5. The concentration of each primer was determined by spectrophotometry, as described in section 4.2.4.

Polymerase Chain Reaction (PCR): Standard Reactions

Two ng of plasmid DNA or 10 ng of genomic DNA template were used in each polymerase chain reaction (PCR). The reactions contained 20 pmol of each required primer, along with 1 µl 10 mM dNTPs, 5 µl of 10 × reaction buffer (100 mM Tris-HCl, pH 8.3, 500 mM KCl, 0.1% (w/v) gelatin and either 10, 15, 20 or 25 mM $MgCl_2$), 0.5 µl Taq DNA polymerase (5 units/µl), and sterile distilled water to make up the final reaction volume to 50 µl. All PCR amplifications were performed on a PTC-200 Peltier Thermal Cycler (Bresatech Pty. Ltd.). Ten µl of each reaction was sampled and resolved by agarose gel electrophoresis (section 4.2.5). All PCR cycles used in this study are listed in Appendix 6.

Ligation-mediated PCR (LMPCR)

LMPCR ligations and reactions were set up as described by Prod'hom *et al.* (165) with minor adjustments. Initially, 200-300 ng of transposon mutant genomic DNA was digested with 1 µl of *Sal*I (10 units/µl), including 2 µl of 10 × Buffer H

(Roche) and sterile distilled water to a final volume of 20 µl. The digest was incubated for 2 hours at 37°C, then heat inactivated at 65°C for 20 mins. Five µl of the digest (approx. 50-75 ng) was ligated with 1 µl (approx. 25 pmol) of the *Sal*I linker molecule in the presence of 2 µl of 10 × bacteriophage T4 DNA ligase buffer, 2 µl of 10mM ATP and 10 µl of sterile distilled water to make the final reaction volume 20 µl. The ligation reaction was incubated at 15°C overnight. The *Sal*I linker molecule was produced as described by Prod'hom *et al.* (165), using primers 8670 and 8672 (see Appendix 5 and 6).

After incubation, the ligation reaction was heat inactivated at 70°C for 15 mins, then re-digested with *Sal*I by adding 2.5 µl 10 × Buffer H (Roche), 0.5 µl *Sal*I (10 units/µl) and 2 µl sterile distilled water to make the final reaction volume 25 µl. The digest was incubated for 15 mins at 37°C, then heat inactivated at 65°C for 20 mins. The digest was then diluted 10-fold with sterile distilled water, and used as the template in a PCR reaction. In this case, the AmpliTaq Gold polymerase system (Roche) was used. The reaction contained 5 µl template, 5 µl dimethyl sulphoxide (DMSO), 5µl 10 × AmpliTaq reaction buffer, 3µl 25 mM $MgCl_2$, 1 µl 10 mM dNTPs, 1 µl primer 8672 ("Salgd"), 1 µl primer 8665 ("F") or 8671 ("G"), 0.2 µl AmpliTaq Gold polymerase (5 units/µl) and 28.8 µl of sterile distilled water to a final reaction volume of 50 µl. The LMPCR cycle is listed in Appendix 6. The resulting products were then visualised by agarose gel electrophoresis, purified (section 4.2.5) and sequenced with either the "F" or "G" primer.

DNA Sequencing and Subsequent Analysis

Plasmid DNA to be used for sequencing was prepared with the High Pure Plasmid Isolation Kit (Roche), in accordance with the manufacturers instructions. For PCR product sequencing, the DNA was purified using the method described in section 4.2.5. Cycle sequencing reactions to generate DNA sequence were performed and processed in accordance with the protocol recommended by Perkin Elmer Corporation. Sequencing reactions for plasmids contained 500 ng of template DNA, 3.2 pmol of primer, 8 µl of BigDye terminator pre-mix (Perkin Elmer), and adjusted to a final reaction volume of 20 µl with sterile distilled water. Sequencing reactions for purified PCR products contained 10-50 ng of template

DNA. The reaction was performed using a PTC-200 Peltier Thermal Cycler (Bresatech Pty. Ltd.). The sequencing cycle is listed in Appendix 6.

The sequencing products were precipitated (section 4.2.4) and resolved on an ABI 373A Automated Fluorescent Sequencing Apparatus (Applied Biosystems Inc.). The computer program Sequencher™ Version 3.0 (Gene Codes Corporation) and the various BLAST algorithms (Basic Local Alignment Search Tool, accessible through http://www.ncbi.nlm.nih.gov/BLAST/) were used to analyse the DNA sequences.

M. tuberculosis $H_{37}R_v$ (47), *M. bovis* AF2122/97 and *M. leprae* TN strain (48) genomic sequences were accessed through the Wellcome Trust Sanger Institute (http://www.sanger.ac.uk/Projects/Microbes/), while *M. smegmatis* mc^2155 and *M. avium* 104 sequence data was obtained from TIGR (The Institute for Genomic Research, http://tigrblast.tigr.org/ufmg/). The TubercuList database hosted by Insitut Pasteur (http://genolist.pasteur.fr/TubercuList/) was also useful for accessing annotated *M. tuberculosis* $H_{37}R_v$ genomic data.

4.2.8 Transformation of DNA into E. coli

E. coli XL1-Blue MRF' and DH5α cells (Stratagene) were made electrocompetant following the procedure described by Smith *et al.* (187). Electrotransformation was performed using a Bio-Rad Gene Pulser™ and a Bio-Rad Gene Controller™, according to the manufacturers instructions.

4.2.9 DNA Hybridisation

Southern Hybridisation

The DNA probes used for Southern hybridisation experiments were generated from either purified restriction fragments (section 4.2.5) or PCR products (section 4.2.7). In each case, the DNA was quantitated as described in section 4.2.4. The required amount of DNA was then labelled, precipitated and quantitated using the DIG DNA Labelling Kit (Roche), as per the suppliers instructions. This kit employs the method of random priming to label the DNA.

After restriction digestion and electrophoresis (section 4.2.5), the DNA was transferred to a nylon membrane as described by Sambrook *et al.* (174). This was done by initially soaking the gel in 500 ml of 0.25 M HCl for 15 mins, with gentle

agitation. The gel was then soaked in 500 ml of 0.5 M HCl, 1.5 M NaCl for a further 15 mins. The DNA was subsequently transferred to a positively charged nylon membrane (Roche) according to the capillary transfer method described by Sambrook *et al.* (174). After transfer, the DNA was cross-linked to the nylon by exposing the membrane to ultraviolet light for 90 secs. The membrane was then rinsed in 2 × SSC (diluted from a 20 × stock, per litre: 175.3 g NaCl, 88.2 g tri-sodium citrate, pH 7.0) and either stored at -20°C or hybridised.

Nylon filters were initially pre-hybridised in 50 ml of blocking solution (12.5 ml 20 × SSC, 0.5 ml 10% (w/v) sodium lauryl sarcosinate, 0.1 ml 10% (w/v) SDS, 0.5 g skim milk powder and 36.9 ml distilled water) at 65°C for 3 hours, with gentle agitation. After this incubation, the prehybridisation solution was discarded and the membrane was incubated in 10 ml of hybridisation solution (identical to blocking solution, except with the addition of the DIG-labelled probe). The membrane was allowed to hybridise overnight at 65°C. A Robins Scientific Hybridisation Incubator Model 1000 was used to maintain hybridisation temperature.

After hybridisation, the membrane was subjected to a series of stringency washes. These were as follows: 2 × SSC, 0.1% (w/v) SDS (10 mins at room temperature); 2 × SSC, 0.1% (w/v) SDS (10 mins at 65°C); 0.1 × SSC, 0.1% (w/v) SDS (10 mins at 65°C).

Hybridisation of the DIG-labelled DNA probe to the membrane was detected using the DIG Luminescent Detection Kit for Nucleic Acids (Roche), according to the manufacturers instructions. CDP-Star (Roche) was used as the chemiluminescent substrate. The result was visualised by exposing the treated membrane to Fuji Medical X-Ray film. The film was developed using a Fuji RGII X-Ray Film Processor. When required, nylon membranes were stripped of their probe by washing the membrane twice in 0.2 M NaOH, 0.1% (w/v) SDS for 20 mins at 65°C.

Colony Transfer and Hybridisation

E. coli colonies were grown as patches on LB agar plates. The patches were lysed and the DNA transferred to Hybond N^+ nylon membranes (Amersham Pharmacia Biotech) according to the "DIG System User's Guide for Filter

Hybridisation", provided by Roche. Subsequent hybridisation and detection was carried out as described above.

4.2.10 The Effect of Culturing Conditions on Transposon Location

The influence of media on the transposon insertion was tested by culturing the mutant in different media combinations. Single colonies were isolated from PPLO agar plates, resuspended in PPLO broth and inoculated onto either PPLO or Middlebrook 7H10 agar. Colonies from both plates were then selected an inoculated into either PPLO or Middlebrook 7H9 broth. The genomic DNA was also extracted from each strain (section 4.2.3), and the presence of the Tn*611* insertion assessed by PCR amplification (section 4.2.7).

4.3 MYCO479 and MYCO481 contain single Tn611 Transposon Insertions in lpqW

4.3.1 Confirmation of Tn611 Insertion

Despite being initially isolated from the same colony, transposon mutants MYCO479 and MYCO481 gave rise to two distinct colony morphotypes. This raised the question as to whether or not both of these strains are in fact derived from a common parent. It remained possible that the distinct growth characteristics seen may have resulted from separate, perhaps unrelated parental strains.

In order to determine whether or not these strains harboured a single copy of the Tn*611*/pCG79 transposon, restriction fragments of transposon mutant genomic DNA were probed by Southern hybridisation with the IS6100 portion of Tn*611* as described by Guilhot *et al.* (85). In the case of a single Tn*611*/pCG79 insertion, transposon mutant genomic DNA digested with *Pst*I and probed with IS6100 should result in three hybridising fragments (Figure 4.1a). Two of the fragments are internal to IS6100, and should therefore be present in all Tn*611*/pCG79 mutants. These two fragments are also present in episomal pCG79, with the expected sizes being approximately 0.9 and 2 kb. The third hybridising band contains the IS6100 duplicate which forms as a part of the integration event, and is therefore variable in size, depending on the location of transposon insertion. Tn*611*/pCG79 insertions into different sites will generate hybridising *Pst*I

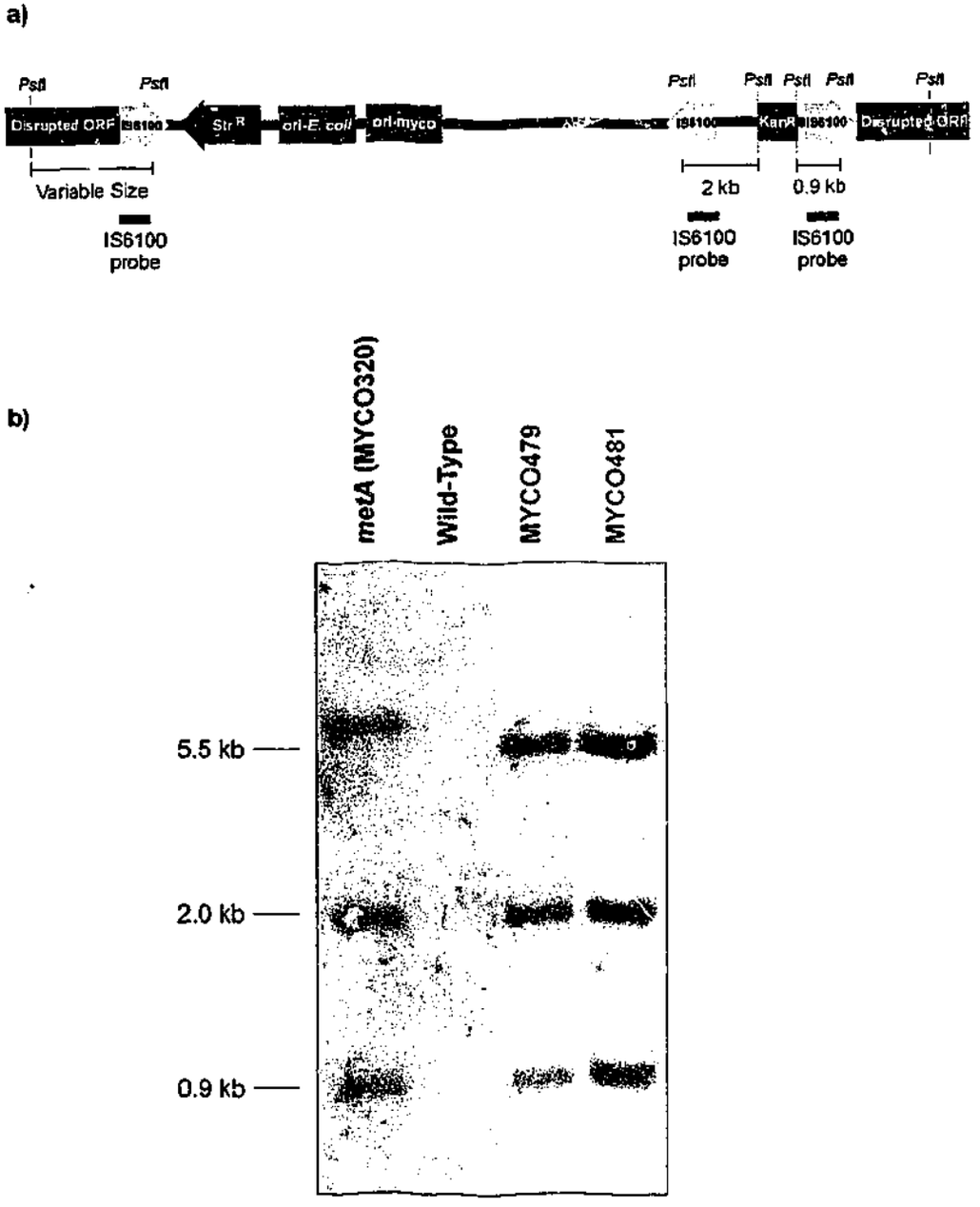

Figure 4.1
MYCO479 and MYCO481 are genetically related Tn*611* transposon mutants.
a) Expected location and size of *Pst*I restriction fragments hybridising to a probe comprising of a section of IS6100 in Tn*611* transposon mutants. Plasmid and genomic DNA was digested with *Pst*I and resolved in 1% (w/v) agarose in TAE.
b) Southern hybridisation showing the resulting restriction fragments hybridised with the IS6100 probe. MYCO320 contains a Tn*611* insertion in the *metA* gene, and was included as a control. The wild-type and the two mutants MYCO479 and MYCO481 were examined for the presence of a Tn*611* insertion. The sizes of hybridising bands in MYCO479 and MYCO481 are indicated in kilobases (kb).

fragments of different sizes. Additionally, the presence of more than one of these variably sized bands would indicate that more than one Tn*611*/pCG79 insertion event has taken place within the genome.

The probe was produced by PCR amplification of IS6100 from pCG79 (85) using the primers 6068 and 6069. Figure 4.1b shows a Southern blot where genomic DNA from the wild-type and the two mutants was *Pst*I-digested and the resulting restriction fragments probed with IS6100. An unrelated transposon mutant, MYCO320, was included as a control. MYCO320 was originally isolated as a methionine auxotroph with a Tn*611*/pCG79 disruption in an ORF highly similar to the *M. tuberculosis* gene *metA* (Rv3341) (47). The *M. smegmatis* wild-type strain was included as a negative control.

In MYCO320, the IS6100 probe hybridised to both the 0.9 and 2 kb fragments, representing two copies of IS6100 present in the insertion on separate *Pst*I fragments. A third fragment of approximately 7 kb also hybridised. This fragment contained the third copy of IS6100, created during the insertion event. The presence of only one band in addition to the 0.9 and 2 kb fragments indicated a single insertion event. The wild-type showed no hybridisation to IS6100. This was to be expected, since the wild-type does not contain a Tn*611*/pCG79 disruption.

In the case of both MYCO479 and MYCO481, the two internal 0.9 and 2 kb hybridising *Pst*I fragments from IS6100 were present along with a third fragment of approximately 5.5 kb in size. The presence of a single fragment of 5.5 kb in addition to the 0.9 and 2 kb fragments in each of these transposon mutants implies that only one transposition event is present in the genome of each strain. Importantly, the 5.5 kb hybridising fragment seen in each case also indicates that the site of Tn*611*/pCG79 insertion is identical in each of these mutants.

4.3.2 *Identification of the Tn*611 *Insertion Site in MYCO479*

With evidence that MYCO479 and MYCO481 have apparently identical transposon insertion points, the seemingly more stable MYCO479 was chosen for detailed genetic analysis. Once the site of insertion was characterised in MYCO479, experiments to confirm an identical site in MYCO481 were carried out. In order to determine the location of the transposon insertion in MYCO479

fragments surrounding the point of Tn*611*/pCG79 integration were identified, isolated and sequenced.

Obtaining Sequence from the Insertion Site

A PCR-based approach initially described by Prod'hom *et al.* (165) and referred to as ligation-mediated PCR (LMPCR) was used to obtain sequence from the Tn*611* insertion point. Briefly, transposon mutant genomic DNA is digested with a specified restriction enzyme and the resulting fragments ligated to a linker fragment of which the sequence is known. PCR amplification of DNA flanking the site of Tn*611* insertion is then achieved using primers which target IS6100 and the attached linker fragment. Using different primers for each terminus of the insertion, distinct amplification products from both ends of the transposon insertion can be obtained. MYCO479 genomic DNA was digested with *Sal*I, ligated to linker molecules and amplified using the linker and IS6100-specific primers 8672 (Salgd), 8665 (F) and 8671 (G). Products from MYCO479 were successfully amplified; the Salgd/F reaction amplified from the insertion terminus near the streptomycin resistance marker and resulted in a product of 402 bp in length. The Salgd/F amplification product was then sequenced with the F primer.

The Salgd/G primers target the insertion terminus nearest to the kanamycin resistance marker, resulting in amplification of a product of 412 bp in length. An amplification product of approximately 1 kb was also generated due to primer target sites internal to the insertion; this product should appear in all Tn*611*/pCG79 transposon mutants. The Salgd/G amplification product was then sequenced using primer G. The resulting sequence showed that the fragment contained 160 bp of ORF, terminated with a TAG stop codon. For future use, the Salgd/G product was re-amplified and cloned into the *Sma*I site of pUC18 to form pHBJ269. To confirm that the Salgd/F amplification product was adjacent to the G-fragment sequence to form the site of transposon insertion, a PCR using primers 7389 and 9276 was performed on wild-type genomic DNA. This primer pair was found to amplify a 483 bp fragment which was purified and sequenced. The sequence obtained aligned with both the F-fragment and the G-fragment sequence to confirm the insertion site of the transposon. An 8 base overlap between the two sides of the insertion was seen when the collected sequences were aligned (GGCGGTGG), suggesting that the insertion event led to a duplication of 8 bases in the target sequence.

A Putative Lipoprotein of Unknown Function

The sequences from the F- and G-fragment were assembled and searched against the available *M. smegmatis* genome sequence. The sequence matched an ORF which represented the putative gene disrupted by Tn*611* in MYCO479. In order to assign a possible function, the ORF sequence was analysed using various bioinformatic algorithms.

The Tn*611*/pCG79 insertion disrupted an open reading frame of 1884 bp (Figure 4.2), with the transposon disruption site occurring 1724 bp into the ORF. Bacterial consensus sequences for promoter features such as -10/-35 boxes and the ribosome binding site were not observed upstream of the ORF. Additionally, the predicted start codon may not be the methionine-encoding ATG, and it remains possible that the third codon in the sequence, encoding for valine (GTG), may be the true initiation codon. Start codons encoding for valine have been identified in the GC-rich genome of *M. tuberculosis* (47).

The ORF encoded for a hypothetical protein of 627 amino acids in length with a predicted molecular mass of approximately 66 kDa. The first 27 residues of the sequence constituted a probable hydrophobic signal peptide (Figure 4.3). This putative signal peptide also included a likely signal peptidase II recognition and cleavage site, in this case LGGC. The cysteine residue within this cleavage site acts as the lipid attachment site. Hence, the hypothetical protein showed the sequence hallmarks of a lipoprotein.

With the observation that MYCO479 shows abnormalities in PIM biosynthesis, the sequence was examined for the presence of any characteristic motifs found in proteins known to be associated with PIM and LAM biosynthesis. No obvious matches to inositol monophosphatase (143), PI synthase (98), GDP-man hydrolase (72) or PPM synthase (86) motifs were observed. However, a weak match to the proposed GDP-man binding site of prokaryotic α-mannosyltransferases (EXFGXXXXE) was observed from residue 228 to 236 (ETIDPWQRDE). Whether this similarity is significant or not is unclear. The presence of the two terminal glutamine residues may be the minimum requirement for the motif (75), however the confirmed mannosyltansferases PimA (ESFGIVLVE), PimB (ETFCQVVQE) and PimC (ETFGLAALE) all show more

```
TACATATTCGCCCCTCGATTGGTAGTGCTTGGCAAAGGAAATTTAGCGCCGACAGCGAATCTTCGCCCTCGAAACC
GAGGGCATGCCCCCAGATCTTTTCTGACGCAAACATCGGACCCGGCAGCGAGTTTGCTGGTCGTGATCTGCCGGTAT
CAGCCAACAGGGCTGTCGACCGAGGGGTGTGTAGCTGGTCCTGGCAACGGATGTGTGAACATTTTCGGGCCCGTCGA
AGTTCTGTTTCTTCGTAATATCGAATGATCTTGCCGATCGTGATTTTTCGGCCGAACGGCCGACATACATCCGCGCG
GCGCGGTGACGAGAATGCTGCGCGGCGTAACGACATGTCGGAATCTGCCGTTTGCTTGTTCATGCCCGTCGCCACAG
ATTCGGGGTTCCAGCAATCCATGCGGCTGGCCGCGACGGCAGCCGGCGAAGTTCTTCCAGGTCAGAGACCCCGTCTC
AACGTGACGTCGCACACGCGGGGCGGCTCGTTACCCTG

0001  ATG GGC GTG CCG ACA CCA GCC CGC CGC GCC CGT TTG ACG TTC GGC GCG CTC CTC
 001   M   G   V   P   T   P   A   R   R   A   R   L   T   F   G   A   L   L

0055  GCG GTG CCG ACA CTG CTG CTC GGC GGC TGC ACG GTG AGC CCG CCT CCC GCG CCG
 019   A   V   P   T   L   L   L   G   G   C   T   V   S   P   P   P   A   P

0109  CAG AGC ACC GAG ACC ACC GAG ACC ACG CCG CCG CCC CCG CCG AAG GCG CCT ACG
 037   Q   S   T   E   T   T   E   T   T   P   P   P   P   P   K   A   P   T

0163  CAG ATC ATC ATG GCC ATC GAC TCG ATC GGC CCG GGG TTC AAT CCG CAC CTG CTG
 054   Q   I   I   M   A   I   D   S   I   G   P   G   F   N   P   H   L   L

0217  TCC GAT CAG TCC CCG GTG AAC GCC GCG ATC GCG TCG CTG GTG CTG CCC AGC TCG
 072   S   D   Q   S   P   V   N   A   A   I   A   S   L   V   L   P   S   S

0271  TTC CGG CCG GTG CCG GAT CCC ACG TCG CCC ACC GGG TCA CGG TGG GAA CTG GAC
 090   F   R   P   V   P   D   P   T   S   P   T   G   S   R   W   E   L   D

0325  ACC ACA CTG CTG GAG TCG GCG GAG GTG ACC AAC GAG AAC CCG TTC ACC GTG ACC
 108   T   T   L   L   E   S   A   E   V   T   N   E   N   P   F   T   V   T

0379  TAC AAG ATC CGG CCG GAA GCG CAG TGG ACC GAC AAC GCG CCG ATC GCC GCC GAT
 126   Y   K   I   R   P   E   A   Q   W   T   D   N   A   P   I   A   A   D

0433  GAC TAC TGG TAT CTG TGG CGG CAG ATG GTC AGC CAG CCC GGT GTC GTC GAC CCG
 144   D   Y   W   Y   L   W   R   Q   M   V   S   Q   P   G   V   V   D   P

0487  GCC GGC TAT GAC CTG ATC ACC GGC GTG CAG TCC GTC GAG GGC GGC AAG CAG GCC
 162   A   G   Y   D   L   I   T   G   V   Q   S   V   E   G   G   K   Q   A

0541  GTC GTG ACG TTC TCG CAG CCG TAC CCG GCG TGG CGT GAA CTG TTC AAC GAC ATC
 180   V   V   T   F   S   Q   P   Y   P   A   W   R   E   L   F   N   D   I

0595  CTT CCC GCG CAC ATC GTC AAG GAC ATC CCG GGC GGG TTC GGC GCG GGC CTG GCC
 198   L   P   A   H   I   V   K   D   I   P   G   G   F   G   A   G   L   A

0649  CGC GCG ATG CCC GTG ACA GGA GGC CAG TTC CGC GTC GAG ACC ATC GAT CCC CAG
 216   R   A   M   P   V   T   G   G   Q   F   R   V   E   T   I   D   P   Q

0703  CGC GAC GAG ATC CTG CTG GCC CGC AAC GAC CGG TTC TGG AGC GTG CCC GCC AAA
 234   R   D   E   I   L   L   A   R   N   D   R   F   W   S   V   P   A   K

0757  CCC GAC CTG GTG CTG TTC CGA CGC GGC GGC GCT CCG GCC GCG CTG GCG GAC TCG
 252   P   D   L   V   L   F   R   R   G   G   A   P   A   A   L   A   D   S

0811  ATC CGC AAC GGT GAC ACA CAG GTC GCC CAG GTG CAC GGC GGC GCA GCG ACT TTC
 270   I   R   N   G   D   T   Q   V   A   Q   V   H   G   G   A   A   T   F
```

Figure 4.2
Complete sequence of the Tn*611*-disrupted ORF in MYCO479.
The nucleotide sequence is 1884 bp in length and shown in black. The transposon insertion site is represented by the 8 bp sequence from nucleotides 1728 to 1735, highlighted in orange. The ORF encodes for a hypothetical protein of 627 amino acids, the sequence of which is shown in blue beneath each of the residues corresponding codon. The 500 bp preceding and following the ORF are also presented. The sequence is continued on the following page.

```
0865  GCC CAG CTC AGC GCC ATC CCC GAC GTC CGG ACC GCA CGC ATC GTG ACC CCG CGC
 288   A   Q   L   S   A   I   P   D   V   R   T   A   R   I   V   T   P   R

0919  GTC ATG CAG CTC ACG CTG CGG GCG CAG CAG CCC AAG CTT GCC GAT CCC CAA GTG
 306   V   M   Q   L   T   L   R   A   Q   Q   P   K   L   A   D   P   Q   V

0973  GTG CGC AAG GCG ATC CTG GGT CTG ATC GAC GTC GAC CTC CTG GCA TCG GTG GGC
 324   V   R   K   A   I   L   G   L   I   D   V   D   L   L   A   S   V   G

1027  GCC GGC GAC GAC AAC ACC GTG ACA CTC GCG CAG GCG CAG GTG CGT TCG CCG TCG
 342   A   G   D   D   N   T   V   T   L   A   Q   A   Q   V   R   S   P   S

1081  GAT CCC GGC TAC GTG CCG ACC GCG CCG CCT GCG ATG ACG CGT GAC GAC GCG CTC
 360   D   P   G   Y   V   P   T   A   P   P   A   M   T   R   D   D   A   L

1135  GAA TTG CTC AGG GAC GCG GGA TAT GTC AGC GAA CCC GTG CCA CCC CCG GAC AAC
 378   E   L   L   R   D   A   G   Y   V   S   E   P   V   P   P   P   D   N

1189  ACC GCG GAC GAT CCG CCG CCC GAC AAC GGG CGT GAA CGA ATC GTG AAA GAT GGG
 396   T   A   D   D   P   P   P   D   N   G   R   E   R   I   V   K   D   G

1243  GTG CCG CTG ACG ATC GTC CTG GGC GTC GCC TCC AAC GAC CCC ACG TCG GTG GCG
 414   V   P   L   T   I   V   L   G   V   A   S   N   D   P   T   S   V   A

1297  GTG GCC AAC ACC GCG GCC GAC CAG TTG CGC AAC GTC GGC ATC GAC GCC TCG GTG
 432   V   A   N   T   A   A   D   Q   L   R   N   V   G   I   D   A   S   V

1351  CTC GCC CTG GAT CCG GTT GCG CTG TAC GGC GAC GCG TTG GTG AAC AAC CGC GTC
 450   L   A   L   D   P   V   A   L   Y   G   D   A   L   V   N   N   R   V

1405  GAC GCC GTC GTC GGC TGG CGC CAG GCC GGT GGT GAC CTC GCG ACC GTT CTG GCG
 468   D   A   V   V   G   W   R   Q   A   G   G   D   L   A   T   V   L   A

1459  TCG CGC TAC GGA TGC CGC GCG CTT GAG GCC ACG CCC GTG GCC ACG GCG GTT CCC
 486   S   R   Y   G   C   R   A   L   E   A   T   P   V   A   T   A   V   P

1513  GGG CCC GCC ACC ACC ACG TCG CAG GCC CCC ACC ACC ACG ACC ACC ACC ACG CCG
 504   G   P   A   T   T   T   S   Q   A   P   T   T   T   T   T   T   T   P

1567  CCT GCG ACC ACC ACA CCG ACG CCC ACC GCG CCG ATC CCG GCG CCG GAG TCC GGT
 522   P   A   T   T   T   P   T   P   T   A   P   I   P   A   P   E   S   G

1621  GAA CTG GTG CAG GCG CCC AGC AAC ATC ACC GGC ATC TGC GAT CGC AGC ATC CAG
 540   E   L   V   Q   A   P   S   N   I   T   G   I   C   D   R   S   I   Q

1675  CCG AGA ATC GAT GCG GCA CTG GAC GGT ACG GAC GAC ATC GCC GAC GTG ATC CAG
 558   P   R   I   D   A   A   L   D   G   T   D   D   I   A   D   V   I   Q

1729  GCG GTG GAA CCG CGG TTG TGG AAC ATG GCG ACC GTG CTG CCG ATC CTG CAG GAC
 576   A   V   E   P   R   L   W   N   M   A   T   V   L   P   I   L   Q   D

1783  ACC ACG ATC GTG GCC GCC GGG CCG AGT GTG CAG AAC GTG AGC CTC ACC GGG GCG
 594   T   T   I   V   A   A   G   P   S   V   Q   N   V   S   L   T   G   A

1837  GTG CCG GTA GGG ATC GTC GGC GAC GCC GGT GAC TGG ACG AAG ACC AAG TAG
 612   V   P   V   G   I   V   G   D   A   G   D   W   T   K   T   K   *

CGCAGGCGGTAGCGTCTGTACACGATGTCATCGCATGAATCGCCCCGGCTGCTGTTCGTCCACGCCCACCCCGACGA
CGAGACCCTGACCACCGGCGGGACCATCGCGCACTACGTCGCGCGCTCGGCCGAGGTCCATGTCGTCACCTGCACGC
TCGGTGAGGAGGGCGAGGTGATCGGCGAGCGCTACGCGCAACTCGCCGTCGACCACGCCGATCAGCTCGGCGGGTAC
CGCATCGCGGAGCTGACGGCCGCGCTGCAGTCTCTCGGGTTGCGGGGCCCGCGGTATCTCGGCGGCGCCGGGCACTG
GCGTGACTCCCGCATGGCAGGCACGCCGTCGCGCGGGCGGCAGCGCTGGGTCGACGCCGACCTCGACGAGGCCGTGG
GTGCACTGGTCGCCGTGATCGGTGAGGTGCGGCCGCACGTCGTCGTCACCTACGACCCCAACGGCGGCTACGGGCAC
CCCGACCACATCCAGACACACGTGGTCACCACGCGGGC
```

Figure 4.2
Complete sequence of the Tn*611* disrupted ORF in MYCO479.
The sequence is continued from the previous page.

```
          10         20         30         40         50
MGVPTPARRARLTFGALLAVPTLLLGGCTVSPPPAPQSTETTETTPPPPP

          60         70         80         90         100
KAPTQIIMAIDSIGPGFNPHLLSDQSPVNAAIASLVLPSSFRPVPDPTSP

          110        120        130        140        150
TGSRWELDTTLLESAEVTNENPFTVTYKIRPEAQWTDNAPIAADDYWYLW

          160        170        180        190        200
RQMVSQPGVVDPAGYDLITGVQSVEGGKQAVVTFSQPYPAWRELFNDILP

          210        220        230        240        250
AHIVKDIPGGFGAGLARAMPVTGGQFRVETIDPQRDEILLARNDRFWSVP

          260        270        280        290        300
AKPDLVLFRRGGAPAALADSIRNGDTQVAQVHGGAATFAQLSAIPDVRTA

          310        320        330        340        350
RIVTPRVMQLTLRAQQPKLADPQVRKAILGLIDVDLLASVGAGDDNTVTL

          360        370        380        390        400
AQAQVRSPSDPGYVPTAPPAMTRDDALELLRDAGYVSEPVPPPDNTADDP

          410        420        430        440        450
PPDNGRERIVKDGVPLTIVLGVASNDPTSVAVANTAADQLRNVGIDASVL

          460        470        480        490        500
ALDPVALYGDALVNNRVDAVVGWRQAGGDLATVLASRYGCRALEATPVAT

          510        520        530        540        550
AVPGPATTTSQAPTTTTTTTPPATTTPTPTAPIPAPESGELVQAPSNITG

          560        570        580        590        600
ICDRSIQPRIDAALDGTDDIADVIQAVEPRLWNMATVLPILQDTTIVAAG

          610        620
PSVQNVSLTGAVPVGIVGDAGDWTKTK
```

Figure 4.3
Features of the hypothetical protein disrupted in MYCO479.
The amino acid sequence contains a hydrophobic signal peptide and putative signal peptidase II recognition site from residues 1 to 27, with the cysteine residue at position 28 being a likely lipid attachment site. A weak match to a GDP-mannose binding site found in prokaryotic α-mannosyltransferases (75) is indicated (residues 229-237). Highlighted in blue are regions of low structural complexity. These stretches are rich in proline and threonine residues. The region highligted in green corresponds to sequence which is similar to that found in bacterial extracellular solute binding proteins.

convincing matches (108, 110, 175).

The sequence was also found to show relatively poor similarity to a domain found in family 5 of the bacterial extracellular solute-binding proteins. These proteins are usually membrane-bound lipoproteins which have roles in chemoreception or transmembrane transport (195).

***The disrupted ORF is most similar to* lpqW**

Using similarity searches, the nucleotide sequence of the disrupted MYCO479 ORF showed a strong match to one entry from the *M. tuberculosis* genome; Rv1166, or *lpqW* (47). The majority of the *M. smegmatis* sequence showed between 80% and 90% identity to *M. tuberculosis lpqW*, with small sections of the sequence showing a relatively poor match. *M. tuberculosis lpqW* has no described function, and has been annotated as a putative lipoprotein. This is due to the presence of a probable hydrophobic signal peptide, corresponding signal peptidase II cleavage site and lipid attachment site (LAGC) within its translated amino acid sequence, which as described for the *M. smegmatis* ORF above, are indicative of a lipoprotein.

Given the strong nucleotide sequence match, it was not suprising to find that in an amino acid sequence comparison of the translated *M. smegmatis* sequence the strongest similarity was seen for the *M. tuberculosis* LpqW protein. A sequence identity of 68% (436/636 residues) and similarity of 76% (487/636) were observed. Only small sections of the alignment showed a poor similarity. Given this degree of similarity, it is highly likely that the ORF disrupted in MYCO479 is the *M. tuberculosis lpqW* homologue. For this reason, the *M. smegmatis* ORF was designated *lpqW*.

Amino acid sequence analysis also revealed secondary matches to LpqW. The *M. smegmatis* sequence showed some similarity to the EppA precursor protein of EDTA-degrading bacterium BNC1, which is involved in EDTA transport. A match to another *M. tuberculosis* protein, OppA (encoded by Rv1280c), was also detected. Both EppA and OppA show similarity to several oligopeptide binding proteins. Indeed, using only two iterations of PSI-BLAST (1) analysis (NCBI) many matches between *M. smegmatis* LpqW and various oligopeptide binding proteins were observed, including EppA and OppA.

4.3.3 LpqW is a Putative Lipoprotein highly conserved among the Mycobacteria

The question as to whether or not *lpqW* was restricted *to M. smegmatis* and *M. tuberculosis* was explored. This was determined by searching for a sequence homologue of the gene in the pathogenic mycobacteria, using data from the available sequencing projects. Clues as to the function of the gene disrupted in the mutants may be obtained by examining the genes surrounding *lpqW*. If the gene forms a part of a functionally related cluster or an operon, such as the proposed PIM biosynthetic cluster (98, 108), the location of *lpqW* may lead to the identification of an additional, novel cluster. Where *lpqW* was found, the surrounding region of the genome was compared to that of *M. smegmatis* to see if any genomic arrangements were shared with the pathogenic mycobacteria.

lpqW *in Other Mycobacteria*

The *M. smegmatis* LpqW sequence was compared to genomic database sequences for *M. bovis*, *M. avium*, *M. leprae* and *M. avium* sub spp. *paratuberculosis* to test for the presence of *lpqW* homologues in mycobacteria other than *M. smegmatis* and *M. tuberculosis*. Alignments for the mycobacterial LpqW homologues are presented in Figure 4.4 and show a strong conservation of the protein sequence amongst the mycobacterial species tested. In each case, hypothetical proteins of high similarity were found to match to the *M. smegmatis* sequence. The *M. bovis* sequence was identical to the *M. tuberculosis* sequence, and hence showed the same degree of matching to the *M. smegmatis* sequence. The *M. leprae* LpqW was 70% identical and 80% similar to *M. smegmatis*, while the *M. avium* LpqW showed 74% identity and 82% similarity. The *M. avium paratuberculosis* LpqW also strongly matches, although the whole gene sequence is not available. One short region of the protein corresponding to residues 500 to 527 of the *M. smegmatis* sequence shows relatively poor conservation. Curiously, the *M. smegmatis* sequence contains a stretch of seven threonine residues in this region, which are not found in the other sequences.

Sequencing of the Genomic Region Disrupted in MYCO479

The chromosomal region surrounding *lpqW* was isolated, sequenced and characterised in order to compare the *M. smegmatis lpqW* locus to those of other, pathogenic mycobacteria. This work was completed prior to the recent and ongoing

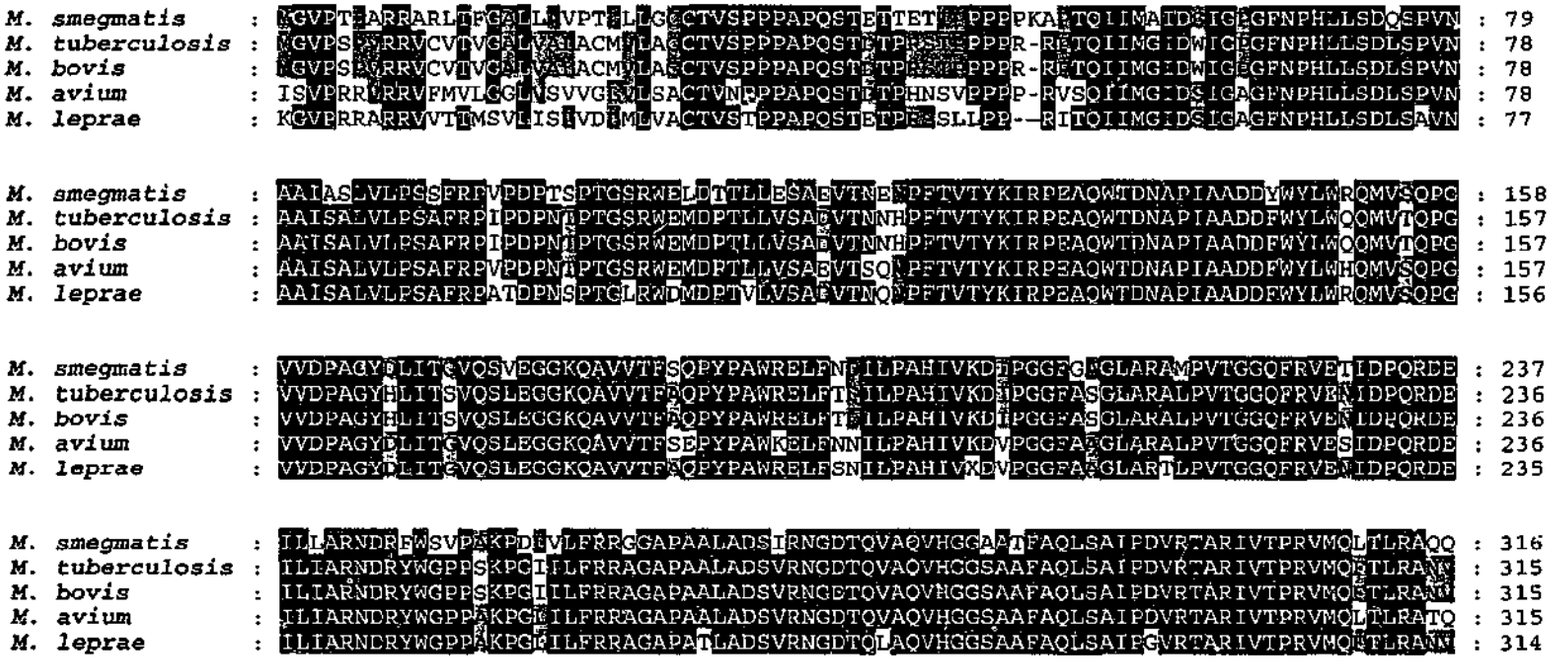

Figure 4.4
LpqW amino acid sequence is conserved in various mycobacteria.
The sequencing projects for *M. tuberculosis* $H_{37}R_v$, *M. bovis* AF2122/97, *M. leprae* TN (Sanger Institute), *M. avium* 104 (TIGR) and *M. smegmatis* mc^2155 (TIGR, this study) were accessed to obtain the sequence of the LpqW protein for each species, based on similarity to the *M. tuberculosis* sequence. Amino acid residues shaded dark blue are residues conserved in each species, with lighter shades indicating less conservation. The yellow box indicates the potential GDP-mannose binding site.
The alignment is continued on the next page.

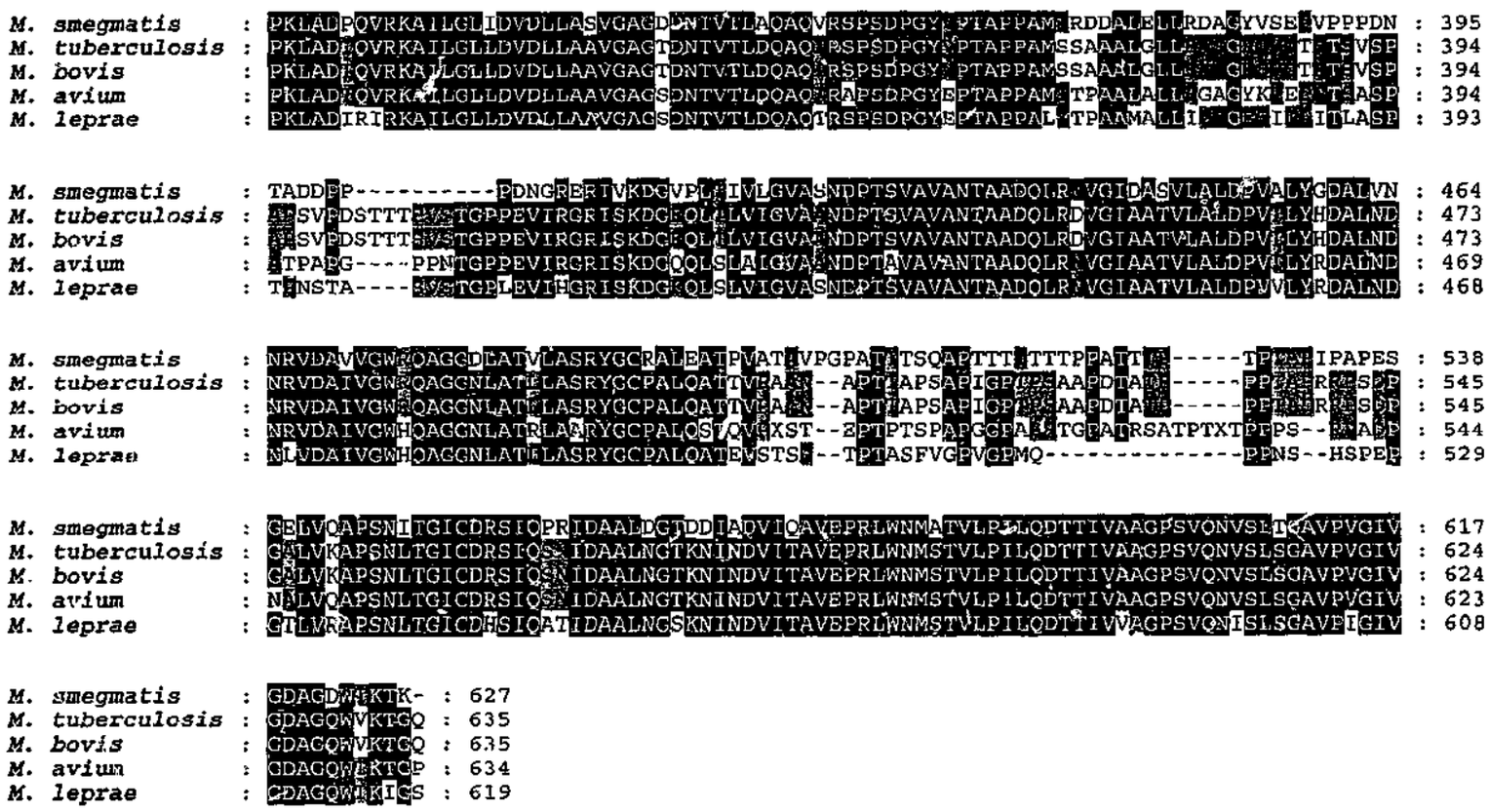

Figure 4.4
LpqW amino acid sequence is conserved in various mycobacteria.
The alignment is continued from the previous page.

release of *M. smegmatis* genomic sequence data (conducted by TIGR). As the sequencing project data was gradually released, the accuracy of the sequences generated in this study were confirmed against that of the TIGR sequencing data.

The arrangement of the various subclones generated for this section of the study are presented in Figure 4.5, together with the location of the primers used to sequence each plasmid. Genomic DNA adjacent to the point of Tn*611*/pCG79 insertion in *lpqW* was initially isolated using an antibiotic resistance marker "rescue", as described in Billman-Jacobe *et al.* (27). This approach allows the isolation of genomic DNA near the terminus of the pCG79 insertion containing the streptomycin resistance marker. Briefly, restriction fragments of transposon mutant DNA are digested with *Eco*RI. One of these fragments will contain a portion of the integrated pCG79 by virtue of a unique *Eco*RI site in the insertion. Due to the position of the pCG79 *Eco*RI site, this fragment will also contain the streptomycin resistance marker and the *E. coli* origin of replication from the inserted plasmid. Hence, transposon mutant *Eco*RI fragments containing the pCG79 streptomycin resistance marker, the *E. coli* replication origin and the adjoining mycobacterial genomic DNA can be isolated by self-ligating the restriction fragment, transforming the ligation products into *E. coli* and selecting for streptomycin resistant clones.

MYCO479 genomic DNA was digested with *Eco*RI, self-ligated and transformed into *E. coli*. Streptomycin resistant transformants were then analysed and one containing a plasmid designated pHBJ115 was identified and chosen for further analysis. The presence of a *Hin*dIII site within IS6100 together with the *Eco*RI site derived from the termini of the original *Eco*RI fragment allows the *lpqW*-derived sequence to be isolated and subcloned from the rescue plasmid. pHBJ115 has an additional internal *Hin*dIII site. One fragment of approximately 5 kb was a *Hin*dIII/*Eco*RI fragment which was subcloned into *Hin*dIII/*Eco*RI-digested pBluescript II SK+ to form pHBJ122. The second, approximately 800 bp *lpqW*-derived fragment from pHBJ115 was generated by *Hin*dIII digest alone and was subcloned into *Hin*dIII-digested pBluescript II SK+ to create pHBJ123.

The inserts of pHBJ122 and pHBJ123 were sequenced using the vector-specific primers T3 and T7. The pHBJ123 insert was found to contain 781 bp of sequence, with the entire insert consisting of *lpqW* ORF. The *lpqW* sequence

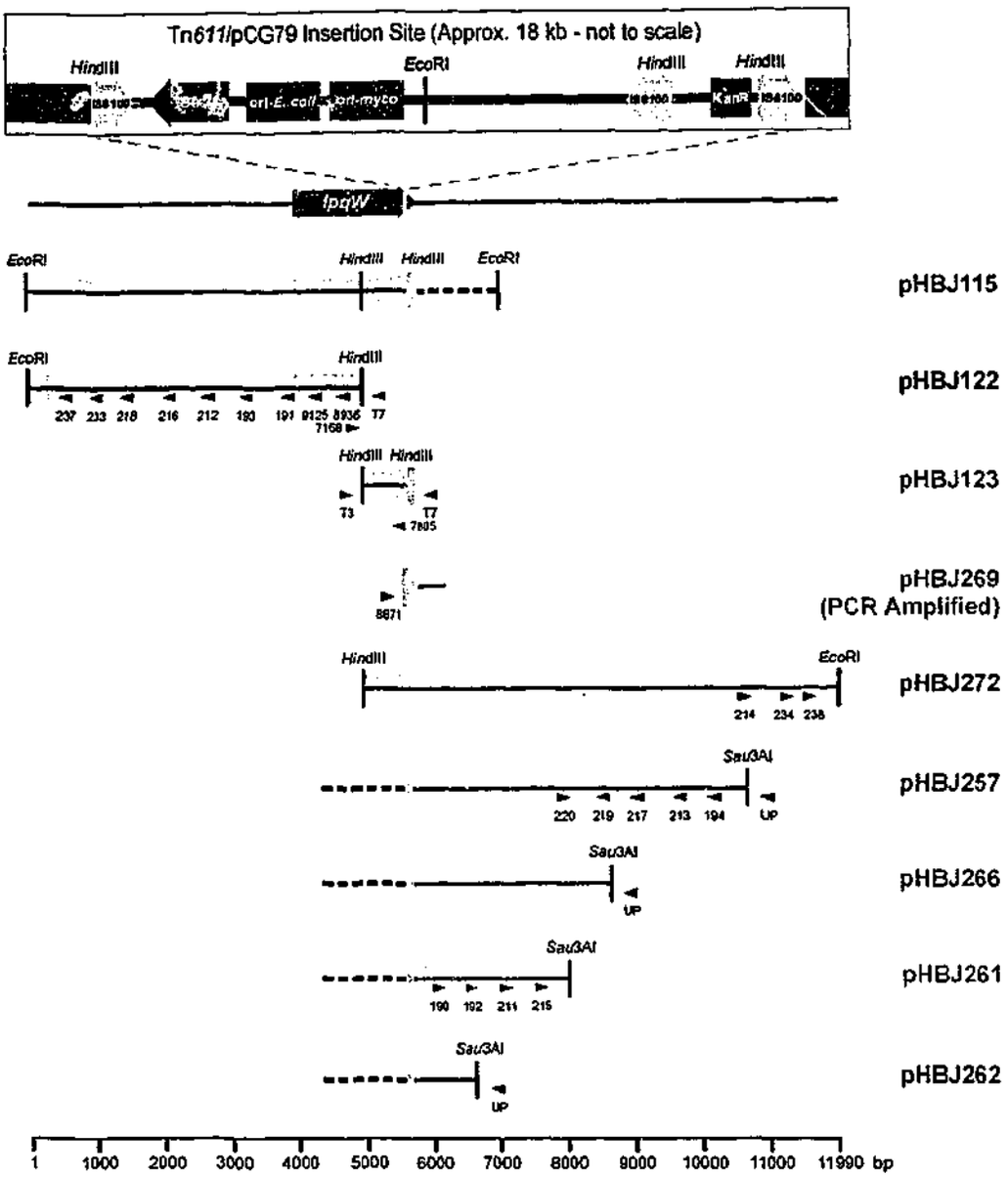

Figure 4.5

Cloning and sequencing of the region surrounding *lpqW* in MYCO479.

Genomic DNA adjacent to the point of Tn*611* insertion in *lpqW* was isolated from MYCO479 and sequenced. Plasmid pHBJ115 was made by self-ligating a pCG79-derived streptomycin resistant *Eco*RI fragment. pHBJ122 and pHBJ123 are subclones of pHBJ115. Plasmid pHBJ269 was made by cloning the PCR amplification product of primers 8671 and 8672. Plasmid pHBJ272 was cloned from the wild-type strain as a *Hin*dIII/*Eco*RI fragment which hybridised to a pHBJ269 probe. pHBJ257, pHBJ261, pHBJ262 and pHBJ266 were randomly cloned from MYCO479 and include the kanamycin resistance marker and further sequence from the Tn*611* insertion (represented by broken lines). The grey arrows in each fragment indicate open reading frames, with the pink arrow representing *lpqW*. Oligonucleotide primers used for sequencing the constructs are also shown at their target site. Primers 7168 and 7805 were used as PCR primers to confirm the arrangement of pHBJ122 and pHBJ123. A total of 11990 bp was compiled.

identified at the *Hin*dIII-terminus of the pHBJ122 insert was extended by primer walking and covered 957 bp of the insert. The sequence upstream of *lpqW* in pHBJ122 was completed by primer walking. A TAA translational stop codon which potentially marked the termination of the ORF upstream of *lpqW* was found 165 bp upstream of the putative *lpqW* initiation codon.

The inserts of pHBJ122 and pHBJ123 were expected to be adjacent to each other in the genome via their *Hin*dIII sites, with one of the terminal *Hin*dIII sites of pHBJ123 being derived from IS6100. This was confirmed by amplifying an 839 bp fragment from wild-type genomic DNA using the primers 7168 and 7805. The product was purified and sequenced. The data showed that the 7168/7805 amplification product overlapped the *Hin*dIII termini of pHBJ122 and pHBJ123, confirming that these restriction fragments were adjacent to each other in the genome. Together, pHBJ122 and pHBJ123 contained 1732 bp of genomically-derived *lpqW* ORF sequence adjoining one side of the insertion. The full sequences of pHBJ123 and pHBJ122 were combined to give 5704 bp of sequence for this side of the Tn*611* insertion.

Strategies involving the random cloning of genomic fragments were employed in order to isolate a genomic fragment from the other terminus of the insertion (i.e. near the kanamycin resistance marker). Genomic fragments adjoining the point of Tn*611* insertion into *lpqW* were isolated using two separate approaches.

The first approach involved partially digesting MYCO479 genomic DNA with *Sau*3AI to generate fragments of approximately 5 kb in size. These fragments were ligated into the *Bam*HI site of pUC19, and transformed into *E. coli*. Kanamycin resistant clones were then selected for. Because the kanamycin resistance marker within the insertion is near the insertion terminus, resistant clones containing sufficiently large *Sau*3AI fragments were likely to contain the resistance marker in addition to a few kilobases of adjoining genomically-derived sequence. Potential clones were digested with *Pst*I, and those found to contain the 0.9 kb *Pst*I fragment of pCG79 were chosen for further analysis. The 0.9 kb *Pst*I fragment is derived from the terminal IS6100 element of this side of the insertion. Qualifying clones were then probed with a *PstI*/*Eco*RI fragment from pHBJ269. The clones which were shown to hybridise to this probe and therefore contained the required

sequence were pHBJ257, pHBJ261, pHBJ262 and pHBJ266. These plasmids were then sequenced using the pUC19-targetting UP and RP primers, with further sequencing being carried out by primer walking.

A second, more direct approach was designed to isolate genomic DNA from this terminus of the insertion. Wild-type genomic DNA was digested with *Hin*dIII/*Eco*RI to generate the fragment which adjoins with pHBJ122 via the *Hin*dIII site. pHBJ123 should also overlap this fragment, sharing its genomically-derived *Hin*dIII site. Southern blot analysis using the *PstI*/*Eco*RI insert from pHBJ269 as a probe showed this fragment to be approximately 7 kb in size.

M. smegmatis wild-type genomic DNA was completely digested with *Hin*dIII/*Eco*RI and fragments of approximately 5-8 kb were purified. These were ligated to *Hin*dIII/*Eco*RI-cleaved pUC18, and clones with the correct insert were identified by colony hybridisation using the pHBJ269 probe. Plasmid DNA from positive clones was isolated, digested with *Hin*dIII/*Eco*RI and re-hybridised with the pHBJ269 probe to identify those with the correct fragment. Plasmid pHBJ272 was then chosen for subsequent sequencing. The section of pHBJ272 which did not overlap with the *Sau*3AI partial digest clones was sequenced by primer walking. When combined with the *Sau*3AI partial digest clones, the total length of sequence generated for this side of the insertion was 6294 bp. Combined with the sequence from pHBJ122 and pHBJ123 isolated from the opposing terminus, the amount of sequence data generated from MYCO479 was compiled to give 11990 bp of contiguous sequence from the *lpqW* region of the *M. smegmatis* genome.

Genetic Arrangement of the* lpqW *Region in Mycobacteria

The *M. smegmatis* sequence generated for this study was compared to recently released data from the *M. smegmatis* sequencing project (TIGR). The sequence generated in this study completely agreed with the data from the genome sequencing project. Using the data obtained in this study to search against the available *M. smegmatis* genome data, approximately 30 kb of sequence was compiled. The sequence was compared to the genomic data available from other mycobacterial species to determine how the arrangement of *lpqW* and its surrounding genes differ between the species tested. The species examined were *M. tuberculosis*, *M. bovis*, *M. leprae*, and *M. avium*. The genomic arrangements were

constructed using the *M. tuberculosis* $H_{37}R_v$ genome and its ORF numbering system as a guide (47).

The analysis showed several similarities and differences between the species (Figure 4.6a). While the gene arrangements varied between the species, in most cases the amino acid sequences derived from each ORF showed strong similarity to each other (Figure 4.6b). A match to Rv1160 (*mutT2*, a putative mutator protein) is not found upstream of an Rv1161 (*narG*) homologue in *M. smegmatis*, rather, a strong match to Rv1737c (*narK2*) is present. The *M. smegmatis* Rv1160 equivalent is located a further three ORFs upstream of the Rv1737c match. The Rv1161 to Rv1164 homologues seem to be a nitrate reductase operon or cluster and is highly conserved among the species. Interestingly, an 1148 bp gap exists between the *M. smegmatis* Rv1164 and Rv1165 matches. This arrangement is not seen in the other species. The gene upstream of *lpqW* in each case was the Rv1165 homologue, a putative GTP binding protein. In *M. smegmatis*, a large gap of 1782 bp is found between *lpqW* and the Rv1165 homologue. This is not seen in other species. The *M. tuberculosis* gene immediately downstream of *lpqW*, Rv1167c, encodes a putative transcriptional regulator and is not present in *M. smegmatis* but is found in the other species. Only *M. tuberculosis* and *M. bovis* contain Rv1168c and Rv1169c, part of the large PE/PPE gene family.

In *M. smegmatis*, the gene immediately downstream of *lpqW* is Rv1170 (*mshB*). The ORF encodes a deacetylase involved in the biosynthesis of the inositol-containing compound mycothiol (139) and is present in all of the species analysed. Homologues to Rv1172c are found in all species except *M. avium*. The matching ORF in *M. smegmatis*, however, is relatively weak and may not represent an actual homologue. The gene is a part of the *M. tuberculosis* PE family. In *M. smegmatis*, regions of 956 bp and 1470 bp flank the Rv1175c (*fadH*) match. *M. smegmatis* homologues to Rv1174c, Rv1176c, Rv1179c (functions unknown) and Rv1180 (polyketide synthase) are absent from the region and are possibly located elsewhere in the genome. Matches to Rv1186c (function unknown), Rv1187 (*rocA*, a probable pyroline-5-carboxylate dehydrogenase) and Rv1188 (proline dehydrogenase) are found downstream of the Rv1178 homologue only in *M. smegmatis*. These observations show that there is some conservation in the *lpqW*

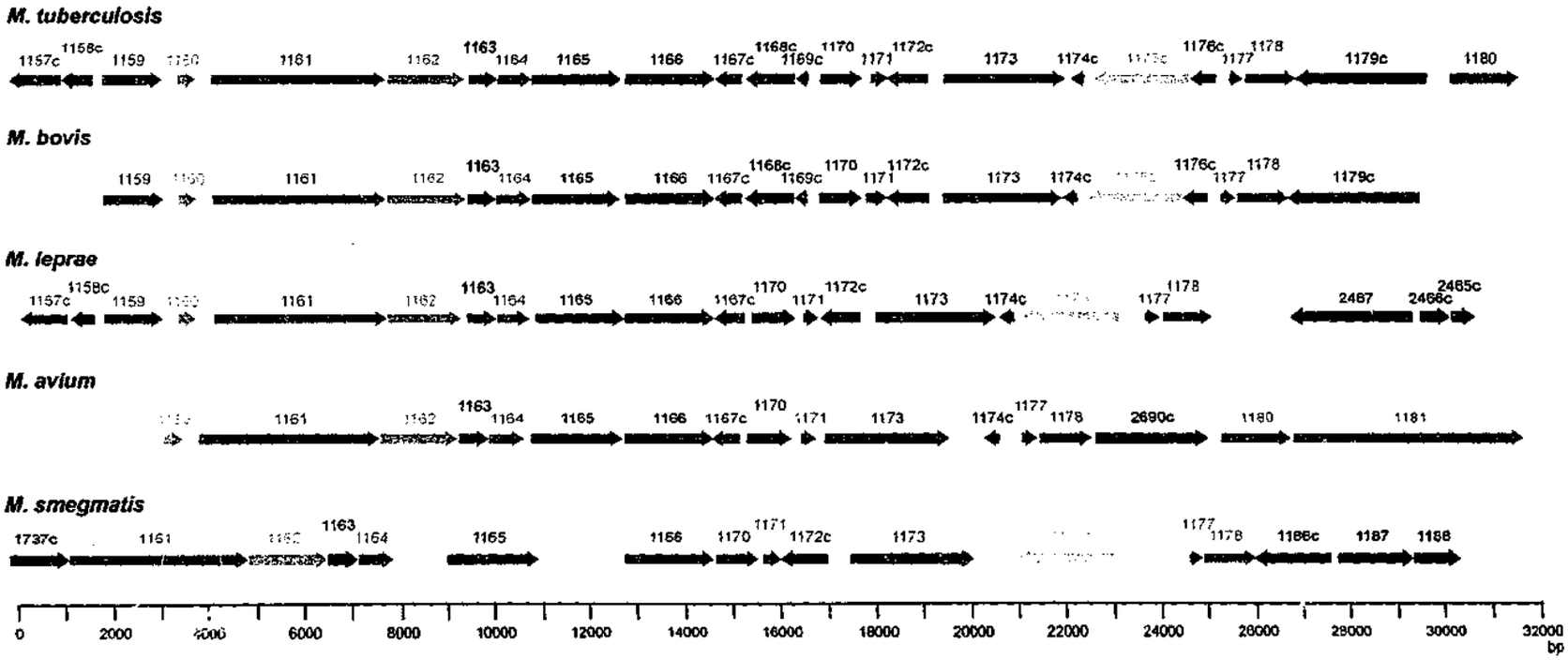

Figure 4.6a
Comparison of the *lpqW* locus in various mycobacteria.
The sequencing projects for *M. tuberculosis* $H_{37}R_v$, *M. bovis* AF2122/97, *M. leprae* TN (Sanger Institute), *M. avium* 104 (TIGR) and *M. smegmatis* mc^2155 (this study, TIGR) were accessed to compile genomic maps of the region surrounding the *lpqW* gene.
The numbers assigned to each ORF are based on the *M. tuberculosis* $H_{37}R_v$ numbering system (47), such that ORFs which matched a particular *M. tuberculosis* ORF were assigned that ORFs number. Matching colours indicate homologous genes between each species. *lpqW* is presented in red as (Rv)1166 (bp: base pairs).

(Figure is continued on next page).

(Figure is continued on next page).

ORF Match	*M. smegmatis* Amino acid Identity/Similarity to:			Proposed Function
	M. tuberculosis/ M. bovis	*M. leprae**	*M. avium*	
Rv1737c	80, 97	NM	NM	*narK2*: nitrate/nitrite transporter
Rv1161	79, 86	34, 43	81, 88	*narG*: nitrate reductase α-subunit
Rv1162	80, 86	47, 56	79, 85	*narH*: nitrate reductase β-chain
Rv1163	65, 74	47, 60	66, 74	*narJ*: nitrate reductase δ-chain
Rv1164	73, 83	37, 47	65, 78	*narI*: nitrate reductase γ-chain
Rv1165	84, 91	88, 93	91, 95	GTP binding protein?
Rv1166	74, 82	70, 80	74, 82	*lpqW*: hypothetical lipoprotein
Rv1170	66, 77	62, 74	66, 73	*mshB*; *myo*-Inosityl-*N*-acetylglucosamine deacetylase
Rv1171	54, 71	48, 67	54, 72	Unknown (hydrophobic protein)
Rv1172c	25, 46	NM	NM	*M. tuberculosis* PE family
Rv1173	86, 91	84, 89	85, 91	Unknown, conserved
Rv1175c	81, 88	36, 47	NM	*fadH*: 2,4-dienoyl coA reductase
Rv1177	87, 92	86, 90	90, 93	*fdxC*: ferredoxin (highly similar to Rv2007c, *fdxA*)
Rv1178	79, 87	78, 85	77, 83	Possible aminotransferase
Rv1186c	70, 80	NM	70, 81	Unknown, contains helix-turn-helix motif
Rv1187	80, 87	NM	81, 89	*rocA*: Probable pyroline-5-carboxylate dehydrogenase
Rv1188	68, 76	NM	70, 77	Probable proline dehydrogenase

Figure 4.6b
Comparison of the *lpqW* locus in various mycobacteria.
(Figure is continued from previous page)

The proposed function of each ORF is listed, together with their amino acid sequence similarities to the likely *M. smegmatis* homologues.
NM: no matches found.

region amongst the species tested. However, no apparent gene clusters which would lend clues to the function of *lpqW* are obvious.

4.3.4 MYCO479 and MYCO481 contain Identical Transposon Insertions into lpqW

The distinct compositional differences seen between MYCO479 and MYCO481 may be a result of the strains containing transposon insertions at different points in the genome, resulting in distinct phenotypes. While both MYCO479 and MYCO481 show the same hybridisation pattern to an IS6100 probe (Figure 4.1b), the extensive sequence data generated from MYCO479 allows for the design of a more specific means of testing for the *lpqW* transposon insertion in the two mutant strains.

Transposon Orientation in MYCO479 and MYCO481 are Identical

The observed difference in phenotype between MYCO479 and MYCO481 may be caused by a difference in the way in which Tn*611*/pCG79 has inserted into the chromosome. It remains a possibility that the Tn*611*/pCG79 could excise by homologous recombination between copies of the IS6100 elements. A change in insert orientation upon reinsertion may have unforeseen effects, such as introducing expression signals which influence the transcription of the genes downstream of *lpqW*.

If MYCO479 genomic DNA was cleaved with *Pvu*II, fragments of 9.3 kb, 8.2 kb and a fragment of approximately 2 kb internal to the insertion should hybridise with an IS6100 probe (Figure 4.7a). Variations in the orientation of the insert can be distinguished since the hybridisation profiles would be detectably different. For any transposon mutant, three hybridising bands corresponding to the three IS6100 elements in the insertion should always be observed. The wild-type is not expected to hybridise, since it does not harbour IS6100.

The wild-type and mutant strains were grown in PPLO broth and exhibited the growth characteristics observed previously (see Sections 2.3.2 and 2.5.1). Genomic DNA was extracted, digested with *Pvu*II and hybridised with IS6100 (Figure 4.7b). The wild-type showed no evidence of hybridisation, as anticipated. The *metA* transposon mutant MYCO320 exhibited the expected 2 kb internal insertion fragment, as well as hybridising fragments of approximately 8.5 and 6 kb.

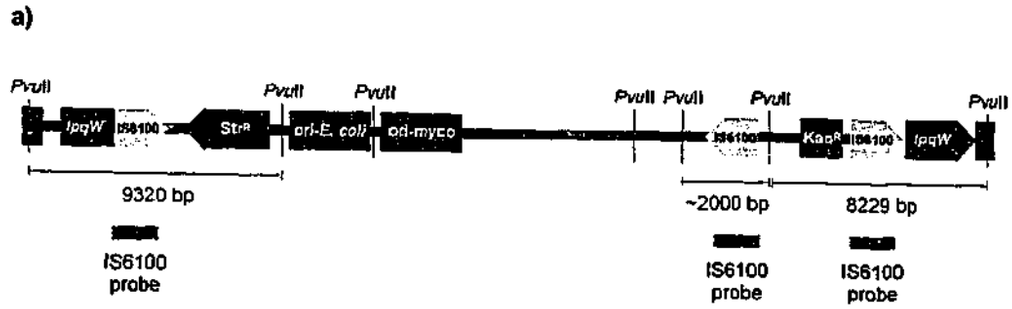

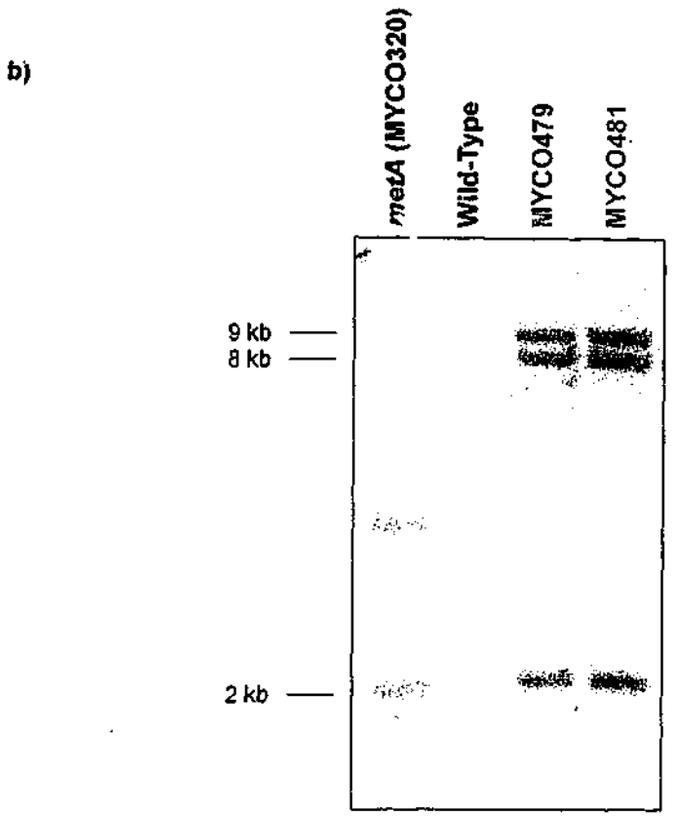

Figure 4.7
MYCO479 and MYCO481 show identical Tn*611* transposon insertions in *lpqW*.
a) Expected location and size of *Pvu*II restriction fragments hybridising to a probe comprising of a section of IS6100 from pCG79. Genomic DNA was digested with *Pvu*II and resolved in 1% (w/v) agarose in TAE.
b) Southern hybridisation showing the resulting restriction fragments hybridised with the IS6100 probe. The wild-type and the two mutants MYCO479 and MYCO481 were examined for the nature of the Tn*611* insertion in *lpqW*. MYCO320 contains a Tn*611* insertion in the *metA* gene and was included as a control. The sizes of hybridising bands are indicated in kilobases (kb).

This profile is distinct from that expected for MYCO479. MYCO481 showed the same hybridisation pattern as in MYCO479, with fragments of approximately 9.3 and 8.2 kb hybridising to IS6100 in addition to the internal 2 kb fragment. Together with the result presented in Figure 4.1, this result provided evidence that despite marked differences in phenotype, MYCO479 and MYCO481 exhibit identical Tn*611*/pCG79 insertions into the *lpqW* gene.

The Site of* lpqW *Insertion is Identical

A PCR-based approach was designed to detect specific transposon insertion events using oligonucleotide primers that specifically target *lpqW* transposon mutant genome. In this case, primer 7389 targetted *lpqW* sequence near the disruption site defined in MYCO479. When used in conjunction with the IS6100-specific primer 3053, an amplification product of 697 bp was expected (Figure 4.8a). Primer 9276, which targets *M. smegmatis* sequence near the opposing side of the insertion, was also used together with the IS6100 specific primer 3054. An amplification product of 291 bp was expected when using these two primers (Figure 4.8b). Both of these products should only amplify in transposon mutants containing a disruption in the same location as that seen in MYCO479. Neither product is expected to amplify from the wild-type or mutants with a Tn*611* insertion in genes other than *lpqW*. Thus, the wild-type and MYCO320 were used as controls.

Genomic DNA extracted from PPLO-grown cells was used as a PCR template for the wild-type, MYCO320, MYCO479 and MYCO481. No amplification products of the expected size were obtained from the negative controls, the wild-type and MYCO320. MYCO479 and MYCO481 yielded identical PCR amplification products in two reactions using primers 7389/3053 and primers 9276/3054, respectively (Figure 4.8). Some unincorporated primers or a non-specific product is visible in the 3053/7389 reaction, probably due to the reaction conditions not being optimal. These results confirm that MYCO481 contains an *lpqW* Tn*611*/pCG79 disruption identical to the one defined in MYCO479. These results also show that the two PCRs used are specific for *lpqW* transposon mutants and do not amplify the expected products from the wild-type and an unrelated Tn*611* mutant.

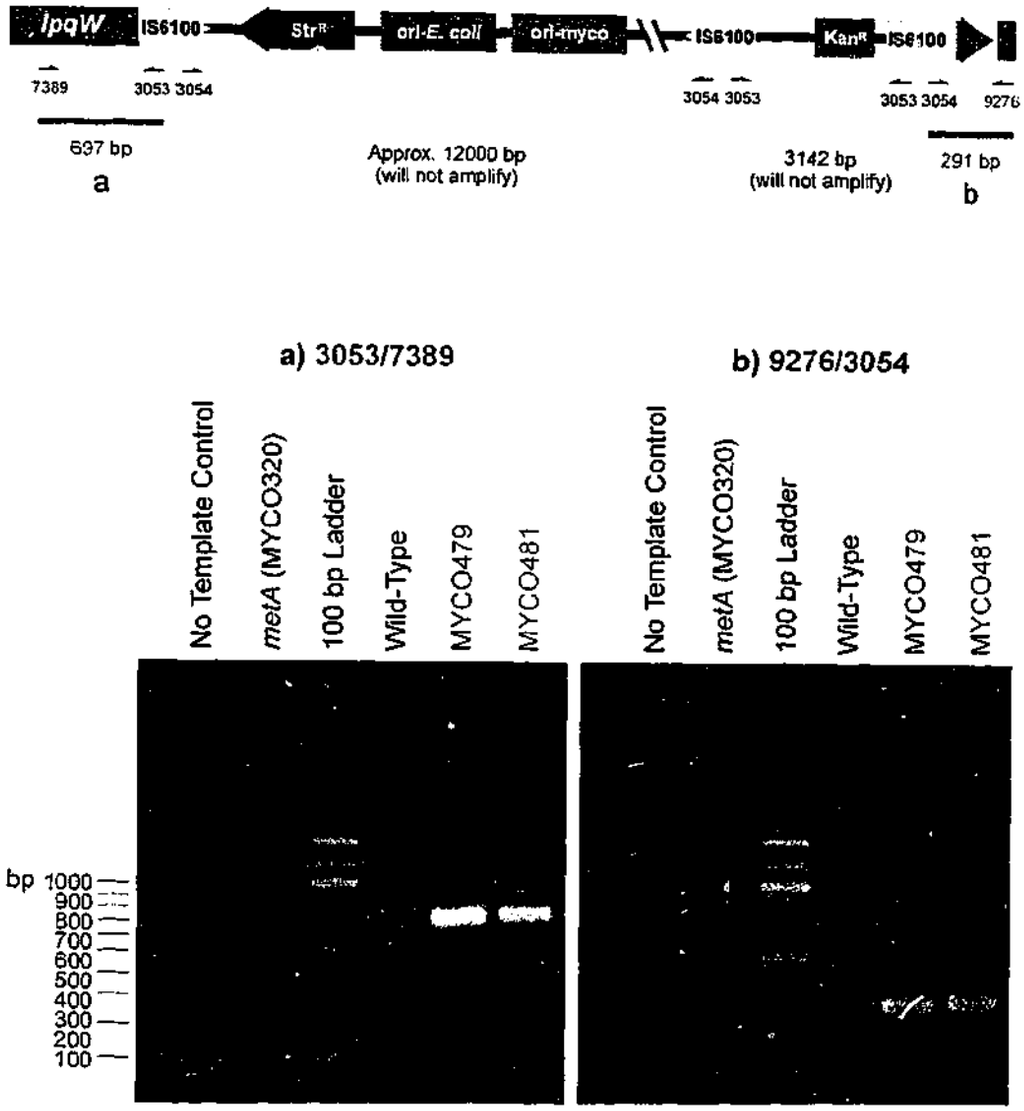

Figure 4.8
The *lpqW* transposon insertion is consistent in MYCO479 and MYCO481.
Two separate PCR amplifications were designed to test for the presence of Tn*611* in *lpqW*. The wild-type and the two transposon mutants were tested for the presence of Tn*611* in *lpqW*. For both reactions, MYCO320 (Tn*611* disruption of *metA*) was included as a negative control. Amplification products were resolved in 1.5% (w/v) agarose in TAE.
a) In the case of *lpqW* insertion which is identical to MYCO479, primers 3053 and 7389 are expected to amplify a 697 bp product. The resulting amplification products are presented.
b) Amplification products using primers 3054 and 9276 are expected to amplify a 291 bp product. The amplification products resulting from this reaction are shown.

Markers are shown in base pairs (bp).

4.3.5 *MYCO81/MYCO479 Colony Morphology and* lpqW *Disruption are Consistent in Different Media*

It is possible that different media conditions may affect the stability of the transposon insertion in the *lpqW* mutants, given that gross phenotypic differences were seen for MYCO481 depending on the media used (Chapter 2). While the transposon appears to be stable in PPLO media (section 4.3.4), the change in MYCO481 colony morphology observed when the mutant was grown on Middlebrook 7H10 agar may be the result of a change in the Tn*611* insertion. It is possible that 7H10 media may select for genetic variants. An experiment was designed to determine if the characteristic colony morphology and *lpqW* insertion of MYCO481 was maintained after incubation in either PPLO or Middlebrook media. Media conditions were also alternated or between PPLO and Middlebrook media to test if this had an effect on the *lpqW* insertion. Colonies which were grown on PPLO agar then subcultured into PPLO broth were designated the "PPLO/PPLO" series, while PPLO-grown colonies subcultured in Middlebrook 7H9 broth (i.e. change of media) were designated as the "PPLO/7H9" series. Conversely, colonies which were grown on Middlebrook 7H10 agar then subcultured into Middlebrook 7H9 broth were designated as the "7H10/7H9" series while those subcultured in PPLO broth (i.e. change of media) were called the "7H10/PPLO" series. The wild-type, MYCO479 and MYCO481 were grown under these media conditions, and genomic DNA subsequently extracted.

Site of Insertion is Identical After Growth on Various Media

To test if the media conditions described above selected for genetic variants that had alterations in the region of *lpqW*, primers 7389/3053 and 9276/3054 were used to amplify genomic DNA from each strain as previously described (section 4.3.4). The results are presented in Figure 4.9. The *metA* transposon mutant MYCO320 was grown in PPLO and its genomic DNA included as a negative control. MYCO320 showed weak amplification of a product of approx. 150 bp, not indicative of an *lpqW* disruption.

Primers 3053 and 7389 yield a product of 697 bp expected for *lpqW* transposon mutants (Figure 4.9a). The results for each of the four media conditions tested were found to be identical. In each case, both MYCO479 and MYCO481 showed amplification of an approx. 700 bp product, consistent with an *lpqW*

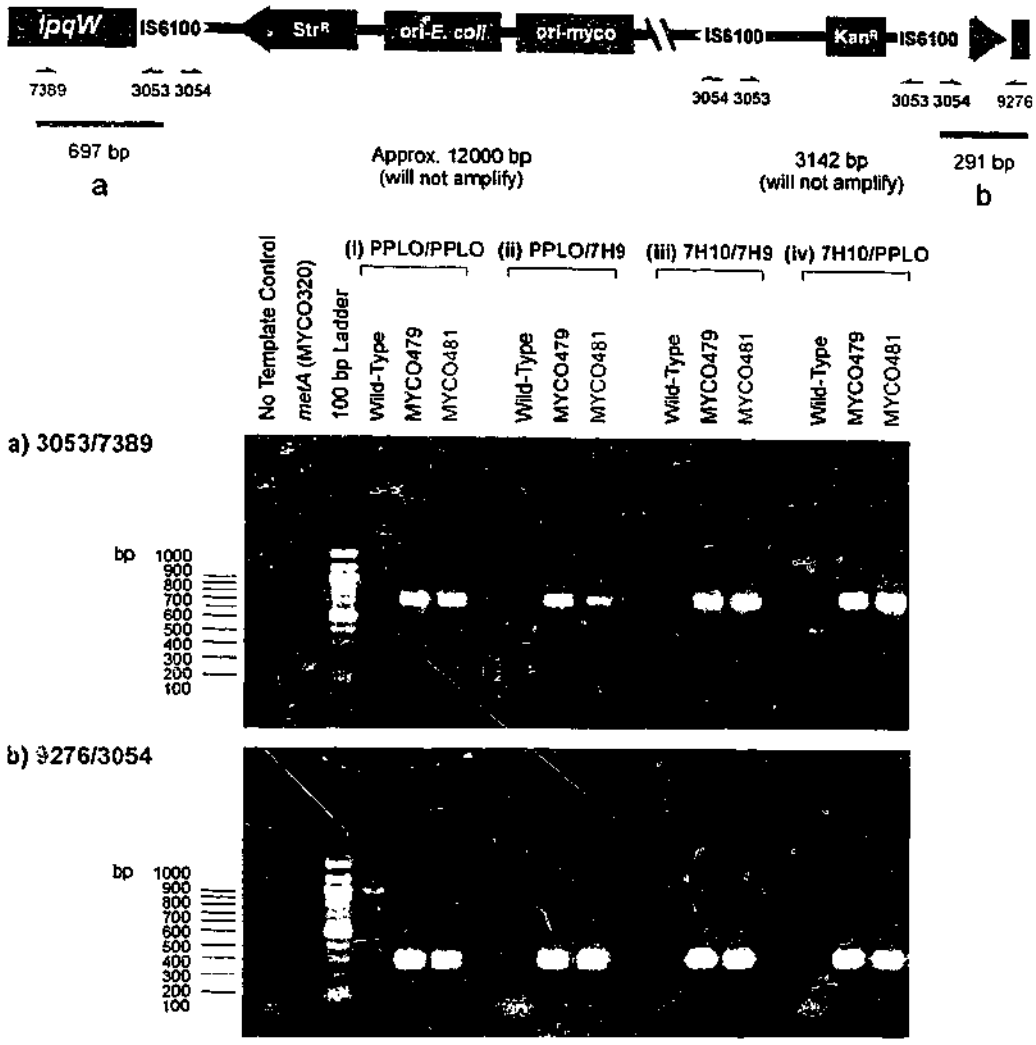

Figure 4.9
The *lpqW* insertion in MYCO479 and MYCO481 is not affected by media conditions.
The wild-type and the *lpqW* mutants MYCO479 and MYCO481 were grown in PPLO and Middlebrook media under various conditions:
(i) PPLO/PPLO series (PPLO colony to PPLO broth).
(ii) PPLO/7H9 series (PPLO colony to Middlebrook 7H9 broth).
(iii) 7H10/7H9 series (Middlebrook 7H10 colony to Middlebrook 7H9 broth).
(iv) 7H10/PPLO series (Middlebrook 7H10 colony to PPLO broth).

Two PCR amplifications were designed to test for the presence of Tn*611* disruption in *lpqW*. For both reactions, MYCO320 (Tn*611* disruption of *metA*) was included as a negative control. Amplification products were resolved in 1.5% agarose in TAE.

a) In the case of *lpqW* insertion which is identical to that found in MYCO479, primers 3053 and 7389 are expected to amplify a 697 bp product. The resulting amplification products are presented.
b) Amplification products using primers 3054 and 9276 are expected to amplify a 291 bp product. The amplification products resulting from this reaction are shown.
Markers are shown in base pairs (bp).

transposon insertion. The wild-type showed no amplification products, which was expected as the strain does not harbour Tn*611*.

The primer combination of 9276 and 3054 was expected to amplify a 291 bp product in the case of the *lpqW* transposon mutant (Figure 4.9b). Both the *metA* mutant MYCO320 and the wild-type did not show amplification of the product, which was as expected. Some amplification was observed, but in both cases the products were weak and clearly not the correct size. For each of the culturing conditions, MYCO479 and MYCO481 showed amplification of the 291 bp product. Together with the 3053/7389 PCR results, this demonstrates that regardless of the media used and the resultant colony morphology, both transposon mutants exhibit the Tn*611* insertion in *lpqW*.

4.4 An lpqW Mutant that shows variation in Colony Morphology and PIM/LAM Content

The results presented in this chapter show that despite different colony morphologies and a distinct PIM/LAM phenotype (Chapter 2, Chapter 3), MYCO481 and MYCO479 were shown to be Tn*611* transposon mutants. Further, the site of Tn*611* insertion was the same in each case, and the arrangement of the transposon insert does not appear to differ between the two mutants. The colony morphology differences seen in different media had no bearing on the location of the Tn*611* insertion, which was shown to be the same under various culture conditions. The difference in colony morphology, concurrent with the observed PIM/LAM phenotype, must be caused by a structural or metabolic difference between the two forms of the mutant. This difference may be caused by mutations which occur elsewhere in the genome.

The Tn*611* disruption was found to be within a putative gene called *lpqW*. In MYCO479 and MYCO481, the Tn*611* insertion is situated near the 3' terminus of the gene, such that most of *lpqW* would be intact in the transposon mutants. It is conceivable that the mutant produces a truncated LpqW which is partially functional. This may be examined further by determining whether a truncated *lpqW* mRNA transcript is present, and whether it is able to facilitate the expression of a truncated protein. Alternatively, the mutant may be expressing a truncated LpqW which may not be functional, since Tn*611* has inserted into a region of the

sequence which is well conserved amongst the species tested and hence may be functionally important.

LpqW has no reported function. The amino acid sequence contains a hydrophobic signal peptide, signal peptidase II cleavage site and a lipid attachment site, and hence seems likely to be a lipoprotein. Signal peptidase II is a post-translational modification enzyme which acts to cleave signal peptides from pro-lipoproteins while they are being translocated across the cytoplasmic membrane (135). After the signal peptide is cleaved, the remaining cysteine residue is substituted with lipid moieties to form a lipoprotein. Lipoproteins are likely to be anchored into to the outer face of the cytoplasmic membrane via the lipid (166, 185). LpqW may therefore be located on the outer leaflet of the cytoplasmic membrane. The role of the gene in PIM/LAM biosynthesis is unclear. The probable function of LpqW as a membrane-bound lipoprotein is consistent with PIM/LAM synthesis being active in membrane fractions (23, 98, 108, 173).

While it is tempting to speculate that the lack of mannosylation from PIM_4 to PIM_6 in MYCO479 could be due to a disrupted mannosyltansferase gene, the match to the reported signature motif is not convincing. LpqW may be a membrane-bound mannosyltransferase which uses PPMs as a direct mannose donor, and therefore may not contain the reported GDP-man binding site of α-mannosyltransferases (75).

The LpqW sequence showed relatively weak matches to various Family 5 extracellular solute binding proteins. The Family 5 category includes several oligopeptide binding proteins found in both Gram-positive and Gram-negative organisms. It is not clear whether LpqW represents one of these proteins, since a consensus sequence observed by Tam and Saier (195) is only partially present in the sequence. Nevertheless, some proteins which show similarly convincing matches to known Family 5 solute binding proteins do not show strict agreement with this consensus, but rather a more scattered similarity to known oligopeptide binding proteins. It is possible that LpqW may have a role in regulating the availablity of substrates or enzymes used in PIM/LAM synthesis.

The characterisation of the PIM biosynthetic cluster in *M. tuberculosis* (98, 108) has shown that at least two of its ORFs, *pgsA* and *pimA*, are essential for mycobacterial survival. The cluster is highly conserved in *M. smegmatis* (Figure

1.7), both in terms of sequence similarity and genetic arrangement. With the observation that the *M. leprae* genome may represent a minimal gene set for the mycobacteria (48), the relative conservation of the *lpqW* locus in *M. leprae* suggests that it is an essential gene. While *lpqW* is not adjacent or in proximity to this cluster in *M. tuberculosis* (47), the location of the gene in *M. smegmatis* was unknown. The PIM cluster contains genes which have so far been involved in the very early stages of PIM biosynthesis. As *lpqW* mutants are affected in the higher PIM and LAM sections of the pathway, it is not suprising that *lpqW* is not linked to the PIM cluster. If *lpqW* is highly conserved in other mycobacteria as it is in *M. tuberculosis*, it is probable that the gene is of importance to the genus.

The *lpqW* gene may be a part of a separate PIM/LAM biosynthetic cluster which may also show high conservation amongst the species, although this was not clear from the *lpqW* region examined in this study. In *M. smegmatis*, six gene homologues upstream of *lpqW* as well as the Rv1170 and Rv1171 homologues all appear to be transcribed in the same direction, forming a cluster which is abutted by the divergently transcribed homologue of Rv1172c. It is interesting that *lpqW*, a gene which is potentially involved in PIM/LAM biosynthesis, is upstream of a gene involved in the production of another inositol containing molecule, mycothiol. The fact that these ORFs have no defined function as yet means that the possibility of a functionally related gene cluster at this locus cannot be dismissed. Analysis of the mRNA for any polycistronic transcripts produced from this locus would provide more information.

Chapter 5
MYCO481 Undergoes Change to Resemble MYCO479

5.1 Rationale and Objectives

5.1.1 Are the Two lpqW Mutants Related?

In Chapter 2, it was established that MYCO481 produced characteristically small colonies in comparison to the wild-type and MYCO479. Curiously, when MYCO481 was subcultured on LB or PPLO agar, the small colony phenotype was lost through subculture and eventually normal "large" colonies were obtained. Large colonies were always evident for MYCO479 and the wild-type. However, these differences were not apparent when the strains were grown and subcultured in Middlebrook 7H10 media, where all strains produced colonies of approximately the same diameter (see Figure 2.3). The results presented also demonstrated that MYCO479 and MYCO481 showed distinct biochemical differences. MYCO479 was deficient in PIM_6 and accumulated PIM_4. In contrast, MYCO481 produced a normal complement of PIMs and showed a marked reduction in the amount of LAM. These major differences were observed regardless of the media used. Further differences between the two strains were observed with respect to their PIM and LAM biosynthetic characteristics, as described in Chapter 3.

It was then established in Chapter 4 that despite these differences in colony morphology and biochemical composition, both MYCO479 and MYCO481 contained a Tn*611* insertion in *lpqW* at identical locations. Hence, two morphologically and biochemically distinct strains contain identical *lpqW* transposon insertions.

The observation that MYCO481 produces an unstable small colony morphology which changes to a normal large morphology through subculture raises the possibility that MYCO481 is altered to a more stable form of the *lpqW* transposon mutant which resembles MYCO479. A correlation in the change of colony phenotype with a change in the PIM/LAM phenotype, together with stability of the *lpqW* transposon insertion would support this theory. With the

identification of the *lpqW* insertion and the differentiation of the two mutants based on biochemical composition, this possibility can be investigated.

5.1.2 Aims of this Section

The main aim of this section is to establish whether or not MYCO479 is derived from MYCO481, using a combination of genetic and biochemical tests. The first aim of this chapter is to recreate the change in colony morphology seen in MYCO481. Subsequently, the aim was to correlate this change in colony morphology with an altered PIM/LAM phenotype. The final objective was to test if any observed change in biochemical profile and colony morphology affected the stability of the Tn*611* insertion into *lpqW*. In each case, the ability of different media to induce any of these changes was examined.

5.2 Materials and Methods

5.2.1 Chemicals, Reagents, Strains and Media

Suppliers for chemicals and reagents used in this study are listed in Section 2.2.1 of Chapter 2. The *M. smegmatis* strains used in this section are listed in Appendix 1. The media was prepared as per Appendix 2, and culturing conditions are described in section 2.2.2.

5.2.2 Subculturing of Strains

In order to monitor possible changes in MYCO481 colony morphology, single colonies of the wild-type, MYCO479 and MYCO481 were isolated from PPLO agar plates and resuspended in 200 µL of LB broth, PPLO broth or Middlebrook 7H9 broth. A characteristically small colony of MYCO481 was chosen for analysis, while normal (large) colonies of the wild-type and MYCO479 were selected. One hundred µL of resuspended colony was then inoculated into 30 mL of the same type of media, and incubated for four days at 39°C with shaking.

After incubation, each strain was subcultured by sampling 300 µL of culture to inoculate into a fresh 30 mL broth of the same media. The subculture was then incubated for a further four days. This subculturing cycle was repeated for a total of five subcultures.

5.2.3 Colony Morphology on PPLO Agar

At the end of each subculturing cycle 1 mL of culture was sampled, serially diluted, and plated onto PPLO agar to determine the colony morphology. In this case, PPLO was used as an "indicator" media for differentiating between the large and small colony morphology. Previous experience had shown that the small colony form was more reliably produced on PPLO media through subculture, while LB agar seemed to be more strongly selective against the small colony type. The plates were incubated for four days, and following incubation those with well isolated, countable colonies were scored for the proportion of large and small colonies in the population.

5.2.4 Biochemical Analysis

After being sampled to inoculate the next subculture (section 5.2.2) and plated for PPLO colony morphology (section 5.2.3), the remaining culture was harvested by centrifugation and stored at -20°C. Once all of the subcultures were collected, they were analysed for their PIM profile by HPTLC (sections 2.2.3, 2.2.4) and LAM content by GC-MS (sections 2.2.3, 2.2.5). The raw GC-MS data is included in Appendix 3.

5.2.5 Genetic Analysis

One hundred µL of the originally resuspended PPLO agar-grown colony (section 5.2.2) was inoculated into 30 mL of LB, PPLO or Middlebrook 7H9 broth and grown for four days. Genomic DNA was then extracted from the cultures. These were designated as "Initial" samples. Following the fifth and final subculture (section 5.2.2), 300 µL of culture was sampled and inoculated into a fresh 30 mL of the corresponding broth. This broth was incubated overnight, and genomic DNA then extracted. The DNA from these cultures were labelled as "Final" samples.

The genomic DNA was digested with *Pvu*II, resolved by agarose gel electrophoresis and immobilised to nylon membrane. The DNA was then probed with labelled IS6100 via Southern hybridisation to test for the characteristic presence of the Tn*611* disruption in *lpqW*. The techniques used for mycobacterial DNA isolation and Southern hybridisation are described in sections 4.2.3 and 4.2.9.

5.3 MYCO479 is Derived from MYCO481

5.3.1 MYCO481 Colony Morphology Changes through Subculture

The PPLO agar colony morphology from each subculture was scored with respect to the number of large and small colonies on a countable plate. In each case, the wild-type and MYCO479 showed a consistently normal ("large") colony morphology on PPLO agar throughout the subculturing period. This was the case for colonies plated from LB, PPLO or Middlebrook 7H9 broth. MYCO481 colonies, however, changed throughout the period of the experiment. The large and small colony morphology numbers recorded for MYCO481 are presented in Table 5.1.

Subculturing in LB Broth

When first cultured in LB broth, the MYCO481 culture consisted of predominantly small colonies characteristic of the mutant. Only 1 of the 219 colonies counted was found to be large. However, by the second subculture no small colonies were seen and the population was only comprised of the large colony types. The homogeneous large colony population was maintained throughout the remainder of the subculturing period. This demonstrated that in LB, MYCO481 initially consisted of a population of cells which formed small colonies on PPLO agar; subculturing MYCO481 in LB broth quickly converted this initial population to one which was dominated by cells able to form normal, large-sized colonies on PPLO agar.

Subculturing in PPLO Broth

Subculturing MYCO481 through PPLO had a similar effect to that observed for LB broth. In the first subculture, the majority of colonies were small in size. By Subculture 2, 17% of the cells in the population generated large colonies, while in Subculture 3, 84% of the cells grew into large colonies. Subcultures 4 and 5 consisted of almost entirely large colonies. These numbers indicated that in PPLO, a form of MYCO481 that generated large colonies on PPLO agar was gradually selected. The conversion of a culture which consisted of small colony forming cells to one which contained cells that formed large colonies was not as rapid as that seen in LB broth.

MYCO481 Subculture Media	Colonies Counted on PPLO Agar	
	Large	Small
LB broth		
Subculture 1	1	218
Subculture 2	58	0
Subculture 3	115	3
Subculture 4	38	0
Subculture 5	76	0
PPLO broth		
Subculture 1	2	386
Subculture 2	48	226
Subculture 3	21	4
Subculture 4	287	5
Subculture 5	126	0
Middlebrook 7H9 broth		
Subculture 1	2	187
Subculture 2	0	47
Subculture 3	11	281
Subculture 4	8	311
Subculture 5	3	89

Table 5.1
MYCO481 colony morphology on PPLO agar changes through subculture.
MYCO481 was subcultured five times in either LB, PPLO or Middlebrook 7H9 broth. At the end of each round, the culture was serially diluted and spread plated onto PPLO agar. Plates which yielded colony numbers of between 25 and 400 were then scored for the number of small colonies typical of the mutant, and for normal ("large") colonies.

Subculturing in Middlebrook 7H9 Broth

When subcultured through Middlebrook 7H9 broth, MYCO481 behaved differently to that observed for LB or PPLO broth. At subculture 1, two large colonies out of 189 were observed, showing that the population consisted predominantly of cells which formed small colonies on PPLO agar. Throughout the subsequent subcultures, the maximum proportion of large colonies was 4%. This demonstrated that throughout the subculturing process, MYCO481 did not lose its ability to produce the small colony phenotype. The results implied that Middlebrook 7H9 broth exerted little or no selective pressure on MYCO481.

5.3.2 MYCO481 PIM_6 is Lost and LAM Increased through Subculture

At each subculture, PIMs were extracted and examined by HPTLC. The corresponding LAM content for subcultures 1 and 5 was analysed by GC-MS compositional analysis.

Subculturing in LB Broth

The PIM profiles of the strains subcultured in LB broth are shown in Figure 5.1. The results show that throughout the subculture period, the wild-type strain demonstrated a consistently normal PIM profile, where PIM_2 and PIM_6 accumulate (Figure 5.1a). This result shows that the PIM profile of *M. smegmatis* is not drastically altered throughout the course of multiple LB broth subcultures.

The MYCO481 subculture series contained the wild-type PIM profile only in subculture 1. Subculture 2 contained a novel, mixed PIM profile, where PIM_2, PIM_4 and PIM_6 are apparent. In addition, the amounts of PIM_6 were reduced when compared to Subculture 1. For the remainder of the subculturing period, PIM_4 accumulated while PIM_6 was completely absent, resembling the expected PIM profile of MYCO479. This result shows that subculturing MYCO481 through LB broth results in the loss of PIMs by the second or third subculture coinciding with the accumulation of PIM_4.

The PIM profile of MYCO479 remained stable throughout the subculturing period. In each case, its characteristic PIM_6-deficient, PIM_4 accumulating phenotype was observed (Figure 5.1c). This result demonstrates that the PIM profile of MYCO479 is not affected by serial subculture through LB broth.

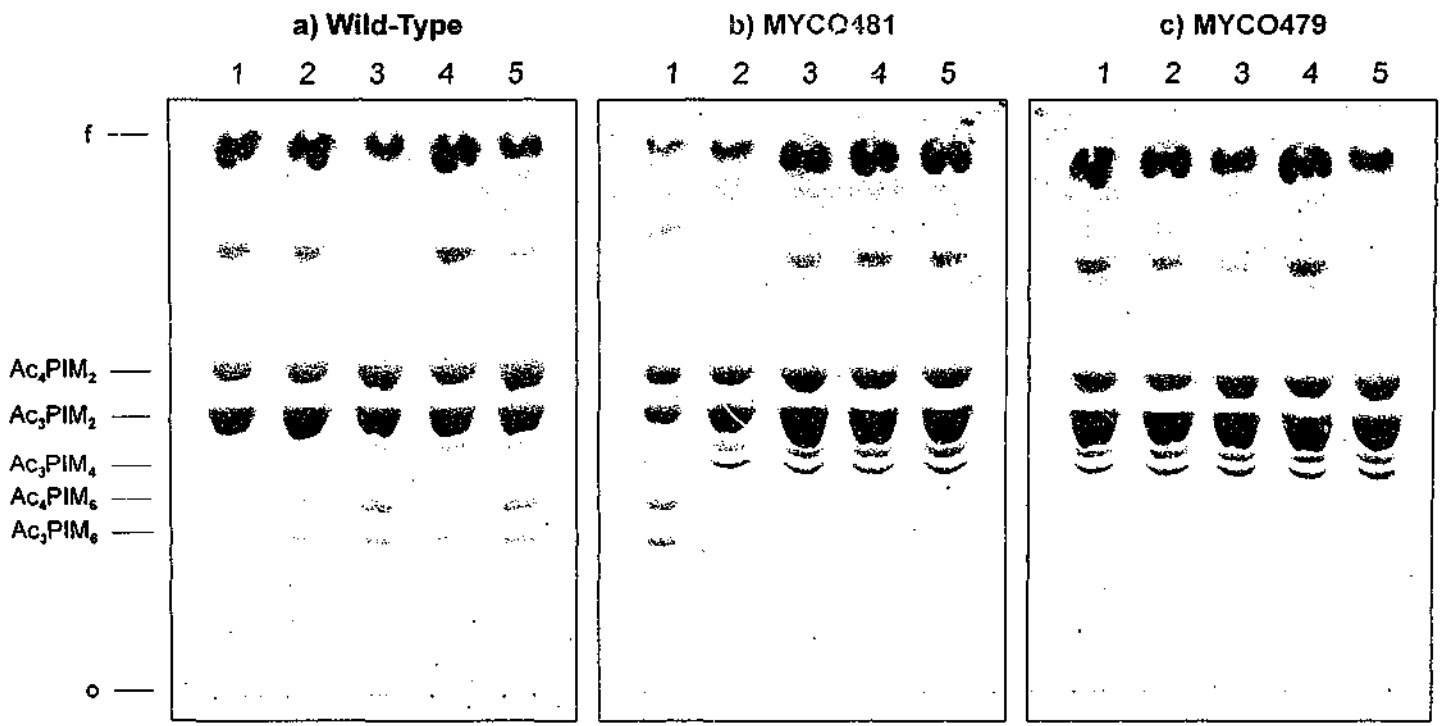

Figure 5.1

PIM profiles of strains serially subcultured through LB broth.

The wild-type and the *lpqW* transposon mutants (MYCO481 and MYCO479) were serially subcultured five times (1 to 5) through LB broth. At the end of each subculture, the cells were collected and PIMs extracted. PIMs were resolved by HPTLC and developed using Solvent System A. The plates were then stained with orcinol. The positions of Ac_4/Ac_3PIM_2, Ac_3PIM_4 and Ac_4/Ac_3PIM_6 are also marked. a) Wild-Type serial subculture. b) MYCO481 serial subculture. c) MYCO479 serial subculture.

The position of the sample origin is indicated by an "o", while the solvent front is indicated by an "f".

The LAM content of selected subcultures were then examined (Figure 5.2). Between Subcultures 1 and 5, the wild-type extracts demonstrated little difference in the amount LAM-derived sugars. The three-fold increase in arabinose may be due to the often variable nature of the arabinose measurements encountered throughout this study (see Chapter 2). MYCO481 extracts had markedly less inositol, mannose and arabinose in Subculture 1 when compared to the wild-type, consistent with its expected LAM-deficient phenotype. Subculture 2 of MYCO481, which demonstrated a mixed PIM profile (Figure 5.2b), showed markedly elevated sugar levels when compared to subculture 1, while still being considerably lower than those seen in the wild-type. By Subculture 5, these levels had increased more, to a point where the amount of inositol and mannose was approaching those seen in Subculture 5 of the wild-type. The arabinose levels measured were, however, still low. This result suggests that when subcultured through LB, MYCO481 cells with increased LAM levels are selected for. This increase coincides with the loss of PIM_6 and the accumulation of PIM_4 in the corresponding PIM profiles.

When the LAM content of MYCO479 was examined for Subculture 1, sugar levels similar to those of Subculture 1 from the wild-type were recorded. By Subculture 5, these levels were reduced by approximately 2.5-fold, a reduction greater than normally expected for this mutant. This suggested that some sample loss may have occurred during the extraction or analysis. Nevertheless, it was demonstrated that the LAM content does not resemble that of the typically LAM-deficient MYCO481 seen in Subculture 1.

Subculturing in PPLO Broth

The PIMs extracted from strains subcultured through PPLO broth are presented in Figure 5.3. The wild-type showed a stable PIM profile throughout the subculturing period (Figure 5.3a). This result demonstrates that in PPLO, serial subculture does not affect the PIMs of the wild-type strain.

When MYCO481 is subcultured through PPLO broth, a change in PIM profile is evident (Figure 5.3b). At Subcultures 1 and 2, a normal PIM profile is observed. At Subculture 3, the mixed PIM_4/PIM_6 profile similar to the profile seen in Subculture 2 of the LB broth series (Figure 5.1b) was observed. It appears as though PIM_6 was depleting while PIM_4 was accumulating. By Subculture 4, PIM_6

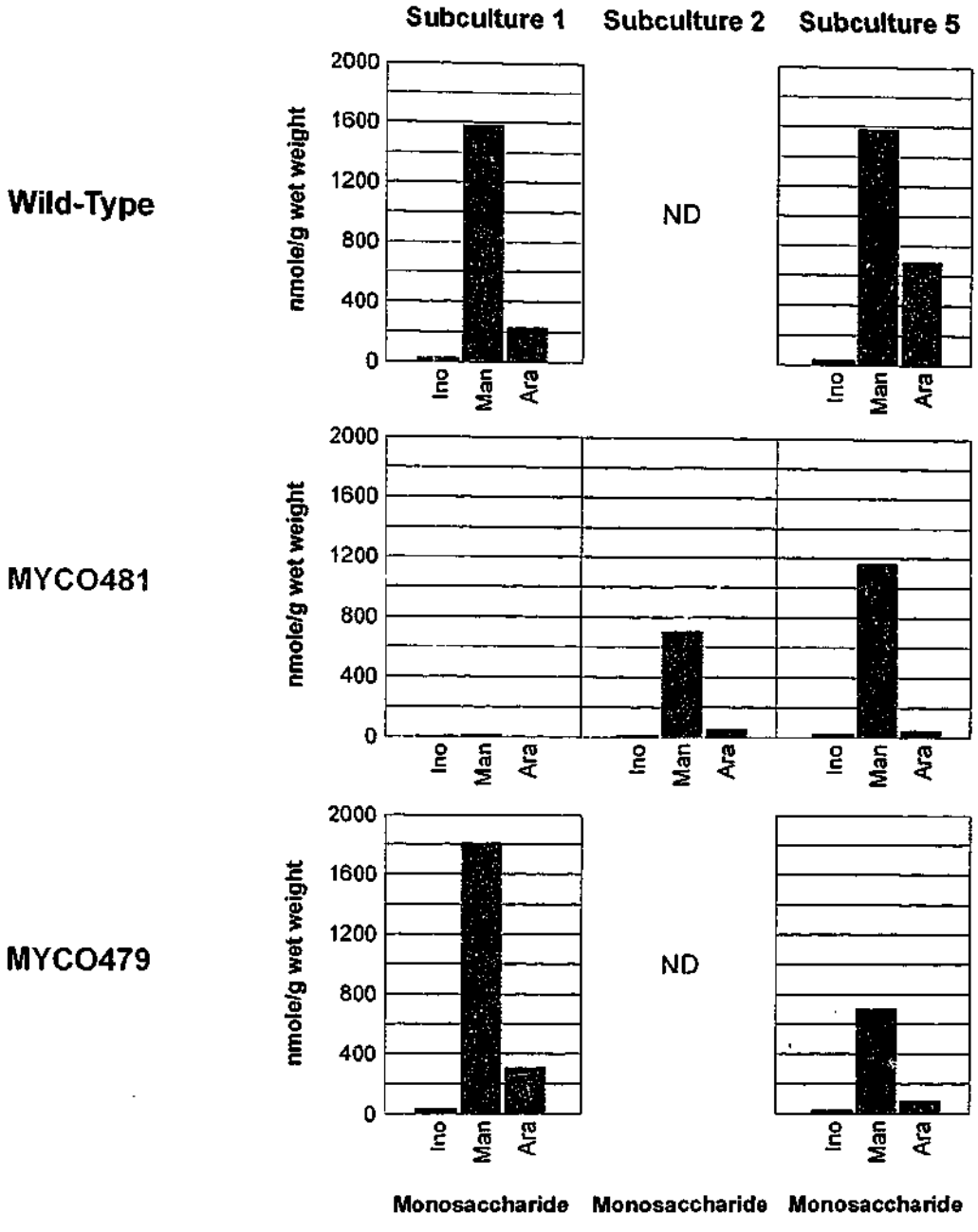

Figure 5.2
LAM content of strains serially subcultured through LB broth.
The wild-type and the *lpqW* transposon mutants (MYCO481 and MYCO479) were serially subcultured five times through LB broth. At the end of selected subcultures, LAMs were extracted. Samples were then subjected to methanolysis and TMS derivatisation, and analysed by GC-MS. Subcultures 1 and 5 were analysed for the wild-type, along with subcultures 1, 2 and 5 for MYCO481 and subcultures 1 and 5 for MYCO479 (ND: analysis not done).

The constituent monosaccharides of LAM are presented are: *myo*-inositol (Ino), D-mannose (Man) and D-arabinose (Ara). The values given are nmole of sugar per gram of cell pellet wet weight (nmole/g wet weight).

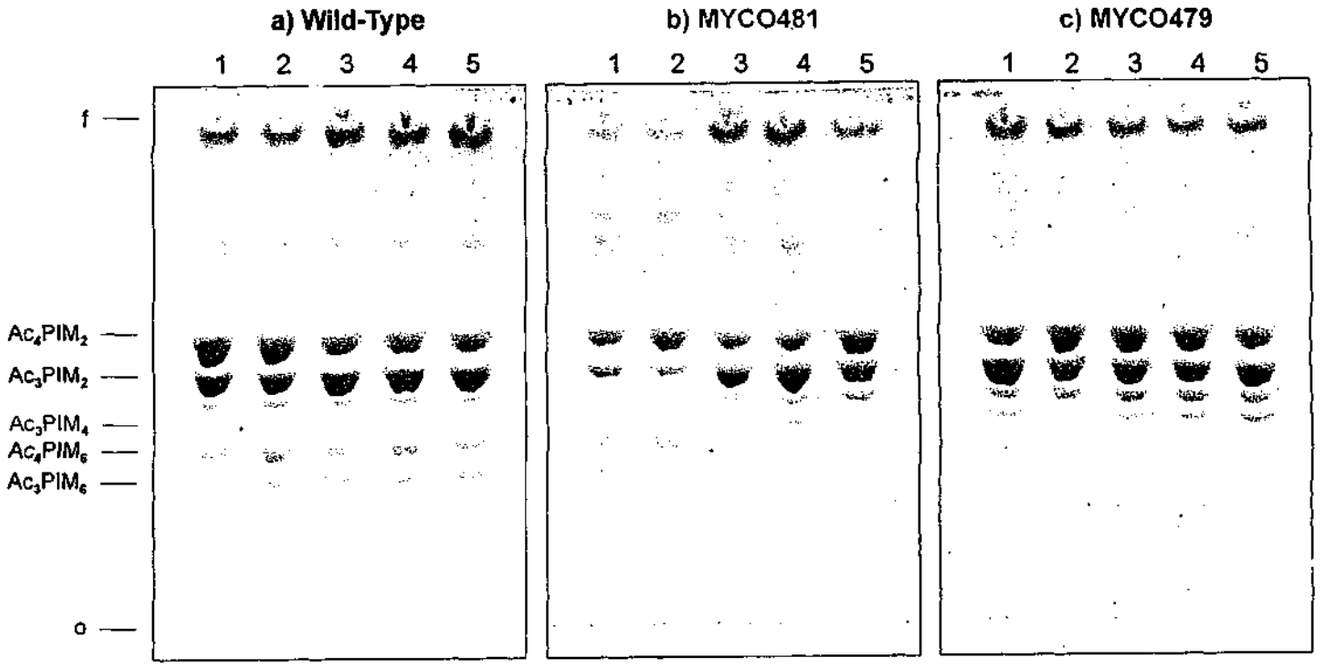

Figure 5.3
PIM profiles of strains serially subcultured through PPLO broth.
The wild-type and the *lpqW* transposon mutants (MYCO481 and MYCO479) were serially subcultured five times (1 to 5) through PPLO broth. At the end of each subculture, the cells were collected and PIMs extracted. PIMs were resolved by HPTLC and developed using Solvent System A. The plates were then stained with orcinol. The positions of Ac_4/Ac_3PIM_2, Ac_3PIM_4 and Ac_4/Ac_3PIM_6 are also marked. a) Wild-Type serial subculture. b) MYCO481 serial subculture. c) MYCO479 serial subculture.
The position of the sample origin is indicated by an "o", while the solvent front is indicated by an "f".

The position of the sample origin is indicated by an "o", while the solvent front is indicated by an "f".

was absent and PIM_4 present in a greater amount. This profile was also seen in Subculture 5. These results suggest that subculturing MYCO481 in PPLO broth results in the gradual loss of PIM_6 and the appearance of PIM_4, as observed in the LB broth subculturing experiment. The change from the profiles resembling the wild-type to that of MYCO479 appears to be more gradual than the change observed in the LB subcultures.

Subculturing MYCO479 through PPLO had no effect on its PIM profile (Figure 5.3c). As with the cultures propagated in LB broth, this result demonstrates that the MYCO479 PIM profile remains stable throughout serial subculturing in PPLO.

The LAM content of selected PPLO subcultures was then analysed (Figure 5.4). From Subculture 1 to Subculture 5, the wild-type showed an approx. 2-fold increase in sugar levels. At Subculture 1, MYCO481 showed the expected low levels of each sugar. When Subculture 3 was examined, the inositol, mannose and arabinose levels all increased markedly but were still somewhat lower than those seen in the wild-type. This subculture of MYCO481 contained a mixed PIM profile (Figure 5.3b). At Subculture 5, the sugar levels were slightly lower than those seen at subculture 3, but still greatly increased compared to those of Subculture 1. The sugar levels were approx. 5-fold lower than those of Subculture 5 of the wild-type. This result suggests that when subcultured through PPLO broth, MYCO481 cells with increased LAM levels are selected for. As with the LB subculture series, this observed increase in LAM coincides with the loss of PIM_6 and the accumulation of PIM_4 in the corresponding PIM profiles. However, the increase of LAM levels are not as marked as those induced by LB broth in subcultures of MYCO481.

Subculturing MYCO479 through PPLO had no major effect on its LAM content. While some difference was observed between Subculture 1 and 5, the difference was clearly not as large as that seen in the MYCO481 subculturing experiment. The very low sugar levels expected of MYCO481 were not seen in MYCO479.

Subculturing in Middlebrook 7H9 Broth

The PIMs extracted from strains serially subcultured through Middlebrook 7H9 broth are shown in Figure 5.5. The subculturing process had no major effect on the PIM profile of the wild-type, which yielded normal PIMs throughout (Figure

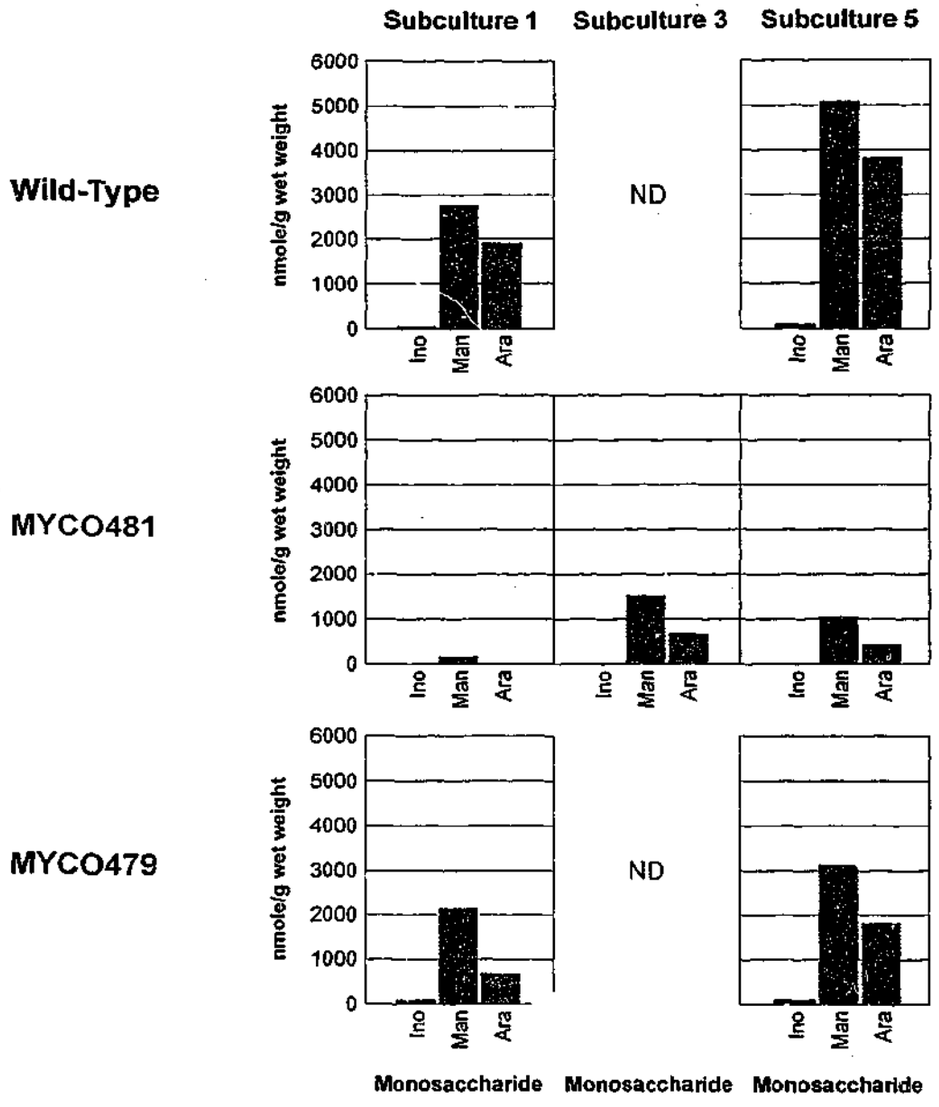

Figure 5.4
LAM content of strains serially subcultured through PPLO broth.
The wild-type and the *lpqW* transposon mutants (MYCO481 and MYCO479) were serially subcultured five times through PPLO broth. At the end of selected subcultures, LAMs were extracted. Samples were then subjected to methanolysis and TMS derivatisation, and analysed by GC-MS. Subcultures 1 and 5 were analysed for the wild-type, along with subcultures 1, 3 and 5 for MYCO481 and subcultures 1 and 5 for MYCO479 (ND: analysis not done).

The constituent monosaccharides of LAM are presented are: *myo*-inositol (Ino), D-mannose (Man) and D-arabinose (Ara). The values given are nmole of sugar per gram of cell pellet wet weight (nmole/g wet weight).

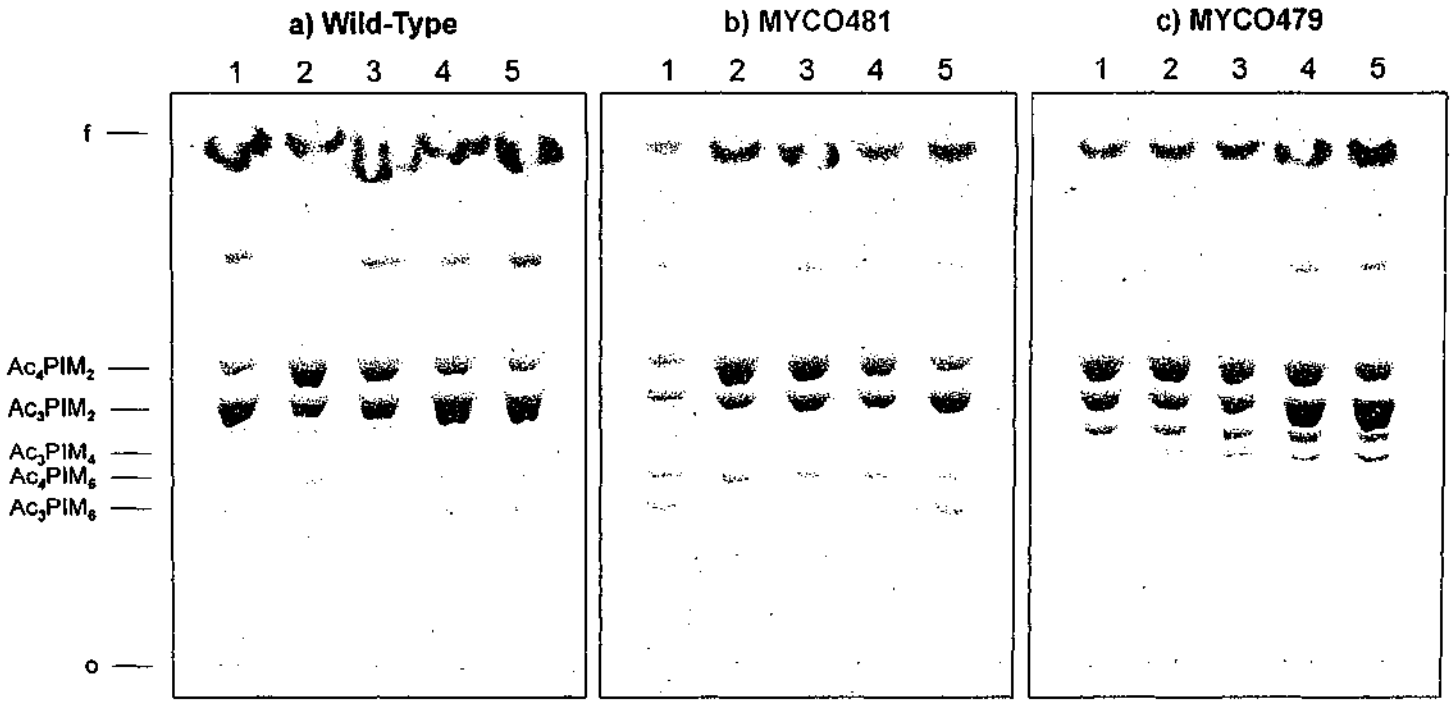

Figure 5.5
PIM profiles of strains serially subcultured through Middlebrook 7H9 broth.
The wild-type and the *lpqW* transposon mutants (MYCO481 and MYCO479) were serially subcultured five times (1 to 5) through Middlebrook 7H9 broth. At the end of each subculture, the cells were collected and PIMs extracted. PIMs were resolved by HPTLC and developed using Solvent System A. The plates were then stained with orcinol. The positions of Ac_4/Ac_3PIM_2, Ac_3PIM_4 and Ac_4/Ac_3PIM_6 are also marked. a) Wild-Type serial subculture. b) MYCO481 serial subculture. c) MYCO479 serial subculture.
The position of the sample origin is indicated by an "o", while the solvent front is indicated by an "f".

5.5a). It was also shown that subculturing MYCO481 in Middlebrook 7H9 broths had no effect on the strains normal PIM profile, which was shown to be stable throughout all five subcultures (Figure 5.5b). This was a suprising result, given the apparent effect of growth in LB and PPLO broth. These results demonstrated that the normal PIM profiles of the wild-type and MYCO481 remained stable in Middlebrook 7H9, with no apparent loss of PIM_6 or accumulation of PIM_4. The characteristic PIM profile of MYCO479 was also shown to be stable in this media (Figure 5.5c), as it was in LB and PPLO broth.

The LAMs extracted from the subcultured strains were then examined (Figure 5.6). The wild-type showed little variation between subculture 1 and 5, showing that the subculturing process had no major effect on its LAM content. Subculture 1 of MYCO481 showed very low sugar levels when compared to the wild-type, as expected. These levels were somewhat increased in subculture 5, but were still approx. 10-fold or more lower than those seen in subculture 5 of the wild-type, and as such were still very low. This result suggested that in addition to maintaining a stable PIM profile, serial subculture of MYCO481 through Middlebrook 7H9 broth also maintained a very low LAM content.

The sugar levels seen for subculture 1 of MYCO479 were lower than those of the wild-type, but much greater than those of the LAM-deficient MYCO481. The levels recorded for Subculture 5 showed an increase in each sugar, being approx. 1.5-fold greater than those seen in subculture 5 of the wild-type. Again, these levels do not resemble those of the LAM-deficient MYCO481.

5.3.3 *The* lpqW *Transposon Insertion Remains Stable*

In order to test whether or not the serial subculturing process resulted in a change in the *lpqW* Tn*611* insertion, genomic DNA from the beginning and end of the subculturing period was probed with the IS6100 probe. By digesting the genomic DNA with *Pvu*II, fragments characteristic of a Tn*611* insertion into *lpqW* were detected by hybridisation with IS6100, as described in section 4.3.4 (see Figure 4.7). Briefly, the probe hybridises to fragments of 9320 bp, 8229 bp and approx. 2000 bp in the *lpqW* transposon mutants MYCO479 and MYCO481. Major rearrangements in the transposon insertion can be detected as fragments of sizes which differ to those expected for the two mutants. Also, these fragments are

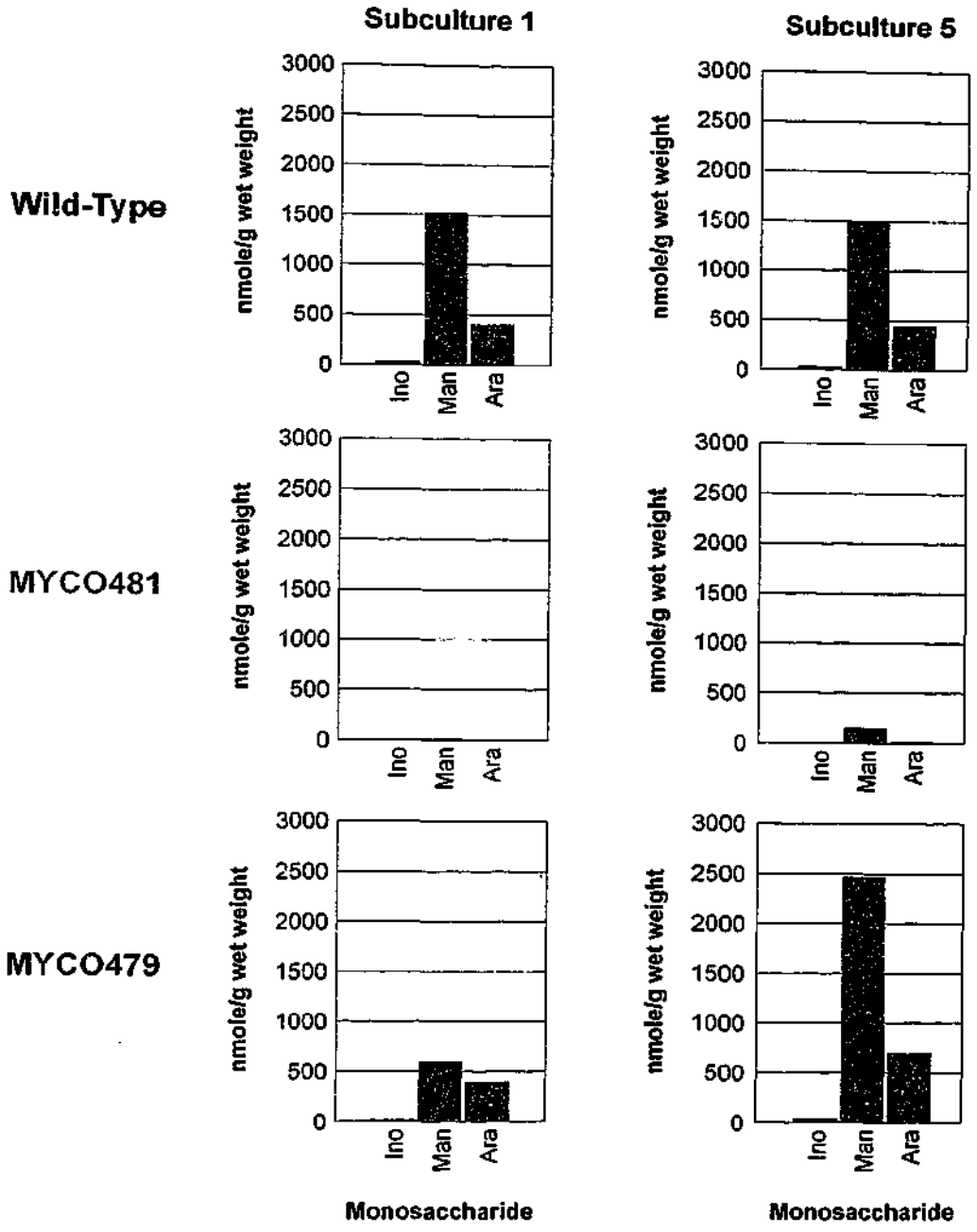

Figure 5.6
LAM content of strains serially subcultured through Middlebrook 7H9 broth.
The wild-type and the *lpqW* transposon mutants (MYCO481 and MYCO479) were serially subcultured five times through Middlebrook 7H9 broth. At the end of selected subcultures, LAMs were extracted. Samples were then subjected to methanolysis and TMS derivatisation, and analysed by GC-MS. Subcultures 1 and 5 were analysed for the wild-type, MYCO481 and MYCO479.

The constituent monosaccharides of LAM are presented are: *myo*-inositol (Ino), D-mannose (Man) and D-arabinose (Ara). The values given are nmole of sugar per gram of cell pellet wet weight (nmole/g wet weight).

characteristic of the *lpqW* insertion and any variation in the observed hybridising fragments would imply that the transposon has changed location within the genome.

The results for genomic DNA extracted as "Initial" and "Final" samples are presented in Figure 5.7. In the case of LB broth (Figure 5.7a), PPLO broth (Figure 5.7b) and Middlebrook 7H9 broth (Figure 5.7c), no difference was observed between the beginning and the end of the subculturing period. The DNA extracted from the wild-type showed no hybridisation, confirming that the transposon is absent from the strain. In the case of MYCO481 and MYCO479, hybridising bands of approx. 9 kb, 8 kb and 2 kb were observed.

These results suggest that the serial subculturing of MYCO481 and MYCO479 through each media had no effect on the presence or location of the transposon. Despite MYCO481 showing changes in colony morphology, PIM profile and LAM content through subculture in LB and PPLO, the strain remained an *lpqW* transposon mutant.

5.4 *Two Phenotypically Distinct* lpqW *Mutants are Related*

The results presented in this chapter provide biochemical and genetic evidence that MYCO479 is derived from MYCO481. To demonstrate this, a change in MYCO481 colony morphology was created by serial subculturing through liquid media. This allowed the resulting colony morphologies and PIM profiles to be examined at each subculture. LAMs were also investigated at selected steps in the process, and genomic DNA was examined at the beginning and end of the subculturing procedure.

It was found that depending on the media used, the MYCO481 population changes from its original phenotype to one which more closely resembles that of MYCO479. At the beginning of the experiment, MYCO481 displays its characteristic small colonies on PPLO agar, produces a very low level of LAM, contains a normal PIM profile and includes a Tn*611* insertion into *lpqW*. After subculture in LB or PPLO broth, MYCO481 produces normal ("large") PPLO colonies, shows an elevated amount of LAM in relation to the start of the experiment, lacks PIM_6, accumulates PIM_4 and retains a transposon insertion in *lpqW*. In other words, MYCO481 undergoes a change into a strain resembling

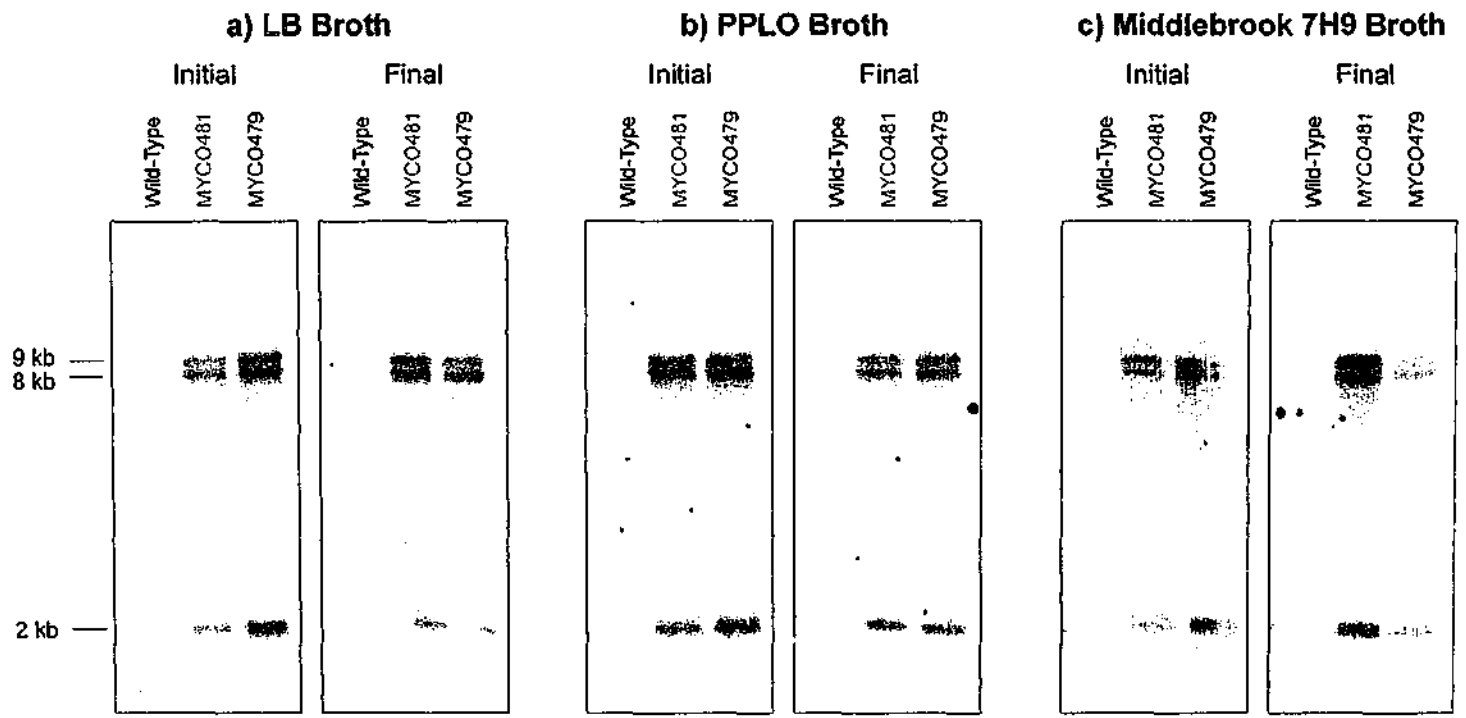

Figure 5.7
The *lpqW* transposon insertion is stable through subculture.
The wild-type and *lpqW* mutant (MYCO481 and MYCO479) strains were subcultured through LB, PPLO or Middlebrook 7H9 broth. Genomic DNA was extracted at the beginning ("Initial") and end ("Final") of the subculturing period. The DNA was digested with *Pvu*II and resolved in 0.8% (w/v) agarose in TAE. The resulting restriction fragments were probed with IS6100 and hybridisation detected. A Tn*611* insertion into *lpqW* is confirmed when the probe hybridises to *Pvu*II fragments of 9.23 kb, 8.22 kb and approx. 2 kb.
a) Subculture through LB broth. b) Subculture through PPLO broth. c) Subculture through Middlebrook 7H9 broth. Sizes of hybridising fragments are indicated to the left of the figure in kilobases (kb).

MYCO479. Furthermore, this change appears to be stable and irreversible under these culturing conditions. When MYCO479 was subjected to the subculturing procedure, its PIM profile was stable and its LAM content was not vastly reduced. Additionally, the subcultured MYCO479 strain always produced large PPLO colonies and still maintained the transposon insertion in *lpqW*. Therefore, it appears that once MYCO481 changes its phenotype to that of MYCO479, its phenotype is stabilised.

The strains different responses in different media were interesting. MYCO481 did not produce the change to the MYCO479-like phenotype after subculturing through Middlebrook 7H9. In this case, most of the strains resulting PPLO colonies remained small. The few large colonies that were seen may have been a result of plating the culture onto PPLO media, which was shown to promote the conversion in phenotype. At the end of subculture, the PIM profile remained normal, LAM levels were still very low in comparison to the wild-type, and the *lpqW* insertion remained. An increase in LAM is evident through Middlebrook 7H9 subculture, but the low LAM content characteristic of MYCO481 is maintained. This result also confirmed that Middlebrook 7H9 is useful as a media which is able to stably support the phenotype of MYCO481 through any future experiments. In the case of LB and PPLO media, the MYCO481 LAM levels were not restored to those of the wild-type or MYCO479. This implies that the PIM profile is more rapidly changed in the population, while change in LAM levels occurs more gradually. Growing MYCO481 for further subcultures in LB and PPLO broth may show this to be the case.

It is not clear why such differences were observed between the different media. Neither PPLO nor LB are defined media, while Middlebrook 7H9 is. It is therefore difficult to make an accurate comparison of the ingredients of each media to try to identify components that may influence the change in MYCO481. It is also unclear why the presumably more nutritious formulations of PPLO and LB are less able to support the phenotype which is stable in the defined and less nutritious Middlebrook media.

One difference that may be important is the amount of salt in each media. LB contains 1% (w/v) NaCl, PPLO contains 0.5% (w/v) NaCl, while Middlebrook 7H9 contains just 0.085% (w/v) NaCl. These salt concentrations correlate with the

relative ability of the media to induce the phenotypic change in MYCO481; LB broth produced the most rapid change, PPLO resulted in a rapid change but was more gradual that that seen in LB, and little or no change was seen in Middlebrook 7H9. Being a LAM-deficient mutant, MYCO481 possesses a cell envelope defect that may greatly change its osmotic properties and therefore render the mutant at a disadvantage when growing in LB and PPLO. It would be interesting to examine this theory further. For instance, MYCO481 can be subcultured in LB and PPLO with varying salt levels, including those equivalent to Middlebrook 7H9, to see if these modified media induce any change in the mutant. An alternative strategy would be to test the cell permeability of each mutant in comparison to the wild-type, using an approach similar to that applied for a penicillin binding protein-deficient mutant of *M. smegmatis* (25). It remains possible that Middlebrook 7H9 can select for the change in phenotype, perhaps over a much longer subculturing period.

The observation that subculturing MYCO479 through LB or PPLO media led to no major changes in its PIM/LAM phenotype demonstrated that the MYCO479 phenotype was permanent, and not reversed to that of MYCO481. The biochemical changes seen in MYCO481 through subculture are therefore likely to be a result of permanent secondary genetic mutations in addition to the *lpqW* transposon disruption, rather than metabolic changes which are more likely to be reversible.

These secondary genetic mutations may arise from an undefined selective pressure. It is plausible that the earlier form of the *lpqW* mutant, the LAM-deficient MYCO481, is disadvantaged when grown in LB or PPLO. Under these conditions, mutations that overcome this disadvantage are desirable and are hence selected for. These secondary mutations accumulate until the MYCO479 phenotype is created, at which point the cells viability is restored and the new phenotype remains stable. The "mixed" PIM profile observed as MYCO481 changes through subculture possibly reflects a mixed population of cells, where some contain normal PIMs while others lack PIM_6 and accumulate PIM_4. This possibility is supported by the observation that such "mixed" PIM cultures result in a mixture of large and small colony morphologies.

The number and nature of these secondary mutations would prove difficult to identify. It remains possible that the "early" form of the transposon mutant, MYCO481, has already accumulated secondary mutations in addition to the *lpqW* disruption, and that MYCO479 represents a version of the strain with additional mutations. Clearly, the mutations result in the loss of PIM_6 and presumably PIM_5, and hence may be involved in PIM biosynthesis. Since the structures of PIM_5 and PIM_6 are not consistent with the structure of LAM, these mutations are not likely to be located in genes involved in LAM biosynthesis. Applying the same logic, if genes involved in LAM biosynthesis were mutated, the LAM levels observed in MYCO481 undergoing the changes should further decline rather than rise. However, it remains possible that the secondary mutations result in the increased activity of LAM biosynthetic genes, either through elevated promoter activity or by resulting in a more structurally stable or enzymatically efficient altered gene product. Determining the identity of these genes would be of great interest, as they may represent novel genetic determinants involved in the PIM/LAM biosynthetic pathway.

Chapter 6
lpqW and the PIM/LAM Phenotype

6.1 Rationale and Objectives

6.1.1 Is lpqW involved in the PIM/LAM Phenotype?

Although MYCO481 and MYCO479 share identical Tn*611* insertions within the *lpqW* gene (Chapter 4), the two mutants show distinct biochemical differences (Chapters 2 and 3). The results presented in Chapter 5 also imply that MYCO481 is an earlier, ancestral form of the mutant MYCO479. Clearly, if there is a reproducible biochemical difference between the two strains and the *lpqW* disruption is unchanged, then other genetic differences must exist. The changes in phenotype through subculture raise questions as to whether the role of the *lpqW* disruption in the PIM/LAM phenotype is merely coincidental and whether its disruption is actually responsible for the observed biochemical discrepancies. The observed switching of phenotypes from MYCO481 to MYCO479 makes this a significant likelihood. While the fact that *lpqW* transposon mutants show the PIM/LAM phenotype does suggest that the disrupted gene is somehow responsible for the observed biochemical profiles, further evidence is required to connect the *lpqW* mutations to the phenotype.

A means of addressing this question is to provide the transposon mutants with an intact copy of *lpqW*. The gene would be isolated from the wild-type and provided episomally on an expression vector. If the gene disruption is responsible for the PIM/LAM phenotype, then the intact *lpqW* should complement the mutation and therefore restore a normal biochemical phenotype. Another possibility is that the Tn*611* disruption of *lpqW* is not only affecting that gene but also those genes which are transcribed downstream of *lpqW*. It is apparent from Figure 4.6 that there are two ORFs downstream of *lpqW*, representing likely homologues of the *M. tuberculosis* ORFs Rv1170 and Rv1171 (47). These ORFs were therefore designated as ORF-1170 and ORF-1171. Both ORFs would be transcribed in the same direction as *lpqW*, and hence may form an operon. ORFs within operons are often functionally related, encoding for products which are involved in assembling

particular structures or constitute a part of the same biosynthetic pathway. Based on similarity searching (see Chapter 4, section 4.3.3) a functional relationship between *lpqW*, ORF-1170 and ORF-1171 is not obvious, but cannot be discounted. The lack of any clear promoter signals for these genes does not help to determine whether or not *lpqW* is part of an operon. If these ORFs do form an operon, then disrupting *lpqW* may affect the transcription of downstream genes which in turn may cause the PIM/LAM phenotype. These are often referred to as polarity effects.

6.1.2 Aims of this Section

The results presented in this chapter aim to establish whether or not the *lpqW* disruption in MYCO481 and MYCO479 is the cause of the PIM/LAM phenotype. The question was addressed in two parts.

The aim of the first part of this chapter is to provide MYCO481 and MYCO479 with an intact copy of *lpqW* to determine if the wild-type phenotype can be restored in the mutants. If complementation is successful, the LAM levels in MYCO481 should be elevated to a near wild-type level, while MYCO479 should produce a normal PIM profile. The restoration of a normal phenotype in both of the *lpqW* transposon mutants would implicate the gene as being responsible for the observed phenotype.

The second part of this chapter aims to disrupt the ORF directly downstream of *lpqW*, ORF-1170. If the *lpqW* transposon insertion is causing polarity effects on ORF-1170, then independently disrupting this gene may also produce the PIM/LAM phenotype.

6.2 Materials and Methods

6.2.1 Chemicals, Reagents, Strains and Media

Suppliers for chemicals and reagents used in this study are listed in Section 2.2.1 of Chapter 2. The *M. smegmatis* and *E. coli* strains used in this section are listed in Appendix 1. The media was prepared as per Appendix 2.

6.2.2 Bacteriological Culture

The culturing conditions for *M. smegmatis* are described in section 2.2.2 of Chapter 2. *E. coli* was grown according to the method described in section 4.2.2 of Chapter 4.

6.2.3 Complementation of MYCO481 and MYCO479

Wild-type, MYCO481 and MYCO479 cells were transformed with a construct containing the intact *lpqW* gene cloned into the *E. coli*/Mycobacterial shuttle vector pMV261 (192).

***Preparation and Transformation of Electrocompetant* M. smegmatis**

M. smegmatis electrocompetant cells were prepared according to a protocol described by Jacobs *et al.* (100). Plasmid DNA was prepared using the High Pure Plasmid Isolation Kit (Roche), in accordance with the manufacturers instructions. Approximately 1 µg of plasmid DNA was transformed into *M. smegmatis*. Electrotransformation was performed using a Bio-Rad Gene Pulser™ and a Bio-Rad Gene Controller™, according to the manufacturers instructions and the settings described by Jacobs *et al.* (100). *M. smegmatis* transformants were propagated on Middlebrook media (Appendix 2).

Analysis of Transformants

Putative transformants were then analysed for the presence of the complementation plasmid by transforming a crude mycobacterial lysate into *E. coli* and performing a plasmid DNA miniprep extraction on the resulting transformants. A single *M. smegmatis* transformant colony was resuspended in 100 µl of sterile distilled water. Approximately 100 mg of 0.10-0.11 mm glass beads (B. Braun Biotech International) was then added, and the cells homogenised by cell disruption for 40 secs at the medium speed setting using the Biospec Products Cell Disruptor. The resulting cell debris was then collected by centrifugation at 13000 rpm for 5 mins, and 50 µl of plasmid-containing supernatant decanted to a new tube. Plasmid DNA was then transferred to *E. coli* by transforming 2 µl of the crude extract into electrocompetent *E. coli* cells (section 4.2.8), and extracting plasmid DNA from the resulting *E. coli* transformants (section 4.2.3). Plasmids were analysed by restriction enzyme digestion and agarose gel electrophoresis. Methods for the cloning procedures and transformation of *E. coli* are described in detail in sections

4.2.3 to 4.2.9 of Chapter 4. Plasmid constructs used in this chapter are listed in Appendix 4, while the sequences of oligonucleotide primers are included in Appendix 5. PCR cycles are provided in Appendix 6.

Biochemical Analysis

Mycobacterial transformants containing recovered plasmids which resulted in the expected restriction maps were then analysed further. Each strain was tested for PIM profile and LAM composition, and compared to the non-transformed wild-type, MYCO481 and MYCO479 strains. Extraction and analysis of PIMs and LAM were performed as described previously in Sections 2.2.3 to 2.2.5 of Chapter 2. The raw GC-MS data is included in Appendix 3.

6.2.4 Targetted Disruption of ORF-1170

Wild-type cells were transformed with a pUC18-based (210) plasmid construct containing the ORF-1170 gene disrupted by a kanamycin resistance marker. The resistance marker is inserted into the wild-type ORF-1170 by virtue of homologous recombination with the ORF-1170 sequences flanking the kanamycin resistance marker in the plasmid. Transformants were then selected for on LB media (Appendix 2), and disruption of ORF-1170 by homologous recombination assessed by Southern hybridisation. Genomic DNA was probed with purified pHBJ269 insert to identify a strain that showed the desired recombination event. Methods for the cloning procedures, transformation of *E. coli* and Southern hybridisation are described in detail in sections 4.2.3 to 4.2.9 of Chapter 4. The strain was then analysed for its PIM profile and LAM composition together with the wild-type, MYCO481 and MYCO479 strains according to Sections 2.2.3 to 2.2.5 of Chapter 2. The raw GC-MS data is included in Appendix 3.

6.3 *Disruption in* lpqW *may be Responsible for the PIM/LAM Phenotype*

6.3.1 *Intact* lpqW *Partially Complements the PIM/LAM Phenotype*

Preparation of Complementation Constructs

Oligonucleotide primers 48 and 9276 were used to PCR amplify the *lpqW* ORF from *M. smegmatis* wild-type genomic DNA. Primer 48 was designed to incorporate an *Eco*RI site into the 5' end of the amplicon, facilitating the cloning of the fragment into the *Eco*RI site of the *E. coli/Mycobacterium* shuttle vector pMV261 (192). As a result, the ORF would be in frame with the pMV261 *hsp60* sequence and expressed via the constitutive *hsp60* promoter as a *hsp60/lpqW* fusion protein.

The primers PCR amplified a 1943 bp product. The product was purified, the termini modified and cloned into *Sma*I-digested pUC18. The resulting plasmid, pHBJ197, was sequenced using primers UP, RP, 317, 318, 320 and 394 to confirm that the sequence of the amplified and cloned *lpqW* matched that of the *M. smegmatis* genomic sequence data (TIGR). A single base change was detected at position 309 of the ORF sequence. It was found that the adenosine residue in codon 103 (TCA) was substituted with a guanidine (TC*G*). The change should not alter the expressed protein sequence, since both codons encode for a serine residue. Indeed, the use of TCG as a serine codon is heavily favoured in *M. tuberculosis* and *M. leprae*, while TCA is relatively uncommon (3, 57). In the *M. smegmatis* LpqW sequence, there are 30 serine residues of which 14 are encoded by TCG, whereas the only TCA codon present in the sequence is the one which is mutated in pHBJ197.

Plasmid pHBJ197 contained the *lpqW* ORF in an orientation where the *Eco*RI site introduced into the ORF by the PCR primer 48 was at the opposite end to the vector-derived *Eco*RI site. Hence, the entire 1.9 kb *lpqW* ORF was isolated from pUC18 with an *Eco*RI digest and subcloned into the *Eco*RI site of pMV261. The *lpqW* fragment was cloned in two orientations; pHBJ201 contained the *lpqW* ORF in an opposing direction to the *hsp60* promoter while pHBJ202 contained the ORF in a direction consistent with the *hsp60* promoter, and was therefore in the

orientation required for the expression of *lpqW*. The plasmids were analysed by sequencing pHBJ201 and pHBJ202 with the *hsp60*-based primer 6457. The resulting sequence confirmed the reverse orientation of *lpqW* in pHBJ201 as well as an *lpqW* transcriptional fusion with *hsp60* in pHBJ202.

Since the transposon mutants into which the constructs would be transformed are already kanamycin resistant by virtue of their pCG79/Tn*611* insertions, the kanamycin resistance gene of the pMV261-based constructs was not useful and needed to be replaced with another selection marker. A hygromycin resistance marker was chosen to replace the kanamycin resistance gene in pHBJ210 and pHBJ202. To this end, the hygromycin resistance gene of pEP3 (167) was PCR amplified from the plasmid using primers 8598 and 8599 to genrate a product of 1918 bp. Both pHBJ201 and pHBJ202 were then digested with *Nsi*I, which cleaves twice within the plasmids kanamycin gene. These fragments were then ligated to the hygromycin gene amplified from pEP3. Plasmid pHBJ201 containing the hygromycin gene was designated pHBJ210, while pHBJ202 containing the hygromycin gene was called pHBJ212.

The plasmid pHBJ212 contains an *lpqW* ORF cloned in frame with *hsp60* and should therefore be expressed via the upstream *hsp60* promoter. By comparison, pHBJ210 was identical to pHBJ212 except that the *lpqW* ORF was cloned in the opposite orientation. Plasmid pHBJ210 was included in the complementation experiment as a negative control. As an additional vector control, pHBJ164 was constructed by ligating the pEP3 hygromycin amplicon as a blunt-ended fragment into the *Sma*I site of pMV261, which also disrupts the kanamycin resistance marker of the vector. The main features of pHBJ164, pHBJ210 and pHBJ212 are shown in Figure 6.1, presented with restriction maps that will be referred to in the following experiments.

***Transformation into* M. smegmatis**

Plasmids pHBJ164, pHBJ210 and pHBJ212 were transformed into electrocompetant wild-type, MYCO481 and MYCO479. Hygromycin resistant transformants of the wild-type and hygromycin/kanamycin resistant transformants of MYCO481 and MYCO479 were selected, and the transformation efficiencies were determined (Table 6.1).

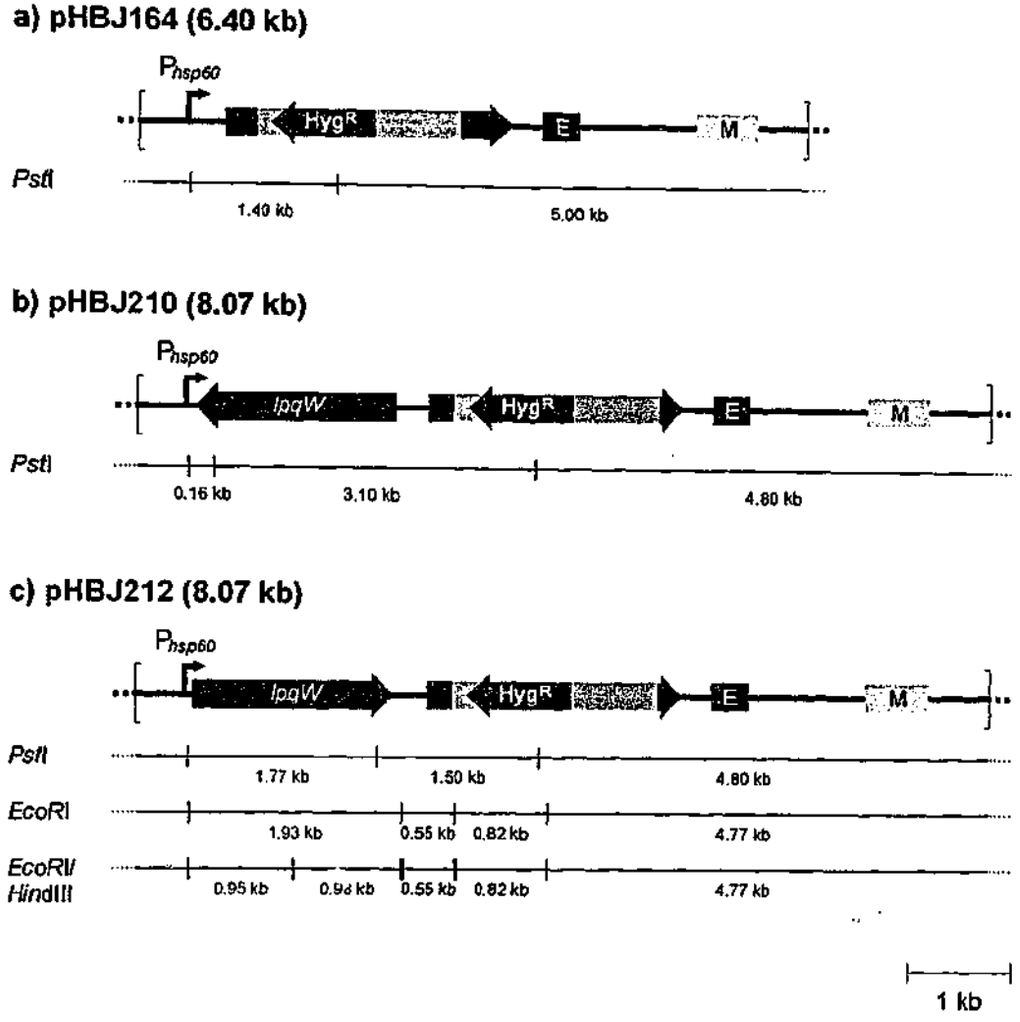

Figure 6.1
Plasmid constructs used for complementation.
These diagrams represent linear maps of the three plasmid constructs used in the complementation experiments. The broken lines at the ends of each figure indicate an arbitrary point at which the circular plasmid was linearised for the map.
Each construct was based on the *E. coli*/mycobacterial shuttle vector pMV261 (192). pMV261 includes origins of replication for *E. coli* (E) and mycobacteria (M). The red rightward-facing arrow (P_{hsp60}) indicates the location of the *hsp60* promoter and the first few residues of the corresponding *hsp60* ORF. In each case, a fragment containing the hygromycin resistance marker (Hyg^R) from pEP3 (167) was amplified and cloned into sites within the pMV261 kanamycin resistance gene (the remnants of which are represented in green). Hence, each vector confers hygromycin resistance.
a) pHBJ164, presented with its *Pst*I restriction map. b) pHBJ210 contains the full length *lpqW* ORF cloned in the opposite orientation to the *hsp60* promoter; the *Pst*I restriction map is also shown. c) pHBJ212 contains the full length *lpqW* cloned in frame with the *hsp60* ORF and should therefore express a *hsp60*/*lpqW* hybrid protein; the corresponding restriction maps for *Pst*I, *Eco*RI and *Eco*RI/*Hin*dIII are shown.

	Wild-Type	MYCO481	MYCO479
pHBJ164	8.52×10^5	0.50×10^1	3.40×10^5
pHBJ210	7.74×10^5	3.40×10^5	2.18×10^5
pHBJ212	5.16×10^5	1.56×10^5	1.90×10^1

Table 6.1
Transformation efficiencies of constructs in *M. smegmatis* strains.
One μg of plasmid DNA was electroporated into each strain. Hygromycin resistant transformants of the wild-type were selected for, while hygromycin/kanamycin resistant transformants were isolated in the case of the *lpqW* transposon mutants MYCO481 and MYCO479. Transformation efficiencies were calculated as the number of colony forming units generated per μg of DNA transformed (cfu/μg DNA).

In the case of the wild-type, transformation efficiencies were in the order of 10^5 transformants per μg of DNA transformed. This efficiency is typical of what is expected in wild-type *M. smegmatis* electrocompetant cells (100). The *lpqW* transposon mutant MYCO481 had lower transformation efficiencies for pHBJ210 and pHBJ212. Strikingly, MYCO481 was transformed with pHBJ164 at a greatly reduced efficiency of 5 cfu/μg of DNA. This low efficiency was reproducible in two separate transformation attempts.

Plasmids pHBJ164 and pHBJ210 transformed into MYCO479 at efficiencies less than those of the wild-type, while pHBJ212 transformed at a very poor efficiency of 19 cfu/μg of DNA. This was the highest efficiency obtained in previous attempts to transform pHBJ212 into MYCO479. Transformation of MYCO479 with pHBJ212 was attempted four times, with transformants only obtained in one experiment.

Confirmation of Transformation

Crude lysates of selected transformants were prepared by homogenising a single *M. smegmatis* colony. The homogenised material was used as a source of plasmid DNA to electroporate into *E. coli*. Hygromycin resistant *E. coli* transformants were isolated. Plasmids from the *E. coli* transformants were recovered, digested with *Pst*I, and the resulting fragments resolved to generate a restriction profile. The expected *Pst*I restriction maps for pHBJ164, pHBJ210 and pHBJ212 are shown in Figure 6.1.

Digesting pHBJ164 with *Pst*I results in restriction fragments of 5.0 and 1.4 kb in size. This profile was demonstrated for pHBJ164 and the plasmids derived from the wild-type, MYCO481 and MYCO479 transformants. The strains harbouring pHBJ164 were designated wild-type-pHBJ164, MYCO481-pHBJ164 and MYCO479-pHBJ164 (Figure 6.2a).

Plasmid pHBJ210 was then digested with *Pst*I, resulting in restriction fragments of 4.80 and 3.10 kb in size (Figure 6.2b). The expected 0.16 kb fragment is not obvious as it would not be well resolved in this gel system. Plasmids derived from the wild-type, MYCO481 and MYCO479 transformants demonstrated this profile. The successful pHBJ210 transformants of each strain were designated wild-type-pHBJ210, MYCO481-pHBJ210 and MYCO479-pHBJ210.

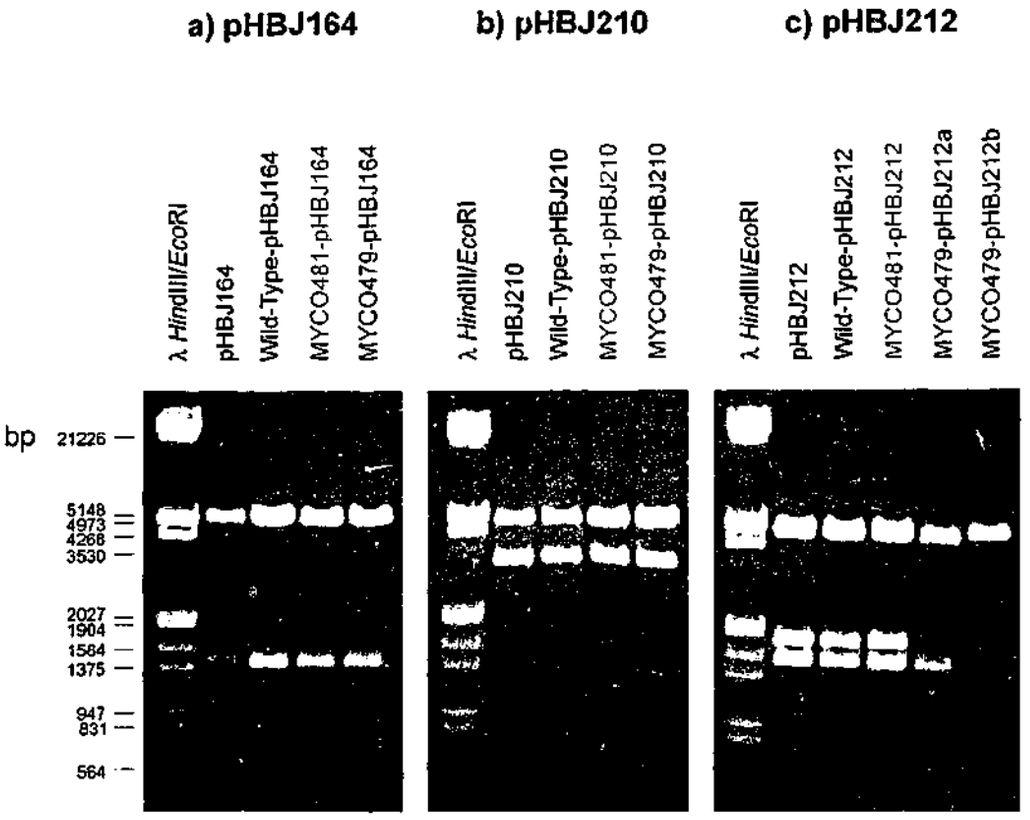

Figure 6.2
Confirming the nature of the transformants.
To confirm that mycobacterial transformants harboured the correct plasmid, a crude lysate preparation was transformed into *E. coli*. The resulting transformants were isolated, their plasmids extracted, and digested with *Pst*I. Digests were resolved in 1% (w/v) agarose in TAE, electrophoresed and stained with ethidium bromide.
The *Pst*I restriction maps of pHBJ164, pHBJ210 and pHBJ212 are presented in Figure 6.1.
Digests of the plasmids derived from transformants of the wild-type, MYCO481 and MYCO479 were resolved alongside a control plasmid.

a) pHBJ164
b) pHBJ210
c) pHBJ212

Molecular weight markers are in base pairs (bp).

A *Pst*I digest of pHBJ212 is expected to yield fragments of 4.80, 1.77 and 1.50 kb in size. This was observed, and the plasmids derived from the wild-type and MYCO481 transformants also demonstrated this profile. The transformants were designated wild-type-pHBJ212 and MYCO481-pHBJ212 (Figure 6.2c). The plasmids derived from two MYCO479 transformants, however, resulted in restriction profiles which did not match that seen for pHBJ212. Notably, the 1.77 kb fragment which includes most of *lpqW* is missing in both cases. These plasmids represent truncated or modified versions of pHBJ212, where the *lpqW* gene is absent. These truncated plasmids were designated pHBJ212a and pHBJ212b.

pHBJ212 is Not Stably Transformed into MYCO479

Given the low transformation efficiency of pHBJ212 into MYCO479, the question as to whether any of the few transformants generated contained the correct plasmid was raised. To investigate this, a further five transformants of MYCO479 were analysed to bring the total number of potential transformants analysed to seven. The plasmids extracted were designated pHBJ212c, pHBJ212d, pHBJ212e, pHBJ212f and pHBJ212g, in addition to pHBJ212a and pHBJ212b. As controls, the plasmids derived from wild-type-pHBJ212 and MYCO481-pHBJ212 were included.

Along with pHBJ212, the plasmids were digested with *Pst*I (Figure 6.3a). Plasmids from wild-type-pHBJ212 and MYCO481-pHBJ212 digested as expected. On the other hand, the plasmids derived from MYCO479 transformants showed in variation in their *Pst*I restriction profiles. Plasmid pHBJ212a and pHBJ212c resulted in an identical profile, lacking the 1.77 kb *lpqW*-derived band. Plasmid pHBJ212e demonstrated further truncation, while pHBJ212d and pHBJ212b only demonstrated a single *Pst*I cut site and probable truncation of the vector. Plasmid pHBJ212f, while larger in size, also only demonstrated a single *Pst*I site. Since each of these plasmids were selected for hygromycin resistance (in both *M. smegmatis* and *E. coli* hosts), it seemed likely that at least an intact hygromycin gene was present in each case.

Interestingly, pHBJ212g was the only MYCO479 derived plasmid that had an intact, pHBJ212-like *Pst*I fragment profile. Each expected restriction fragment was present and the correct size. To further demonstrate the loss of *lpqW* in the

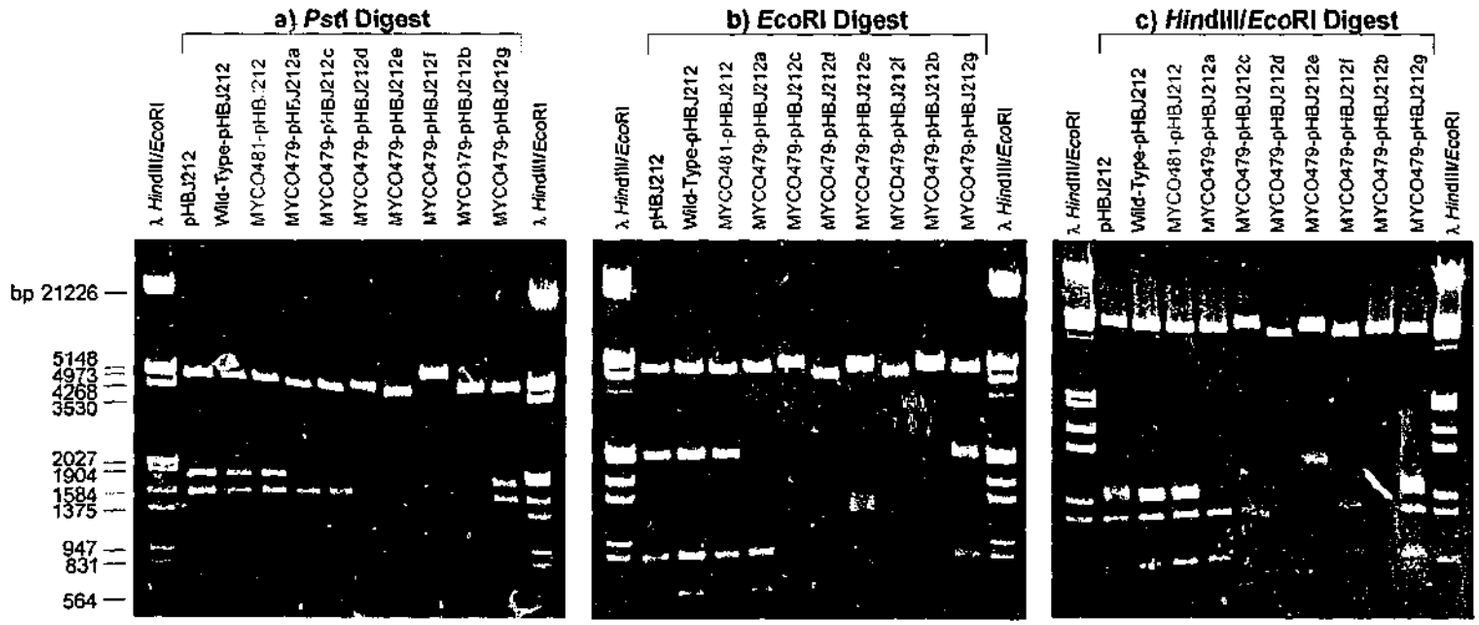

Figure 6.3

MYCO479 transformants harbour variants of pHBJ212 with truncated *lpqW*.

It was found that MYCO479 transformants of pHBJ212 yielded truncated or modified versions of the plasmid. Restriction digests were performed to demonstrate the nature of the truncations. Digests were resolved in 1.5% (w/v) agarose in TAE, electrophoresed and stained with ethidium bromide. The *Pst*I, *Eco*RI and *Eco*RI/*Hin*dIII restriction maps of pHBJ212 are included in Figure 6.1.

The results of the following digests are shown. a) *Pst*I; b) *Eco*RI; c) *Eco*RI/*Hin*dIII.

Each digest includes pHBJ212, a plasmid derived from the wild-type transformant (wild-type-pHBJ212) and a plasmid derived from the MYCO481 transformant (MYCO481-pHBJ212) as controls. A series of plasmids derived from various MYCO479 transformants (MYCO479-pHBJ212a, -c, -d, -e, -f and -b) were digested, demonstrating the lack of the *lpqW*-derived fragments. MYCO479-pHBJ212g appears to be intact.

Molecular weight markers are shown in base pairs (bp).

truncated plasmids, *Eco*RI and *Hin*dIII/*Eco*RI digests characteristic for an intact *lpqW* were performed. An *Eco*RI digest would release the 1.9 kb *lpqW* insert in its entirety while a *Hin*dIII/*Eco*RI digest would generate an *lpqW* derived doublet of 0.95 kb and 0.98 kb (Figure 6.1). These additional digests also serve to confirm the identity of pHBJ212g as being like pHBJ212. When digested with *Eco*RI, pHBJ212 and the plasmids derived from the wild-type and MYCO481 transformants each showed the expected profile (Figure 6.3b). Plasmid pHBJ212g was also found to contain the correct profile, consistent with the expected pHBJ212 fragments. Each of the MYCO479-derived plasmids showing a truncated *Pst*I profile were also found to lack the 1.93 kb *lpqW* fragment, and in the case on pHBJ212b, pHBJ212d and pHBJ212e, a part of the 0.55 kb fragment immediately downstream of *lpqW*. The *Hin*dIII/*Eco*RI digests were found to be consistent with the *Pst*I and *Eco*RI digests, in that the plasmids which had previously demonstrated a truncation of *lpqW* also lacked the 0.98 and 0.95 kb fragments indicative of the gene (Figure 6.3c). The control plasmid pHBJ212, as well as plasmids derived from wild-type-pHBJ212, MYCO481-pHBJ212 and MYCO479-pHBJ212g all demonstrated the correct restriction fragment profile. Hence, not only did pHBJ212 transform into MYCO479 at a low efficiency, but also the majority of the transformants contained truncated variants of the plasmid with a partially or completely deleted *lpqW*. The MYCO479 transformant harbouring an intact pHBJ212 was designated MYCO479-pHBJ212g.

The wild-type, MYCO481 and MYCO479 together with their confirmed transformants of pHBJ164, pHBJ210 and pHBJ212 were further analysed. Each strain was examined for its PIM profile by HPTLC and LAM composition by GC-MS analysis.

pHBJ212g Complements the PIM Phenotype in MYCO479

The PIM profiles of the pHBJ164 transformants are shown in Figure 6.4a. The results show that wild-type-pHBJ164, MYCO481-pHBJ164 and MYCO479-pHBJ164, when compared with their corresponding parent strains, show an unchanged PIM profile. The wild-type and MYCO481 extracts contained the expected PIMs, where the PIM_2 and PIM_6 species dominate. The same is seen with their transformants. The mutant MYCO479 extract showed its expected PIM_6-deficient, PIM_4-positive profile, as did its corresponding pHBJ164 transformant.

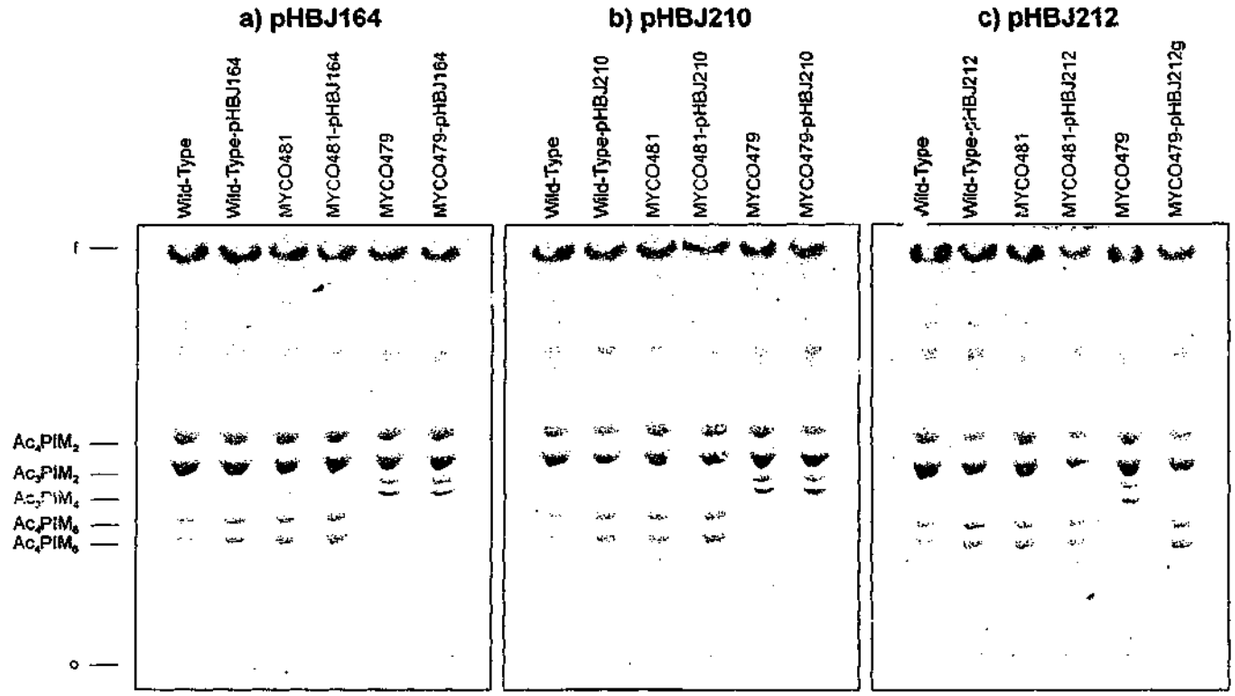

Figure 6.4
Plasmid pHBJ212 may complement the PIM deficiency of MYCO479.
PIMs were extracted from control strains and their corresponding transformants, and resolved by HPTLC. Plates were developed in Solvent System A and stained with orcinol. Extracts from the wild-type, MYCO481 and MYCO479 were resolved alongside PIMs from their respective transformants of a) pHBJ164, b) pHBJ210 and c) pHBJ212.
The positions of the main PIM_2 and PIM_6 species are indicated, as is the position of Ac_2PIM_4. The sample origin is indicated by an "o", while the solvent front is indicated by an "f".

The positions of the main PIM_2 and PIM_6 species are indicated, as is the position of Ac_2PIM_4. The sample origin is indicated by an "o", while the solvent front is indicated by an "f".

This result demonstrates that pHBJ164 alone does not complement the PIM defect seen in MYCO479.

The PIMs extracted from the pHBJ210 transformants were then visualised (Figure 6.4b). Wild-type-pHBJ210, MYCO481-pHBJ210 and MYCO479-pHBJ210, when compared with their corresponding parent strains, show an unchanged PIM profile. The wild-type and MYCO481 show a normal PIM profile, while MYCO479 showed the expected PIM_6-deficient, PIM_4-accumulating profile. The corresponding transformants appear unchanged by the addition of pHBJ210. As with pHBJ164, the addition of pHBJ210 does not restore the wild-type PIM profile.

The PIMs extracted from the pHBJ212 transformants were then resolved (Figure 6.4c). With respect to PIMs, the wild-type and its transformed equivalent show a normal PIM profile. The same result was observed with MYCO481 and the corresponding MYCO481-pHBJ212, where normal PIMs were observed with no change in the transformant.

MYCO479 showed its expected PIM profile, being deficient in PIM_6 while accumulating PIM_4. When transformed with pHBJ212g, however, the profile is restored to that of the wild-type where PIM_6 is produced and PIM_4 no longer accumulates. This result suggests that pHBJ212g, containing an intact *lpqW* provided in frame with *hsp60* to facilitate expression, is able to restore the PIM deficient phenotype seen in MYCO479 to that of a wild-type PIM profile.

pHBJ212g May Complement the LAM Phenotype in MYCO481

The GC-MS analysis of the same set of strains and transformants was then conducted to assess the affect of pHBJ164, pHBJ210 and pHBJ212 on LAM production (Figure 6.5). In each case the sugar amounts in the mutants were compared to the wild-type control. When compared to the wild-type, MYCO481 showed a marked reduction in each of these sugars, typical of its reduced LAM phenotype. In this case, the sugar levels seen are 31% of the wild-type inositol, 19% of the mannose and 11% of the arabinose. In comparison to the wild-type, MYCO479 showed approximately equal amounts (98%) of inositol, 72% of the wild-type mannose and elevated arabinose, 154% of that seen in the wild-type.

The wild-type, MYCO481 and MYCO479 transformed with pHBJ164 were then analysed. In comparison to wild-type-pHBJ164, MYCO481-pHBJ164 LAM

yielded a low amount of inositol (13%), low mannose (49%) but elevated arabinose (306%). MYCO479-pHBJ164 LAM contained reduced inositol (23% of wild-type-pHBJ164), identical amounts of mannose (96%) and elevated arabinose (493%). Given this deviation from the expected trends seen in the untransformed controls, and the lack of consistency in which sugars are elevated or reduced after transformation, drawing a conclusion from these results is difficult. With respect to the LAM-reduced mutant MYCO481, its pHBJ164 transformant does not show inositol or mannose levels comparable to those of wild-type-pHBJ164, although arabinose levels were elevated in both MYCO481-pHBJ164 and MYCO479-pHBJ164.

The strains transformed with pHBJ210 were analysed next. When compared to wild-type-pHBJ210, LAM purified from MYCO481-pHBJ210 contained a reduced amount of inositol (47% of wild-type-pHBJ210), reduced mannose (78%), and reduced arabinose (48%). While reduced LAM sugars are expected in the MYCO481 transformant, these differences are less obvious than those seen between the untransformed wild-type and MYCO481, as described above. Hence, pHBJ210 does seem to at least partially restore the strains LAM. The MYCO479-pHBJ210 transformant showed similar sugar levels to wild-type-pHBJ210, demonstrating that the presence of pHBJ210 had also elevated LAM sugar levels in the mutant compared to the untransformed control.

The strains containing the *lpqW* complementation plasmid, pHBJ212, were then analysed. In comparison to the wild-type transformant, the MYCO481-pHBJ212 showed 68% as much inositol, 79% mannose and 52% arabinose. While these levels are high with respect to the comparison between untransformed wild-type and MYCO481, and hence may represent partial complementation, these levels are not greatly higher than those obtained in the pHBJ210 transformation. It is therefore unclear as to whether or not pHBJ212 complements the LAM phenotype seen in MYCO481. The results obtained for MYCO479-pHBJ212g are also unusual. The transformant showed 50% inositol, 52% mannose and 36% arabinose in comparison to wild-type-pHBJ212. This indicates that LAM levels are reduced when comparing these differences to those seen between untransformed wild-type and MYCO479, and to the differences between the pHBJ210

transformed strains. Interestingly, both pHBJ210 and pHBJ212 had the effect of increasing the overall LAM sugar levels in each of the strains tested (Figure 6.5).

Confirming the Presence of Complementation Constructs

To confirm that the cultures used for PIM and LAM analysis contained the expected plasmids, a sample of the culture was lysed and used to transform *E. coli*. The plasmids recovered from the resulting transformants were isolated and digested with *Pst*I (see Figure 6.1). In each case, the expected fragment sizes were observed. Plasmids isolated from wild-type-pHBJ164, MYCO481-pHBJ164 and MYCO479-pHBJ164 generated the 5.0 and 1.4 kb bands of pHBJ164 (Figure 6.6a). Wild-type-pHBJ210, MYCO481-pHBJ210 and MYCO479-pHBJ210 derived plasmids yielded restriction fragments of 4.8 and 3.1 kb characteristic of pHBJ210 (Figure 6.6b). Wild-type-pHBJ212, MYCO481-pHBJ212 and MYCO479-pHBJ212g derived plasmids produced fragments of 4.8, 1.77 and 1.55 kb which are characteristic of pHBJ212 (Figure 6.6c).

Antibiotic Resistance of the Transformed Strains

To demonstrate the identity of wild-type-pHBJ212, MYCO481-pHBJ212 and MYCO479-pHBJ212g as the respective transformants of the wild-type, MYCO481 and MYCO479, each strain was plated onto Middlebrook 7H10 agar containing either kanamycin, streptomycin or hygromycin. The wild-type strain is expected to be sensistive to each of the three antibiotics, while its transformed counterpart should be resistant to hygromycin by virtue of pHBJ212. Conversely, MYCO481 and MYCO479 are expected to be resistant to kanamycin and streptomycin due to the Tn*611*/pCG79 insertion, with their corresponding transformants showing additional resistance to hygromycin via the resistance marker on pHBJ212. Following incubation, the plates were scored for growth on the different antibiotics (Table 6.2).

The wild-type, MYCO481 and MYCO479 were found to respond to each antibiotic as expected. Wild-Type-pHBJ212 showed resistance to hygromycin, as expected. Also as expected, MYCO481-pHBJ212 and MYCO479-pHBJ212 showed resistance to kanamycin and hygromycin. Unexpectedly however, both strains were sensitive to streptomycin. This result implied that the streptomycin resistance marker in MYCO481-pHBJ212 and MYCO479-pHBJ212g was either

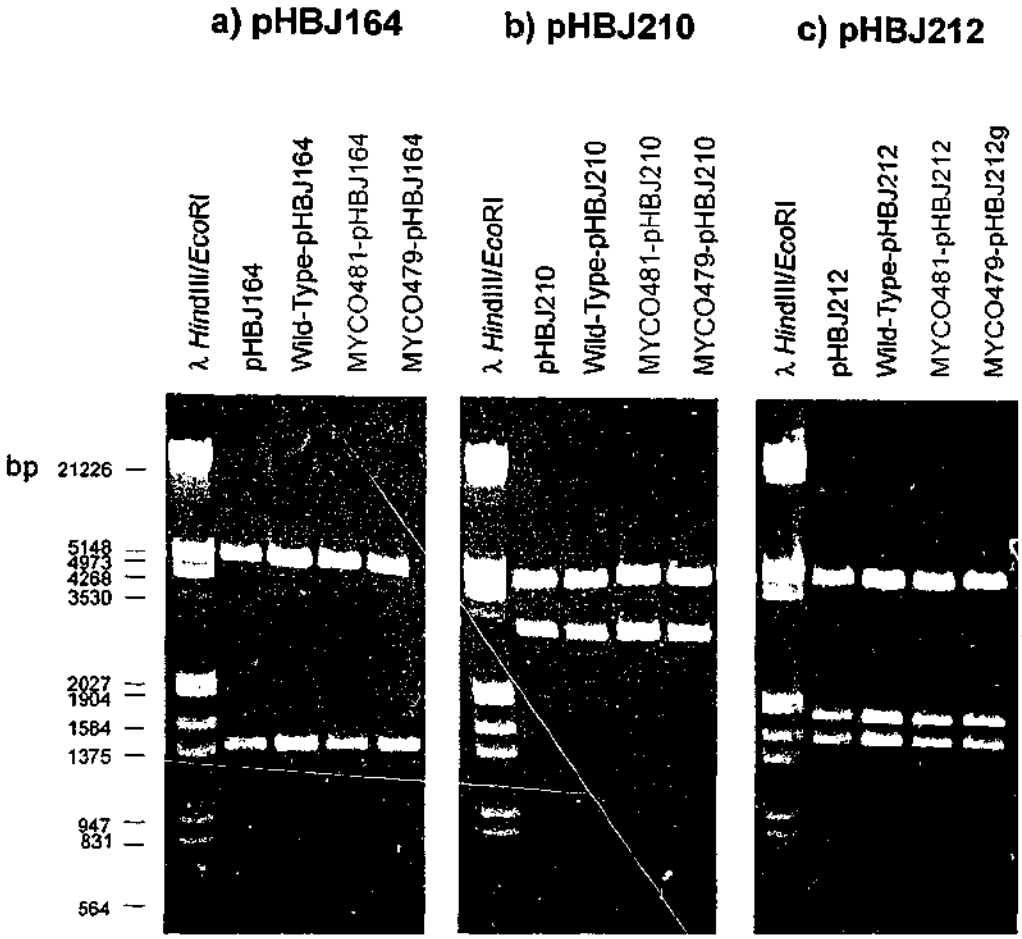

Figure 6.6
Confirming the presence of plasmids in the transformants.
To confirm that mycobacterial transformants harboured the expected plasmid, a crude lysate preparation was transformed into *E. coli*. The resulting transformants were isolated, their plasmids extracted, and digested with *Pst*I. Digests were resolved in 1% (w/v) agarose in TAE, electrophoresed and stained with ethidium bromide.
The *Pst*I restriction maps of pHBJ164, pHBJ210 and pHBJ212 are presented in Figure 6.1.
Digests of the plasmids derived from transformants of the wild-type, MYCO481 and MYCO479 were resolved alongside a control plasmid.

a) pHBJ164
b) pHBJ210
c) pHBJ212

Molecular weight markers are in base pairs (bp).

lost, truncated or mutated such that both strains were now sensitive to the antibiotic.

***Confirmation of Tn611 insertion in* lpqW**

To show that the pHBJ212 transformants MYCO481-pHBJ212 and MYCO479-pHBJ212g harboured a Tn*611* insertion in *lpqW*, the PCR using the primer pairs 7389/3053 and 3054/9276 was performed on genomic DNA extracted from the strains. The PCR specifically amplifies fragments from strains harbouring an *lpqW* insertion identical to that of MYCO481/MYCO479, as established in Chapter 4 (see section 4.3.4). Wild-Type-pHBJ212 was included as a negative control, as it should not contain the *lpqW* disruption. As further controls, genomic DNA from the wild-type, MYCO481 and MYCO479 were also included. The results of the PCR are presented in Figure 6.7. As expected, the wild-type and its corresponding pHBJ212 transformant showed no amplification of the expected product using either of the primer pairs. Some relatively weak, non-specific amplification products were observed in the 3053/7389 reaction. These products were approximately 150 bp in size, as distinct from the expected 697 bp amplification product. In contrast, PCR products of the expected sizes were amplified from MYCO481-pHBJ212 and MYCO479-pHBJ212g genomic DNA, while the expected amplification products were also seen in MYCO481 and MYCO479. This result indicated that both MYCO481-pHBJ212 and MYCO479-pHBJ212g harboured the Tn*611* insertion in *lpqW*, at a location identical to that in MYCO481 and MYCO479.

6.3.2 *Disruption of ORF-1170 (*mshB*) does not result in the PIM/LAM Phenotype*

Mycobacterial Mycothiol

Mycothiol (1-D-*myo*-inosityl-2-(*N*-acetyl-L-cysteinyl)amido-2-deoxy-α-D-glucopyranoside, or MSH) (171) is a low molecular weight thiol first characterised in *M. bovis* (189). MSH is thought to act as an antioxidant, protecting the cell against oxidative damage in the same way as the common cellular reducing agent glutathione. In support of this view, *M. smegmatis* MSH mutants have an increased sensitivity to hydrogen peroxide (141). Interestingly, MSH seems to be restricted to actinomycetes. *M. avium*, *M. chelonae*, *M. fortuitum*, *M. smegmatis* and *M.*

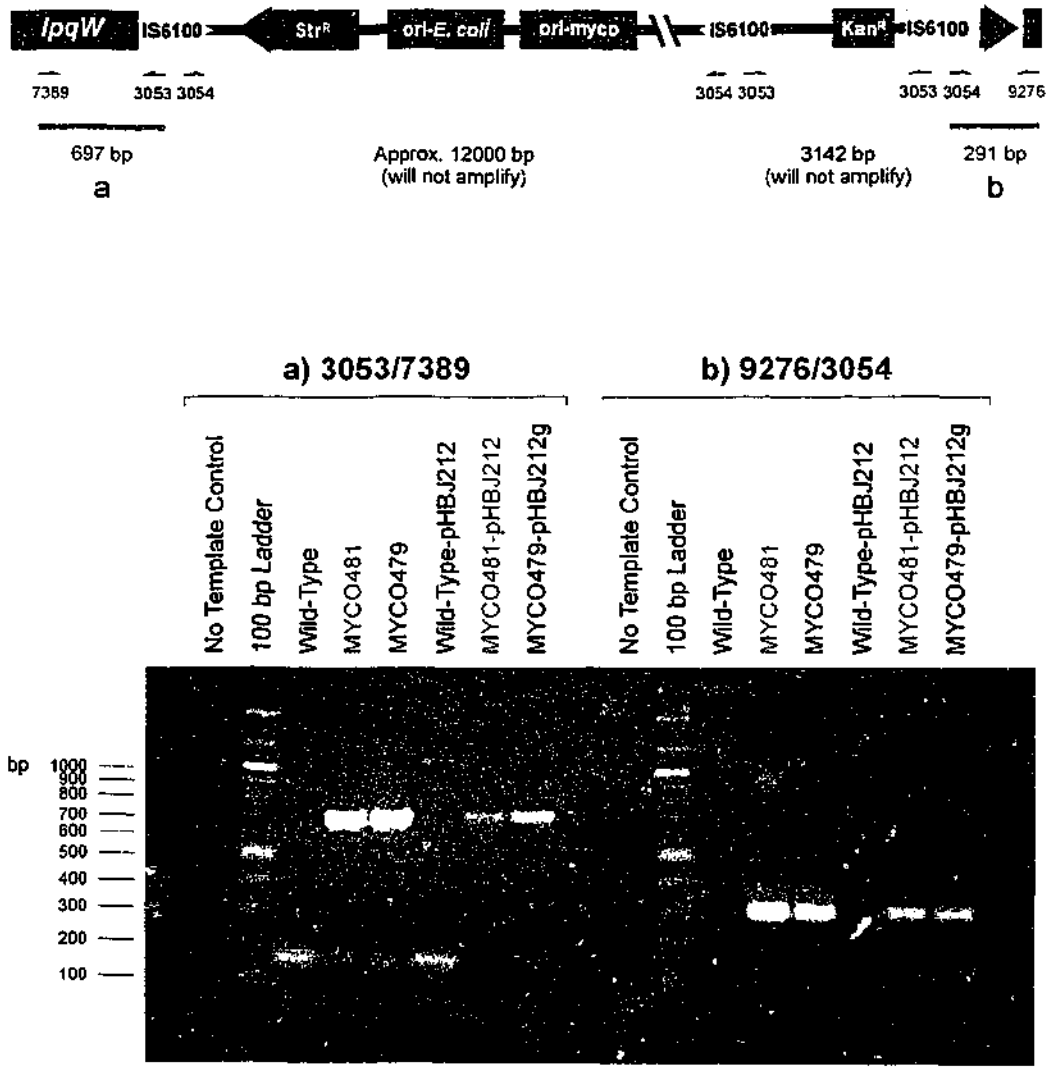

Figure 6.7
The *lpqW* transposon insertion is present in complemented mutants.
Genomic DNA was extracted from the wild-type, *lpqW* transposon mutants and their pHBJ212-transfomed counterparts (Wild-Type-pHBJ212, MYCO481-pHBJ212 and MYCO479-pHBJ212g). The presence of Tn*611* in *lpqW* was tested for using two separate PCR amplifications. Amplification products were resolved in 1.5% (w/v) agarose in TAE.
a) In the case of an *lpqW* Tn*611* insertion identical to that in MYCO479, primers 3053 and 7389 are expected to amplify a 697 bp product. The resulting amplification products are presented.
b) Amplification products using primers 3054 and 9276 are expected to amplify a 291 bp product. The amplification products resulting from this reaction are shown.

Markers are shown in base pairs (bp).

tuberculosis all contain MSH, along with species from closely related genera such as *Nocardia*, *Rhodococcus* and *Streptomyces* (138). This finding has sparked interest in studying the MSH biosynthetic pathway, as it offers promise as a target for novel drugs which are specific for the mycobacteria.

Newton *et al.* (140) were able to purify an enzyme that had MSH-S-conjugate amidase activity in *M. smegmatis*, and identified the enzyme sequence as being encoded by a *M. tuberculosis* Rv1082 (47) homologue. The gene was designated mycothiol amidase, or "*mca*". The role of *mca* was not clear, but it was proposed that the enzyme functions as a component of a MSH-dependant detoxification system in mycobacteria. Patel and Blanchard (154) were also able to identify an enzyme which was classified as a mycothione reductase (*mtr*), expressed from *M. tuberculosis* Rv2855. The enzyme shows similarity with other members of the class I flavoprotein disulfide reductase family which are involved in substrate disulfide reduction.

***ORF-1170 and Mycothiol Production:* mshB**

In an effort to find additional MSH biosynthetic genes, Newton *et al.* (139) identified Rv1170 as a sequence homologue to Rv1082. Rv1082 shows 42% amino acid sequence identity to Rv1170, and when expressed in *E. coli* showed some amidase activity and considerable *myo*-inosityl-*N*-acetylglucosamine deacetylase activity. The discovery of this enzyme advanced the theory of mycothiol biosynthesis, and led to the proposal of a biosynthetic pathway (Figure 6.8). Briefly, a cysteine is coupled with the amine group of a *myo*-inosityl-glucosamine and *N*-acetylated to form MSH. With the emergence of a pathway, the enzymes responsible for each step and their corresponding genes are being identified. Based on the proposed order of intermediate synthesis, hypothetical genes were assigned *mshA*, *mshB* (deacetylase), *mshC* (cysteine ligase) and *mshD* (transacetylase) (29, 139).

The gene downstream of *lpqW*, ORF-1170, was named as such because of its high sequence similarity to *M. tuberculosis* Rv1170. The *M. smegmatis* sequence is 66% identical to the *M. tuberculosis* sequence at the amino acid sequence level. For this reason, ORF-1170 was renamed *mshB*. Further examination of the *M. smegmatis* genome sequencing project data revealed a likely *M. smegmatis* homologue of *M. tuberculosis* Rv1082 (*mca*), with a 74% amino

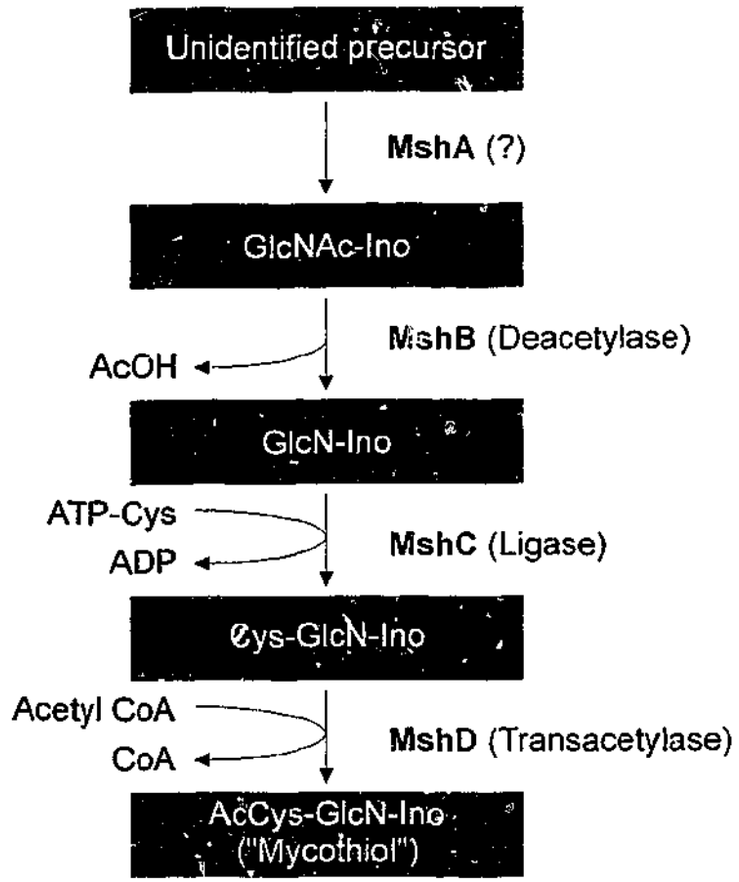

Figure 6.8
Proposed biosynthetic pathway for Mycothiol.
Mycothiol biosynthesis is predicted to proceed as follows. *myo*-inosityl-*N*-acetylglucosamine (GlcNAc-Ino) is synthesised from an unknown precursor by the hypothetical enzyme MshA. GlcNAc-Ino is then de-acetylated by MshB to form to *myo*-inosityl-*N*-glucosamine (GlcN-Ino). Cysteine is then ligated to GlcN-Ino in an ATP-dependant manner to form cysteinyl-*myo*-inosityl-*N*-glucosamine (Cys-GlcN-Ino), hypothetically catalysed by a cysteine ligase, MshC. Finally, Cys-GlcN-Ino is transacetylated by MshD to form 1-D-*myo*-inosityl-2-(*N*-acetyl-L-cysteinyl)amido-2-deoxy-α-D-glucopyranoside (AcCys-GlcN-Ino, or mycothiol) (Adapted from 29, 139 and 140).

acid sequence match. When comparing *M. smegmatis mshB* to the putative *mca* homologue, 34% amino acid identity is observed. This is low compared to the 42% amino acid identity between the *M. tuberculosis mshB* and *mca* sequences.

Preparation of the Targetted Disruption Construct

To test whether or not the *lpqW* transposon insertion of MYCO481 and MYCO479 is affecting the transcription of *mshB* via polarity affects, *mshB* was inactivated by targetted gene disruption. This was achieved by the use of a pUC18-based construct which was designed to recombine with the *M. smegmatis* genome. The vector pUC18 (210) only contains an *E. coli* origin of replication, and is therefore unable to replicate in *M. smegmatis*. Targetted disruption of *M. smegmatis mshB* was mediated by the use of the pUC18-based construct pHBJ280 (Figure 6.9).

To achieve this, a 2549 bp *Dde*I fragment was excised from pHBJ272. This fragment contained a region of genomic DNA that spanned the entire 873 bp *mshB* ORF with an additional 773 bp upstream and 906 bp downstream of the ORF. The fragment was cloned into a modified *Kpn*I restriction site in pUC18 to form pHBJ273. This cloning step was designed such that the unique *Kpn*I site 203 bp into the *mshB* ORF was available for inserting a selectable marker, thereby disrupting *mshB*.

The kanamycin resistance cassette from pUC18K (127) was then inserted into the *Kpn*I site within the *mshB* ORF of pHBJ273. The pUC18K cassette contains a kanamycin resistance gene flanked by translational regulatory sequences. Translational stop codons occur in all three reading frames immediately before the start codon of the kanamycin resistance gene to ensure that the *mshB* sequence preceding the site of the kanamycin cassette insertion is not translated past this point. Downstream of these stop codons are a ribosome binding site and translational start codon for an ORF of 795 bp which encodes for kanamycin resistance. Downstream of this ORF is another ribosome binding site and translational start codon. If the cassette is cloned in such a way that a translational fusion is created between the 3' start codon of the cassette and the genomic sequence downstream of the point of cassette insertion, then translation of the genes downstream of *mshB* should not be affected.

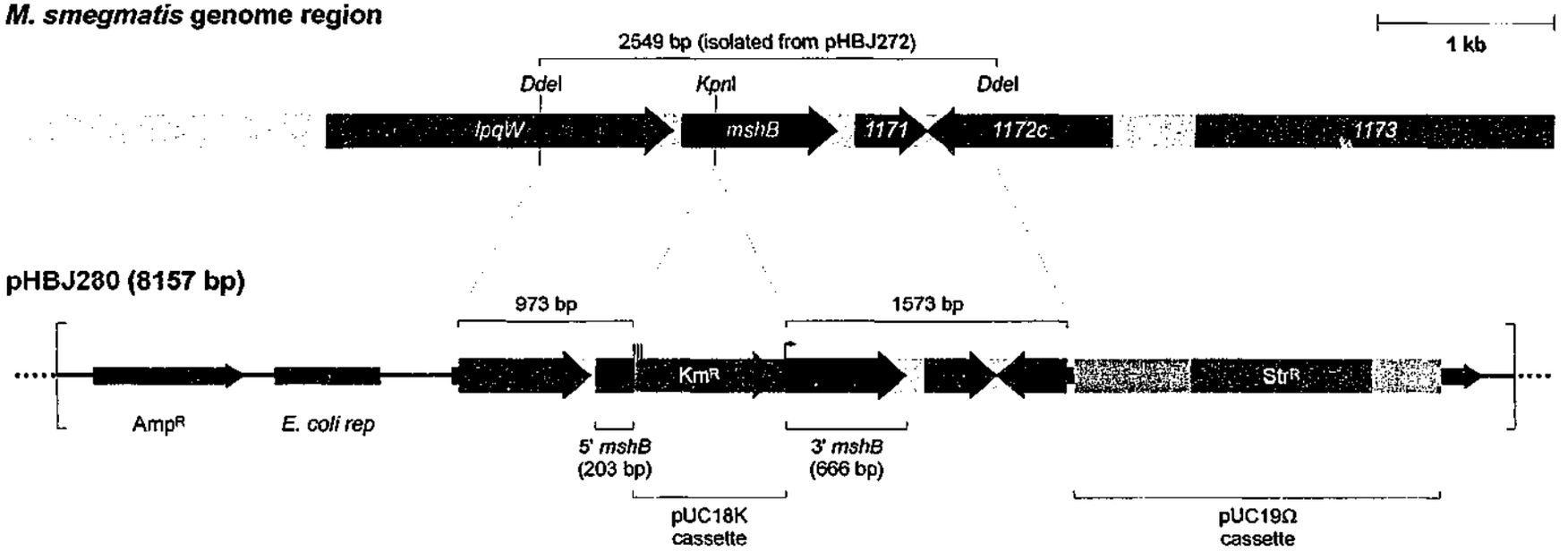

Figure 6.9
Main features of pHBJ280.
M. smegmatis mshB is flanked by *lpqW* and ORF-1171. This region of the genome is contained within the pHBJ272 insert (see Chapter 4, Figure 4.5). A 2549 bp *DdeI* fragment from pHBJ272 was subcloned into pUC18 (210).
The pUC18 vector backbone provided the ampicillin resistance marker (Amp^R) and the *E. coli* replicative origin (*E. coli rep*). The lack of a mycobacterial replicative origin meant that the construct was unable to replicate in *M. smegmatis*. The kanamycin resistance cassette (Km^R) from pUC18K (127) was used to disrupt the *mshB* sequence; the three red lines preceding the Km^R ORF represent stop codons in all three translation frames, while the red arrow downstream of the Km^R gene represents a ribosome binding site and start codon in frame with the sequence downstream to it. The streptomycin resistance cassette (Str^R) was cloned from pUC19Ω (163) and incorporated as a counterselectable marker.

The kanamycin cassette was PCR amplified from pUC18K using the UP and RP primers to give a product of approx. 850 bp. The ampification product was then digested with *Kpn*I/*Hin*cII and the termini modified for subsequent cloning. Plasmid pHBJ273 was then digested with *Kpn*I, which lies within *mshB*. This cloning step resulted in the insertion of the pUC18K kanamycin resistance cassette in a non-polar fashion. The cassette was ligated to the linearised pHBJ273 and the orientation of the cassette confirmed by *Xho*I/*Eco*RV restriction digests. The *Eco*RV site is conveniently unique to the kanamycin cassette, allowing the orientation of the cassette to be determined. Correct insertion was then confirmed by sequencing with the kanamycin cassette-targeting primer KanC, and the construct was named pHBJ278.

The insertion of the kanamycin cassette into the wild-type *mshB* ORF is mediated by a double cross-over event, where homologous recombination takes place between the *mshB* sequences flanking the cassette in the construct and their genomic counterparts. If recombination only occurs with one of the flanking sequences, the entire construct is inserted into the genome and produces an intact copy of *mshB*. To enable this event to be detected, an additional selection marker was incorporated into the construct. Resistance to this selection marker implies that a single cross-over event has occurred and the entire construct has inserted. Conversely, sensitivity to the additional marker along with resistance to the kanamycin cassette suggests that only the cassette has inserted, as a result of the required double cross-over event. In this case streptomycin resistance was used as the additional selectable marker. The streptomycin resistance cassette from pUC19Ω (163) was excised as an approx. 2 kb *Sma*I fragment. pHBJ278 was then cleaved with *Hin*dIII, the resulting fragments termini modified, and the streptomycin resistance cassette was cloned into this site to form pHBJ280.

***Transformation into* M. smegmatis**

Plasmid pHBJ280 was electroporated in wild-type *M. smegmatis* and kanamycin resistant transformants were selected for. A total of 30 transformants were obtained. These colonies were then patched onto kanamycin and streptomycin plates to screen for kanamycin resistant, streptomycin sensitive transformants. These were expected to result from putative double cross-over events where the

tor. The streptomycin resistance cassette (Str^r) was cloned from pUC19Ω(163) and incorporated as a counterselectable marker.

vector has recombined with the genome to introduce the kanamycin resistance cassette. Transformants which were found to be resistant to both antibiotics probably arose from a single cross-over event, where the entire vector has incorporated into the genome. In this case, *mshB* would be disrupted, but the recombination event would result in the formation of a separate, intact copy of the gene. Hence, transformants which showed kanamycin resistance and streptomycin sensitivity were selected. Of the 30 transformants, four showed the required resistance profile. These potential *mshB* mutants were designated *mshB*-AX-7, *mshB*-AX-9, *mshB*-AX-17 and *mshB*-AX-18.

Confirmation of* mshB *disruption

To test which of the four mutants contained an *mshB* disruption, the genomic DNA was analysed for evidence of the recombination event. Differences in restriction fragment profile, as a result of the insertion of the kanamycin resistance cassette, can be detected by Southern hybridisation. The kanamycin resistance cassette contains a unique *Eco*RV restriction site which can be exploited to test for the cassettes presence in the genome. Therefore, *Eco*RV can be used in combination with another enzyme to test for an *mshB* disruption. The restriction enzyme *Eco*RI, which has relatively infrequent target sites within the *M. smegmatis* genome, was used for this purpose.

A scheme was designed to differentiate between wild-type genomic DNA, an *mshB* disruption as a result of a double recombination event, and mutants derived from a single recombination event (Figure 6.10). The probe used was the 0.4 kb *PstI*/*Eco*RI insert from pHBJ269, which spans the 3' end of *lpqW* and the 5' end of *mshB* (see Figure 4.5). Since wild-type DNA does not contain any *Eco*RV restriction sites near *mshB*, the probe should bind to a single *Eco*RI fragment of 11985 bp (Figure 6.10a). In the case of a double cross-over event the insertion of the kanamycin cassette would introduce an *Eco*RV site within the *Eco*RI fragment seen in the wild-type. Hence, cleaving *mshB*-disrupted genomic DNA with *Eco*RI/*Eco*RV would split the 11985 bp wild-type *Eco*RI fragment into two fragments of 6802 bp and 6044 bp. The pHBJ269 probe targets the 6802 bp fragment (Figure 6.10b). The occurrence of single cross-over events in the four mutants, while selected against based on streptomycin sensitivity, are still possible. These can be detected by the presence of two fragments of 13341 and 6802 bp

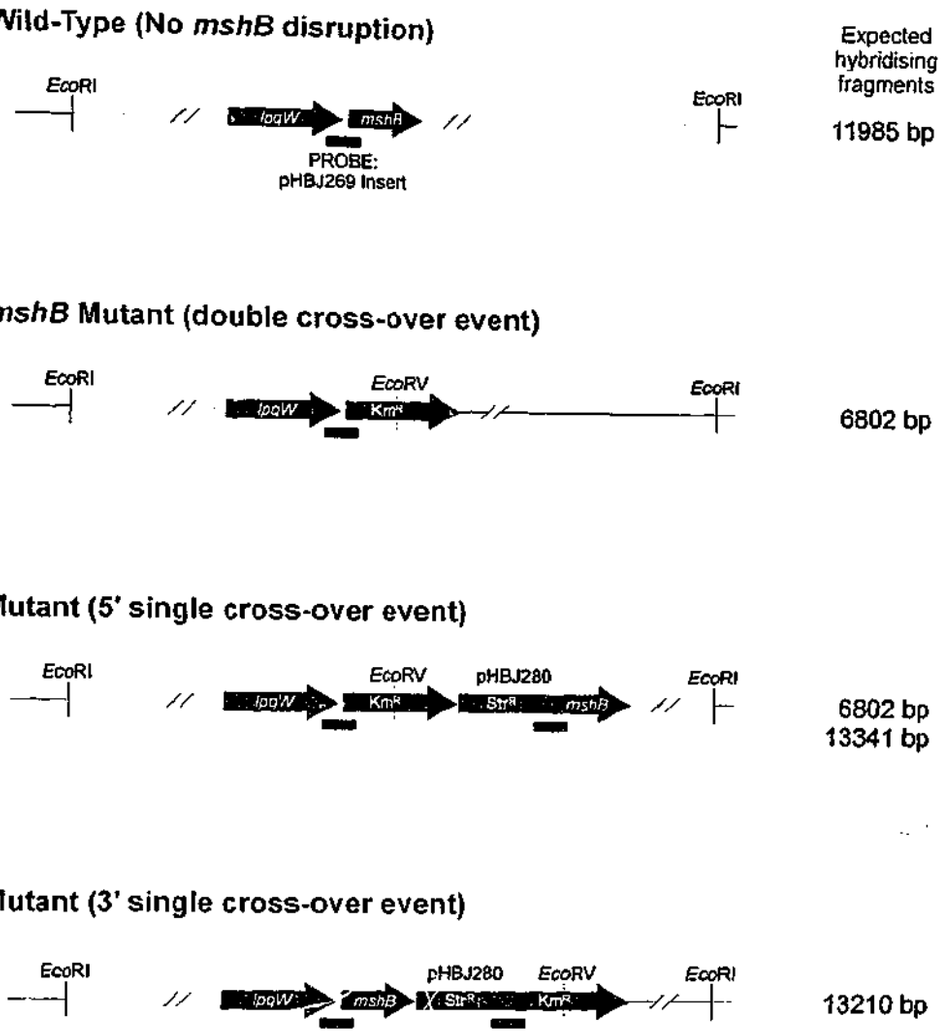

Figure 6.10
Detecting disruption of *mshB* with pHBJ280.
Homologous recombination between pHBJ280 and the *M. smegmatis* genome can be detected by Southern hybridisation. Genomic DNA is digested with *Eco*RV/*Eco*RI and probed with the pHBJ269 *Pst*I/*Eco*RI insert, which targets the 3' end of *lpqW* and the 5' end of *mshB*.

a) The expected genomic arrangement in the wild-type, indicating no pHBJ280 recombination event.
b) Disruption of *mshB* resulting from a double cross-over event.
c) A single cross-over event in the 5' region of *mshB*, resulting in an intact copy of the gene which is a hybrid of pHBJ280 and genomically-derived sequence.
d) As with c), except the single recombination event has occurred in the 3' region of *mshB*.

The diagram is not to scale.

(Figure 6.10c) or a 13210 bp hybridising fragment (Figure 6.10d), depending on the nature of recombination.

Genomic DNA was extracted from the four putative mutants and along with wild-type DNA, digested with *Eco*RI/*Eco*RV and probed with the pHBJ269 insert (Figure 6.11). The pHBJ269 probe hybridised to a fragment of approx. 12 kb in size, consistent with the expected *Eco*RI fragment size.

In *mshB*-AX-7, *mshB*-AX-9 and *mshB*-AX-17, the probe hybridised to a fragment of approx. 7 kb in size. This was consistent with the expected *Eco*RV/*Eco*RI fragment of the double cross-over mutant, suggesting that these three strains were *mshB* knock-outs. This was also consistent with their resistance to kanamycin and sensitivity to streptomycin.

When *mshB*-AX-18 DNA was probed, hybridising fragments of approx. 12 kb and 4.2 kb were observed. This profile was not consistent with any of the expected genetic arrangments (Figure 6.10). The presence of a 12 kb band implies that *mshB* is not disrupted, while the origin of the other hybridising fragment is unknown. The *mshB*-AX-18 strain may be an example of an illegitimate recombination event.

The *mshB*-AX-9 mutant strain was renamed MYCO504 and chosen for further analysis. To this point, MYCO504 was generated and propagated in LB media. The colonies formed on LB agar resembled those of the wild-type and the mutants growth in LB broth did not appear to differ greatly to the wild-type. At no point throughout its isolation did MYCO504 colonies resemble those of MYCO481 on LB agar. Through a small number of subcultures on LB agar, MYCO504 showed no change in colony morphology.

MYCO504 extracts contain normal PIM and LAM

To examine the affect to the *mshB* mutant on the PIM/LAM phenotype, MYCO504 was subjected to a PIM and LAM extraction alongside the wild-type, MYCO481 and MYCO479. Each strain was grown on Middlebrook media for biochemical analysis.

PIMs were extracted from each strain and resolved by HPTLC (Figure 6.12). The results showed that the wild-type and MYCO481 contained the normal complement of PIMs and MYCO479 lacked PIM_6 and accumulated Ac_3PIM_4, as seen previously. The PIM profile of the *mshB* mutant MYCO504 resembled the

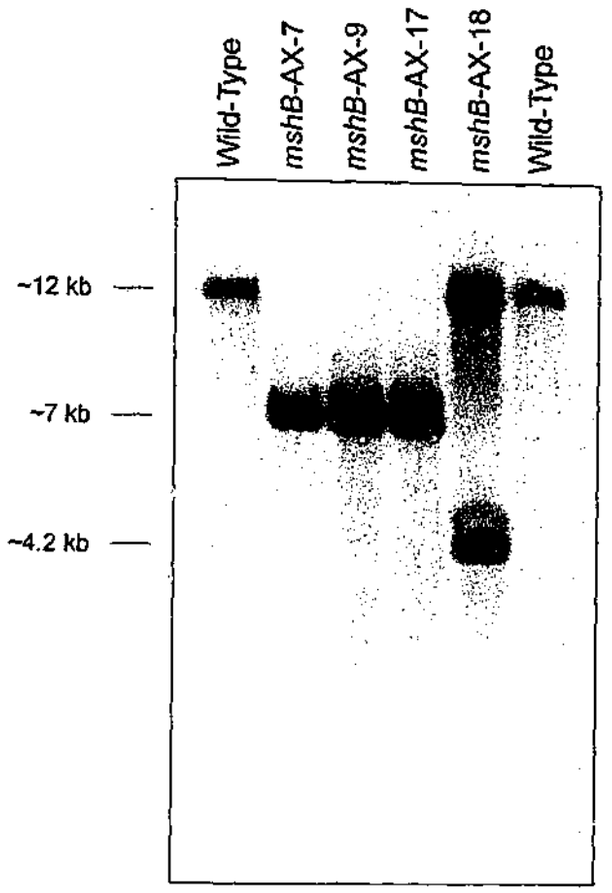

Figure 6.11
Detection of *mshB* disruption in *M. smegmatis*.
The nature of pHBJ280 recombination was examined by Southern hybridisation with the pHBJ269 *PstI*/*Eco*RI insert fragment as a probe. Genomic DNA from the wild-type and four kanamycin resistant, streptomycin sensitive pHBJ280 transformants (*mshB*-AX-7, *mshB*-AX-9, *mshB*-AX-17 and *mshB*-AX-18) was digested with *Eco*RV/*Eco*RI and resolved in 1% (w/v) agarose in TAE. The restriction fragments were hybridised with the probe, and hybridisation detected.

Genomic DNA from *mshB*-AX-7, *mshB*-AX-9 and *mshB*-AX-17 contained a 7 kb hybridising fragment, consistent with an *mshB* disruption arising from a double cross-over event.

The size of each hybridising band is indicated in kilobases (kb).

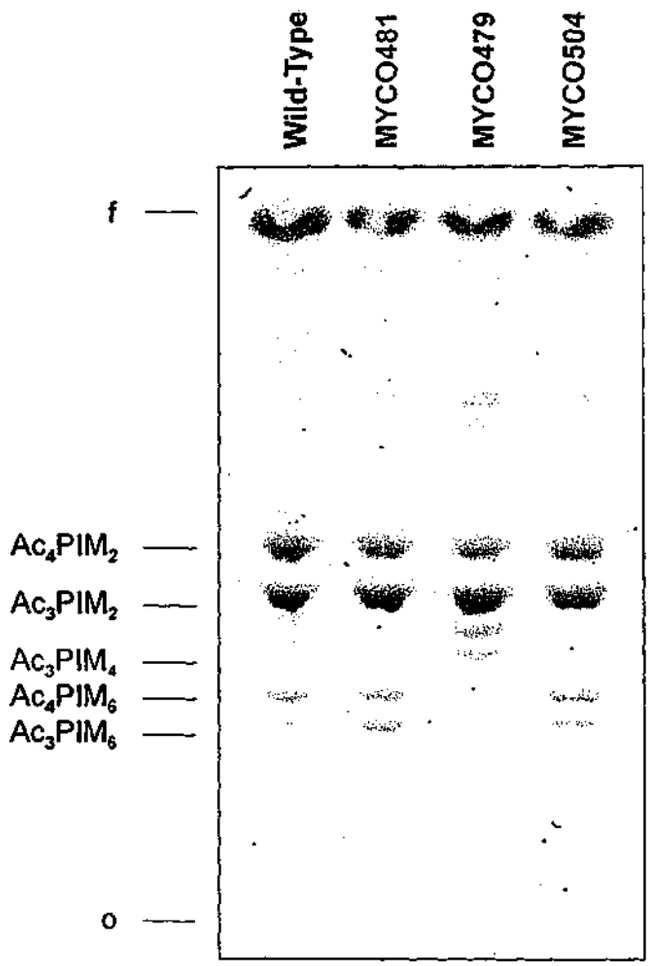

Figure 6.12
Disruption of *mshB* does not affect PIMs.
PIMs were extracted from the wild-type, the *lpqW* transposon mutants MYCO481 and MYCO479 (*lpqW*::Tn*611*), and the *mshB* targetted disruption mutant MYCO504 (*mshB*::Kan^R). PIMs were resolved by HPTLC using Solvent System A, and stained with orcinol.
The position of the main PIM_2 and PIM_6 species are indicated, as is the position of Ac_3PIM_4. The sample origin is indicated by an "o", while the solvent front is indicated by an "f".

wild-type pattern. Additionally, MYCO504 had a stable phenotype with respect to PIM synthesis. MYCO504 was serially subcultured seven times in LB broth and showed no change in PIM profile (data not shown).

LAMs were then extracted and purified from each strain, and subjected to a compositional analysis by GC-MS (Figure 6.13). When compared to the wild-type, MYCO481 showed the reduced sugar levels typical of the mutant. MYCO481 contained 21% of the wild-type inositol, 19% of the mannose and 5% of the arabinose. MYCO479 showed reduced sugar levels when compared to the wild-type, containing 86% of the inositol, 83% of the mannose and a highly reduced arabinose at 29%. The *mshB* knock-out MYCO504 was found to show similar LAM sugar levels to that of the wild-type. The mutant contained 81% inositol, 90% mannose and 91% arabinose in comparison to the wild-type. This implied that an *mshB* disruption had no effect of LAM production, and hence did not reproduce the reduced LAM phenotype characteristic of MYCO481.

These data indicate that disrupting *mshB* had no effect on the PIM/LAM phenotype therefore it is unlikely that polar effects from a *lpqW*::Tn*611* mutation contribute significantly to the phenotypes of MYCO479 and MYCO481.

6.4 Is lpqW Responsible for the PIM/LAM Phenotype?

The main objective of this chapter was to determine whether or not the *lpqW* transposon insertion in MYCO481 and MYCO479 was responsible for the PIM/LAM phenotype which was defined in the two strains. This was examined using two separate approaches. Firstly, an intact copy of *lpqW* isolated from the wild-type was provided to the mutants to test if the gene complements the PIM/LAM phenotype. Secondly, the gene downstream of *lpqW*, *mshB*, was disrupted to examine the possibility that the *lpqW* transposon insertion in MYCO481 and MYCO479 interfered with the transcription of any downstream genes, which in turn causes the PIM/LAM phenotype.

6.4.1 Complementation with lpqW

Analysis of the PIMs from the complemented strains showed that pHBJ212 was able to restore a normal PIM profile in MYCO479 while the construct had no

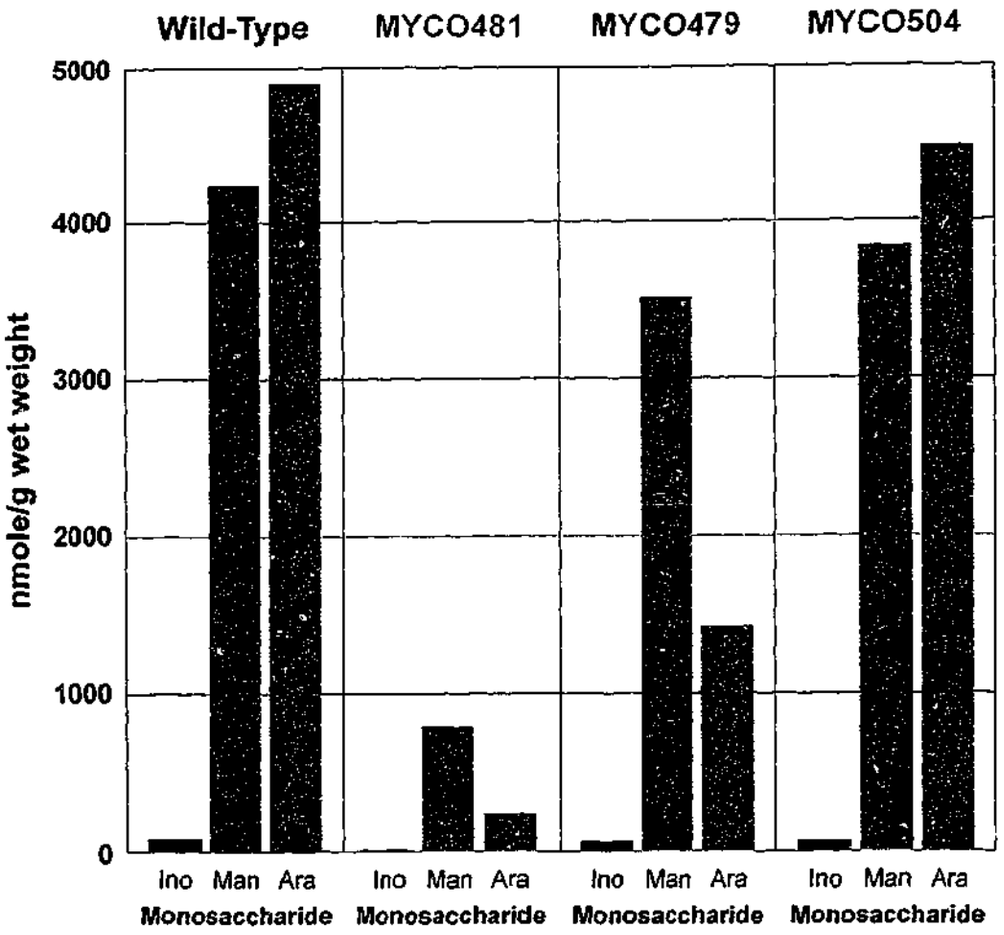

Figure 6.13
Disruption of *mshB* does not result in the LAM-deficienct phenotype of MYCO481.
LAMs were extracted and purified from the wild-type, the *lpqW* transposon mutants MYCO481 and MYCO479 (*lpqW*::Tn*611*), and the *mshB* targetted disruption mutant MYCO504 (*mshB*::Kan^R).

LAM-containing fractions were subjected to methanolysis and analysed for composition by TMS-derivatisation and GC-MS. The monosaccharides presented are: *myo*-inositol (Ino), D-mannose (Man) and D-arabinose (Ara).

The values given are nmole of sugar per gram of cell pellet wet weight (nmole/g wet weight).

apparent effect on the PIM profiles of MYCO481 and the wild-type. The control plasmids pHBJ164 and pHBJ210 had no effect on the PIM profiles of each strain.

While the PIM defect appears to have been complemented in MYCO479, the ability of *lpqW* to restore LAM levels in MYCO481 was not clear. Unlike the qualitative nature of PIM analysis, LAMs were assessed by quantitative, compositional means. Throughout the course of the study, it was found that the LAM compositional data tended to reveal trends rather than offer reproducible, comparable numbers. This may be a reflection on the LAM extraction technique, which is relatively crude compared to the procedure on which this method was based (144).

When compared to the wild-type transformed with the control plasmids pHBJ164 and pHBJ210, the amount of mannose and arabinose seen in MYCO481 is appreciably higher than that seen in the untransformed controls. This is also observed for pHBJ212. Given the general increase in mannose and arabinose seen in the transformants, the effect of pHBJ212 cannot be concluded with confidence.

The inositol measurements, however, indicate that pHBJ212 is partially complementing the deficiency seen in MYCO481. While the pHBJ164 and pHBJ212 control transformants show low inositol levels when compared to the wild-type, the MYCO481-pHBJ212 transformant shows an appreciable increase in inositol. Inexplicably, MYCO479 transformed with pHBJ164 shows reduced inositol. Further independent extractions and compositional analyses may clarify these results.

It is interesting to note that both pHBJ210 and pHBJ212 resulted in a general increase of LAM sugars in the wild-type and mutant transformants. This raises the possibility that both constructs are expressing a complementing product. While LpqW expression is expected in pHBJ212, no expression is anticipated for pHBJ210. It is possible that *lpqW* is being expressed in pHBJ210 under the control of an unknown regulatory element in the vector. For instance, the promoter driving expression of the hygromycin resistance gene, which is transcribed in the same direction as *lpqW*, may be involved (Figure 6.1). Expression of LpqW by either pHBJ210 or pHBJ212 can be tested for by examining whole-cell lysates or membrane fractions. Anti-sera can be raised against LpqW and used as a detection reagent to assess expression levels in the transformants.

Another possibility to consider is the choice of pMV261 as the expression vector. The vector expresses cloned genes via the constitutive *hsp60* promoter, which is highly active in mycobacteria (192). The level of LpqW expression from pHBJ212 is not likely to be comparable to the expression levels of genomic LpqW. Analysis of the differences in LpqW expression levels between transposon mutants and the pHBJ212 transformants would address this question.

A difference in expression levels may affect the constructs ability to complement the mutation. This problem can be overcome by using a construct which employs a less active promoter, or ideally, incorporates the native *lpqW* promoter. The *lpqW* promoter has not been identified; consensus sequences were not apparent upstream of the gene, and analysis of the *lpqW* transcript was not attempted.

The observation that only one successful pHBJ212 transformant of MYCO479 exists is of concern and raises questions as to why the transformation frequency was so low. Plasmid pHBJ212 was able to transform into the wild-type and the *lpqW* transposon mutant MYCO481 at a relatively high efficiency, while MYCO479 transformants were rare. In several previous attempts to transform the plasmid into MYCO479, no transformants were obtained. The results reported in this chapter represent the most successful attempt to transform the plasmid into MYCO479. Further, all but one of the transformants tested were found to contain modified or truncated forms of the plasmid which for the least part were missing the *lpqW* ORF. It appears that while MYCO481 accepts pHBJ212 with no apparent effect on its viability, MYCO479 only accepts the plasmid if it lacks *lpqW*. This implies that the presence of an intact *lpqW* in MYCO479 is lethal. The existence of pHBJ212g contradicts this theory. It is also unlikely that overexpression of the protein causes lethality, as wild-type transformants were easily obtained.

As MYCO481 seems to "evolve" into MYCO479 (Chapter 5), perhaps through selective pressure, it is possible that the mutations which change MYCO481 to MYCO479 are conditional on the absence of a functional LpqW. Hence, MYCO481 may accept pHBJ212 because the mutations which convert it to MYCO479 have not yet occurred. Conversely, MYCO479 has undergone those mutations and is unable to accept the intact *lpqW* provided by pHBJ212. This theory can be tested by serially subculturing the MYCO481 transformant in LB or

PPLO broth in the presence of kanamycin and hygromycin, and determining the viable count at each subculture. The hypothesis would be supported if a marked drop in viable count is observed, concurrent with a conversion to the PIM deficient phenotype of MYCO479.

The finding that both MYCO481-pHBJ212 and MYCO479-pHBJ212g were sensitive to streptomycin raises further questions. Both transformants should be resistant to the antibiotic by virtue of the streptomycin resistance marker contained within the pCG79 insertion. This result implied that the streptomycin resistance marker was absent or non-functional, or that in both cases the transposon insertion had undergone some sort of rearrangement such that streptomycin resistance was lost. One possible mechanism for this would involve homologous recombination between the IS6100 elements flanking the streptomycin resistance gene, resulting in the excision of a large portion of the transposon insert. It is unlikely that this had occurred in either strain since both mutants yielded the expected amplification products using the primers 3053 and 7389. This product would not be seen in the case of the recombination event described above. Hence, the streptomycin resistance genes may harbour single base changes which result in a loss of streptomycin resistance. The fact that both MYCO481-pHBJ212 and MYCO479-pHBJ212g were streptomycin sensitive is unexplained and requires further investigation. The identity of MYCO479-pHBJ212g as a true derivative of MYCO479 needs to be questioned, certainly since it is the sole example of such a transformant. While the characteristic transposon insertion into *lpqW* was demonstrated by PCR amplification, the region of insertion should be examined for any differences in sequence or organisation compared to MYCO479.

Plasmid pHBJ212g should be cured from the transformant to test whether the complemented PIM phenotype can be reversed to the PIM-deficient profile of MYCO479. Conversely, curing the plasmid from MYCO481-pHBJ212 should result in a reduction in the abundance of LAM-derived sugars in the strain, characteristic of MYCO481. It is possible that pHBJ212g is a rare example of pHBJ212 with a mutation that affects successful LpqW expression. Such a defect was not apparent with restriction mapping, and is therefore likely to be a single base addition or deletion leading to a frameshift. This can be addressed by sequencing pHBJ212g, or testing for the expression of LpqW from the plasmid.

Further evidence is required to connect *lpqW* to the PIM/LAM phenotype. An alternative approach to addressing this question involves disrupting *lpqW* by different means, such as targeted gene disruption. In effect, this approach results in an genetic "knock-out" which is analogous to the *lpqW* transposon mutants. Mutants of *lpqW* with disruptions in different parts of the ORF may be informative. If secondary mutations are responsible for the PIM/LAM phenotype in the transposon mutants, then disrupting *lpqW* in a strain which should not have these secondary changes (i.e. the wild-type) will demonstrate whether or not *lpqW* disruption causes the phenotype independently from secondary genetic events. *lpqW* disruption in the wild-type was attempted throughout the course of the study, and a successful *lpqW* knock-out strain could not be generated. Given the strong conservation of LpqW in various mycobacteria (see Figure 4.4), it is possible that the gene is essential and therefore could not be disrupted. The mutants of this study may represent rare examples of a viable *lpqW* disruption, where Tn*611* has inserted near the 3' end of the gene. The *lpqW*::Tn*611* mutants may express a truncated, partially functional protein. This question was not examined in this study.

6.4.2 *Disruption of* mshB *does not cause the PIM/LAM Phenotype*

The targetted disruption of *mshB* did not result in the loss of PIM_6, the accumulation of PIM_4 or the depletion of LAM. The colony morphology and instability of PIM profile characteristic of MYCO481 were not evident in the *mshB* mutant. These results imply that the transposon insertion into *lpqW* does not cause the PIM/LAM phenotype solely by affecting the transcription of the gene immediately downstream of it. One possibility is that the Tn*611* insertion in *lpqW* does cause a disruption in *mshB* transcription, and that the loss of function in both genes causes the PIM/LAM phenotype. This possibility can be explored by disrupting *lpqW* and *mshB* simultaneously.

The gene *mshB* is involved in mycothiol biosynthesis (139), and is therefore unlikely to be involved in PIM or LAM biosynthesis. While mycothiol contains inositol, a key component of PIMs and LAMs, there is no obvious relationship between the mycothiol and PIM/LAM biosynthetic pathways. Therefore, the lack of involvement of *mshB* in the PIM/LAM phenotype is not unexpected.

The *mshB* knock-out mutant MYCO504 can be of use in studying the mycothiol biosynthetic pathway. If the function of *mshB* is as Newton *et al.* (139) predicts, then MYCO504 may accumulate *myo*-inositol-*N*-acetylglucosamine. Newton *et al.* (141) isolated chemically-mutagenised mycothiol deficient strains which were found to be more sensitive to hydrogen peroxide and rifampicin, while being more resistant to isoniazid. MYCO504 can be tested for its response to these agents. The mutants response to *in vivo* oxidative stress, in the form of the intracellular environment of the macrophage, may also help to clarify the role of mycothiols in mycobacterial infection and persistence.

Chapter 7
An Unusual Pair of Mutants with Great Potential

The results presented in the preceding chapters describe a pair of mutants with a complex, unusual phenotype. The phenotype is characterised by a set of abnormalities that affect the PIM/LAM biosynthetic pathway. Given that mutants in this pathway are very rare, the observation that MYCO481 and MYCO479 have numerous defects is particularly interesting.

Transposon mutant MYCO481 shows a major reduction in the amount of LM/LAM. The mutant also oversynthesises PIM species, in particular the early precursor PIM_1, and also shows elevated production of the biosynthetic mannose donor HPM. MYCO481 generates small colonies on selected media which are unstable through subculture, giving rise to a form of the mutant which produces colonies that more closely resemble the wild-type. This secondary form of the mutant, MYCO479, also shows some interesting defects. The mutant does not synthesise the more polar PIM_6 species and accumulates PIM_4, which acts as a biosynthetic precursor for the polar PIMs in the wild-type and MYCO481. The more advanced form of the mutant also oversynthesises HPM, and its LAM levels are intermediate to that of the wild-type and MYCO481. Furthermore, both the primary and secondary forms of the mutant contain a Tn*611* insertion in the same gene, *lpqW*. The gene has no known function, and bears the sequence hallmarks of a lipoprotein. The transposon disruption was shown to be stable despite the shift in phenotype from MYCO481 to MYCO479.

7.1 The Change from MYCO481 to MYCO479

The biochemical observations provide clues as to how the change in mutant phenotype occurs, allowing a hypothetical sequence of events to be proposed. Before transposon mutagenesis, the *M. smegmatis* wild-type shows normal PIM, LAM and HPM synthesis (Figure 7.1a). The *lpqW* gene is then disrupted with Tn*611* to form the mutant strain MYCO481. This leads to a loss of normal LpqW

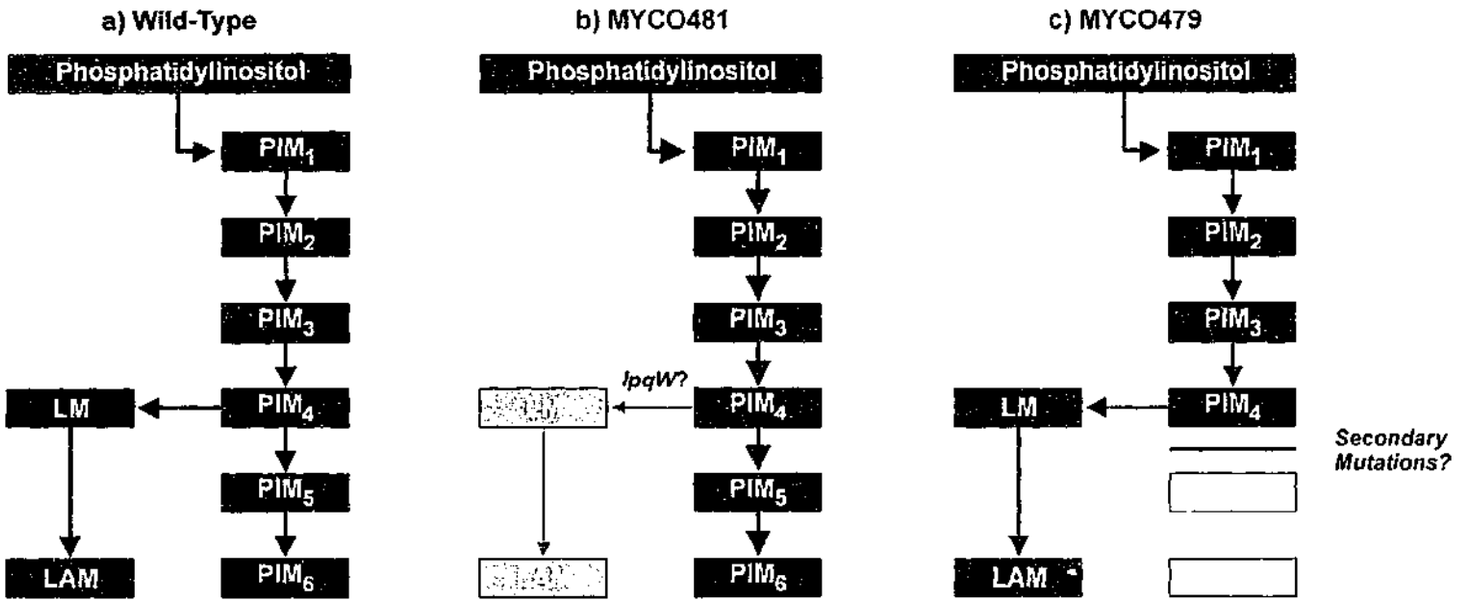

Figure 7.1
Proposed alterations to the PIM/LAM biosynthetic pathway in MYCO481 and MYCO479.
This diagram attempts to summarise the aberrant PIM/LAM biosynthetic phenotypes of two *lpqW* transposon mutants, MYCO481 and MYCO479. Accumulating end-products are shown in navy, while intermediates are presented in blue. In the mutants, products of abundance are shown in grey while absent molecules are shown in white.
a) *M. smegmatis* wild-type accumulates acylation variants of PIM_2 and PIM_6, while also producing LAM.
b) After transposon mutagenesis of *lpqW*, MYCO481 produces greatly reduced amounts of LAM while also showing elevated PIM production. It is possible that the LAM deficiency results in enfeebled cells with a growth disadvantage, as demonstrated on selected media.
c) Secondary mutations which compensate for the defect are selected for, resulting in a loss of PIM_5 and PIM_6 production and the accumulation of PIM_4. LAM levels are consequently restored to a point where the cells viability is not affected. This form of the mutant is called MYCO479.

c) Secondary mutations which compensate for the defect are selected for, resulting in loss of PIM_6 and PIM_5 synthesis and the production of PIM_4. LAM levels are consequently restored to a point where the cells viability is not affected. This form of the mutant is called MYCO479.

function, which results in the oversynthesis of HPM and PIMs together with a reduction in LAM synthesis (Figure 7.1b). It is important to note that LAM synthesis is not completely inhibited, as MYCO481 accumulates up to 30% of the level of LAM seen in the wild-type.

It is possible that the mutation affects LAM synthesis first, and the elevation of HPM and PIM synthesis is a result of the increased availability of precursors, enzymes or substrates which would normally be utilised in LAM production. This series of biosynthetic defects result in the production of a small, perhaps enfeebled colony on selected media. Given that a major cell envelope component such as LAM is greatly depleted, the cell wall architecture is likely to be compromised. MYCO481 may respond by regulating the synthesis of other cell envelope components to compensate for the absence of LAM. This was not obvious in the compositional analyses performed in this study, but a more thorough analysis of the cell envelope composition and architecture would be interesting. A major LAM defect may be observed by electron microscopy of the MYCO481 cell envelope. Any differences may be informative as to the location of LAM, which to date is poorly understood.

The MYCO481 phenotype is unstable and shifts to one that is typified by a colony morphology that closely resembles the wild-type. This implies that selective pressure is applied to the MYCO481 population, where cells with mutations that compensate for the absence of LAM are selected for. Interestingly, culture media plays an important role in this process. Cells with secondary, compensatory mutations are likely to confer a growth advantage and gradually dominate the population as MYCO479. What causes this change is not known. The site of these secondary mutations, and indeed whether it is one or many mutations, is also unknown.

What is apparent is that the secondary mutations result in the loss of PIM_6 and presumably PIM_5 synthesis, leading to the accumulation of PIM_4. This was a particularly interesting finding, as the point of divergence between PIM and LAM biosynthesis in the biosynthetic pathway is not clear (see Figure 1.6). A previous report implicates Ac_3PIM_2 as the point of pathway divergence (23). PIM_2 would be a logical candidate as the LAM precursor, as it accumulates in the cell envelope and is therefore abundant and freely available for use in the synthesis of a major

glycolipid such as LAM. However, based on structural similarity acylation variants of PIM_3 or PIM_4 can also fulfil this role.

It is tempting to speculate that PIM_4 acts as the direct precursor to LM/LAM synthesis, based on the observations made in MYCO481 and MYCO479. The secondary mutations in MYCO479 have the effect of halting PIM_5/PIM_6 production, such that their immediate precursor PIM_4 now accumulates and is oversynthesised. This provides the mutant with a greater amount of precursor for LAM synthesis, boosting the branch of the pathway involved in LAM production. LAM synthesis is partially restored, perhaps to a point at which the fitness of the cell is comparable to the wild-type (Figure 7.1c). The significance of elevated HPM synthesis in MYCO479 is not clear. It is possible that the secondary mutations cause in an increase in HPM, in turn increasing PIM_4 synthesis. If PIM_5/PIM_6 production is sensitive to the amount of PIM_4 precursor, it is conceivable that an overabundance of PIM_4 may result in the inhibition of polar PIM synthesis. The observation that MYCO479 has no obvious growth defects implies that the polar PIMs are expendable, unlike the apolar PIM_1 (108). Once the change from the LAM-deficient to the polar PIM-deficient phenotype has been made, the phenotype is stabilised and permanent.

7.2 lpqW and the Possibility of Secondary Mutations

While MYCO481 and MYCO479 are both *lpqW* mutants, the role of the gene in this complex set of phenomena is not known. The likely nature of the gene product as a lipoprotein is consistent with PIM and presumably LAM biosynthesis being based at the cytoplasmic membrane. To explore the subcellular location of the protein, antisera can be raised against recombinant LpqW and used as a reagent to localise the protein to subcellular compartments, either by immunogold electron microscopy or by examining cell-free subcellular fractions of *M. smegmatis* via polyacrylamide gel electrophoresis. Another approach involves constructing translational fusions with β-galactosidase or alkaline phosphatase to test if LpqW resides in the cytoplasm or is exported beyond the plasma membrane. This experiment can be attempted in *E. coli*, but would ultimately need to be done in *M. smegmatis*.

The identity of LpqW as a lipoprotein should also be confirmed. This can be addressed by testing whether or not radiolabelled lipid incorporates into the mature form of LpqW via an *in vivo* metabolic labelling experiment. Testing the ability of LpqW to be cleaved by signal petidase II (SPaseII) may be dificult, as the pre-protein form is not likely to accumulate in the cell. Further, SPaseII activity may be difficult to reconstitute in an *in vitro* assay. Mutagenesis of the signal peptidase II cleavage and lipid attachment sites may overcome these potential problems, where the mutated protein is unable to incorporate radiolabelled lipid *in vivo*. Alternatively, antisera raised against LpqW can be used to detect mobility shifts in polyacrylamide gels between the wild-type protein and the mutated protein.

The LpqW sequence showed a weak match to the proposed GDP-mannose binding motif of bacterial α-mannosyltransferases (75). While the match was not convincing, the defects in PIM biosynthesis implied that mannosyltransferase activity was aberrant. An enzymatic assay to test if the protein has the ability to transfer radiolabelled mannose from GDP-man to purified PIM species can be attempted to explore the possibility that LpqW has mannosyltransferase activity.

The results from the complementation experiments do not conclusively demonstrate the genes role in the PIM/LAM phenotype. Interestingly, a plasmid containing intact *lpqW* is deleterious to MYCO479. Of the rare transformants generated for MYCO479, the majority were found to harbour truncated variants of the complementing plasmid pHBJ212 that lacked a complete *lpqW* ORF. Only one successful transformant, MYCO479-pHBJ212g, was isolated and subsequently shown to contain a normal set of PIMs while maintaining the Tn*611* insertion into *lpqW*. The observation that intact *lpqW* is not lethal against the genetic background of MYCO479-pHBJ212g, as is the case with MYCO481 transformants, raises the possibility that the transformant is a rare example of a MYCO479 strain that has reverted back to a genotype resembling MYCO481. While this is contrary to evidence that the conversion from MYCO481 to MYCO479 is stable, the uniqueness of MYCO479-pHBJ212g supports the notion of a very rare genetic event. Comparing the wild-type, MYCO481 and MYCO479 to their respective pHBJ212 transformants by genomic microarray analysis would be useful for exploring this possibility. This approach would identify similarities or differences

in transcript levels between the strains, but would not detect point mutations that may be important. The generation of similar transformants would also be useful in investigating this phenomena as a rare genetic event, but problematic given the difficulty of transforming pHBJ212 into MYCO479. The frequency of reversion may be increased on media which promotes a less stable genetic enviroment for MYCO479, such as LB or PPLO. Alternatively, reducing the strength of the promoter in the *lpqW* complementation construct may reduce its lethality in MYCO479 and thereby affect the occurance of the reversion mutations. It should be emphasised that the ability of the apparently intact plasmid in MYCO479-pHBJ212g to express LpqW has not been examined and should be confirmed.

If MYCO479-pHBJ212g is a MYCO481-like revertant, the elevated LAM sugars detected in each of the *lpqW*-complemented strains suggests that *lpqW* is involved in the LAM biosynthetic branch of the PIM/LAM pathway. The observation that the change from MYCO481 to MYCO479 affects PIM synthesis would therefore imply that the secondary changes specifically affect PIM biosynthetic genes. It remains possible that the gene is involved in both branches of the biosynthetic pathway. Hence, the findings of this study do not conclusively prove that *lpqW* is responsible for the PIM/LAM phenotype, although its involvement seems likely.

The identity of the proposed secondary genetic changes that result in the loss of PIMs and restoration of LAM remain unknown. Several approaches can be used to search for the additional mutations that may change the MYCO481 phenotype to that of MYCO479. Transposon mutant MYCO479 can be transformed with a *M. smegmatis* cosmid library in an attempt to complement the secondary mutations with random fragments of the genome. In this case, complementation would be defined as the restoration of a normal PIM profile to MYCO479. However, screening for such complementation events would be laborious, as PIM extractions would have to be done for each transformant. It is not known whether complementation of the secondary defects in MYCO479 would result in a complete reversion to the MYCO481 phenotype. If so, the transformants can be screened for the small colony phenotype. However, a reversion of colony phenotype may not be a very reliable indicator of successful complementation. A crude screening method using an anti-PIM monoclonal antibody, such as the anti-

polar PIM antibody reported by Hoppe *et al* (90), could be used in the development of a screening assay for the presence or absence of polar PIMs. Ultimately, the cosmid complementation approach may not be feasible. If multiple secondary mutations are present, successfully complementing MYCO479 with a single cosmid would be difficult and unlikely.

An alternate approach would involve the use of a *M. smegmatis* genomic microarray. Hybridising the MYCO479 transcriptome to the genome array would allow the identification of gene/s with altered expression in the mutant, perhaps being due to these secondary mutation events. The recent reports identifying genes involved in PIM biosynthesis such as *impA* (153), *pgsA* (98), *pimA* (108), *pimB* (175) and *ppm1* (86) provide a good list of candidates which may be the targets for the secondary mutations. The microarray approach could identify other novel cell envelope biosynthetic genes if MYCO479 or MYCO481 alter the synthesis of other cell envelope components to compensate for the loss of PIM or LAM. As mentioned previously, microarray analysis would not necessarily reveal secondary chages that are point mutations. If the complementation or microarray approaches are unsuccessful, then the sequences of the genes mentioned above can be examined for sequence mutations in MYCO479.

In order to further explore the role of *lpqW*, attempts were made to knock out the gene by targetted disruption. The attempts were unsuccessful, raising the possibility that *lpqW* is essential to *M. smegmatis*. Given its high conservation amongst the genus, it may be essential to all mycobacteria. The conditional knock-out system successfully used to demonstrate that *pgsA* and *pimA* are essential (98, 108) may be useful in demonstrating the importance of *lpqW*. The existence of MYCO481/MYCO479 as Tn*611* mutants of *lpqW* suggests that it is possible to disrupt the gene. Further, the truncated LpqW which may be expressed by the mutants is apparently sufficient for cell viability and perhaps partially functional. The existence of the truncated protein was not examined in this study and should be investigated.

In addition to the various outstanding questions regarding *lpqW* and the nature of the secondary genetic changes, further biochemical studies need to be completed to better understand the PIM/LAM phenotype. This study offered a limited analysis of the composition of crude LM/LAM extracts. A detailed

examination of the MYCO481 LAM structure may reveal structural anomalies indicative of specific defects in the mutant. The ability of MYCO481 to oversynthesise PIMs facilitates the purification of novel, previously unidentified PIM and LAM precursors. A detailed structural characterisation of these precursors would undoubtedly improve our understanding of the PIM/LAM biosynthesis. Given the number of defects observed in the mutants, a more thorough examination of the mutants ability to synthesise other components of the PIM and LAM pathway, particularly LAM precursors, would also be interesting.

The results presented demonstrate that the change in phenotype is dependant on the media used. In Middlebrook, a standard media used in the propagation of mycobacteria, the change is prevented or at the very least delayed. In contrast, when a more general media such as LB is used the change in phenotype is rapid. Hence, the instability of MYCO481 can be delayed through the use of Middlebrook as a growth medium. This is an important finding, as further study of MYCO481 will require its phenotype to be stable. The reasons as to why LAM deficiencies are a great disadvantage on some media and but not Middlebrook are unclear.

7.3 Scope for Further Studies

The unique nature of the MYCO481 and MYCO479 phenotypes offers great potential for a broad range of studies. Most directly, the ability of MYCO479 to produce abundant quantities of PIM_4 provides a useful substrate for studying the branching point between PIM and LAM synthesis. For instance, MYCO479 cultures can be labelled with [^{3}H]mannose, and the resulting PIM_4 isolated. The purified PIM_4 can then be used in a metabolic labelling experiment to test whether the label from PIM_4 is incorporated into $PIM_{5/6}$ exclusively, or into LAM. The incorporation of label into LAM would implicate PIM_4 as its biosynthetic precursor. This experiment would rely on the ability of purified, labelled PIM_4 to enter live cells. An analogous experiment involving the use of cell-free reactions may avoid this problem. Sub-cellular fractions from a wild-type strain that overexpresses LpqW can be assayed for the ability to enhance PIM/LAM production. The strain generated in this study, wild-type-pHBJ212, may be useful

for these types of experiments. It would be interesting to examine the capability of excess LpqW to catalyse the formation of PIM_5 from PIM_4 in a cell-free fraction.

As described in detail in Chapter 1 of this study, PIMs and LAM play an important, multifunctional role in the abilty of mycobacteria to interact and interfer with the host immune system. MYCO481 and MYCO479 provide a unique opportunity to study the effect of PIM or LAM deficiency in the infected macrophage. The ability of the mutants to bind to macrophages would be of particular interest, given the role of PIMs and LAM in binding to host cells (67). The ability of MYCO479 to bind to macrophages would be interesting as polar PIMs have been shown to act as host cell ligands (90). The effect of a polar PIM deficiency can be tested, as well as the ability of PIM_4 to bind to host cells.

The unique nature of PIM and LAM structure has made the biosynthetic pathway an attractive target for the development of novel, highly specific anti-mycobacterial drugs. The *lpqW* mutants provide a unique opportunity to examine the effect of PIM or LAM deficiency on drug sensitivity, addressing the question as to whether or not the search for new drugs which target PIM/LAM biosynthesis is worthwhile. Previous studies have shown that PIMs do have influence on the drug sensitivity of mycobacteria. Parish *et al.* (153) found that the *impA* transposon mutant, which showed a reduced amount of PIM_2, to be more sensitive to ampicillin. Conversely, the over-expression of PimA increased resistance to ampicillin three to four fold (108). A detailed examination of drug resistance in MYCO481 and MYCO479 would be of great interest.

It is clear that the data presented in this study only partially defines what appears to be a highly complex interplay between unknown genetic determinants and the PIM/LAM biosynthetic pathway. The attempts to characterise MYCO481 and MYCO479 raised many unresolved questions. Perhaps more importantly, the *lpqW* mutants offer numerous opportunities to explore these questions and study various aspects of mycobacterial pathogenesis, structure and metabolism. Given the importance of PIMs and LAM in the mycobacterial cell envelope, together with their poorly defined and seemingly complex role in disease, the need for further study is highly warranted.

Appendix 1

Bacterial Strains

Mycobacterium smegmatis Strains		
Strain	**Description**	**Source**
mc²155	Wild-type strain, high transformation efficiency	(192)
MYCO320	Tn*611* transposon mutant of mc²155 (*metA*::Tn*611*)	Dr. H. Billman-Jacobe
MYCO479	Tn*611* transposon mutant of mc²155 (*lpqW*::Tn*611*)	Dr. H. Billman-Jacobe
MYCO481	Tn*611* transposon mutant of mc²155 (*lpqW*::Tn*611*)	Dr. H. Billman-Jacobe
MYCO504	Targetted disruption mutant of mc²155 (*mshB*::Kan^R)	This study
Wild-Type-pHBJ164	mc²155 containing plasmid pHBJ164	This study
MYCO479-pHBJ164	MYCO479 containing plasmid pHBJ164	This study
MYCO481-pHBJ164	MYCO481 containing plasmid pHBJ164	This study
Wild-Type-pHBJ210	mc²155 containing plasmid pHBJ210	This study
MYCO479-pHBJ210	MYCO479 containing plasmid pHBJ210	This study
MYCO481-pHBJ210	MYCO481 containing plasmid pHBJ210	This study
Wild-Type-pHBJ212	mc²155 containing plasmid pHBJ212	This study
MYCO479-pHBJ212	MYCO479 containing plasmid pHBJ212	This study
MYCO481-pHBJ212	MYCO481 containing plasmid pHBJ212	This study

Table A1.1
***Mycobacterium smegmatis* strains used in this study.**
All mycobacterial strains used in this study were derived from the *M. smegmatis* mc²155.

Escherichia coli Strains		
Strain	**Genotype**	**Source**
XL1-Blue MRF'	Δ(*mcrA*)183 Δ(*mcrCB-hsdSMR-mrr*)173 *endA1 supE44 thi-1 recA1 gyrA96 relA1 lac* [F'*proAB lacI*^{q}Z ΔM15 Tn10 (Tet^R)]	Stratagene
DH5α	*supE44* Δ*lacU169*(*ϕ80lacΔZM15*) *hsdR17 recA1 gyrA96 thi-1 relA1*	Stratagene

Table A1.2
***Escherichia coli* strains used in this study.**
The *E. coli* XL1-Blue MRF' and DH5α strains were used as hosts for all plasmids and cloning procedures described in this study.

Appendix 2

Bacteriological Media Formulations

Antibiotic Supplement

Ampicillin	100 µg/ml
Hygromycin	200 µg/ml (*M. smegmatis*), 100 µg/ml (*E. coli*)
Kanamycin	20 µg/ml
Streptomycin	20 µg/ml

Beef-Yeast (BY) Agar

0.3% (w/v) beef extract

0.6% (w/v) yeast extract

1.2% (w/v) peptone

1% (w/v) NaCl

1.5% (w/v) bacteriological agar

Sterilise by autoclaving at 121°C for 20 minutes.

Luria-Bertani (LB) Broth

1% (w/v) bacto-tryptone

0.5% (w/v) yeast extract

1% (w/v) NaCl

Sterilise by autoclaving at 121°C for 20 minutes.

Luria-Bertani (LB) Agar

1% (w/v) bacto-tryptone

0.5% (w/v) yeast extract

1% (w/v) NaCl

1.5% (w/v) bacteriological agar

Sterilise by autoclaving at 121°C for 20 minutes.

Middlebrook 7H9 Broth

Per litre: Resuspend 4.7 g of Middlebrook 7H9 (Difco Laboratories) in 900 ml of distilled water containing 2 ml of glycerol

Sterilise by autoclaving at 121°C for 20 minutes

Supplement with 100 ml sterile modified DC enrichment.

Middlebrook 7H10 Agar

Per litre: Resuspend 19 g of Middlebrook 7H10 (Difco Laboratories) in 900 ml of distilled water containing 5 ml of glycerol

Sterilise by autoclaving at 121°C for 20 minutes

Supplement with 100 ml sterile modified DC enrichment.

Modified DC Enrichment

2% (w/v) glucose

0.85% (w/v) NaCl

Sterilise by autoclaving at 121°C for 10 minutes.

Pleuropneumonia-like organism (PPLO) Broth

5% (w/v) brain heart infusion

1% (w/v) bacto-peptone

0.5% (w/v) NaCl

Sterilise by autoclaving at 121°C for 20 minutes.

Pleuropneumonia-like organism (PPLO) Agar

5% (w/v) brain heart infusion

1% (w/v) bacto-peptone

0.5% (w/v) NaCl

1.4% (w/v) bacteriological agar

Sterilise by autoclaving at 121°C for 20 minutes.

Sauton's Minimal Media

0.05% (w/v) KH_2PO_4

0.05% (w/v) $MgSO_4.7H_2O$

0.2% (w/v) citric acid

0.005% (w/v) ferric ammonium citrate

6% (v/v) glycerol

0.4% (w/v) asparagine

Adjust to pH 7.4

Sterilise by autoclaving at 121°C for 15 minutes.

Appendix 3

Gas Chromatography - Mass Spectroscopy

Raw Data

Data from Chapter 2

Strain	Extract	nmole / g wet weight					
		Inositol	Mannose	Arabinose	Galactose	Rhamnose	Glucose
Wild-Type	Chloroform : Methanol (2 : 1, v/v)	1248	2486	4	0	654	0
	Chloroform : Methanol : Water (1 : 2 : 0.8, v/v/v)	95	833	0	12	1	53
	Total	**1343**	**3319**	**4**	**12**	**655**	**53**
MYCO481	Chloroform : Methanol (2 : 1, v/v)	1435	3185	15	0	720	0
	Chloroform : Methanol : Water (1 : 2 : 0.8, v/v/v)	147	1298	0	36	2	0
	Total	**1582**	**4483**	**15**	**36**	**722**	**0**
MYCO479	Chloroform : Methanol (2 : 1, v/v)	1890	3835	7	0	969	0
	Chloroform : Methanol : Water (1 : 2 : 0.8, v/v/v)	47	227	0	2	0	39
	Total	**1937**	**4062**	**7**	**2**	**969**	**39**

Table A3.1
Data for Figure 2.4a

Strain	Extract	nmole / g wet weight					
		Inositol	Mannose	Arabinose	Galactose	Rhamnose	Glucose
Wild-Type	Chloroform : Methanol (2 : 1, v/v)	37	69	0	17	1	1550
	Chloroform : Methanol : Water (1 : 2 : 0.8, v/v/v)	92	61	2	9	0	2460
	Total	**129**	**130**	**2**	**26**	**1**	**4010**
MYCO481	Chloroform : Methanol (2 : 1, v/v)	25	93	0	17	2	2048
	Chloroform : Methanol : Water (1 : 2 : 0.8, v/v/v)	89	139	4	14	2	3315
	Total	**114**	**232**	**4**	**31**	**4**	**5363**
MYCO479	Chloroform : Methanol (2 : 1, v/v)	28	56	0	14	1	1818
	Chloroform : Methanol : Water (1 : 2 : 0.8, v/v/v)	77	75	2	9	2	2248
	Total	**105**	**131**	**2**	**23**	**3**	**4066**

Table A3.2
Data for Figure 2.4a

Strain	nmole / g wet weight					
	Inositol	Mannose	Arabinose	Galactose	Glucose	Rhamnose
Wild-Type	74	3288	6564	94	141	1803
MYCO481	19	800	991	102	147	319
MYCO479	48	2405	3449	72	182	1038

Table A3.3
Data for Figure 2.8a

Strain	nmole / g wet weight					
	Inositol	Mannose	Arabinose	Galactose	Glucose	Rhamnose
Wild-Type	111	581	606	95	525	2293
MYCO481	107	246	190	213	866	0
MYCO479	83	618	211	74	433	662

Table A3.4
Data for Figure 2.8b

Strain	nmole / g wet weight					
	Inositol	Mannose	Arabinose	Galactose	Glucose	Rhamnose
Wild-Type	1	21	21	7	36	6
MYCO481	1	8	48	13	63	15
MYCO479	0	8	21	6	37	8

Table A3.5
Data for Figure 2.10

Strain	nmole / g wet weight					
	Inositol	Mannose	Arabinose	Galactose	Glucose	Rhamnose
Wild-Type	0	9	12422	2162	369	4680
MYCO481	1	17	11416	2385	460	4088
MYCO479	1	29	8250	1874	715	3011

Table A3.6
Data for Figure 2.11

Strain	nmole / g wet weight		
	Inositol	Mannose	Arabinose
a) 7H10/PPLO			
Wild-Type	182	3470	2561
MYCO481	11	111	19
MYCO479	83	1767	855
b) PPLO/PPLO			
Wild-Type	195	3103	6504
MYCO481	7	206	149
MYCO479	67	1960	2275

Table A3.7
Data for Figure 2.13

Data from Chapter 5

Strain	*LB broth*	*nmole/gram wet weight*		
	Subculture	**Inositol**	**Mannose**	**Arabinose**
Wild-Type	Subculture 1	33	1584	242
	Subculture 5	30	1499	700
MYCO481	Subculture 1	0	12	0
	Subculture 2	11	707	59
	Subculture 5	24	1162	53
MYCO479	Subculture 1	34	1809	314
	Subculture 5	16	703	92

Table A3.8
Data for Figure 5.2

Strain	*PPLO broth*	*nmole/gram wet weight*		
	Subculture	**Inositol**	**Mannose**	**Arabinose**
Wild-Type	Subculture 1	53	2780	1932
	Subculture 5	110	5088	3843
MYCO481	Subculture 1	1	192	16
	Subculture 3	26	1562	695
	Subculture 5	18	1082	471
MYCO479	Subculture 1	47	2129	685
	Subculture 5	55	3122	1814

Table A3.9
Data for Figure 5.4

Strain	*7H9 broth*	*nmole /gram wet weight*		
	Subculture	**Inositol**	**Mannose**	**Arabinose**
Wild-Type	Subculture 1	24	1520	405
	Subculture 5	28	1499	446
MYCO481	Subculture 1	0	12	4
	Subculture 5	3	162	17
MYCO479	Subculture 1	13	609	410
	Subculture 5	45	2483	710

Table A3.10
Data for Figure 5.6

Data from Chapter 6

Strain	nmole/g wet weight		
	Inositol	Mannose	Arabinose
Wild-Type	25	941	78
Wild-Type-pHBJ164	33	658	41
Wild-Type-pHBJ210	19	1369	977
Wild-Type-pHBJ212	29	1950	1690
MYCO481	7	181	8
MYCO481-pHBJ164	4	320	127
MYCO481-pHBJ210	9	1064	467
MYCO481-pHBJ212	20	1537	888
MYCO479	24	677	121
MYCO481-pHBJ164	7	631	205
MYCO481-pHBJ210	21	1692	890
MYCO481-pHBJ212	14	1015	603

Table A3.11
Data for Figure 6.5

Strain	nmole/g wet weight		
	Inositol	Mannose	Arabinose
Wild-Type	76	4245	4903
MYCO481 (*lpqW*::Tn*611*)	16	804	248
MYCO479 (*lpqW*::Tn*611*)	65	3525	1435
MYCO504 (*mshB*::Kan^R)	62	3839	4490

Table A3.12
Data for Figure 6.13

Appendix 4

Plasmid Constructs

Plasmid	Description
pBluescript SK+	Multipurpose cloning vector; *lacZ*, Amp (Stratagene)
pCG79	*Mycobacterium/E. coli* shuttle vector; harbours Tn*611*, which contains a kanamycin resistance marker flanked by two copies of IS6100 (Str, Km) (85)
pEP3	*Mycobacterium/E. coli* shuttle vector; hygromycin-resistant derivative of pEP2 (Hyg) (167)
pHBJ115	Marker rescue plasmid from MYCO479 (Str, Km)
pHBJ122	4929 bp *Hin*dIII/*Eco*RI subclone from pHBJ115 into pBluescript II SK+ (Amp)
pHBJ123	781 bp *Hin*dIII subclone from pHBJ115 into pBluescript II SK+ (Amp)
pHBJ164	PCR-amplified Hygromycin resistance marker from pEP3 (primers 8598/8599) cloned into *Sma*I site of pMV261 (Hyg)
pHBJ197	PCR product of primers 48/9276 cloned into *Sma*I site of pUC18 (Amp)
pHBJ201	pHBJ197 *Eco*RI fragment cloned into *Eco*RI site of pMV261 (Km)
pHBJ202	As with pHBJ201, except insert cloned in opposite orientation; this results in an *hsp60/lpqW* transcriptional fusion
pHBJ210	PCR-amplified Hygromycin resistance marker from pEP3 (primers 8598/8599) cloned into the *Nsi*I sites of pHBJ201 (Hyg, Km)
pHBJ212	PCR-amplified Hygromycin resistance marker from pEP3 (primers 8598/8599) cloned into the *Nsi*I sites of pHBJ202 (Hyg, Km)
pHBJ257	*Sau*3AI partial digest fragment from MYCO479, cloned into the *Bam*HI site of pUC19 (Km, Amp)
pHBJ261	*Sau*3AI partial digest fragment from MYCO479, cloned into the *Bam*HI site of pUC19 (Km, Amp)
pHBJ262	*Sau*3AI partial digest fragment from MYCO479, cloned into the *Bam*HI site of pUC19 (Km, Amp)
pHBJ266	*Sau*3AI partial digest fragment from MYCO479, cloned into the *Bam*HI site of pUC19 (Km, Amp)
pHBJ269	PCR amplification product from MYCO479 (primers 8671/8672) cloned into *Sma*I site of pUC18 (Amp)
pHBJ272	Approx. 6 kb *Hin*dIII/*Eco*RI fragment from the wild-type genome cloned into the *Hin*dIII/*Eco*RI sites of pUC18 (Amp)
pHBJ273	Approx. 2.5 kb *Dde*I fragment from pHBJ272, blunt-ended and cloned into a blunt-ended *Kpn*I site in pUC18 (Amp)
pHBJ278	PCR-amplified kanamycin resistance marker from pUC18K (primers UP and RP) digested with *Kpn*I/*Hin*cII and blunt-ended, cloned into the blunt-ended *Kpn*I site of pHBJ273 (Amp, Km)
pHBJ280	*Sma*I digested Omega cassette from pUC19Ω cloned into blunt-ended *Hin*dIII site of pHBJ278 (Amp, Km, Str)
pMV261	*Mycobacterium/E. coli* shuttle vector; *hsp60* promoter for mycobacterial gene expression (Km) (192)
pUC18/pUC19	Multipurpose cloning vector; *lacZ*, Amp (210)
pUC18K	pUC18 containing a kanamycin resistance cassette (Amp, Km) (127)
pUC19Ω	pUC19 containing the omega cassette, which encodes streptomycin resistance (Amp, Str) (163)

Table A4
Plasmids used in this study.
Indicated are the antibiotic resistance markers contained within the plasmid: Amp (ampicillin); Hyg (hygromycin); Km (kanamycin); Str (streptomycin).
All plasmids were generated for this study, except where indicated with the relevant reference.

Appendix 5

Oligonucleotide Primers

The following tables include the sequences (**Table A5.1**) and the experimental applications (**Table A5.2**) of each of the oligonucleotide primers used in this study. Relevant references are included in Table A5.2.

Primer	Sequence
48	5′ AAA GAA TTC ATG GGC GTG CCG 3′
190	5′ GGT GAG GAG GGC GAG GTG 3′
191	5′ TCT GTG GCG ACG GGC ATG 3′
192	5′ GCA CAC GCC ACG CAG ATC 3′
193	5′ TGA TCC CGC TGG TCG AGG 3′
194	5′ GGT ACT CGT CGT CGC TGC 3′
211	5′ ACT GGG CCG ACT CAC TGC 3′
212	5′ CCG ACG GCA ACC ACA ACG 3′
213	5′ ACA CCA GGT TCG GCG GCG 3′
214	5′ GTC GAT CCG TGA ATG GCT G 3′
215	5′ CCG GTG CAT CTG GCG TC 3′
216	5′ GCA CCC GGA CCA CCT CG 3′
217	5′ ACC CAG TTC AGC TCC TTG 3′
218	5′ CTT GCC GAC GGT GAG CTC 3′
219	5′ GTG CCG ACC TGC CCG CG 3′
220	5′ CCA CCG CAC CGA ACC CG 3′
233	5′ CTT CTT GAG CTT GCC GTT G 3′
234	5′ CCC CTG GCC GCG TAG AG 3′
237	5′ ACC GCG TTC CAC CTC ACC 3′
238	5′ CCA CCG ACC TGA CCA CCG 3′
317	5′ CGC GTC GCA TAT GCT GCC CAG CT 3′
318	5′ TGC TCT CGA GGC GGA ACT G 3′
320	5′ TCG GCT CGA GGA TGC CGG TGA 3′
394	5′ GCA ACG GTG ACA CAC AGG T 3′
3053	5′ GAA CCG CTT CGC TGC CTT G 3′
3054	5′ AAC CAC CAT TTC GCA GCA GC 3′
6068	5′ GCA TGC TTG GCG GAG ATT GG 3′
6069	5′ GCA CCA GGG GCG AGC CTG T 3′
6457	5′ GCC CGG CCA GCG TAA GTA G 3′
7168	5′ CAG CGC CAT CCC CGA CGT C 3′
7389	5′ GGC GTC GCG CTA CGG ATG 3′

Primer	Sequence
7805	5' CGA TGT CGT CCG TAC CGT C 3'
8598	5' AAA AAC CGC GGC TCC GCC ATA ACC TCA CC 3'
8599	5' GGG GGA ATA TTC AGA AAC AAC TCT GGC GCA T 3'
8665	5' AAG AAT TCA TCG TTC CGT CCG TCC AAT CTC C 3'
8670	5' TCG AGC TCG TGC 3'
8671	5' GAG CGA CAG CCT ACC TCT GAC T 3'
8672	5' TAG CTT ATT CCT CAA GGC ACG AGC 3'
8936	5' CCA GCA GGA TCT CGT CGC GC 3'
9125	5' TGG GCG ACG TGG GAT CCG 3'
9276	5' AGC CGG GGC GAT TCA TGC 3'
KanC	5' GTG GTA TGA CAT TGC CTT CTG C 3'
UP	5' GTA AAA CGA CGG CCA GT 3'
RP	5' GGA AAC AGC TAT GAC CA 3'
T3	5' ATT AAC CCT CAC TAA AGG GA 3'
T7	5' TAA TAC GAC TCA CTA TAG GG 3'

Table A5.1
Oligonucleotide primer sequences.

Primer	Purpose
48	PCR amplification of *lpqW* for cloning into pMV261
190	Sequencing of pHBJ261
191	Sequencing of pHBJ122
192	Sequencing of pHBJ261
193	Sequencing of pHBJ122
194	Sequencing of pHBJ257
211	Sequencing of pHBJ261
212	Sequencing of pHBJ122
213	Sequencing of pHBJ257
214	Sequencing of pHBJ272
215	Sequencing of pHBJ261
216	Sequencing of pHBJ122
217	Sequencing of pHBJ257
218	Sequencing of pHBJ122
219	Sequencing of pHBJ257
220	Sequencing of pHBJ257
233	Sequencing of pHBJ122
234	Sequencing of pHBJ272
237	Sequencing of pHBJ122

Primer	Purpose
238	Sequencing of pHBJ272
317	Sequencing of pHBJ197
318	Sequencing of pHBJ197
320	Sequencing of pHBJ197
394	Sequencing of pHBJ197
3053	PCR Amplification of IS6100, used with 7389 to test for *lpqW* insertion
3054	PCR Amplification of IS6100, used with 9276 to test for *lpqW* insertion
6068	PCR Amplification of IS6100, used with 6069 for production of hybridisation probe
6069	PCR Amplification of IS6100, used with 6068 for production of hybridisation probe
6457	Sequencing of pMV261-based constructs, targets *hsp60* promoter
7168	PCR Amplification of *lpqW*, used with 7805 to test arrangement of pHBJ122/pHBJ123
7389	PCR Amplification of *lpqW*
7805	PCR Amplification of *lpqW*, used with 7168 to test arrangement of pHBJ122/pHBJ123
8598	PCR Amplification of hygromycin resistance gene in pEP3
8599	PCR Amplification of hygromycin resistance gene in pEP3
8665	"Primer F"; PCR amplification/sequencing of IS6100-containing insertion site (165)
8670	"Primer Salpi"; used to construct LM-PCR linker fragment (165)
8671	"Primer G"; PCR amplification/sequencing of IS6100-containing insertion site (165)
8672	"Primer Salgd"; linker primer, PCR amplification of IS6100-containing insertion site (165)
8936	Sequencing of pHBJ122
9125	Sequencing of pHBJ122
9276	PCR Amplification of *lpqW*
KanC	Sequencing of pUC18K kanamycin resistance cassette
UP	pUC18/19 "Universal primer" for amplification/sequencing (Amersham Pharmacia Biotech Pty. Ltd, Australia)
RP	pUC18/19 "Reverse primer" for amplification/sequencing (Amersham Pharmacia Biotech Pty. Ltd, Australia)
T3	Sequencing primer for pBluescript SK+ (Novagen)
T7	Sequencing primer for pBluescript SK+ (Novagen)

Table A5.2
Oligonucleotide primers used in this study.
Primers were used for PCR amplification and/or DNA sequencing purposes.
All primers were designed for this study, except where referenced.

Appendix 6

Polymerase Chain Reaction Cycles

Cycle Sequencing

Step	Number of Cycles	Temperature	Time
Denaturation	25	96°C	10 secs
Annealing		50°C	5 secs
Extension		60°C	4 mins

PCR Amplification

Amplification of IS6100 Probe
(Primers 6068/6069)

Step	Number of Cycles	Temperature	Time
Denaturation	35	95°C	30 secs
Annealing		55°C	30 secs
Extension		72°C	15 secs

Ligation-Mediated PCR Linker Molecule (165)
(Primers 8670/8672)

Step	Temperature
Annealing	80°C to 4°C gradient over 60 mins

Ligation-Mediated PCR (165)
(Primers 8672/8665 or 8671)

Step	Number of Cycles	Temperature	Time
Denaturation/Enzyme "Hot Start"	1	95°C	9 mins
Denaturation	40	95°C	30 secs
Annealing		55°C	30 secs
Extension		72°C	90 secs
Final Extension	1	72°C	10 mins

Amplification across pHBJ122/pHBJ123 Junction
(Primers 7168/7805)

Step	Number of Cycles	Temperature	Time
Initial Denaturation	1	95°C	5 mins
Denaturation	35	95°C	30 secs
Annealing		60°C	30 secs
Extension		72°C	90 secs
Final Extension	1	72°C	5 mins

Amplification across site of MYCO479 Tn*611* insertion in wild-type genome
(Primers 7389/9276)

Step	Number of Cycles	Temperature	Time
Initial Denaturation	1	95°C	5 mins
Denaturation	35	95°C	30 secs
Annealing		55°C	30 secs
Extension		72°C	90 secs
Final Extension	1	72°C	5 mins

Specific Detection of Tn*611* insertion in *lpqW*
(Primers 9276/3054 and 3053/7389)

Step	Number of Cycles	Temperature	Time
Initial Denaturation	1	95°C	5 mins
Denaturation	35	95°C	30 secs
Annealing		55°C	30 secs
Extension		72°C	60 secs
Final Extension	1	72°C	5 mins

Amplification of hygromycin resistance marker from pEP3 (167)
(Primers 8598/8599)

Step	Number of Cycles	Temperature	Time
Initial Denaturation	1	95°C	10 mins
Denaturation	35	95°C	30 secs
Annealing		55°C	30 secs
Extension		72°C	90 secs
Final Extension	1	72°C	7 mins

Amplification of *lpqW* for cloning into pMV261 (192)
(Primers 48/9276)

Step	*Number of Cycles*	*Temperature*	*Time*
Initial Denaturation	1	95°C	5 mins
Denaturation	35	95°C	30 secs
Annealing		57°C	30 secs
Extension		72°C	2 mins plus additional 20 secs extension per cycle
Final Extension	1	72°C	7 mins

Amplification of kanamycin resistance cassette from pUC18K (127)
(Primers UP/RP) (Amersham Pharmacia Biotech Pty. Ltd, Australia)

Step	*Number of Cycles*	*Temperature*	*Time*
Initial Denaturation	1	95°C	5 mins
Denaturation	35	95°C	30 secs
Annealing		50°C	30 secs
Extension		62°C	30 secs
Final Extension	1	62°C	3 mins

References

1. **Altschul, S. F., T. L. Madden, A. A. Schaffer, J. Zhang, Z. Zhang, W. Miller, and D. J. Lipman** 1997. Gapped BLAST and PSI-BLAST: a new generation of protein database search programs. *Nucleic Acids Res.* **25**:3389-3402.

2. **Anderberg, R. J., J. A. Strachan, and G. A. Cangelosi** 1995. Purification of DNA from *Mycobacterium* species without sonication or phenol. *Biotechniques.* **18**:217-219.

3. **Andersson, G. E., and P. M. Sharp** 1996. Codon usage in the *Mycobacterium tuberculosis* complex. *Microbiology.* **142**:915-925.

4. **Aspinall, G. O., D. Chatterjee, and P. J. Brennan** 1995. The variable surface glycolipids of mycobacteria: structures, synthesis of epitopes, and biological properties. *Adv Carbohydr Chem Biochem.* **51**:169-242.

5. **Ausubel, F. M., R. Brent, R. E. Kingston, D. D. Moore, J. G. Seidman, J. A. Smith, and K. Struhl** 1994. Current protocols in Molecular Biology. John Wiley and Sons, Inc., New York.

6. **Azuma, I., Y. Yamamura, and K. Fukushi** 1968. Fractionation of mycobacterial cell wall. Isolation of arabinose mycolate and arabinogalactan from cell wall fraction of *Mycobacterium tuberculosis* strain Aoyama B. *J Bacteriol.* **96**:1885-1887.

7. **Bachhawat, N., and S. C. Mande** 1999. Identification of the INO1 gene of *Mycobacterium tuberculosis* $H_{37}R_v$ reveals a novel class of inositol-1-phosphate synthase enzyme. *J Mol Biol.* **291**:531-536.

8. **Banerjee, A., E. Dubnau, A. Quemard, V. Balasubramanian, K. S. Um, T. Wilson, D. Collins, G. de Lisle, and W. R. Jacobs, Jr.** 1994. *inhA*, a gene encoding a target for isoniazid and ethionamide in *Mycobacterium tuberculosis*. *Science.* **263**:227-230.

9. **Banerjee, A., M. Sugantino, J. C. Sacchettini, and W. R. Jacobs, Jr.** 1998. The *mabA* gene from the *inhA* operon of *Mycobacterium tuberculosis* encodes a 3-ketoacyl reductase that fails to confer isoniazid resistance. *Microbiology.* **144**:2697-2704.

10. **Barnes, P. F., D. Chatterjee, J. S. Abrams, S. Lu, E. Wang, M. Yamamura, P. J. Brennan, and R. L. Modlin** 1992. Cytokine production induced by *Mycobacterium*

tuberculosis lipoarabinomannan. Relationship to chemical structure. *J Immunol.* **149:**541-547.

11. **Beatty, W. L., E. R. Rhoades, H. J. Ullrich, D. Chatterjee, J. E. Heuser, and D. G. Russell** 2000. Trafficking and Release of Mycobacterial Lipids from Infected Macrophages. *Traffic.* **1:**235-247.

12. **Belanger, A. E., G. S. Besra, M. E. Ford, K. Mikusova, J. T. Belisle, P. J. Brennan, and J. M. Inamine** 1996. The *embAB* genes of *Mycobacterium avium* encode an arabinosyl transferase involved in cell wall arabinan biosynthesis that is the target for the antimycobacterial drug ethamoutol. *Proc Natl Acad Sci U S A.* **93:**11919-11924.

13. **Belanger, A. E., J. C. Porter, and G. F. Hatfull** 2000. Genetic analysis of peptidoglycan biosynthesis in mycobacteria: characterization of a *ddlA* mutant of *Mycobacterium smegmatis*. *J Bacteriol.* **182:**6854-6856.

14. **Belisle, J. T., and P. J. Brennan** 1989. Chemical basis of rough and smooth variation in mycobacteria. *J Bacteriol.* **171:**3465-3470.

15. **Belisle, J. T., M. R. McNeil, D. Chatterjee, J. M. Inamine, and P. J. Brennan** 1993. Expression of the core lipopeptide of the glycopeptidolipid surface antigens in rough mutants of *Mycobacterium avium*. *J Biol Chem.* **268:**10510-10516.

16. **Belisle, J. T., L. Pascopella, J. M. Inamine, P. J. Brennan, and W. R. Jacobs, Jr.** 1991. Isolation and expression of a gene cluster responsible for biosynthesis of the glycopeptidolipid antigens of *Mycobacterium avium*. *J Bacteriol.* **173:**6991-6997.

17. **Belisle, J. T., V. D. Vissa, T. Sievert, K. Takayama, P. J. Brennan, and G. S. Besra** 1997. Role of the major antigen of *Mycobacterium tuberculosis* in cell wall biogenesis. *Science.* **276:**1420-1422.

18. **Berton, G., C. Laudanna, C. Sorio, and F. Rossi** 1992. Generation of signals activating neutrophil functions by leukocyte integrins: LFA-1 and gp150/95, but not CR3, are able to stimulate the respiratory burst of human neutrophils. *J Cell Biol.* **116:**1007-1017.

19. **Besra, G. S., R. C. Bolton, M. R. McNeil, M. Ridell, K. E. Simpson, J. Glushka, H. van Halbeek, P. J. Brennan, and D. E. Minnikin** 1992. Structural elucidation of a novel family of acyltrehaloses from *Mycobacterium tuberculosis*. *Biochemistry.* **31:**9832-9837.

20. **Besra, G. S., and P. J. Brennan** 1997. The mycobacterial cell wall: biosynthesis of arabinogalactan and lipoarabinomannan. *Biochem Soc Trans.* **25:**845-850.

21. **Besra, G. S., and D. Chatterjee** 1994. Lipids and Carbohydrates of *Mycobacterium tuberculosis.*, p. 285-306. *In* B. R. Bloom (ed.), Tuberculosis: Pathogenesis, Protection, and Control. American Society for Microbiology, Washington DC.

22. **Besra, G. S., K. H. Khoo, M. R. McNeil, A. Dell, H. R. Morris, and P. J. Brennan** 1995. A new interpretation of the structure of the mycolyl-arabinogalactan complex of *Mycobacterium tuberculosis* as revealed through characterization of oligoglycosylalditol fragments by fast-atom bombardment mass spectrometry and 1H nuclear magnetic resonance spectroscopy. *Biochemistry.* **34:**4257-4266.

23. **Besra, G. S., C. B. Morehouse, C. M. Rittner, C. J. Waechter, and P. J. Brennan** 1997. Biosynthesis of mycobacterial lipoarabinomannan. *J Biol Chem.* **272:**18460-18466.

24. **Besra, G. S., T. Sievert, R. E. Lee, R. A. Slayden, P. J. Brennan, and K. Takayama** 1994. Identification of the apparent carrier in mycolic acid synthesis. *Proc Natl Acad Sci U S A.* **91:**12735-12739.

25. **Billman-Jacobe, H., R. E. Haites, and R. L. Coppel** 1999. Characterization of a *Mycobacterium smegmatis* mutant lacking penicillin binding protein 1. *Antimicrob Agents Chemother.* **43:**3011-3013.

26. **Billman-Jacobe, H., M. J. McConville, R. E. Haites, S. Kovacevic, and R. L. Coppel** 1999. Identification of a peptide synthetase involved in the biosynthesis of glycopeptidolipids of *Mycobacterium smegmatis. Mol Microbiol.* **33:**1244-1253.

27. **Billman-Jacobe, H., J. Sloan, and R. L. Coppel** 1996. Analysis of isoniazid-resistant transposon mutants of *Mycobacterium smegmatis. FEMS Microbiol Lett.* **144:**47-52.

28. **Bloom, B. R., and C. J. Murray** 1992. Tuberculosis: commentary on a reemergent killer. *Science.* **257:**1055-1064.

29. **Bornemann, C., M. A. Jardine, H. S. Spies, and D. J. Steenkamp** 1997. Biosynthesis of mycothiol: elucidation of the sequence of steps in *Mycobacterium smegmatis. Biochem J.* **325:**623-629.

30. **Boshoff, H. I., and V. Mizrahi** 2000. Expression of *Mycobacterium smegmatis* pyrazinamidase in *Mycobacterium tuberculosis* confers hypersensitivity to pyrazinamide and related amides. *J Bacteriol.* **182:**5479-5485.

31. **Braunstein, M., T. I. Griffin, J. I. Kriakov, S. T. Friedman, N. D. Grindley, and W. R. Jacobs, Jr.** 2000. Identification of genes encoding exported *Mycobacterium tuberculosis* proteins using a Tn*552'phoA in vitro* transposition system. *J Bacteriol.* **182:**2732-2740.

32. **Brennan, P., and C. E. Ballou** 1968. Biosynthesis of mannophosphoinositides by *Mycobacterium phlei*. Enzymatic acylation of the dimannophosphoinositides. *J Biol Chem.* **243:**2975-2984.

33. **Brennan, P., and C. E. Ballou** 1967. Biosynthesis of mannophosphoinositides by *Mycobacterium phlei*. The family of dimannophosphoinositides. *J Biol Chem.* **242:**3046-3056.

34. **Brennan, P. J., and G. S. Besra** 1997. Structure, function and biogenesis of the mycobacterial cell wall. *Biochem Soc Trans.* **25:**188-194.

35. **Brennan, P. J., and P. Draper** 1994. Ultrastructure of *Mycobacterium tuberculosis.*, p. 271-284. *In* B. R. Bloom (ed.), Tuberculosis: Pathogenesis, Protection, and Control. American Society for Microbiology, Washington DC.

36. **Brennan, P. J., and H. Nikaido** 1995. The envelope of mycobacteria. *Annu Rev Biochem.* **64:**29-63.

37. **Caceres, N. E., N. B. Harris, J. F. Wellehan, Z. Feng, V. Kapur, and R. G. Barletta** 1997. Overexpression of the D-alanine racemase gene confers resistance to D-cycloserine in *Mycobacterium smegmatis*. *J Bacteriol.* **179:**5046-5055.

38. **Camacho, L. R., D. Ensergueix, E. Perez, B. Gicquel, and C. Guilhot** 1999. Identification of a virulence gene cluster of *Mycobacterium tuberculosis* by signature-tagged transposon mutagenesis. *Mol Microbiol.* **34:**257-267.

39. **Chan, J., X. D. Fan, S. W. Hunter, P. J. Brennan, and B. R. Bloom** 1991. Lipoarabinomannan, a possible virulence factor involved in persistence of *Mycobacterium tuberculosis* within macrophages. *Infect Immun.* **59:**1755-1761.

40. **Chatterjee, D., C. M. Bozic, M. McNeil, and P. J. Brennan** 1991. Structural features of the arabinan component of the lipoarabinomannan of *Mycobacterium tuberculosis*. *J Biol Chem.* **266**:9652-9660.

41. **Chatterjee, D., S. W. Hunter, M. McNeil, and P. J. Brennan** 1992. Lipoarabinomannan. Multiglycosylated form of the mycobacterial mannosylphosphatidylinositols. *J Biol Chem.* **267**:6228-6233.

42. **Chatterjee, D., and K. H. Khoo** 1998. Mycobacterial lipoarabinomannan: an extraordinary lipoheteroglycan with profound physiological effects. *Glycobiology.* **8**:113-120.

43. **Chatterjee, D., and K. H. Khoo** 2001. The surface glycopeptidolipids of mycobacteria: structures and biological properties. *Cell Mol Life Sci.* **58**:2018-2042.

44. **Chatterjee, D., K. H. Khoo, M. R. McNeil, A. Dell, H. R. Morris, and P. J. Brennan** 1993. Structural definition of the non-reducing termini of mannose-capped LAM from *Mycobacterium tuberculosis* through selective enzymatic degradation and fast atom bombardment-mass spectrometry. *Glycobiology.* **3**:497-506.

45. **Chatterjee, D., K. Lowell, B. Rivoire, M. R. McNeil, and P. J. Brennan** 1992. Lipoarabinomannan of *Mycobacterium tuberculosis*. Capping with mannosyl residues in some strains. *J Biol Chem.* **267**:6234-6239.

46. **Chatterjee, D., A. D. Roberts, K. Lowell, P. J. Brennan, and I. M. Orme** 1992. Structural basis of capacity of lipoarabinomannan to induce secretion of tumor necrosis factor. *Infect Immun.* **60**:1249-1253.

47. **Cole, S. T., R. Brosch, J. Parkhill, T. Garnier, C. Churcher, D. Harris, S. V. Gordon, K. Eiglmeier, S. Gas, C. E. Barry, 3rd, F. Tekaia, K. Badcock, D. Basham, D. Brown, T. Chillingworth, R. Connor, R. Davies, K. Devlin, T. Feltwell, S. Gentles, N. Hamlin, S. Holroyd, T. Hornsby, K. Jagels, B. G. Barrell, and *et al.*** 1998. Deciphering the biology of *Mycobacterium tuberculosis* from the complete genome sequence [see comments] [published erratum appears in *Nature* 1998 Nov 12;396(6707):190]. *Nature.* **393**:537-544.

48. **Cole, S. T., K. Eiglmeier, J. Parkhill, K. D. James, N. R. Thomson, P. R. Wheeler, N. Honore, T. Garnier, C. Churcher, D. Harris, K. Mungall, D. Basham, D. Brown, T. Chillingworth, R. Connor, R. M. Davies, K. Devlin, S. Duthoy, T. Feltwell, A. Fraser, N. Hamlin, S. Holroyd, T. Hornsby, K. Jagels, C. Lacroix, J. Maclean, S. Moule, L.**

Murphy, K. Oliver, M. A. Quail, M. A. Rajandream, K. M. Rutherford, S. Rutter, K. Seeger, S. Simon, M. Simmonds, J. Skelton, R. Squares, S. Squares, K. Stevens, K. Taylor, S. Whitehead, J. R. Woodward, and B. G. Barrell 2001. Massive gene decay in the leprosy bacillus. *Nature.* **409:**1007-1011.

49. **Cywes, C., H. C. Hoppe, M. Daffe, and M. R. Ehlers** 1997. Nonopsonic binding of *Mycobacterium tuberculosis* to complement receptor type 3 is mediated by capsular polysaccharides and is strain dependent. *Infect Immun.* **65:**4258-4266.

50. **Daffe, M., P. J. Brennan, and M. McNeil** 1990. Predominant structural features of the cell wall arabinogalactan of *Mycobacterium tuberculosis* as revealed through characterization of oligoglycosyl alditol fragments by gas chromatography/mass spectrometry and by ^{1}H and ^{13}C NMR analyses. *J Biol Chem.* **265:**6734-6743.

51. **Daffe, M., and P. Draper** 1998. The envelope layers of mycobacteria with reference to their pathogenicity. *Adv Microb Physiol.* **39:**131-203.

52. **Daffe, M., C. Lacave, M. A. Laneelle, M. Gillois, and G. Laneelle** 1988. Polyphthienoyl trehalose, glycolipids specific for virulent strains of the tubercle bacillus. *Eur J Biochem.* **172:**579-584.

53. **Daffe, M., and M. A. Laneelle** 1988. Distribution of phthiocerol diester, phenolic mycosides and related compounds in mycobacteria. *J Gen Microbiol.* **134:**2049-2055.

54. **Daffe, M., M. A. Laneelle, and C. Lacave** 1991. Structure and stereochemistry of mycolic acids of *Mycobacterium marinum* and *Mycobacterium ulcerans. Res Microbiol.* **142:**397-403.

55. **Dahl, K. E., H. Shiratsuchi, B. D. Hamilton, J. J. Ellner, and Z. Toossi** 1996. Selective induction of transforming growth factor beta in human monocytes by lipoarabinomannan of *Mycobacterium tuberculosis. Infect Immun.* **64:**399-405.

56. **David, H. L., K. Takayama, and D. S. Goldman** 1969. Susceptibility of mycobacterial D-alanyl-D-alanine synthetase to D-cycloserine. *Am Rev Respir Dis.* **100:**579-581.

57. **de Miranda, A. B., F. Alvarez-Valin, K. Jabbari, W. M. Degrave, and G. Bernardi** 2000. Gene expression, amino acid conservation, and hydrophobicity are the main factors shaping codon preferences in *Mycobacterium tuberculosis* and *Mycobacterium leprae. J Mol Evol.* **50:**45-55.

58. **De Smet, K. A., A. Weston, I. N. Brown, D. B. Young, and B. D. Robertson** 2000. Three pathways for trehalose biosynthesis in mycobacteria. *Microbiology.* **146**:199-208.

59. **Delmas, C., M. Gilleron, T. Brando, A. Vercellone, M. Gheorghui, M. Riviere, and G. Puzo** 1997. Comparative structural study of the mannosylated-lipoarabinomannans from *Mycobacterium bovis* BCG vaccine strains: characterization and localization of succinates. *Glycobiology.* **7**:811-817.

60. **Deng, L., K. Mikusova, K. G. Robuck, M. Scherman, P. J. Brennan, and M. R. McNeil** 1995. Recognition of multiple effects of ethambutol on metabolism of mycobacterial cell envelope. *Antimicrob Agents Chemother.* **39**:694-701.

61. **Dhariwal, K. R., Y. M. Yang, H. M. Fales, and M. B. Goren** 1987. Detection of trehalose monomycolate in *Mycobacterium leprae* grown in armadillo tissues. *J Gen Microbiol.* **133**:201-209.

62. **Draper, P., O. Kandler, and A. Darbre** 1987. Peptidoglycan and arabinogalactan of *Mycobacterium leprae. J Gen Microbiol.* **133**:1187-1194.

63. **Drickamer, K., and M. E. Taylor** 1993. Biology of animal lectins. *Annu Rev Cell Biol.* **9**:237-264.

64. **Dubnau, E., M. A. Laneelle, S. Soares, A. Benichou, T. Vaz, D. Prome, J. C. Prome, M. Daffe, and A. Quemard** 1997. *Mycobacterium bovis* BCG genes involved in the biosynthesis of cyclopropyl keto- and hydroxy-mycolic acids. *Mol Microbiol.* **23**:313-322.

65. **Dye, C., M. A. Espinal, C. J. Watt, C. Mbiaga, and B. G. Williams** 2002. Worldwide incidence of multidrug-resistant tuberculosis. *J Infect Dis.* **185**:1197-1202.

66. **Eckstein, T. M., F. S. Silbaq, D. Chatterjee, N. J. Kelly, P. J. Brennan, and J. T. Belisle** 1998. Identification and recombinant expression of a *Mycobacterium avium* rhamnosyltransferase gene (*rtfA*) involved in glycopeptidolipid biosynthesis. *J Bacteriol.* **180**:5567-5573.

67. **Ehlers, M. R., and M. Daffe** 1998. Interactions between *Mycobacterium tuberculosis* and host cells: are mycobacterial sugars the key? *Trends Microbiol.* **6**:328-335.

68. **Escuyer, V. E., M. A. Lety, J. B. Torrelles, K. H. Khoo, J. B. Tang, C. D. Rithner, C. Frehel, M. R. McNeil, P. J. Brennan, and D. Chatterjee** 2001. The role of the *embA* and

embB gene products in the biosynthesis of the terminal hexaarabinofuranosyl motif of *Mycobacterium smegmatis* arabinogalactan. *J Biol Chem.* **276**:48854-48862.

69. **Fitzmaurice, A. M., and P. E. Kolattukudy** 1997. Open reading frame 3, which is adjacent to the mycocerosic acid synthase gene, is expressed as an acyl coenzyme A synthase in *Mycobacterium bovis* BCG. *J Bacteriol.* **179**:2608-2615.

70. **Folch, J., M. Lee, and G. H. Sloane Stanley** 1957. A simple method for the isolation and purification of total lipides from animal tissues. *J Biol Chem.* **226**:497-509.

71. **Forman, H. J., H. Zhou, E. Gozal, and M. Torres** 1998. Modulation of the alveolar macrophage superoxide production by protein phosphorylation. *Environ Health Perspect.* **106 Suppl 5**:1185-1190.

72. **Frick, D. N., B. D. Townsend, and M. J. Bessman** 1995. A novel GDP-mannose mannosyl hydrolase shares homology with the MutT family of enzymes. *J Biol Chem.* **270**:24086-24091.

73. **Gelber, R. H.** 1995. Leprosy (Hansen's Disease)., p. 2243-2250. *In* G. L. Mandell, J. E. Bennet, and R. Dolin (eds), Mandell, Douglas & Bennet's Principles and Practice of Infectious Diseases, 4th ed. Churchill-Livingston, New York.

74. **George, K. M., D. Chatterjee, G. Gunawardana, D. Welty, J. Hayman, R. Lee, and P. L. Small** 1999. Mycolactone: a polyketide toxin from *Mycobacterium ulcerans* required for virulence. *Science.* **283**:854-857.

75. **Geremia, R. A., E. A. Petroni, L. Ielpi, and B. Henrissat** 1996. Towards a classification of glycosyltransferases based on amino acid sequence similarities: prokaryotic alpha-mannosyltransferases. *Biochem J.* **318**:133-138.

76. **Gilleron, M., L. Bala, T. Brando, A. Vercellone, and G. Puzo** 2000. *Mycobacterium tuberculosis* $H_{37}R_v$ parietal and cellular lipoarabinomannans. Characterization of the acyl- and glyco-forms. *J Biol Chem.* **275**:677-684.

77. **Gilleron, M., N. Himoudi, O. Adam, P. Constant, A. Venisse, M. Riviere, and G. Puzo** 1997. *Mycobacterium smegmatis* phosphoinositols-glyceroarabinomannans. Structure and localization of alkali-labile and alkali-stable phosphoinositides. *J Biol Chem.* **272**:117-124.

78. **Gilleron, M., J. Nigou, B. Cahuzac, and G. Puzo** 1999. Structural study of the lipomannans from *Mycobacterium bovis* BCG: characterisation of multiacylated forms of the phosphatidyl-myo- inositol anchor. *J Mol Biol.* 285:2147-2160.

79. **Gilleron, M., C. Ronet, M. Mempel, B. Monsarrat, G. Gachelin, and G. Puzo** 2001. Acylation state of the phosphatidylinositol mannosides from *Mycobacterium bovis* bacillus Calmette Guerin and ability to induce granuloma and recruit natural killer T cells. *J Biol Chem.* 276:34896-34904.

80. **Glickman, M. S., S. M. Cahill, and W. R. Jacobs, Jr.** 2000. The *Mycobacterium tuberculosis cmaA2* gene encodes a mycolic acid trans cyclopropane synthetase. *J Biol Chem.*

81. **Goodfellow, M., and J. G. Magee** 1998. Taxonomy of Mycobacteria., p. 1-71. *In* P. R. J. Gangadharam, and P. A. Jenkins (eds), Mycobacteria, vol. 1: Basic aspects. Chapman & Hall, New York.

82. **Goren, M. B.** 1984. Biosynthesis and structures of phospholipids and sulfatides., p. 379-415. *In* G. P. Kubica, and G. Wayne (eds), The Mycobacteria: A Sourcebook, vol. A. Marcel Dekker, Inc., New York.

83. **Grange, J. M.** 1998. Pathogenesis of Mycobacterial Disease., p. 145-177. *In* P. R. J. Gangadharam, and P. A. Jenkins (eds), Mycobacteria, vol. 1: Basic Aspects. Chapman & Hall, New York.

84. **Guerardel, Y., E. Maes, E. Elass, Y. Leroy, P. Timmerman, G. S. Besra, C. Locht, G. Strecker, and L. Kremer** 2002. Structural study of lipomannan and lipoarabinomannan from *Mycobacterium chelonae*. Presence of unusual components with alpha 1,3-mannopyranose side chains. *J Biol Chem.* 277:30635-30648.

85. **Guilhot, C., I. Otal, I. Van Rompaey, C. Martin, and B. Gicquel** 1994. Efficient transposition in mycobacteria: construction of *Mycobacterium smegmatis* insertional mutant libraries. *J Bacteriol.* 176:535-539.

86. **Gurcha, S. S., A. R. Baulard, L. Kremer, C. Locht, D. B. Moody, W. Muhlecker, C. E. Costello, D. C. Crick, P. J. Brennan, and G. S. Besra** 2002. Ppm1, a novel Polyprenol Monophosphomannose Synthase from *Mycobacterium tuberculosis*. *Biochem J.* 365:441-450.

87. **Haas, D. W., and R. M. Des Prez** 1995. *Mycobacterium tuberculosis*, p. 2213-2243. *In* G. L. Mandell, J. E. Bennet, and R. Dolin (eds), Mandell, Douglas & Bennet's Principles and Practice of Infectious Diseases, 4th ed. Churchill-Livingston, New York.

88. **Hamid, M. E., D. E. Minnikin, and M. Goodfellow** 1993. A simple chemical test to distinguish mycobacteria from other mycolic- acid-containing actinomycetes. *J Gen Microbiol.* 139:2203-2213.

89. **Hockmeyer, W. T., R. E. Krieg, M. Reich, and R. D. Johnson** 1978. Further characterization of *Mycobacterium ulcerans* toxin. *Infect Immun.* 21:124-128.

90. **Hoppe, H. C., B. J. de Wet, C. Cywes, M. Daffe, and M. R. Ehlers** 1997. Identification of phosphatidylinositol mannoside as a mycobacterial adhesin mediating both direct and opsonic binding to nonphagocytic mammalian cells. *Infect Immun.* 65:3896-3905.

91. **Horgen, L., E. L. Barrow, W. W. Barrow, and N. Rastogi** 2000. Exposure of human peripheral blood mononuclear cells to total lipids and serovar-specific glycopeptidolipids from *Mycobacterium avium* serovars 4 and 8 results in inhibition of TH1-type responses. *Microb Pathog.* 29:9-15.

92. **Horowitz, E. A., and W. E. J. Sanders** 1995. Other *Mycobacterium* Species., p. 2264-2273. *In* G. L. Mandell, J. E. Bennet, and R. Dolin (eds), Mandell, Douglas & Bennet's Principles and Practice of Infectious Diseases, 4th ed. Churchill-Livingston, New York.

93. **Horsburgh, C. R., Jr.** 1991. *Mycobacterium avium* complex infection in the acquired immunodeficiency syndrome. *N Engl J Med.* 324:1332-1338.

94. **Horsburgh, C. R., Jr., J. Gettings, L. N. Alexander, and J. L. Lennox** 2001. Disseminated *Mycobacterium avium* complex disease among patients infected with human immunodeficiency virus, 1985-2000. *Clin Infect Dis.* 33:1938-1943.

95. **Hunter, S. W., and P. J. Brennan** 1990. Evidence for the presence of a phosphatidylinositol anchor on the lipoarabinomannan and lipomannan of *Mycobacterium tuberculosis*. *J Biol Chem.* 265:9272-9279.

96. **Hunter, S. W., H. Gaylord, and P. J. Brennan** 1986. Structure and antigenicity of the phosphorylated lipopolysaccharide antigens from the leprosy and tubercle bacilli. *J Biol Chem.* 261:12345-12351.

97. **Ilangumaran, S., S. Arni, M. Poincelet, J. M. Theler, P. J. Brennan, D. Nasir ud, and D. C. Hoessli** 1995. Integration of mycobacterial lipoarabinomannans into glycosylphosphatidylinositol-rich domains of lymphomonocytic cell plasma membranes. *J Immunol.* 155:1334-1342.

98. **Jackson, M., D. C. Crick, and P. J. Brennan** 2000. Phosphatidylinositol is an essential phospholipid of mycobacteria. *J Biol Chem.* 275:30092-30099.

99. **Jackson, M., C. Raynaud, M. A. Laneelle, C. Guilhot, C. Laurent-Winter, D. Ensergueix, B. Gicquel, and M. Daffe** 1999. Inactivation of the antigen 85C gene profoundly affects the mycolate content and alters the permeability of the *Mycobacterium tuberculosis* cell envelope. *Mol Microbiol.* 31:1573-1587.

100. **Jacobs, W. R., Jr., G. V. Kalpana, J. D. Cirillo, L. Pascopella, S. B. Snapper, R. A. Udani, W. Jones, R. G. Barletta, and B. R. Bloom** 1991. Genetic systems for mycobacteria. *Methods Enzymol.* 204:537-555.

101. **Jarlier, V., and H. Nikaido** 1994. Mycobacterial cell wall: structure and role in natural resistance to antibiotics. *FEMS Microbiol Lett.* 123:11-18.

102. **Kaufmann, S. H.** 1993. Immunity to intracellular bacteria. *Annu Rev Immunol.* 11:129-163.

103. **Khoo, K. H., A. Dell, H. R. Morris, P. J. Brennan, and D. Chatterjee** 1995. Inositol phosphate capping of the nonreducing termini of lipoarabinomannan from rapidly growing strains of *Mycobacterium*. *J Biol Chem.* 270:12380-12389.

104. **Khoo, K. H., A. Dell, H. R. Morris, P. J. Brennan, and D. Chatterjee** 1995. Structural definition of acylated phosphatidylinositol mannosides from *Mycobacterium tuberculosis*: definition of a common anchor for lipomannan and lipoarabinomannan. *Glycobiology.* 5:117-127.

105. **Khoo, K. H., E. Douglas, P. Azadi, J. M. Inamine, G. S. Besra, K. Mikusova, P. J. Brennan, and D. Chatterjee** 1996. Truncated structural variants of lipoarabinomannan in ethambutol drug- resistant strains of *Mycobacterium smegmatis*. Inhibition of arabinan biosynthesis by ethambutol. *J Biol Chem.* 271:28682-28690.

106. **Kindler, V., A. P. Sappino, G. E. Grau, P. F. Piguet, and P. Vassalli** 1989. The inducing role of tumor necrosis factor in the development of bactericidal granulomas during BCG infection. *Cell.* 56:731-740.

107. **Knutson, K. L., Z. Hmama, P. Herrera-Velit, R. Rochford, and N. E. Reiner** 1998. Lipoarabinomannan of *Mycobacterium tuberculosis* promotes protein tyrosine dephosphorylation and inhibition of mitogen-activated protein kinase in human mononuclear phagocytes. Role of the Src homology 2 containing tyrosine phosphatase 1. *J Biol Chem.* **273**:645-652.

108. **Kordulakova, J., M. Gilleron, K. Mikusova, G. Puzo, P. J. Brennan, B. Gicquel, and M. Jackson** 2002. Definition of the first mannosylation step in phosphatidylinositol mannoside synthesis: PimA is essential for growth of Mycobacteria. *J Biol Chem.* **14**:14.

109. **Kremer, L., J. D. Douglas, A. R. Baulard, C. Morehouse, M. R. Guy, D. Alland, L. G. Dover, J. H. Lakey, W. R. Jacobs, Jr., P. J. Brennan, D. E. Minnikin, and G. S. Besra** 2000. Thiolactomycin and related analogues as novel anti-mycobacterial agents targeting KasA and KasB condensing enzymes in *Mycobacterium tuberculosis*. *J Biol Chem.* **275**:16857-16864.

110. **Kremer, L., S. S. Gurcha, P. Bifani, P. G. Hitchen, A. Baulard, H. R. Morris, A. Dell, P. J. Brennan, and G. S. Besra** 2002. Characterization of a putative alpha-mannosyltransferase involved in phosphatidylinositol trimannoside biosynthesis in *Mycobacterium tuberculosis*. *Biochem J.* **363**:437-447.

111. **Larson, R. S., and T. A. Springer** 1990. Structure and function of leukocyte integrins. *Immunol Rev.* **114**:181-217.

112. **Lee, R. E. K. Mikusova, P. J. Brennan and G. S. Besra** 1995. Synthesis of the Arabinose Donor .beta.-D-arabinofuranosyl-1-monophosphoryldecaprenol. Development of a basic arabinosyl-transferase assay, and identification of ethambutol as an arabinosyl transferase inhibitor. *J. Am. Chem. Soc.* **117**:11829-11832.

113. **Lee, Y. C., and C. E. Ballou** 1965. Complete structures of the glycophospholipids of mycobacteria. *Biochemistry.* 4:1395-1404.

114. **Lemassu, A., and M. Daffe** 1994. Structural features of the exocellular polysaccharides of *Mycobacterium tuberculosis*. *Biochem J.* **297**:351-357.

115. **Lemassu, A., A. Ortalo-Magne, F. Bardou, G. Silve, M. A. Laneelle, and M. Daffe** 1996. Extracellular and surface-exposed polysaccharides of non-tuberculous mycobacteria. *Microbiology.* **142**:1513-1520.

116. **Leopold, K., and W. Fischer** 1993. Molecular analysis of the lipoglycans of *Mycobacterium tuberculosis*. *Anal Biochem.* **208**:57-64.

117. **Liu, J., E. Y. Rosenberg, and H. Nikaido** 1995. Fluidity of the lipid domain of cell wall from *Mycobacterium chelonae*. *Proc Natl Acad Sci U S A.* **92**:11254-11258.

118. **Luquin, M., V. Ausina, F. Lopez Calahorra, F. Belda, M. Garcia Barcelo, C. Celma, and G. Prats** 1991. Evaluation of practical chromatographic procedures for identification of clinical isolates of mycobacteria. *J Clin Microbiol.* **29**:120-130.

119. **Ma, Y., J. A. Mills, J. T. Belisle, V. Vissa, M. Howell, K. Bowlin, M. S. Scherman, and M. McNeil** 1997. Determination of the pathway for rhamnose biosynthesis in mycobacteria: cloning, sequencing and expression of the *Mycobacterium tuberculosis* gene encoding alpha-D-glucose-1-phosphate thymidylyltransferase. *Microbiology.* **143**:937-945.

120. **Maiti, D., A. Bhattacharyya, and J. Basu** 2001. Lipoarabinomannan from *Mycobacterium tuberculosis* Promotes Macrophage Survival by Phosphorylating Bad through a Phosphatidylinositol 3- Kinase/Akt Pathway. *J Biol Chem.* **276**:329-333.

121. **Majumder, A. L., M. D. Johnson, and S. A. Henry** 1997. 1L-*myo*-inositol-1-phosphate synthase. *Biochim Biophys Acta.* **1348**:245-256.

122. **Marklund, B. I., and R. W. Stokes** 1998. Gene replacement in *Mycobacterium intracellulare*. *Methods Mol Biol.* **101**:217-224.

123. **Marques, M. A., S. Chitale, P. J. Brennan, and M. C. Pessolani** 1998. Mapping and identification of the major cell wall-associated components of *Mycobacterium leprae*. *Infect Immun.* **66**:2625-2631.

124. **McNeil, M., M. Daffe, and P. J. Brennan** 1990. Evidence for the nature of the link between the arabinogalactan and peptidoglycan of mycobacterial cell walls. *J Biol Chem.* **265**:18200-18206.

125. **McNeil, M., M. Daffe, and P. J. Brennan** 1991. Location of the mycolyl ester substituents in the cell walls of mycobacteria. *J Biol Chem.* **266**:13217-13223.

126. **McNeil, M. R., and P. J. Brennan** 1991. Structure, function and biogenesis of the cell envelope of mycobacteria in relation to bacterial physiology, pathogenesis and drug resistance; some thoughts and possibilities arising from recent structural information. *Res Microbiol.* **142**:451-463.

127. **Menard, R., P. J. Sansonetti, and C. Parsot** 1993. Nonpolar mutagenesis of the *ipa* genes defines IpaB, IpaC, and IpaD as effectors of *Shigella flexneri* entry into epithelial cells. *J Bacteriol.* **175**:5899-5906.

128. **Meyers, P. R., W. R. Bourn, L. M. Steyn, P. D. van Helden, A. D. Beyers, and G. D. Brown** 1998. Novel method for rapid measurement of growth of mycobacteria in detergent-free media. *J Clin Microbiol.* **36**:2752-2754.

129. **Mikusova, K., R. A. Slayden, G. S. Besra, and P. J. Brennan** 1995. Biogenesis of the mycobacterial cell wall and the site of action of ethambutol. *Antimicrob Agents Chemother.* **39**:2484-2489.

130. **Mikusova, K., T. Yagi, R. Stern, M. R. McNeil, G. S. Besra, D. C. Crick, and P. J. Brennan** 2000. Biosynthesis of the galactan component of the mycobacterial cell wall. *J Biol Chem.* **275**:33890-33897.

131. **Minnikin, D. E.** 1982. Lipids: Complex Lipids, Their Chemistry, Biosynthesis and Roles., p. 95-184. *In* C. Ratledge, and J. Stanford (eds), The Biology of the Mycobacteria, vol. 1: Physiology, Identification and Classification. Academic Press, London.

132. **Minnikin, D. E., L. Alshamaony, and M. Goodfellow** 1975. Differentiation of *Mycobacterium, Nocardia* and related taxa by thin-layer chromatographic analysis 0f whole-organism methanolysates. *J Gen Microbiol.* **88**:200-204.

133. **Moreno, C., A. Mehlert, and J. Lamb** 1988. The inhibitory effects of mycobacterial lipoarabinomannan and polysaccharides upon polyclonal and monoclonal human T cell proliferation. *Clin Exp Immunol.* **74**:206-210.

134. **Moreno, C., J. Taverne, A. Mehlert, C. A. Bate, R. J. Brealey, A. Meager, G. A. Rook, and J. H. Playfair** 1989. Lipoarabinomannan from *Mycobacterium tuberculosis* induces the production of tumour necrosis factor from human and murine macrophages. *Clin Exp Immunol.* **76**:240-245.

135. **Munoa, F. J., K. W. Miller, R. Beers, M. Graham, and H. C. Wu** 1991. Membrane topology of *Escherichia coli* prolipoprotein signal peptidase (signal peptidase II). *J Biol Chem.* **266**:17667-17672.

136. **Nalini, P., and G. K. Khuller** 1982. Biosynthesis of hexamannophosphoinositides in *Mycobacterium smegmatis* ATCC 607. *Arch Microbiol.* **132**:87-90.

137. **Neuwald, A. F., J. D. York, and P. W. Majerus** 1991. Diverse proteins homologous to inositol monophosphatase. *FEBS Lett.* **294**:16-18.

138. **Newton, G. L., K. Arnold, M. S. Price, C. Sherrill, S. B. Delcardayre, Y. Aharonowitz, G. Cohen, J. Davies, R. C. Fahey, and C. Davis** 1996. Distribution of thiols in microorganisms: mycothiol is a major thiol in most actinomycetes. *J Bacteriol.* **178**:1990-1995.

139. **Newton, G. L., Y. Av-Gay, and R. C. Fahey** 2000. N-Acetyl-1-D-*myo*-inosityl-2-amino-2-deoxy-alpha-D-glucopyranoside deacetylase (MshB) is a key enzyme in mycothiol biosynthesis. *J Bacteriol.* **182**:6958-6963.

140. **Newton, G. L., Y. Av-Gay, and R. C. Fahey** 2000. A novel mycothiol-dependent detoxification pathway in mycobacteria involving mycothiol S-conjugate amidase. *Biochemistry.* **39**:10739-10746.

141. **Newton, G. L., M. D. Unson, S. J. Anderberg, J. A. Aguilera, N. N. Oh, S. B. delCardayre, Y. Av-Gay, and R. C. Fahey** 1999. Characterization of *Mycobacterium smegmatis* mutants defective in 1-D-*myo*-inosityl-2-amino-2-deoxy-alpha-D-glucopyranoside and mycothiol biosynthesis. *Biochem Biophys Res Commun.* **255**:239-244.

142. **Niederweis, M., S. Ehrt, C. Heinz, U. Klocker, S. Karosi, K. M. Swiderek, L. W. Riley, and R. Benz** 1999. Cloning of the *mspA* gene encoding a porin from *Mycobacterium smegmatis*. *Mol Microbiol.* **33**:933-945.

143. **Nigou, J., L. G. Dover, and G. S. Besra** 2002. Purification and biochemical characterization of *Mycobacterium tuberculosis* SuhB, an inositol monophosphatase involved in inositol biosynthesis. *Biochemistry.* **41**:4392-4398.

144. **Nigou, J., M. Gilleron, B. Cahuzac, J. D. Bounery, M. Herold, M. Thurnher, and G. Puzo** 1997. The phosphatidyl-myo-inositol anchor of the lipoarabinomannans from *Mycobacterium bovis* bacillus Calmette Guerin. Heterogeneity, structure, and role in the regulation of cytokine secretion. *J Biol Chem.* **272**:23094-23103.

145. **Nigou, J., M. Gilleron, and G. Puzo** 1999. Lipoarabinomannans: characterization of the multiacylated forms of the phosphatidyl-*myo*-inositol anchor by NMR spectroscopy. *Biochem J.* **337**:453-460.

146. **Nikaido, H., S. H. Kim, and E. Y. Rosenberg** 1993. Physical organization of lipids in the cell wall of *Mycobacterium chelonae*. *Mol Microbiol.* **8**:1025-1030.

147. **Norman, E.** 1998. Gene replacement in *Mycobacterium bovis* BCG. *Methods Mol Biol.* **101**:225-233.

148. **Ortalo-Magne, A., A. B. Andersen, and M. Daffe** 1996. The outermost capsular arabinomannans and other mannoconjugates of virulent and avirulent tubercle bacilli. *Microbiology.* **142**:927-935.

149. **Ortalo-Magne, A., M. A. Dupont, A. Lemassu, A. B. Andersen, P. Gounon, and M. Daffe** 1995. Molecular composition of the outermost capsular material of the tubercle bacillus. *Microbiology.* **141**:1609-1620.

150. **Ortalo-Magne, A., A. Lemassu, M. A. Laneelle, F. Bardou, G. Silve, P. Gounon, G. Marchal, and M. Daffe** 1996. Identification of the surface-exposed lipids on the cell envelopes of *Mycobacterium tuberculosis* and other mycobacterial species. *J Bacteriol.* **178**:456-461.

151. **Palella, F. J., Jr., K. M. Delaney, A. C. Moorman, M. O. Loveless, J. Fuhrer, G. A. Satten, D. J. Aschman, and S. D. Holmberg** 1998. Declining morbidity and mortality among patients with advanced human immunodeficiency virus infection. HIV Outpatient Study Investigators. *N Engl J Med.* **338**:853-860.

152. **Pangborn, M. C., and J. A. McKinney** 1966. Purification of serologically active phosphoinositides of *Mycobacterium tuberculosis*. *J Lipid Res.* **7**:627-633.

153. **Parish, T., J. Liu, H. Nikaido, and N. G. Stoker** 1997. A *Mycobacterium smegmatis* mutant with a defective inositol monophosphate phosphatase gene homolog has altered cell envelope permeability. *J Bacteriol.* **179**:7827-7833.

154. **Patel, M. P., and J. S. Blanchard** 1999. Expression, purification, and characterization of *Mycobacterium tuberculosis* mycothione reductase. *Biochemistry.* **38**:11827-11833.

155. **Patterson, J. H., M. J. McConville, R. E. Haites, R. L. Coppel, and H. Billman-Jacobe** 2000. Identification of a methyltransferase from *Mycobacterium smegmatis* involved in glycopeptidolipid synthesis. *J Biol Chem.* **275**:24900-24906.

156. **Paul, T. R., and T. J. Beveridge** 1994. Preservation of surface lipids and determination of ultrastructure of *Mycobacterium kansasii* by freeze-substitution. *Infect Immun.* **62:**1542-1550.

157. **Paul, T. R., and T. J. Beveridge** 1992. Reevaluation of envelope profiles and cytoplasmic ultrastructure of mycobacteria processed by conventional embedding and freeze-substitution protocols. *J Bacteriol.* **174:**6508-6517.

158. **Paulus, H., and E. P. Kennedy** 1960. The enzymatic synthesis of inositol monophosphatide. *J Biol Chem.* **235:**1303-1311.

159. **Pavelka, M. S., Jr., and W. R. Jacobs, Jr.** 1999. Comparison of the construction of unmarked deletion mutations in *Mycobacterium smegmatis*, *Mycobacterium bovis* bacillus Calmette-Guerin, and *Mycobacterium tuberculosis* $H_{37}R_v$ by allelic exchange. *J Bacteriol.* **181:**4780-4789.

160. **Pelicic, V., M. Jackson, J. M. Reyrat, W. R. Jacobs, Jr., B. Gicquel, and C. Guilhot** 1997. Efficient allelic exchange and transposon mutagenesis in *Mycobacterium tuberculosis*. *Proc Natl Acad Sci U S A.* **94:**10955-10960.

161. **Pettipher, C. A., A. S. Karstaedt, and M. Hopley** 2001. Prevalence and clinical manifestations of disseminated *Mycobacterium avium* complex infection in South Africans with acquired immunodeficiency syndrome. *Clin Infect Dis.* **33:**2068-2071.

162. **Polotsky, V. Y., J. T. Belisle, K. Mikusova, R. A. Ezekowitz, and K. A. Joiner** 1997. Interaction of human mannose-binding protein with *Mycobacterium avium*. *J Infect Dis.* **175:**1159-1168.

163. **Prentki, P., and H. M. Krisch** 1984. *In vitro* insertional mutagenesis with a selectable DNA fragment. *Gene.* **29:**303-313.

164. **Prinzis, S., D. Chatterjee, and P. J. Brennan** 1993. Structure and antigenicity of lipoarabinomannan from *Mycobacterium bovis* BCG. *J Gen Microbiol.* **139:**2649-2658.

165. **Prod'hom, G., B. Lagier, V. Pelicic, A. J. Hance, B. Gicquel, and C. Guilhot** 1998. A reliable amplification technique for the characterization of genomic DNA sequences flanking insertion sequences. *FEMS Microbiol Lett.* **158:**75-81.

166. **Pugsley, A. P.** 1993. The complete general secretory pathway in gram-negative bacteria. *Microbiol Rev.* **57:**50-108.

167. **Radford, A. J., and A. L. Hodgson** 1991. Construction and characterization of a *Mycobacterium-Escherichia coli* shuttle vector. *Plasmid.* **25:**149-153.

168. **Rastogi, N., C. Frehel, and H. L. David** 1986. Triple-layered structure of mycobacterial cell wall: Evidence for the existence of a polysaccharide-rich outer layer in 18 mycobacterial species. *Current Microbiology.* **13:**237-242.

169. **Roach, T. I., C. H. Barton, D. Chatterjee, and J. M. Blackwell** 1993. Macrophage activation: lipoarabinomannan from avirulent and virulent strains of *Mycobacterium tuberculosis* differentially induces the early genes c-fos, KC, JE, and tumor necrosis factor-alpha. *J Immunol.* **150:**1886-1896.

170. **Roach, T. I., D. Chatterjee, and J. M. Blackwell** 1994. Induction of early-response genes KC and JE by mycobacterial lipoarabinomannans: regulation of KC expression in murine macrophages by Lsh/Ity/Bcg (candidate Nramp). *Infect Immun.* **62:**1176-1184.

171. **Sakuda, S., Z. Y. Zhou, and Y. Yamada** 1994. Structure of a novel disulfide of 2-(N-acetylcysteinyl) amido-2-deoxy-alpha-D-glucopyranosyl-*myo*-inositol produced by *Streptomyces* sp. *Biosci Biotechnol Biochem.* **58:**1347-1348.

172. **Salman, M., P. J. Brennan, and J. T. Lonsdale** 1999. Synthesis of mycolic acids of mycobacteria: an assessment of the cell- free system in light of the whole genome. *Biochim Biophys Acta.* **1437:**325-332.

173. **Salman, M., J. T. Lonsdale, G. S. Besra, and P. J. Brennan** 1999. Phosphatidylinositol synthesis in mycobacteria. *Biochim Biophys Acta.* **1436:**437-450.

174. **Sambrook, J., E. F. Fritsch, and T. Maniatis** 1989. Molecular Cloning: A Laboratory Manual, 2nd Edition ed. Cold Spring Harbour Press.

175. **Schaeffer, M. L., K. H. Khoo, G. S. Besra, D. Chatterjee, P. J. Brennan, J. T. Belisle, and J. M. Inamine** 1999. The *pimB* gene of *Mycobacterium tuberculosis* encodes a mannosyltransferase involved in lipoarabinomannan biosynthesis. *J Biol Chem.* **274:**31625-31631.

176. **Schlesinger, L. S.** 1993. Macrophage phagocytosis of virulent but not attenuated strains of *Mycobacterium tuberculosis* is mediated by mannose receptors in addition to complement receptors. *J Immunol.* **150:**2920-2930.

177. **Schlesinger, L. S., and M. A. Horwitz** 1991. Phenolic glycolipid-1 of *Mycobacterium leprae* binds complement component C3 in serum and mediates phagocytosis by human monocytes. *J Exp Med.* **174:**1031-1038.

178. **Schlesinger, L. S., S. R. Hull, and T. M. Kaufman** 1994. Binding of the terminal mannosyl units of lipoarabinomannan from a virulent strain of *Mycobacterium tuberculosis* to human macrophages. *J Immunol.* **152:**4070-4079.

179. **Schlesinger, L. S., T. M. Kaufman, S. Iyer, S. R. Hull, and L. K. Marchiando** 1996. Differences in mannose receptor-mediated uptake of lipoarabinomannan from virulent and attenuated strains of *Mycobacterium tuberculosis* by human macrophages. *J Immunol.* **157:**4568-4575.

180. **Schulbach, M. C., P. J. Brennan, and D. C. Crick** 2000. Identification of a short (C15) chain Z-isoprenyl diphosphate synthase and a homologous long (C50) chain isoprenyl diphosphate synthase in *Mycobacterium tuberculosis*. *J Biol Chem.* **275:**22876-22881.

181. **Scorpio, A., and Y. Zhang** 1996. Mutations in *pncA*, a gene encoding pyrazinamidase/nicotinamidase, cause resistance to the antituberculous drug pyrazinamide in tubercle bacillus. *Nat Med.* **2:**662-667.

182. **Severn, W. B., R. H. Furneaux, R. Falshaw, and P. H. Atkinson** 1998. Chemical and spectroscopic characterisation of the phosphatidylinositol manno-oligosaccharides from *Mycobacterium bovis* AN5 and WAg201 and *Mycobacterium smegmatis* mc^2155. *Carbohydr Res.* **308:**397-408.

183. **Sibley, L. D., L. B. Adams, and J. L. Krahenbuhl** 1990. Inhibition of interferon-gamma-mediated activation in mouse macrophages treated with lipoarabinomannan. *Clin Exp Immunol.* **80:**141-148.

184. **Sibley, L. D., S. W. Hunter, P. J. Brennan, and J. L. Krahenbuhl** 1988. Mycobacterial lipoarabinomannan inhibits gamma interferon-mediated activation of macrophages. *Infect Immun.* **56:**1232-1236.

185. **Simonen, M., and I. Palva** 1993. Protein secretion in Bacillus species. *Microbiol Rev.* **57:**109-137.

186. **Singh, A. P., and G. K. Khuller** 1994. Induction of immunity against experimental *tuberculosis* with mycobacterial mannophosphoinositides encapsulated in liposomes containing lipid A. *FEMS Immunol Med Microbiol.* **8:**119-126.

187. **Smith, M., J. Jesse, T. Landers, and J. Jordan** 1990. High efficiency bacterial transformation: $1x10^{10}$ *E. coli* transformants/μg. *Focus.* **12**:38-40.

188. **Snapper, S. B., R. E. Melton, S. Mustafa, T. Kieser, and W. R. Jacobs, Jr.** 1990. Isolation and characterization of efficient plasmid transformation mutants of *Mycobacterium smegmatis*. *Mol Microbiol.* **4**:1911-1919.

189. **Spies, H. S., and D. J. Steenkamp** 1994. Thiols of intracellular pathogens. Identification of ovothiol A in Leishmania donovani and structural analysis of a novel thiol from *Mycobacterium bovis*. *Eur J Biochem.* **224**:203-213.

190. **Stahl, D. A., and J. W. Urbance** 1990. The division between fast- and slow-growing species corresponds to natural relationships among the mycobacteria. *J Bacteriol.* **172**:116-124.

191. **Stinear, T., J. K. Davies, G. A. Jenkin, J. A. Hayman, F. Oppedisano, and P. D. Johnson** 2000. Identification of *Mycobacterium ulcerans* in the environment from regions in southeast australia in which It is endemic with sequence capture-PCR. *Appl Environ Microbiol.* **66**:3206-3213.

192. **Stover, C. K., V. F. de la Cruz, T. R. Fuerst, J. E. Burlein, L. A. Benson, L. T. Bennett, G. P. Bansal, J. F. Young, M. H. Lee, G. F. Hatfull, and et al.** 1991. New use of BCG for recombinant vaccines. *Nature.* **351**:456-460.

193. **Summerfield, J. A.** 1993. The role of mannose-binding protein in host defence. *Biochem Soc Trans.* **21**:473-477.

194. **Takayama, K., and D. S. Goldman** 1969. Pathway for the synthesis of mannophospholipids in *Mycobacterium tuberculosis*. *Biochim Biophys Acta.* **176**:196-198.

195. **Tam, R., and M. H. Saier, Jr.** 1993. Structural, functional, and evolutionary relationships among extracellular solute-binding receptors of bacteria. *Microbiol Rev.* **57**:320-346.

196. **Taylor, M. E.** 1993. Recognition of complex carbohydrates by the macrophage mannose receptor. *Biochem Soc Trans.* **21**:468-473.

197. **Tereletsky, M. J., and W. W. Barrow** 1983. Postphagocytic detection of glycopeptidolipids associated with the superficial L1 layer of *Mycobacterium intracellulare*. *Infect Immun.* **41**:1312-1321.

198. **Thornton, B. P., V. Vetvicka, M. Pitman, R. C. Goldman, and G. D. Ross** 1996. Analysis of the sugar specificity and molecular location of the beta- glucan-binding lectin site of complement receptor type 3 (CD11b/CD18). *J Immunol.* **156**:1235-1246.

199. **Treumann, A., F. Xidong, L. McDonnell, P. J. Derrick, A. E. Ashcroft, D. Chatterjee, and S. W. Homans** 2002. 5-Methylthiopentose: a New Substituent on Lipoarabinomannan in *Mycobacterium tuberculosis*. *J Mol Biol.* **316**:89-100.

200. **Trias, J., and R. Benz** 1994. Permeability of the cell wall of *Mycobacterium smegmatis*. *Mol Microbiol.* **14**:283-290.

201. **Trias, J., V. Jarlier, and R. Benz** 1992. Porins in the cell wall of mycobacteria. *Science.* **258**:1479-1481.

202. **Venisse, A., M. Riviere, J. Vercauteren, and G. Puzo** 1995. Structural analysis of the mannan region of lipoarabinomannan from *Mycobacterium bovis* BCG. Heterogeneity in phosphorylation state. *J Biol Chem.* **270**:15012-15021.

203. **Vercellone, A., J. Nigou, and G. Puzo** 1998. Relationships between the structure and the roles of lipoarabinomannans and related glycoconjugates in *tuberculosis* pathogenesis. *Front Biosci.* **3**:e149-163.

204. **Weber, P. L., and G. R. Gray** 1979. Structural and immunochemical characterization of the acidic arabinomannan of *Mycobacterium smegmatis*. *Carbohydr Res.* **74**:259-278.

205. **Weston, A., R. J. Stern, R. E. Lee, P. M. Nassau, D. Monsey, S. L. Martin, M. S. Scherman, G. S. Besra, K. Duncan, and M. R. McNeil** 1997. Biosynthetic origin of mycobacterial cell wall galactofuranosyl residues. *Tuber Lung Dis.* **78**:123-131.

206. **Wolucka, B. A., M. R. McNeil, E. de Hoffmann, T. Chojnacki, and P. J. Brennan** 1994. Recognition of the lipid intermediate for arabinogalactan/arabinomannan biosynthesis and its relation to the mode of action of ethambutol on mycobacteria. *J Biol Chem.* **269**:23328-23335.

207. **World Health Organisation** 2001. Global Tuberculosis Control. WHO Report 2001. World Health Organisation.

208. **World Health Organisation** 2000. Tuberculosis: WHO Fact Sheet No. 104. World Health Organisation.

209. **Xin, Y., R. E. Lee, M. S. Scherman, K. H. Khoo, G. S. Besra, P. J. Brennan, and M. McNeil** 1997. Characterization of the *in vitro* synthesized arabinan of mycobacterial cell walls. *Biochim Biophys Acta.* **1335**:231-234.

210. **Yanisch-Perron, C., J. Vieira, and J. Messing** 1985. Improved M13 phage cloning vectors and host strains: nucleotide sequences of the M13mp18 and pUC19 vectors. *Gene.* **33**:103-119.

211. **Yuan, Y., and C. E. Barry, 3rd** 1996. A common mechanism for the biosynthesis of methoxy and cyclopropyl mycolic acids in *Mycobacterium tuberculosis*. *Proc Natl Acad Sci U S A.* **93**:12828-12833.

212. **Yuan, Y., R. E. Lee, G. S. Besra, J. T. Belisle, and C. E. Barry, 3rd** 1995. Identification of a gene involved in the biosynthesis of cyclopropanated mycolic acids in *Mycobacterium tuberculosis*. *Proc Natl Acad Sci U S A.* **92**:6630-6634.

213. **Zhang, Y., M. Broser, H. Cohen, M. Bodkin, K. Law, J. Reibman, and W. N. Rom** 1995. Enhanced interleukin-8 release and gene expression in macrophages after exposure to *Mycobacterium tuberculosis* and its components. *J Clin Invest.* **95**:586-592.

214. **Zhang, Y., M. Broser, and W. N. Rom** 1994. Activation of the interleukin 6 gene by *Mycobacterium tuberculosis* or lipopolysaccharide is mediated by nuclear factors NF-IL6 and NF-kappa B [published erratum appears in Proc Natl Acad Sci U S A 1995 Apr 11;92(8):3632]. *Proc Natl Acad Sci U S A.* **91**:7225-2229.

215. **Zhang, Y., and W. N. Rom** 1993. Regulation of the interleukin-1 beta (IL-1 beta) gene by mycobacterial components and lipopolysaccharide is mediated by two nuclear factor-IL6 motifs. Mol Cell Biol. **13**:3831-3837.

216. **Zimhony, O., J. S. Cox, J. T. Welch, C. Vilcheze, and W. R. Jacobs, Jr.** 2000. Pyrazinamide inhibits the eukaryotic-like fatty acid synthetase I (FASI) of *Mycobacterium tuberculosis* [see comments]. *Nat Med.* **6**:1043-1047.

217. **Zumla, A., and J. M. Grange** 2001. Multidrug-resistant *tuberculosis*--can the tide be turned? *Lancet Infect Dis.* **1**:199-202.

Department of Microbiology
P. O. Box 53, Wellington Road
Clayton, Victoria 3800
Melbourne, Australia
Tel +61 3 9905 1378
Fax +61 3 9905 4811